

The Society of Thoracic Radiology
Thoracic Imaging 2003

March 2 - 6, 2003
Loews Miami Beach Hotel
Miami Beach, Florida



pulmonary vessels mediastinum heart aorta
lungs coronary arteries pleura pulmonary vessels
mediastinum heart aorta lungs coronary
arteries pleura pulmonary vessels mediastinum
heart aorta lungs coronary arteries pleura
pulmonary vessels mediastinum heart aorta
lungs coronary arteries pleura pulmonary
vessels mediastinum heart aorta lungs
coronary arteries pleura pulmonary vessels

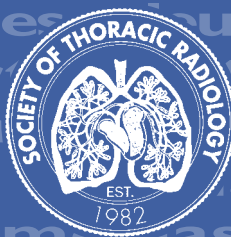


Table of Contents

President's Letter	3
Course Description, Objectives and Highlights	4
Credit, Disclosures and Target Audience	5
Faculty	6-9
General Information	11
Officers and Past Presidents	12
Program Committee and Guest Speaker	13
Future Meetings	10
Posters	23-25
Program Schedule	
Sunday, March 2nd, 2003	14-15
Monday, March 3rd, 2003	16-17
Tuesday, March 4th, 2003	18-19
Wednesday, March 5th, 2003	20-21
Thursday, March 6th, 2003	22

President's Letter

Dear Friends,

Welcome to Miami Beach and the 21st annual meeting of the Society of Thoracic Radiology. This should be a wonderful meeting in a wonderful location. The course director, Ella Kazerooni, has gathered a truly outstanding group of faculty for the meeting. You will be getting the latest and the greatest information on all the current issues in thoracic imaging. Don't forget -- thoracic imaging encompasses both pulmonary and cardiac imaging, and we have great speakers in both of these areas. We will cover controversial subjects, such as lung cancer screening, and issues important to the clinical and academic workplace, such as new technologies, PACs and ergonomics, the workforce shortage and current/future developments in research and research funding, with experts from the NCI, NIBIB and ACR. Overall, it should be a great meeting at a truly outstanding hotel!

This year the Benjamin Felson Memorial Lecture will be given by Thomas Brady, who will present "Cardiac Imaging: Role of CT and MR," a very hot topic given the rapid advances in technology. Another highlight is the Scanlon Symposium on Lung Cancer. A meeting favorite, the unknown film panel, has been revived with a group of STR presidents challenging the newcomers in taking a series of truly unknown cases. Fun should be had by all!

Thank you for coming to the meeting. If there is anything I can do to improve the meeting and your meeting experience, please do not hesitate to let me know or contact one of our meeting planners from Matrix Meetings if you need assistance.

Lastly, mark you calendars for the 2004 meeting at the beautiful Westin Mission Hills Resort in Rancho Mirage, California on March 28-April 1, 2004.

Sincerely,



Robert D. Tarver, M.D.
President, Society of Thoracic Radiology

Course Description

The course is designed for radiologists and other physicians with an interest in cardiopulmonary imaging. Thoracic Imaging 2003 is the Twenty-First Annual Meeting and Postgraduate Course of the Society of Thoracic Radiology. This five day course features internationally recognized experts in thoracic imaging, including the lungs, airway, heart, and thoracic vasculature.

Dedicated symposia on the following subjects will be presented.

- Lung Cancer Screening, Diagnosis and Staging
- Cardiac Imaging (CXR, CT and MR) of Atherosclerotic Disease, Valvular Disease, Cardiomyopathy and Cardiac Tumors
- New Imaging Technologies
- Infiltrative Lung Disease
- Small Airway Disease
- The Central Airway
- The Pleura, including Intervention
- Clinical Workflow, including PACS and Voice Recognition
- Thoracic Infection
- Electronic Presentation and Web-Based Education Resources

Two scientific sessions and scientific posters

Course Objectives

At the completion of the course, the attendee will be able to:

- Describe the current state of imaging technology, including digital radiography, PACS, voice recognition, and advances in multidetector CT and MR
- Summarize the current status and role of cardiovascular imaging using multidetector CT and MRI, particularly with respect to atherosclerotic coronary artery disease
- Summarize the current controversies related to the screening and diagnosis of lung cancer
- Describe the appearance and role of radiology in the evaluation of infiltrative and obstructive lung disease, thoracic neoplasms and abnormalities of the central airway
- Use digital resources to enhance evidence based on-line continuous education and to prepare electronic presentations

Course Highlights

- *Unknown Cases of the Day* – Two cases will be posted daily for attendees to review and submit a diagnosis. The cases are then presented and discussed the following day during the morning session. On Thursday, the awards will be given for the most correct answers in several categories, including non-STR members and STR members.
- *Unknown Film Panel* – features “past presidents” versus the “up and coming” with true unknown cases. Attendees will see how experts work through cases based in imaging findings as well as relevant clinical history.
- *Clinical and Academic Workplace Issues* – include PACS, PACS ergonomics, voice recognition, the manpower shortage in radiology with Jonathan Sunshine (ACR), research directions for the future with Edward Staab (NCI) and Richard Swaya (NIBB).

Continuing Medical Education Credit

This activity has been planned and implemented in accordance with the Essential Areas and Policies of the Accreditation Council for Continuing Medical Education (ACCME) through the joint sponsorship of the Minnesota Medical Association and the Society of Thoracic Radiology (STR). The Minnesota Medical Association is accredited by the ACCME to provide continuing medical education for physicians.

The Minnesota Medical Association designates this activity for a maximum of 33.25 category 1 credits toward the AMA Physician's Recognition Award. Each physician should claim only those credits that he/she actually spent in the activity.

Disclosures

The Accreditation Council for Continuing Medical Education requires the Minnesota Medical Association, as an accredited provider of CME, to provide faculty disclosure information to all attendees prior to the beginning of the CME activity. Faculty members are expected to disclose the existence of any significant financial or other relationship with the manufacturer(s) of any commercial product (s) discussed in an educational presentation. The requirement applies to relationships that are in place at the time of the presentation or in the 12 months preceding the meeting date. Faculty members are also required to disclose discussion of unlabeled use of commercial products or investigational use not yet approved for any purpose. Disclosure information, including a list of faculty failing to provide disclosure information prior to the Society of Thoracic Radiology Meeting, will be available onsite.

Target Audience

This meeting is designed for general diagnostic radiologists, thoracic radiologists, cardiac radiologists, pulmonologist, internists, family physicians, thoracic surgeons, and thoracic-oriented residents and fellows.

Faculty

Gerald F. Abbott, MD
Brown University
Providence, RI

Suzanne L. Aquino, MD
Massachusetts General Hospital
Boston, MA

Alexander A. Bankier, MD
University of Vienna
Vienna, Austria

Poonam Batra, MD
University of California – Los Angeles
Los Angeles, CA

William Berger, MD
University of Arizona
Tucson, AZ

Phillip M. Boiselle, MD
Beth Israel Deaconess Medical Center
Boston, MA

Lawrence M. Boxt, MD
Columbia-Presbyterian Medical Center
New York, NY

Thomas J. Brady, MD
Massachusetts General Hospital
Boston, MA

Lynn S. Broderick, MD
University of Wisconsin
Madison, WI

Denis H. Carr, MD
Royal Brompton Hospital
London, England

Philip N. Cascade, MD
University of Michigan
Ann Arbor, MI

Marvin H. Chasen, MD
MD Anderson Cancer Center
Houston, TX

Caroline Chiles, MD
Wake Forest University
Winston-Salem, NC

Jannette Collins, MD, MEd
University of Wisconsin
Madison, WI

Sujal R. Desai, MBBS
King's College
London, England

Jeffrey D. Edelman, MD
Oregon Health and Sciences University
Portland, OR

Jeremy J. Erasmus, MD
MD Anderson Cancer Center
Houston, TX

Joel E. Fishman, MD, PhD
University of Miami
Miami, FL

Tomas C. Franquet, MD
Hospital de Sant Pau
Barcelona, Spain

Aletta A. Frazier, MD
Armed Forces Institute of Pathology
Washington, DC

Donald P. Frush, MD
Duke University
Durham, NC

Carl R. Fuhrman, MD
University of Pittsburgh
Pittsburgh, PA

Jeffrey R. Galvin, MD
Armed Forces Institute of Pathology
Washington, DC

Gordon Gamsu, MD
Cornell University
New York, NY

Warren B. Gefter, MD
University of Pennsylvania
Philadelphia, PA

Robert C. Gilkeson, Jr., MD
University Hospitals of Cleveland
Cleveland, OH

Michelle S. Ginsberg, MD
Memorial Sloan-Kettering Cancer Center
New York, NY

Lawrence R. Goodman, MD
Medical College of Wisconsin
Milwaukee, WI

Marc V. Gosselin, MD
Oregon Health and Sciences University
Portland, OR

Michael B. Gotway, MD
San Francisco General Hospital
San Francisco, CA

George W. Gross, MD
University of Maryland
Baltimore, MD

James F. Gruden, MD
Emory University
Atlanta, GA

Jud W. Gurney, MD
University of Nebraska
Omaha, NE

Fernando R. Gutierrez, MD
Mallinckrodt Institute of Radiology
St. Louis, MO

Linda B. Haramati, MD
Albert Einstein College of Medicine
New Rochelle, NY

Thomas E. Hartman, MD
Mayo Clinic
Rochester, MN

Hiroto Hatabu, MD, PhD
Beth Israel Deaconess Medical Center
Boston, MA

Todd R. Hazelton, MD
H. Lee Moffitt Cancer Center
Tampa, FL

Laura E. Heyneman, MD
Duke University
Durham, NC

Francine L. Jacobson, MD, MPH
Brigham & Women's Hospital
Boston, MA

Peter V. Kavanagh, MD
Wake Forest University
Winston-Salem, NC

Gregory J. L. Kaw, MD
Singapore

Ella A. Kazerooni, MD
University of Michigan
Ann Arbor, MI

Aine M. Kelly, MD
University of Michigan
Ann Arbor, MI

Loren H. Ketai, MD
University of New Mexico
Albuquerque, NM

Arfa Khan, MD
Long Island Jewish Medical Center
New Hyde Park, NY

Jin-Kwan Kim, MD
Mallinckrodt Institute of Radiology
St. Louis, MO

Jeffrey S. Klein, MD
University of Vermont
Williston, VT

Jane P. Ko, MD
New York University
New York, NY

Sandra S. Kramer, MD
Children's Hospital - Philadelphia
Philadelphia, PA

Kyung Soo Lee, MD
Sungkyunkwan University
Seoul, Korea

Ann N. C. Leung, MD
Stanford University
Stanford, CA

Martin J. Lipton, MD
University of Chicago
Chicago, IL

David A. Lynch, MD
University of Colorado
Denver, CO

Richard I. Markowitz, MD
Children's Hospital - Philadelphia
Philadelphia, PA

Edith M. Marom, MD
MD Anderson Cancer Center
Houston, TX

H. Page McAdams, MD
Duke University
Durham, NC

Georgeann McGuinness, MD
New York University
New York, NY

Theresa C. McCloud, MD
Massachusetts General Hospital
Boston, MA

Patricia J. Mergo, MD
University of Florida
Gainesville, FL

Stephen W. Miller, MD
Massachusetts General Hospital
Boston, MA

Paul L. Molina, MD
University of North Carolina
Chapel Hill, NC

Elizabeth H. Moore, MD
University of California - Davis
Sacramento, CA

Brian F. Mullan, MD
University of Iowa
Iowa City, IA

Reginald F. Munden, DMD, MD
MD Anderson Cancer Center
Houston, TX

John D. Newell, MD
University of Colorado
Denver, CO

Mark S. Parker, MD
Medical College of Virginia
Richmond, VA

Smita Patel, MBBS
University of Michigan
Ann Arbor, MI

Gregory D.N. Pearson, MD, PhD
New York Presbyterian Hospital
New York, NY

Steven L. Primack, MD
Oregon Health and Sciences University
Portland, OR

Robert D. Pugatch, MD
University of Maryland
Baltimore, MD

James G. Ravenel, MD
Medical University of South Carolina
Charleston, SC

Carl E. Ravin, MD
Duke University
Durham, NC

Gautham P. Reddy, MD
University of California--San Francisco
San Francisco, CA

James C. Reed, MD
University of Kentucky
Lexington, KY

Melissa L. Rosado de Christenson, MD
Uniformed Services University of the
Health Sciences
Bethesda, MD

Santiago E. Rossi, MD
Capital Federal, Argentina

Anna Rozenshtein, MD
Columbia University
New York, NY

Ernest M. Scalzetti, MD
SUNY Upstate Medical University
Syracuse, NY

U. Joseph Schoepf, MD
Brigham & Women's Hospital
Boston, MA

David S. Schwartz, MD
University of Miami
Miami, FL

Kitt Shaffer, MD, PhD
Dana Farber Cancer Institute
Boston, MA

Rosita M. Shah, MD
Thomas Jefferson University
Philadelphia, PA

David K. Shelton, MD
University of California - Davis
Sacramento, CA

Jo-Anne O. Shepard, MD
Massachusetts General Hospital
Boston, MA

Maria C. Shiau, MD
Columbia-Presbyterian Medical Center
New York, NY

Satinder P. Singh, MD
University of Alabama
Birmingham, AL

Michael B. Sneider, MD
University of Michigan Hospital
Ann Arbor, MI

Edward Staab, MD
National Cancer Institute
Bethesda, MD

William Stanford, MD
University of Iowa
Iowa City, IA

Robert M. Steiner, MD
University of Pennsylvania
Philadelphia, PA

Eric J. Stern, MD
University of Washington
Seattle, WA

Diane C. Strollo, MD
University of Pittsburgh
Pittsburgh, PA

Jonathan H. Sunshine, PhD
American College of Radiology
Reston, VA

Richard Swaja, PhD
National Institute of Health
Bethesda, MD

Robert D. Tarver, MD
Indiana University
Indianapolis, IN

Nisa Thoongsuwan, MD
University of Washington
Seattle, WA

Kay H. Vydareny, MD
Emory University
Atlanta, GA

Lacey Washington, MD
Medical College of Wisconsin
Milwaukee, WI

Gordon L. Weisbrod, MD
Toronto Hospital General Division
Toronto, ON

Charles S. White, MD
University of Maryland
Baltimore, MD

Helen T. Winer-Muram, MD
Indiana University
Indianapolis, IN

Pamela K. Woodard, MD
Mallinckrodt Institute of Radiology
St. Louis, MO

Carl J. Zylak, MD
Henry Ford Hospital
Detroit, MI

Upcoming Meetings

Society of Thoracic Radiology

2004

March 28 – April 1, 2004
(Sunday – Thursday)
Westin Mission Hills Resort
Rancho Mirage, California

Westin Mission Hills Resort

Set in Rancho Mirage, California, the Westin Mission Hills Resort provides all that makes the Palm Springs area unique. Surrounded by the Mission Hills Country Club, this Westin resort provides outstanding golf in the “Golf Capitol of the World.”

Golf, waterways and mountain views combine to enhance the spectacular desert setting. The low-rise Classic-Moroccan architecture complements the desert environment. Guest pavilions are surrounded by lush gardens, meandering lagoons, spectacular pools and waterfalls.

Two championship golf courses, seven tennis courts, the Las Brisas pool, and the health club offer a full range of resort activities. Oversized guest rooms feature private patios, refreshment centers, and a host of thoughtful amenities.

Registration Hours

Saturday, March 1, 2003	4:00 pm – 6:00 pm
Sunday, March 2, 2003	7:00 am – 6:30 pm
Monday, March 3, 2003	7:00 am – 5:30 pm
Tuesday, March 4, 2003	7:00 am – 5:30 pm
Wednesday, March 5, 2003	7:00 am – 5:30 pm
Thursday, March 6, 2003	7:00 am – 12:30 pm

The registration desk will be located in the Americana Foyer, 2nd floor of the hotel.

Speaker Preview Room

The speaker room will be open as follows:

Saturday, March 1, 2003	2:00 pm – 10:00 pm
Sunday, March 2, 2003	7:00 am - 6:30 pm
Monday, March 3, 2003	7:00 am - 5:30 pm
Tuesday, March 4, 2003	7:00 am - 5:30 pm
Wednesday, March 5, 2003	7:00 am - 5:30 pm
Thursday, March 6, 2003	7:00 am - 10:00 am

The speaker preview room will be located in the Sundial Room, 3rd floor of the hotel.

Society Membership Information

Membership in the Society of Thoracic Radiology is open to any radiologist who has an interest in thoracic radiology. If you are interested in receiving further information, contact:

Society of Thoracic Radiology
P.O. Box 1026
Rochester, MN 55903-1026
Telephone (507)288-5620
Fax (507)288-0014
E-mail: str@thoracicrad.org

Officers

Robert D. Tarver, MD, President

Ella A. Kazerooni, MD, President-Elect and Course Director

Reginald F. Munden, DMD, MD, Secretary

Jeffrey S. Klein, MD, Treasurer

Past Presidents

S. David Rockoff, MD

Harold Baltaxe, MD (deceased)

Eric N.C. Milne, MD

W. Richard Webb, MD

Frederick P. Stitik, MD

Carl J. Zylak, MD

Theresa C. McLoud, MD

Robert D. Pugatch, MD

Lawrence R. Goodman, MD

Ernest J. Ferris, MD

David J. Delancy, MD

Sanford A. Rubin, MD

Jack L. Westcott, MD (deceased)

J. David Goodwin II, MD

Nestor L. Müller, MD, PhD

Denise R. Aberle, MD

Robert M. Steiner, MD

Stephen J. Swensen, MD

Gordon Gamsu, MD

Jeffrey R. Galvin, MD

Program Committee

Program Committee

Ella A. Kazerooni, MD, Chair
Reginald F. Munden, DMD, MD
Jeffrey S. Klein, MD
Philip N. Cascade, MD

Scientific Program Committee

Jeremy J. Erasmus, MD, Chair
Santeev Bhalla, MD
Joel E. Fishman, MD
H. Page McAdams, MD
Smita Patel, MD
Gauthum P. Reddy, MD
Eric J. Stern, MD

Benjamin Felson Memorial Lecturer

Thomas J. Brady, MD
Massachusetts General Hospital
Boston, Massachusetts

Society of Thoracic Radiology Scientific Program

March 2, 2003 General Session

Sunday

7:00 - 8:00 am	Continental Breakfast	Americana 4
8:00 - 11:00 am	Guest Hospitality Suite	Moon Room
7:20 - 7:30 am	Welcome and Introduction <i>Ella Kazerooni, MD</i>	Americana 3
Technology Update		Americana 3
Moderator: Suzanne Aquino, MD		
7:50 - 8:10	Chest Radiography: FS, CR, DR <i>Carl Ravin, MD</i>	
8:10 - 8:30	Multidetector CT: More Slices and Beyond <i>Patricia Mergo, MD</i>	
8:50 - 9:10	Functional Imaging <i>Hiroto Hatabu, MD, PhD</i>	
9:10 - 9:30	Radiofrequency Ablation in Thoracic Intervention <i>Peter Kavanagh, MD</i>	
9:30 - 9:50	Session Discussion	
9:50 - 10:10 am	Coffee Break	Americana 4
Interstitial Lung Disease		Americana 3
Moderator: David Lynch, MD		
10:10 - 10:30	The Idiopathic Interstitial Pneumonias <i>Jeffrey Galvin, MD</i>	
10:30 - 10:50	Occupational Lung Disease <i>David Lynch, MD</i>	
10:50 - 11:10	Sarcoidosis <i>John Newell, Jr., MD</i>	
11:10 - 11:30	The Expanded Spectrum of Smoking-Related Lung Disease <i>Rosita Shah, MD</i>	
11:30 - 11:50	Hypersensitivity Pneumonitis <i>Aine Kelly, MD</i>	
11:50 - 12:00	Session Discussion	
12:00 - 1:00 pm	Lunch (on your own)	

March 3, 2003

General Session

Monday

7:00 - 8:00 am Continental Breakfast Americana 4
8:00 - 11:00 am Guest Hospitality Suite Moon Room

Cardiovascular Imaging: Heart I

Moderator: Curtis Green, MD

Americana 3

8:50 - 9:10 Cardiac MR: Established Indications
Charles White, MD

9:10 - 9:30 Cardiac MR: New Developments
Gautham Reddy, MD

9:30 - 9:50 Session Discussion

9:50 - 10:10 am Coffee Break

Americana 4

Cardiovascular Imaging: Aorta and Other

Moderator: Stephen Miller, MD

Americana 3

10:10 - 10:30 CT Angiography of the Thoracic Aorta
Poonam Batra, MD

10:30 - 10:50 Acute Aortic Syndromes
Ernest Scalzeiti, MD

11:10 - 11:30 Pulmonary Veins: Imaging for Radiofrequency Ablation Procedures
Michael Sneider, MD

11:30 - 11:50 Imaging of Cardiopulmonary Support Technology
Philip Cascade, MD

11:50 - 12:00 Session Discussion

12:00 - 2:00 pm STR Annual Business Meeting/Lunch

Americana 4

Cardiovascular Imaging: Pulmonary Vascular

Moderator: Lawrence Goodman, MD

Americana 3

2:00 - 2:20 Epidemiology of Venous Thromboembolic Disease
Lacey Washington, MD

2:20 - 2:40 MDCT Pulmonary Angiography
James Gruden, MD

2:40 - 3:00 CT Structural and Functional Imaging of PE
Joseph Schoepf, MD

3:00 - 3:20 Non Thrombotic Pulmonary Embolism
Lawrence Goodman, MD

3:20 - 3:40 Pulmonary Hypertension
Aletta Frazier, MD

3:40 - 4:00 Session Discussion

4:00 - 4:15 pm Coffee Break

Americana 4

Benjamin Felson Memorial Lecture
Moderator: Ella Kazerooni, MD

5:30 - 7:30 PM General Reception

Americana 3

Americana Lawn

Monday

March 4, 2003

General Session

Tuesday

7:00 - 8:00 am Continental Breakfast Americana Foyer
8:00 - 11:00 am Guest Hospitality Suite Moon Room

Session 1-A Concurrent Session Cardiovascular Imaging: Heart II
Moderator: Pamela Woodard, MD Americana 3

7:50 - 8:10 Adult Manifestations of Congenital Heart Disease: CT& MR
Gregory Pearson, MD, PhD
8:10 - 8:30 Imaging of the Pericardium
Paul Molina, MD
8:30 - 8:50 Cardiomyopathy
Martin Lipton, MD
9:10 - 9:30 Nuclear Cardiology Update
David Shelton, Jr., MD
9:30 - 9:50 Session Discussion

Session 1-B Concurrent Session Clinical & Academic Workplace Issues I
Moderator: Robert Tarver, MD Americana 4

8:15 - 8:40 Manpower Shortage in Radiology: Solutions
Kay Vydareny, MD
8:40 - 9:05 NCI Update for Thoracic Radiology
Edward Staab, MD
9:05 - 9:30 NIBIB Update for Thoracic Radiology
Richard Swaja, PhD
9:30 - 9:50 Session Discussion
9:50 - 10:10 am Coffee Break Americana Foyer

Session 2-A Concurrent Session Pediatric Imaging
Moderator: Sandra Kramer, MD Americana 3

10:10 - 10:30 Thoracic Vascular Abnormalities in Children
Sandra Kramer, MD
10:30 - 10:50 Multidetector Pediatric Chest CT: Practical Approach
Donald Frush, MD
10:50 - 11:10 Pulmonary Disease in the Immunocompromised Child
Richard Markowitz, MD
11:30 - 11:50 Session Discussion

**Session 2-B Concurrent Session
Clinical & Academic Workplace Issues II**

Americana 4

Moderator: Jud Gurney, MD

- 10:50 - 11:10 Voice Recognition
Theresa McCloud, MD
- 11:10 - 11:30 The Internet & the Practice of Radiology: A New Educational Paradigm
Jud Gurney, MD
- 11:30 - 11:50 Session Discussion
- 11:50 - 1:00 pm Lunch (on your own)

Workshops (choose 1)

- 1:00 - 1:45 A1: Lymphoma: Spectrum of Disease
Kitt Shaffer, MD, PhD Americana 3
- 1:00 - 1:45 A2: Digital Images: Camera to Powerpoint
Eric Stern, MD Americana 4
- 1:45 - 2:30 B1: Analysis of Mediastinal Contours
James Reed, MD Americana 3
- 2:30 - 3:15 C2: Unusual Manifestations of Lung Cancer
Michelle Ginsberg, MD Americana 4
- 3:15 - 3:30 pm Coffee Break Americana Foyer
- 3:30 - 5:30 pm **Scientific Session I**
(non-CME Session)
Moderators: Jeremy Erasmus, MD and Joel Fishman, MD, PhD
- 5:30 - 7:00 pm Fellow/Resident/Student Reception Venus Room

March 5, 2003

General Session

Wednesday

7:00 – 8:00 am Continental Breakfast Americana Foyer

8:00 - 11:00 am Guest Hospitality Suite Moon Room

Scanlon Symposium Part I: Lung Cancer Screening & Detection

Moderator: Reginald Munden, DMD, MD

Americana 3

7:50 - 8:10 Screening: Ethics & Principles
Caroline Chiles, MD

8:10 - 8:30 Lung Cancer Screening Trials: An Update
Thomas Hartman, MD

8:30 - 8:50 Lung Cancer Detection Failures (CXR & CT)
Phillip Boiselle, MD

8:50 - 9:10 Role of Computer Aided Diagnosis in Lung Cancer Screening
Jane Ko, MD

9:10 - 9:30 Small T1 Lung Cancer: Imaging & Prognostic Implications
Kyung Soo Lee, MD

9:30 - 9:50 Session Discussion

9:50 - 10:10 am Coffee Break Americana Foyer

Scanlon Symposium Part II: Lung Cancer Diagnosis

Moderator: Robert Pugatch, MD

Americana 3

10:10 - 10:30 Reporting Tumor Measurements in Oncology
Todd Hazelton, MD

10:30 - 10:50 Assessing Growth of Indeterminate Nodules
Helen Winer-Muram, MD

10:50 - 11:10 Lung Cancer Staging
Ann Leung, MD

11:10 - 11:30 Role of Endoscopic US in Staging
James Ravenel, MD

11:50 - 12:00 Session Discussion

12:00 - 1:00 pm Lunch (on your own)

Workshops (choose 1)

1:00 - 1:45	D1: Metastatic Disease to the Thorax <i>Gordon Weisbrod, MD</i>	Americana 3
1:00 - 1:45	D2: Use of MDCT 3D Reconstructions of Cardiovascular Structures: Clinical & Classroom <i>Anna Rozenshtein, MD and Lawrence Boxt, MD</i>	Americana 4
1:45 - 2:30	E1: Thoracic ICU Radiology <i>Joel Fishman, MD, PhD</i>	Americana 3
2:30 - 3:15	F1: Pulmonary Hypertension: Less Common Causes and New Therapies <i>Marc Gosselin, MD and Jeffrey Edelman, MD</i>	Americana 3
3:15 – 3:30 pm	Coffee Break	Americana Foyer
3:30 – 5:30 pm	Scientific Session II (non-CME Session) Moderators: Smita Patel, MBBS and Eric Stern, MD	Americana 3

March 6, 2003

General Session

Thursday

7:00 - 8:00 am Continental Breakfast Americana Foyer

8:00 - 11:00 am Guest Hospitality Suite Moon Room

Thoracic Infection

Moderator: Robert Tarver, MD

Americana 3

7:50 - 8:10 Pulmonary Tuberculosis
Steven Primack, MD

8:10 - 8:30 Non-tuberculous Mycobacterial Infection
David Schwartz, MD

8:30 - 8:50 HIV: Primary and Secondary Lung Infection
Linda Haramati, MD

8:50 - 9:10 Viral Infection on HRCT
Tomas Franquet, MD

9:10 - 9:30 Imaging of Coccidiomycosis
William Berger, MD

9:30 - 9:50 Session Discussion

9:50 - 10:10 am Coffee Break Americana Foyer

The Airway

Moderator: Georgeann McGuinness, MD

Americana 3

10:10 - 10:30 Tracheobronchial Malignancy
Jo-Anne Shepard, MD

10:30 - 10:50 Inflammatory Disease of the Central Airways
Arfa Khan, MD

11:10 - 11:30 Virtual Bronchoscopy
R.C. Gilkeson, Jr., MD

11:30 - 11:50 Session Discussion

11:50 - 12:15 Scientific Presentation and Case of the Day Awards

12:15 pm Meeting Adjourns

Sunday

March 2, 2003

General Session

Sunday

7:00 - 8:00 am	Continental Breakfast	Americana 4
8:00 - 11:00 am	Guest Hospitality Suite	Neptune Room
7:20 - 7:30 am	Welcome and Introduction <i>Ella Kazerooni, MD</i>	Americana 3

Technology Update Americana 3
Moderator: Suzanne Aquino, MD

7:50 - 8:10	Chest Radiography: FS, CR, DR <i>Carl Ravin, MD</i>	
8:10 - 8:30	Multidetector CT: More Slices and Beyond <i>Patricia Mergo, MD</i>	
8:50 - 9:10	Functional Imaging <i>Hiroto Hatabu, MD, PhD</i>	
9:10 - 9:30	Radiofrequency Ablation in Thoracic Intervention <i>Peter Kavanagh, MD</i>	
9:30 - 9:50	Session Discussion	
9:50 - 10:10 am	Coffee Break	Americana 4

Interstitial Lung Disease Americana 3
Moderator: David Lynch, MD

10:10 - 10:30	The Idiopathic Interstitial Pneumonias <i>Jeffrey Galvin, MD</i>	
10:30 - 10:50	Occupational Lung Disease <i>David Lynch, MD</i>	
10:50 - 11:10	Sarcoidosis <i>John Newell, Jr., MD</i>	
11:10 - 11:30	The Expanded Spectrum of Smoking-Related Lung Disease <i>Rosita Shah, MD</i>	
11:30 - 11:50	Hypersensitivity Pneumonitis <i>Aine Kelly, MD</i>	
11:50 - 12:00	Session Discussion	
12:00 - 1:00 pm	Lunch (on your own)	

Small Airway Disease

Americana 3

Moderator: Melissa Rosado de Christenson, MD

- 1:00 - 1:20 CT of Small Airway Disease With Pathology Correlation
Michael Gotway, MD
- 1:20 - 1:40 Asthma: Role of CT
Denis Carr, MD
- 1:40 - 2:00 "Holes" in the Lung: Radiologic-Pathologic Correlations?
Alexander Bankier, MD
- 2:00 - 2:20 Pulmonary Aspiration: You Are What You Eat
Laura Heyneman, MD
- 2:20 - 2:40 Session Discussion
- 2:40 - 3:00 pm Coffee Break

Americana 4

Pleural Disease

Americana 3

Moderator: Jeffrey Klein, MD

- 3:00 - 3:20 Pleural Effusions
Gerald Abbott, MD
- 3:20 - 3:40 Asbestos Related Pleural Disease & Mesothelioma
Francine Jacobson, MD, MPH
- 3:40 - 4:00 Other Pleural Neoplasms
Sujal Desai, MD
- 4:00 - 4:20 Pleural Intervention
H. Page McAdams, MD
- 4:20 - 4:40 Session Discussion

Unknown Film Panel

Americana 3

Moderator: Phillip Boiselle, MD

- 4:45 - 6:30 pm Gordon Gamsu, MD
Theresa McLoud, MD
Robert Pugatch, MD
Robert Steiner, MD
Robert Tarver, MD
- Ella Kazerooni, MD
Jeffrey Klein, MD
H. Page McAdams, MD
Reginald Munden, DMD, MD
Eric Stern, MD
- 6:30 - 8:00 PM Members' Reception
- St. Moritz Lawn

Chest Radiography: FS, CR, DR

Carl E. Ravin, M.D.

Professor of Radiology

Duke University Medical Center, Durham, North Carolina

OBJECTIVES

- 1) Describe the advantages of computed radiography as compared with film-based radiography.
- 2) Describe the advantages of self-scanning radiography systems as compared to computed radiography and/or film-base systems.
- 3) Describe the advantages of improved DQE in deciding between potential image improvement and potential dose reduction.

INTRODUCTION

Since the initial discovery of the X ray by Roentgen, images have been recorded on film. Over time a number of refinements have been introduced into this basic imaging chain, such as intensifying screens, modifications to film, and fluoroscopic displays, but fundamentally the link between x-ray exposure and image display on film remained. During the past two decades, however, rapid advances in electronics and computer technology created new possibilities for x-ray imaging, including specific receptor systems independent of film which permit image information to be recorded in digital form for improved image transportation, manipulation, display, and storage. These systems include photostimulable phosphor computed radiography systems and a selenium-based digital chest system. Recently, a new generation of direct-readout x-ray detectors based on thin-film transistor (TFT) arrays has emerged, offering unsurpassed image quality from a compact digital detector.

STORAGE PHOSPHOR SYSTEMS

Digital imaging systems using a photostimulable storage phosphor imaging plate were first introduced commercially by Fuji in the mid 1980's. Commonly called Computed Radiography (CR) systems, these devices are now widely used worldwide.

Storage phosphor CR systems employ a reusable imaging plate in place of the traditional screen-film detector. Imaging plates and cassettes are available in standard film sizes, including 14x17 inches, which allows them to be used with conventional radiographic equipment. The imaging plate is coated with a layer of photostimulable phosphor material. When exposed to x-rays, the plate stores some of the incident energy in metastable energy traps within the phosphor layer, forming a latent image on the plate. An automated image readout system scans the plate with a very fine laser beam, and as the laser beam strikes the imaging plate the stored energy is released as visible light, which is captured by the reader's photomultiplier tube and digitized, forming the digital image. The plate is erased by exposure to visible light, an operation performed automatically by the plate reader, and may then be reused.

The introduction of photostimulable phosphors opened the door to commercially feasible direct digital radiography. The linear response of photostimulable phosphors over an extremely wide range of radiation exposures made their application particularly good for bedside radiography. Over the years phosphor plate technology has improved and contrast detail resolution is now significantly better with fourth and fifth generation plates. This has allowed images to be expanded in size and they are now available in 14 by 17 format traditionally used for chest imaging. Ultimately, however, CR image quality is generally only equivalent to that of conventional screen-film radiographs.

SELENIUM-BASED DIGITAL CHEST RADIOGRAPHY (THORAVISION)

In 1993 a new device, based upon a selenium detector, was introduced which produced direct digital images of the chest. Amorphous selenium has long been recognized as an excellent detector of x-rays, and its detective quantum efficiency has been demonstrated to be significantly higher than that of photostimulable phosphors. Like photostimulable storage phosphors, selenium detectors possess a very wide dynamic sensitivity range which makes them well-suited for thoracic imaging; unlike storage phosphor systems, selenium-based detectors do not require stimulation for image readout, which eliminates a source of image noise and improves image quality.

The commercially available selenium-based chest radiography system employs an aluminum drum coated with a thin layer of amorphous selenium as the x-ray detector. Prior to x-ray exposure, the drum is rotated slowly beneath an electrical charging element which deposits a uniform positive charge density on the drum's surface. When the x-ray exposure is initiated, drum rotation is stopped and the x-ray exposure is completed, casting the radiographic image onto the drum. The x-rays discharge the selenium in an amount proportional to the radiation intensity, which results in a latent charge image on the drum face. Immediately after exposure, the drum is rapidly rotated and the charge pattern is read out by microelectrometer probes, forming the digital image.

A number of theoretical, laboratory, and clinical studies of the selenium-based chest imaging system have been reported to date. In a laboratory study, Neitzel et al reported that the detective quantum efficiency of the selenium system exceeds that of both conventional screen-film and photostimulable storage phosphor systems. This suggested that the selenium-based digital images would be of inherently higher quality than previously available from other systems. In a separate study, Chotas et al described a technical evaluation of the selenium system as it is used clinically, reporting excellent image quality, reduced scatter fractions in the lung image regions relative to that found in conventional images, and the potential for reduced patient examination times due to the ease of patient setup and the rapid display of a low-resolution image after exposure (to verify proper patient positioning). Finally, an investigation was reported by Floyd et al which compared radiologists' preference between conventional films and laser-printed films from the selenium system for the visualization of 17 anatomical features in PA and lateral radiographs.

DIRECT-READOUT, THIN-FILM TRANSISTOR (TFT) DETECTORS

A new generation of digital x-ray imaging systems based on flat-panel detectors is now emerging, promising exceptionally good image quality and very rapid, direct access to digital images. Although a variety of approaches, designs, and materials are being used by different manufacturers to devise these new detectors, most are based on large-area, thin-film transistor (TFT) arrays. These multi-layered electronic devices offer compact packaging and direct connection to digital imaging networks, unlike CR systems which have external image readout systems and the selenium drum system which requires a large, free-standing detector unit.

One type of direct-readout system is a large-area, solid-state x-ray detector consisting of a structured Cesium Iodide (CsI) scintillator directly coupled to an array of amorphous silicon thin-film photodiodes and readout electronics. The multi-layered detector is manufactured on a glass substrate, approximately 41 cm square. When exposed to x-rays, the visible light is channeled within the CsI crystal matrix directly to the photodiode array where the electric charge is collected and digitized, forming the digital image. Because of its direct-readout design, structured scintillator, and the use of very-low-noise electronics, this flat-panel detector is anticipated to provide exceptionally high image quality.

Another style of direct-readout digital detectors utilizes the same type of TFT array for charge collection and readout, but the active detector element is amorphous selenium instead of a scintillator and photodiode. Because selenium is an x-ray photoconductor, x-ray photons striking the detector are converted directly to electrical charge with no intermediate (visible light) stage. This direct conversion eliminates one step in image production, and thus removes one opportunity for noise to enter the imaging chain.

Image quality from digital acquisition systems is influenced by detector materials, design, and electronics, and it is unknown at this time which style of direct-readout digital x-ray receptor will offer superior performance. It is clear, however, that large-area, direct-readout digital detectors offer expanded opportunities in the radiology department.

REFERENCES

1. Blume H, Jost RG. Chest imaging within the radiology department by means of photostimulable phosphor computed radiography: a review. [Review]. *J Digit Imaging* 5(2):67-78, 1992.
2. Schaefer CM, Greene R, Oestmann JW, et al. Digital storage phosphor imaging versus conventional film radiography in CT-documented chest disease. *Radiology* 174(1):207-210, 1990.
3. Dobbins JT III, Rice JJ, Beam CA, Ravin CE: Threshold perception performance with computed and screen-film radiography: Implications for chest radiography. *Radiology* 183:179-187, 1992.
4. Kido S, Ikezoe J, Takeuchi N, et al. Interpretation of subtle interstitial lung abnormalities: conventional versus storage phosphor radiography. *Radiology* 187(2):527-533, 1993.
5. Neitzel U, Maack I, Gunther-Kohfahl S. Image quality of a digital chest radiography system based on a selenium detector. *Med Phys* 21:509-516, 1994.
6. Chotas HG, Floyd C Jr., Ravin CE. Technical evaluation of a digital chest radiography system that uses a selenium detector. *Radiology* 195(1):264-270, 1995.
7. Floyd CE, Baker JA, Chotas HG, Delong DM, Ravin CE. Selenium-based digital radiography of the chest: radiologists' preference compared with film-screen radiographs. *AJR* 165(6):1353-1358, 1995.
8. Chotas HG, Dobbins JT, Ravin CE: Principles of digital radiography using large-area, electronically-readable detectors: A review of the basics. *Radiology* 210(3):595-599, March 1999.
9. Floyd CE, Warp RJ, Dobbins JT, Chotas HG, Baydush AH, Vargas-Voracek R, Ravin, CE: Imaging characteristics of an amorphous silicon flat-panel detector for digital chest radiography. *Radiology* 218(3):683-688, March 2001.

Multidetector CT: More Slices and Beyond

Patricia J. Mergo, M.D.

Associate Professor
University of Florida

The development of multidetector CT (MDCT) represents a quantum leap in CT technology. The clinical advances made possible by the advent of MDCT represent one of the largest developments in current technology in radiologic imaging. New 16 slice scanners are in production by several vendors including GE, Siemens, Philips and Toshiba. The biggest clinical advance made possible with MDCT is CT angiography. The capabilities of thoracic imaging are affected significantly with multislice CT with subsequent improved pulmonary arterial CT angiography (CTA), as well as thoracic aortic CTA and more recently coronary artery CTA, using cardiac gating. All these are accountable to the ability to obtain volumetric scanning of the region of interest, with imaging approaching now or equaling isotropic voxels.

When considering multislice CT, important technical considerations need to be taken into account including considerations for pitch, collimation, scan slice profile, noise and radiation dose.

Pitch is an important consideration since with a higher pitch, a given volume of tissue can be scanned in a shorter time period. The advantages for scanning at a higher pitch are well appreciated when fast scanning is needed as in CT angiography. The scanning at a higher pitch does result in widening of the slice width profile, however. The dosage should remain the same, technically speaking, but dosage is in reality potentially increased if adjustments are made in the mA to compensate for limitations in slice width profile. In single slice CT pitch is defined as table movement per rotation / slice collimation. For multislice CT, pitch is defined as table movement per rotation / single slice collimation. This implies that with a 0.5 second scanner, with 2 rotations per second, that if the table travels 16 mm in a second and 1 mm collimation is used, then the pitch would be 8.

With SDCT the true width or the "effective slice thickness" of the reconstructed image is influenced by pitch and the reconstruction algorithm used (wide vs. slim). With a pitch of 2 and a slim algorithm the "effective slice thickness" may increase by 27%. With MDCT these factors are effectively corrected using axial interpolation algorithms.

MDCT yields increased flexibility of scanning relative to slice collimation and slice width. With single detector CT the

slice collimation and the slice width are the same and they cannot be modified once the scans are obtained. In MDCT, the detector collimation is chosen prior to scanning. Once the images are obtained, the images can be reconstructed at varying slice widths, such as 1 mm, 2.5 mm, 5 mm, and 10 mm slice thickness. The thinner section imaging allows higher resolution scanning, albeit with increased noise, for high resolution scanning of pulmonary parenchyma or CTA. The data obtained can be considered true volume data sets for reconstruction at varying slice width. The ability to volumetrically manipulate the data and reconstruct it at various slice widths is dependent on the initial collimation.

Image noise is altered by several factors including mAs, kV, slice thickness, collimation and patient size. These factors are a trade off for thinner section imaging that is often required with CT angiographic studies.

Since with MDCT the acquisition time for CT is significantly shortened, for instance, enabling acquisition of imaging of the thorax for pulmonary embolism detection in time periods as short as 9 seconds, contrast material administration profiles are subsequently altered. New scan protocols are optimized for contrast injections depending on the organ or structure scanned. In general, higher injection rates result in higher level of arterial enhancement suitable for CT angiography. Similarly, protocols with shorter injection times with higher osmolality contrast have been proposed to yield improved imaging. Scan timing can be optimized using bolus triggering or test injection techniques.

The changes in scanning that we have talked about can quickly result in information overload in terms of the amount of data generated from the scans. For this reason, 3D processing of scans becomes crucial in order to adequately display the findings to the clinician. This is especially important in CT angiographic studies, and in the chest can be most helpful for the evaluation of the airways or for the detection of pulmonary embolus.

Ultimately, for many studies, although thin section imaging is obtained, reconstruction at thicker slices for interpretation results in a compromise for ease of interpretation of the axial images, while 3D reconstructions are performed on the thinner section images for improved display of the pertinent findings.

CT-PET Imaging

Suzanne Aquino, M.D.

REFERENCES

- Czernin J, Phelps ME. Positron emission tomography scanning: current and future applications. *Annu Rev Med.* 2002;53:89-112.
- Lowe VJ, Fletcher JW, Gobar L, et al. Prospective investigation of positron emission tomography in lung nodules. *J Clin Oncol* 1998 16:1075-1084.
- Kim BT, Kim Y, Lee KS, et al. Localized form of bronchioloalveolar carcinoma: FDG PET findings. *AJR Am J Roentgenol* 1998 170:935-939.
- Matthies A, Hickeson M, Cuchiara A, Alavi A. Dual time point 18F-FDG PET for the evaluation of pulmonary nodules. *J Nucl Med* 2002 Jul;43:871-875.
- Pieterman RM, van Putten JW, Meuzelaar JJ, et al. Preoperative staging of non-small-cell lung cancer with positron-emission tomography. *N Engl J Med.* 2000;343:254-261.
- Reske SN, Kotzerke J. FDG-PET for clinical use. Results of the 3rd German Interdisciplinary Consensus Conference, "Onko-PET III", 21 July and 19 September 2000. *Eur J Nucl Med.* 2001 Nov;28(11):1707-1723.
- Kaff V, Hicks RJ, MacManus MP, et al. Clinical impact of (18)F fluorodeoxyglucose positron emission tomography in patients with non-small-cell lung cancer: a prospective study. *J Clin Oncol* 2001;19:111-118.
- Rosenman JG, Miller EP, Tracton G, Cullip TJ. Image registration: an essential part of radiation therapy treatment planning. *Int J Radiat Oncol Biol Phys.* 1998;40:197-205.
- Weber DA, Ivanovic M. Correlative image registration. *Semin Nucl Med.* 1994;24:311-323.
- Goerres GW, Kamel E, Seifert B, et al. Accuracy of image coregistration of pulmonary lesions in patients with non-small cell lung cancer using an integrated PET/CT system. *J Nucl Med.* 2002;43:1469-1475.
- Goerres GW, Kamel E, Heidelberg TN, et al. PET-CT image coregistration in the thorax: influence of respiration. *Eur J Nucl Med Mol Imaging.* 2002 29:351-360.
- Antoch G, Freudenberg LS, Stattaus J, et al. Whole-body positron emission tomography-CT: optimized CT using oral and IV contrast materials. *AJR Am J Roentgenol.* 2002 179:1555-1560.
- Antoch G, Freudenberg LS, Egelhof T, et al. Focal tracer uptake: a potential artifact in contrast-enhanced dual-modality PET/CT scans. *J Nucl Med.* 2002; 43:1339-1342.
- Aquino SL, Asmuth JC, Alpert NN, Moore RH, Weise S, Fischman AJ. Improved Image Interpretation with Registered Thoracic CT and PET Datasets. *Am J Roentgenol* 2002;178:939-944.
- Hoh CK, Glaspy J, Rosen P, et al. Whole-body FDG-PET imaging for staging of Hodgkin's disease and lymphoma. *J Nucl Med.* 1997;38:343-348.
- Buchmann I, Moog F, Schirrmeister H, Reske SN. Positron emission tomography for detection and staging of malignant lymphoma. *Recent Results Cancer Res.* 2000;156:78-89.
- Schoder H, Meta J, Yap C, et al. Effect of whole-body (18)F-FDG PET imaging on clinical staging and management of patients with malignant lymphoma. *J Nucl Med.* 2001;42:1139-1143.
- Jerusalem G, Beguin Y, Fassotte MF, et al. Whole-body positron emission tomography using 18F-fluorodeoxyglucose for post-treatment evaluation in Hodgkin's disease and non-Hodgkin's lymphoma has higher diagnostic and prognostic value than classical computed tomography scan imaging. *Blood.* 1999;94:429-433.
- Rostrom AY, Powe J, Kandil A et al. Positron emission tomography in breast cancer: a clinicopathological correlation of results. *Br J Radiol.* 1999;72:1064-1068.
- Adler LP, Faulhaber PF, Schnur KC et al. Axillary lymph node metastases: screening with [F-18]2-deoxy-2-fluoro-D-glucose (FDG) PET. *Radiology.* 1997;203:323-327.

Pulmonary Functional Imaging

Hiroto Hatabu, M.D., Ph.D.

Director, Pulmonary Functional Imaging and Resident Education, Department of Radiology, Beth Israel Deaconess Medical Center, Associate Professor of Radiology, Harvard Medical School

Recent development of fast MR imaging techniques opened a new window for functional assessment of the lung.[1,2] The newer generation MR scanner with its higher-strength gradient system and echo-planner capability can control the gradient very accurately and rapidly. The fast MR techniques, which are facilitated by the emergence of these new MR systems with enhanced gradient, are essential for the MR imaging of the lung. The difficulties in MR imaging of the lung have been posed by lung morphology and its physiological motion.

Fast MR imaging techniques with a very short TE are overcoming the problem of inhomogeneous magnetic susceptibility.[3-5] In addition, the single-shot fast SE sequence can now depict the lung parenchyma, providing a platform for MR imaging of the lung.[6,7]

Pulmonary perfusion can be assessed by the use of T1 weighted ultra-short TE sequence and contrast agents. [8] In an animal model, a perfusion defect due to a pulmonary embolus was clearly shown and confirmed by cine angiography. Based upon these investigations, we conclude that MRI of lung perfusion is feasible. Recent preliminary reports showed the feasibility of the MR perfusion technique in the evaluation of patients with pulmonary embolism [9] and unilateral lung transplantation.[10] This dynamic MR technique may also be used for the characterization of a single pulmonary nodule.[11] Another important application of the technique is the evaluation of pulmonary emphysema before lung volume reduction surgery. [12-14] Moreover, by fitting a portion of the time-intensity curve to a gamma variate function, flow parameters such as peak time, apparent mean transient time, and blood volume can be calculated[15]. The natural extension of this 2D technique is breath-hold contrast-enhanced 3D MR technique with short TR and TE.[16] With the implementation of a short TE of 2 ms, both pulmonary perfusion as well as the pulmonary vasculature were depicted in a 25-second breath-hold. Perfusion defects with accompanying obliteration of the regional pulmonary vasculature were demonstrated in both a porcine model and in patients with pulmonary embolism. Another approach for the evaluation of pulmonary perfusion we have devised is the modification of EPI-STAR sequence.[17] A modified fast gradient echo or single shot turbo spin-echo pulse sequence instead of echo planar imaging is utilized for image acquisition, which is robust for magnetic susceptibility artifacts. Within each breath-holding period, two sets of images are acquired. In only one set of the images, an RF pulse is applied to the right ventricle and main pulmonary artery in order to invert the magnetization of blood within those structures. After an inflow period (TI), which is on the order of a few hundred milliseconds to seconds, data are acquired using fast gradient echo or single-shot, half-Fourier, turbo spin-echo (HASTE) pulse sequences. The subtraction of the two images results in the perfusion image. [18-20] The merit of this technique lies in its potential to provide a non-invasive method for the absolute measurement of pulmonary perfusion by the application of a mathematical model. [20]

The assessment of regional ventilation in human lungs is important for the diagnosis and evaluation of a variety of pulmonary disorders including pulmonary emphysema, diffuse lung disease (i.e., sarcoidosis, pulmonary fibrosis), lung cancer, and pulmonary embolism. Oxygen modulates MR signals of blood and fluid through two different mechanisms; (1) a paramagnetic

property of deoxyhemoglobin and (2) a paramagnetic property of molecular oxygen itself.[21,22] Molecular oxygen is weakly paramagnetic with a magnetic moment of 2.8 Bohr magnetons.[23,24] Young et al demonstrated reduction in T1 relaxation time of blood at 0.15 Tesla after inhalation of oxygen.[22,24] After inhalation of 100% oxygen, the concentration of dissolved oxygen in arterial blood increases by approximately five times.

Recently, we have demonstrated the feasibility of oxygen inhalation to evaluate regional pulmonary ventilation and examined the effect of oxygen inhalation on relaxation times in various tissues.[25,26] Signal changes from the right upper quarter portion of the right lung following alternate administration of 10L/min air (21% oxygen) and 100% oxygen via a mask are demonstrated. Calculated T1 values of the lung with various TIs before and after administration of oxygen were 1336 ± 46 ms and 1162 ± 33 ms, respectively. The observed change in T1 value confirms that molecular oxygen can be used as an effective T1 shortening agent in the assessment of ventilation in humans. Single-shot fast SE sequence was used to obtain MR signal from lung parenchyma, which has very short T2* value. The sequence is T1-weighted by the inversion recovery preparation pulse.

Laser-polarized Xe-129 and He-3 were proposed for ventilation MR imaging.[27-30] These noble gases can be hyperpolarized using optical pumping technique. MR signal from these noble gases may be increased by 100,000 times compared with the MR signal in a thermal equilibrium state. The strong signal from the noble gases enable the acquisition of the data from gas itself. A preliminary clinical study by Kauczor et al demonstrated feasibility in assessing various pulmonary diseases including chronic obstructive lung disease, bronchiectasis, and lung cancer.[31,32] Diffusion of these noble gases impeded by alveolar structure can be measured. In addition, Xe-129 can be dissolved in blood, which may enable perfusion imaging as well as functional brain imaging.[33] Recent spectroscopic technique with Xe-129 demonstrated the possibility of separating the signal from lung parenchyma and blood.[34] Xe-129 may be injected intravenously for delivery to the lung and vasculature.[35] The hyperpolarized noble gas techniques provide new exciting applications.[36]

The oxygen-enhanced MR ventilation technique utilizes conventional proton-based MR imaging. Oxygen is available in most MR units for patients and its administration is safe and inexpensive. Thus the oxygen-enhanced MRI technique for assessing pulmonary ventilation has the potential to provide a noninvasive means of assessing regional pulmonary ventilation at high resolution. Combined with the MRI perfusion studies, this technique has the potential to have a major impact on the diagnosis and assessment of a variety of pulmonary disorders.[37]

MR assessment of pulmonary ventilation-perfusion is possible when combined with recent first-pass contrast-enhanced MR perfusion technique using Gd-DTPA.[8,16,37,38] The combination of ventilation-perfusion techniques is particularly interesting when airway obstruction and pulmonary embolism, two classic disease models of the lung with contrasting radiographic manifestations are studied. Airway obstruction causes regional hypoxemia, which elicits hypoxic vasoconstriction, resulting in

an accompanying decreased regional perfusion. Therefore, matched regional ventilation-perfusion deficit is expected when a combined ventilation-perfusion imaging study is performed. In contrast, pulmonary embolism does not cause airway obstruction. Therefore, regional perfusion deficit without ventilation deficit (mismatched ventilation-perfusion) is expected on the combined ventilation-perfusion imaging study. [37]

MR ventilation-perfusion techniques have the potential to play an important part in 21st century pulmonary function testing. With the availability of high-resolution CT, why do we pursue the development of lung parenchymal imaging by MR? CT diagnosis is based on morphological findings as well as limited density information (calcium, fat, contrast enhancement). MR, on the other hand, has the potential for multi-parametric characterization of pathology based upon relaxation times, perfusion, ventilation, proton density (lung water determination), diffusion, susceptibility-induced T2* changes as reflections of alveolar architecture. Fast MR imaging is opening a new exciting window to multi-functional MR imaging of the lung. [1]

Quantification of pulmonary perfusion can be achieved by first-pass contrast agent technique or arterial spin labeling technique. The first-pass contrast agent method is easily applied and provides pixel-by-pixel mapping of perfusion parameters. However, there are issues to be solved theoretically including deconvolution, leakage of contrast agent, and the definition of output function. Arterial spin labeling technique is non-invasive and can be repeated. However, implementation and application are rather difficult.

Imaging of ventilation can be performed using hyperpolarized noble gas technique or oxygen-enhanced MR imaging. Both methods are relatively new and novel. Hyperpolarized noble gas technique demonstrates the flow of gas itself, while oxygen-enhanced MR imaging shows transfer of molecular oxygen indirectly through enhancement of protons in lungs by the paramagnetic effect of molecular oxygen. The real premises of these methods are dynamic imaging of ventilation and physics-based approaches for analyses of dynamic imaging data.

The registration of quantified ventilation/perfusion images is crucial. However, the fact that ventilation requires motion of lung indeed proposes a fundamental challenge for registration of ventilation/perfusion images. At the same time, a physics-based approach of registration of lung imaging provides a unique mathematical description of lung mechanics. [39-41]

Ventilation, perfusion, and biomechanics are three major components of lung function. MR imaging provides a powerful tool for 21st century functional imaging of the lung.

REFERENCES

- Hatabu H, Chen Q, Stock KW, Gefter WB, Itoh H. Fast MR imaging of the lung. *Eur J Radiol* 1999; 29:114-132.
- Hatabu H, Gefter WB, Kressel HY, Axel L, Lenkinski RE. Pulmonary vasculature: high-resolution MR imaging. *Radiology* 1989; 171: 391-395
- Hatabu H, Alsop DC, Listerud J, Bonnet M, Gefter WB. T2* and proton density measurement of normal human lung parenchyma using submillisecond TE gradient echo MR imaging. *Eur J Radiol* 1999; 29:245-252.
- Hatabu H, Alsop D, Bonnet M, Listerud J, Pietra G, Gefter W. Approaches to MR imaging of lung parenchyma utilizing ultrashort TE gradient echo and fast SE sequences. Proceedings, Society of Magnetic Resonance, Second Meeting. San Francisco, August 6-12, 1994:1474.
- Alsop DC, Hatabu H, Bonnet M, Listerud J, Gefter W. Multi-slice, breathhold imaging of the lung with submillisecond echo times. *Magn Reson Med* 1995; 33:678-692.
- Hatabu H, Gaa J, Tadamura E, Li W, Garpestad E, Edelman RR. Lung parenchyma: MRI with a half-Fourier single-shot turbo SE (HASTE) sequence. Proceedings, Society of Magnetic Resonance, Fourth Meeting. New York, 1996:769.
- Hatabu H, Gaa J, Tadamura E, Stock KW, Garpestad E, Edelman RR. MR imaging of pulmonary parenchyma with a Half-Fourier Single-Shot TurboSE (HASTE) Sequence. *Eur J Radiol* 1999; 29:152-159.
- Hatabu H, Gaa J, Kim D, Li W, Prasad PV, Edelman RR. Pulmonary perfusion: qualitative assessment with dynamic contrast-enhanced MRI using ultra-short TE and inversion recovery turbo FLASH. *Magn. Reson. Med* 1996; 36: 503-508.
- Amundsen T, Kvaerness J, Jones RA, Waage A, Bjermer L, Nilsen G, Haraldseth O. Pulmonary embolism: detection with MR perfusion imaging of lung--a feasibility study. *Radiology* 1997; 203:181-185
- Berthezene Y, Croisille P, Bertocchi M, Houzard C, Bendib K, Revel D. Lung perfusion demonstrated by contrast-enhanced dynamic magnetic resonance imaging. Application to unilateral lung transplantation. *Invest Radiol* 1997; 32:351-356
- Guckel C, Schnabel K, Deimling M, Steinbrich W. Solitary pulmonary nodules: MR evaluation of enhancement patterns with contrast-enhanced dynamic snapshot gradient-echo imaging. *Radiology* 1996; 200:681-686
- Slone RM, Pilgram TK, Gierada DS, et al. Lung volume reduction surgery: comparison of preoperative radiologic features and clinical outcome. *Radiology* 1997; 204:685-693.
- Gierada DS, Slone RM, Bae KT, et al. Pulmonary emphysema: comparison of preoperative quantitative CT and physiologic index values with clinical outcome after lung-volume reduction surgery. *Radiology* 1997;205: 235-242.
- Wang SC, Fischer KC, Slone RM, et al. Perfusion scintigraphy in the evaluation for lung volume reduction surgery: correlation with clinical outcome. *Radiology* 1997; 205:243-248.
- Hatabu H, Tadamura E, Levin DL, Chen Q, Li W, Kim D, Prasad PV, Edelman RR. Quantitative assessment of pulmonary perfusion with dynamic contrast-enhanced MRI. *Magn Reson Med* 1999; 42:1033-1038.
- Hatabu H, Gaa J, Kim D, Li W, Prasad PV, Edelman RR. Pulmonary perfusion and angiography: evaluation with breathhold enhanced three-dimensional fast imaging steady-state precession MR imaging with short TR and TE. *AJR* 1996; 167: 653-655.
- Edelman RR, Siewert B, Adamis M, Gaa J, Laub G, and Wielopolski P. Signal targeting with alternating radiofrequency (STAR) sequences: application to MR angiography. *Magn Reson Med* 1994; 31: 233-238.
- Hatabu H, Wielopolski PA, Edelman RR. Pulmonary perfusion MR imaging with ultrashort TR/TE GRE sequence and signal targeting with alternating RF. *Radiology* 1995; 197(P):231.
- Hatabu H, Wielopolski P, Tadamura E. An attempt of pulmonary perfusion imaging utilizing ultrashort TE turbo FLASH sequence with signal targeting and alternating radio-frequency. *Eur J Radiol* 1999; 29:160-163.
- Hatabu H, Tadamura E, Prasad PV, Buxton R, Edelman RR. Noninvasive pulmonary perfusion imaging by STAR-HASTE sequence. *Magn Reson Med* 2000; 44:808-812.
- Pauling L, Coryell C. The magnetic properties and structure of the hemochromogens and related substances. *Proc Natl Acad Sci USA* 1936; 22:159-163
- Young IR, Clarke GJ, Bailes DR, Pennock JM, Doyle FH, Bydder GM. Enhancement of relaxation rate with paramagnetic contrast agents in NMR imaging. *J Comput Tomogr* 1981; 5:543-546.

23. Gore JC, Doyle FH, Pennock JM. Relaxation rate enhancement observed in vivo by NMR imaging. In: Partain CL, James AE, Rollo FD, Price RR, eds. Nuclear magnetic resonance (NMR) imaging. Philadelphia: WB Saunders, 1983; 94-106.
24. Tripathi A, Bydder GM, Hughes JMB, et al. Effect of oxygen tension on NMR spin-lattice relaxation rate of blood in vivo. *Invest Radiol* 1984; 19:174-178.
25. Edelman RR, Hatabu H, Tadamura E, Li W, Prasad PV. Noninvasive assessment of regional ventilation in the human lung using oxygen-enhanced magnetic resonance imaging. *Nature Med* 1996; 2:1236-1239
26. Tadamura E, Hatabu H, Li W, Prasad PV, Edelman RR. Effect of oxygen inhalation on relaxation times in various tissues. *JMRI* 1997; 7:220-225.
27. Albert MS, Cates GD, Driehuys B et al. Biological magnetic resonance imaging using laser-polarized ^{129}Xe . *Nature* 1994; 370:199-201.
28. Middleton H, Black RD, Saam B et al. MR imaging with hyperpolarized ^3He gas. *Magn Reson Med* 1995; 33:271-275.
29. MacFall JR, Charles HC, Black H, et al. Human lung air spaces: potential for MR imaging with hyperpolarized He-3. *Radiology* 1996; 200:553-558.
30. Ebert M, Grossmann T, Heil W, Otten WE, Surkau R, Leduc M, Bachert P, Knopp MV, Schad LR, Thelen M Nuclear magnetic resonance imaging with hyperpolarised helium-3. *Lancet* 1996; 347:1297-1299
31. Kauczor HU, Hofmann D, Kreitner KF, Nilgens H, Surkau R, Heil W, Potthast A, Knopp MV, Otten EW, Thelen M Normal and abnormal pulmonary ventilation: visualization at hyperpolarized He-3 MR imaging. *Radiology* 1996 Nov;201(2):564-8
32. Kauczor HU, Ebert M, Kreitner KF, Nilgens H, Surkau R, Heil W, Hofmann D, Otten EW, Thelen M Imaging of the lungs using ^3He MRI: preliminary clinical experience in 18 patients with and without lung disease. *J Magn Reson Imaging* 1997; 7:538-543
33. Mugler JP 3rd, Driehuys B, Brookeman JR, Cates GD, Berr SS, Bryant RG, Daniel TM, de Lange EE, Downs JH 3rd, Erickson CJ, Happer W, Hinton DP, Kassel NF, Maier T, Phillips CD, Saam BT, Sauer KL, Wagshul ME. MR imaging and spectroscopy using hyperpolarized ^{129}Xe gas: preliminary human results. *Magn Reson Med* 1997; 37:809-815
34. Wagshul ME, Button TM, Li HF, Liang Z, Springer CS, Zhong K, Wishnia A In vivo MR imaging and spectroscopy using hyperpolarized ^{129}Xe . *Magn Reson Med* 1996; 36:183-191
35. Goodson BM, Song Y, Taylor RE, Schepkin VD, Brennan KM, Chingas GC, Budinger TF, Navon G, Pines A In vivo NMR and MRI using injection delivery of laser-polarized xenon. *Proc Natl Acad Sci U S A* 1997; 23;94:14725-14729
36. Albert MS, Balamore D. Development of hyperpolarized noble gas MRI. *Nucl Instr Meth in Phys Res* 1998; A402:441-453.
37. Hatabu H, Chen Q, Levin DL, Tadamura E, Edelman RR. Ventilation-Perfusion MR imaging of the lung. *MRI Clin North Amer* 1999; 7:379-392.
38. Hatabu H. MR Pulmonary angiography and perfusion imaging: recent advances. *Sem US CT MRI* 1997; 18:349-361.
39. Napadow VJ, Mai V, Bankier A, Gilbert RJ, Edelman R, Chen Q. Determination of regional pulmonary parenchymal strain during normal respiration using spin inversion tagged magnetization MRI. *J Magn Reson Imaging*. 2001 Mar;13(3):467-74.
40. Chen Q, Mai VM, Bankier AA, Napadow VJ, Gilbert RJ, Edelman RR. Ultrafast MR grid-tagging sequence for assessment of local mechanical properties of the lungs. *Magn Reson Med*. 2001 Jan;45(1):24-8.
41. Hatabu H, Ohno Y, Uematsu H, Oshio K, Geftter WB, Gee JC. Lung Biomechanics via non-rigid registration of serial MR images. *Radiology* 2001; 221(P); 630.

Radiofrequency Ablation in Thoracic Intervention

Peter V. Kavanagh, M.D.

Introduction:

Percutaneous radiofrequency ablation (RFA) is a thermal ablative technique used to produce local tissue destruction. Methods of tumor ablation most commonly used in current practice are divided into three broad categories: (1) thermal ablation, which utilizes heat (such as RFA and laser therapy), or cold (e.g. cryotherapy), (2) chemical ablation, where agents such as ethanol and acetic acid are used, and (3) mechanical methods using ultrasound energy, such as high-intensity focused ultrasound (HIFU). RFA is currently the most frequently employed tissue ablation technique in the thorax and is the most effective ablative method for treating intra-thoracic malignancies.

Mechanism of action:

RFA delivers high amounts of thermal energy to produce coagulation necrosis of targeted tissue. Thin, insulated metallic electrode probes, similar to percutaneous biopsy needles, are percutaneously inserted into the lesion under image guidance. The probe is connected to a generator, producing RF waves from the tip of probe, resulting in tissue heating by means of ionic agitation. The resultant coagulative tissue necrosis is induced in a controlled and reproducible manner.

RFA is an evolving technique for the treatment of cancers throughout the body, including lung, liver, kidney, adrenal gland and bone. In addition to treating malignant neoplastic processes, percutaneous RFA is also used to treat osteoid osteomas. Endovascular transcatheter RFA methods are employed in the management of varicose veins, and to treat arrhythmogenic foci that give rise to supraventricular tachycardias.

The technique is dependent on the maintenance of high local temperatures in order to produce its effect. As air is an insulator, normal lung parenchyma acts as a barrier to heat dissipation so this is an advantage when treating patients with malignant lung nodules and masses. The presence of flowing blood adjacent to lesions impairs the technique as it acts as a 'heat sink' preventing the generation of very high local temperatures. Hence, lesions close to the heart and adjacent to major pulmonary vascular structures are less amenable to this form of therapy.

Indications:

- I. Primary lung cancer
 - A. In early stage primary bronchogenic cancer (Stage 1A/1B) RFA is a potentially curative technique. Surgery is the conventional treatment in this group of patients, however, in non-operative candidates RFA is a valuable alternative. Lesions up to 3 cm in diameter can reliably be treated by RFA.
 - B. For more advanced stages of bronchogenic cancer (Stage 2 or greater) the objective in treating patients with RFA is to achieve palliation. For example, painful masses that involve the chest wall can be effectively treated and excellent results for pain relief can be obtained.
- II. Metastatic disease:

RFA is primarily used as a palliative procedure in treating pulmonary metastases secondary to primary renal cell carcinoma, colorectal tumors, breast cancer, and carcinoid tumors. While palliative in these cases, the quality and quantity of the palliation can be superior to other treatments.

Technique:

- A. Image guidance modalities: Computed tomography (CT) is used for the majority of procedures. Fluoroscopic guidance, preferably with C-arm or biplanar capability, is also feasible. CT fluoroscopy, if available, can be an advantage, especially for smaller lesions.
- B. Anesthesia
 - General anesthesia is preferred by some operators. The placement of a double lumen endotracheal tube is a valuable adjunct since it allows isolation of the treated lung should bleeding develop. In this instance, ventilation can be maintained via the contralateral lung.
 - A combination of local anesthesia and conscious sedation is used by many operators.
 - MAC is a valuable alternative in select patients.
- C. Contraindications:
 - Coagulopathy, or patients on anti-coagulation therapy with INR > 1.5. Aspirin should be withheld for 5-7 days prior to the procedure.
 - Contralateral pneumonectomy.
 - Severe bullous emphysema.
 - Severely diminished pulmonary reserve such that a pneumothorax could not be tolerated.
- D. Patient preparation:

In creating an RF circuit, grounding pads are placed away from the operating area, usually on the thighs or lower back. Care must be taken to ensure that these are applied correctly as failure to do so can result in burns. Some operators advocate the use of preprocedural prophylactic antibiotics but there is no universal consensus on the need for this. Informed consent is obtained. Ensure that the platelet count is above 75,000.
- E. Equipment:

For tumors < 3 cm, a single needle electrode is used. Tumors > 3 cm are treated with a cluster of 3 electrodes, or a single electrode with tongs at its distal aspect which expand in an 'umbrella' type configuration. RF applicators come in a variety of needle lengths – a suitable length is selected on the basis of the depth of the lesion from the percutaneous entry site. There is also a choice in the length of the active tip on some single electrode and triple electrode systems – an appropriate choice is made based on lesion size.
- F. Procedural Aspects:

The general principles and approaches used in percutaneous transthoracic needle biopsy of lung lesions are followed. Usually the patient is positioned so that the least distance of lung tissue is traversed en route to the lesion. Traversing fissures is avoided, where possible.

The electrode is placed close to the deepest part of the tumor for the first treatment. Subsequent treatments will then be applied at the more superficial aspects of the lesion. At least one RF treatment is performed with the maximum allowable current for 12 minutes. Intratumoral temperatures > 55° are needed to achieve tissue necrosis. The electrode is

repositioned until all the tumor area has been treated. The extent of the heat induced tissue damage is about 3 cm; therefore, the electrode must be repositioned more than once for any lesion larger than 1.5 cm so that a satisfactory margin is achieved.

The needle electrode is advanced into the lesion using either a single needle puncture method or via a coaxial system. There are 3 major vendors who produce RFA equipment and each has a slightly different needle electrode configuration. Irrespective of the equipment vendor, once the needle electrode is confirmed to be satisfactorily positioned by imaging, the generator is turned on and energy is applied. One vendor allows periprocedural monitoring by indicating the temperature at the needle tip. Other vendors permit periprocedural monitoring by measuring the delivery of energy into tissue as watts. The body core temperature of the patient is monitored during the procedure. During prolonged procedures rises in core body temperature may cause sweating which can result in grounding pad detachment, therefore the pads should be regularly checked to avoid burns.

- G. Follow-up imaging recommendations: Chest radiographs are obtained, at 1 and 2 hours following the procedure, and again on the morning of the day after the procedure. The majority of patients leave hospital the day following the procedure. Further follow-up imaging can be obtained with CT and/or PET imaging. A baseline study can be obtained at 1 month. Then further follow-up imaging at 3 monthly intervals initially, gradually lengthening the interval to annual surveillance examinations.

Results:

Overall, RFA for the treatment of primary and secondary malignancies in the chest is a safe technique. Complication rates are less than with conventional surgery. Reported adverse effects include

- Pleural effusions occur in up to 30% of patients. About half of these will require catheter drainage or needle thoracocentesis.
- COPD exacerbation; IPF exacerbation has also been reported.
- Bronchopleural fistula.
- Pulmonary embolism.
- Mental status changes (reversible) have been reported, possibly due to an embolic phenomenon.
- Hemorrhage – rates are similar to percutaneous needle biopsy of lung nodules. While perilesional hemorrhage is commonly identified on post-procedural CTs, the rate of symptomatic bleeding is considerably less, and severe hemoptysis is rare.
- Pneumothorax – while small pneumothoraces are common, those requiring treatment is similar to the rate is no higher than that seen with percutaneous needle biopsy of lung nodules.
- Pain – some patients experience pain, possibly due to a tumor destruction syndrome. It is managed similar to post-embolization syndrome with liberal use of analgesic agents.
- Subcutaneous emphysema.

Early results indicate that RFA is highly effective in treating bronchogenic carcinoma. 1-year survival rates greater than 70% have been reported. 3-year survival rates exceed 50% in some series. This compares very favorably with other conventional treatment modalities. As RFA is a relatively new technique, long term outcome data is not yet available. Failures of local treatment occur more commonly with mediastinal and perihilar lesions where the 'heat sink' effect may operate. Success rates

are higher with more peripheral lesions. RFA is a safe and effective management tool for controlling patients with more advanced primary bronchogenic cancer. It is also an effective palliative technique in treating pulmonary metastatic disease.

Future directions:

RFA technology is rapidly improving and newer, more powerful delivery systems will allow the treatment of larger lesions. RFA may be synergistic with other treatments and combination therapies may prove superior to any single method.

REFERENCES

1. Parkin DM, Pisani P, Ferlay J. Global cancer statistics. *CA Cancer J Clin* 1999 Jan-Feb;49(1):33-64.
2. National Cancer Institute. SEER cancer statistics review 1973-1999. Bethesda (MD): National Cancer Institute; 1999. Table XV-1 through 18: lung and bronchus cancer (invasive). p. 1-24.
3. Jemal A, Thomas A, Murray T, Thun M. Cancer statistics, 2002. *CA Cancer J Clin* 2002 Jan-Feb;52(1):23-47.
4. National Cancer Institute. What you need to know about lung cancer. [internet]. Bethesda (MD): National Cancer Institute; 2002 Sep 16 [cited 2002 Dec 16]. [16 p]. Available: <http://www.cancer.gov>.
5. Ginsberg RJ, Vokes EE, Rosenzweig K. Non-small cell lung cancer. In: DeVita VT, Hellman S, Rosenberg SA, editors. *Cancer: principles and practice of oncology*. 6 ed. Philadelphia (PA): Lippincott Williams & Wilkins; 2001. p. 925-83.
6. Hoffman PC, Mauer AM, Vokes EE. Lung cancer. *Lancet* 2000 Feb 5;355(9202):479-85.
7. National Cancer Institute. Non-small cell lung cancer (PDQ): treatment. [internet]. Bethesda (MD): National Cancer Institute; 2002 Sep [cited 2002 Dec 09]. [22 p]. Available: <http://www.nci.nih.gov/cancerinfo/pdq/treatment/non-small-cell-lung/healthprofessional/>.
8. Miettinen OS. Screening for lung cancer. *Radiol Clin North Am* 2000 May;38(3):479-86.
9. National Cancer Institute. Small cell lung cancer (PDQ): treatment. Health professional version. [internet]. Bethesda (MD): National Cancer Institute; 2002 Jun [cited 2002 Dec 16]. [17 p]. Available: <http://www.cancer.gov>.
10. Dupuy DE, Mayo-Smith WW, Abbott GF, DiPetrillo T. Clinical applications of radio-frequency tumor ablation in the thorax. *Radiographics* 2002 Oct;22 Spec No:S259-69.
11. Wood BJ, Ramkaransingh JR, Fojo T, Walther MM, Libutti SK. Percutaneous tumor ablation with radiofrequency. *Cancer* 2002 Jan 15;94(2):443-51.
12. Mirza AN, Fornage BD, Sneige N, Kuerer HM, Newman LA, Ames FC, Singletary SE. Radiofrequency ablation of solid tumors. *Cancer J* 2001 Mar-Apr;7(2):95-102.
13. Goldberg SN, Gazelle GS, Mueller PR. Thermal ablation therapy for focal malignancy: a unified approach to underlying principles, techniques, and diagnostic imaging guidance. *AJR Am J Roentgenol* 2000 Feb;174(2):323-30.
14. Gazelle GS, Goldberg SN, Solbiati L, Livraghi T. Tumor ablation with radio-frequency energy. *Radiology* 2000;217:633-46.
15. Dupuy DE, Zagoria RJ, Akerley W, Mayo-Smith WW, Kavanagh PV, Safran H. Percutaneous radiofrequency ablation of malignancies in the lung. *AJR Am J Roentgenol* 2000 Jan;174(1):57-9.
16. New procedure destroys lung cancer in China study. [internet]. Jackson (MI): University of Mississippi Medical Center; 2000 Mar 10 [cited 2002 Dec 09]. [2 p]. Available: <http://www.sciencedaily.com/releases/2000/03/000310080143.htm>.

17. Sewell PE, Vance RB. Radiofrequency ablation of lung tumors: assessment of radiofrequency ablation. [internet]. Jackson (MI): The University of Mississippi Medical Center; [cited 2002 Dec 09]. [4 p]. Available: <http://vir.umc.edu/rflung.html>.
18. Nishida T, Inoue K, Kawata Y, Izumi N, Nishiyama N, Kinoshita H, Matsuoka T, Toyoshima M. Percutaneous radiofrequency ablation of lung neoplasms: a minimally invasive strategy for inoperable patients. *J Am Coll Surg* 2002;195(3):426-430.
19. Zagoria RJ, Chen MY, Kavanagh PV, Torti FM. Radio frequency ablation of lung metastases from renal cell carcinoma. *J Urol* 2001 Nov;166(5):1827-8.
20. National Institute for Occupational Safety and Health (NIOSH). Radiofrequency (RF) sealers and heaters: potential health hazards and their prevention. Cincinnati (OH): National Institute for Occupational Safety and Health (NIOSH); 1979 Dec 4. 15 p. (Joint NIOSH/OSHA current intelligence bulletin; no. 33).
21. Dupuy DE, Goldberg SN. Image-guided radiofrequency tumor ablation: challenges and opportunities--part II. *J Vasc Interv Radiol* 2001 Oct;12(10):1135-48.
22. Dupuy DE, Mayo-Smith WW, DiPetrillo T, Ridlen MS, Murphy BL, Cronan JJ. Clinical experience of pulmonary radiofrequency ablation in 27 patients. *Radiol* 2001, 221(P):314.
23. Sewell Jr PE, Jackson MS, Vance RB, Wang YD. Assessing radiofrequency ablation of non-small cell lung cancer with positron emission tomography (PET). *Radiol* 2000, 217(P):334.
24. Sewell Jr PE, Jackson MS. Percutaneous radiofrequency ablation of primary and secondary pulmonary malignancies using CT guidance. *Radiol* 2002, 225(P):291.
25. Goldberg, SN, Gazelle GS, Compton CC, Mueller PR, McLoud TC. Radio-frequency tissue ablation of VX2 tumor nodules in the rabbit lung. *Acad Radiol* 1996; 3:929-935.
26. Goldberg SN, Gazelle GS, Compton CC, McLoud TC. Radiofrequency tissue ablation in the rabbit lung: efficacy and complications. *Acad Radiol* 1995; 2:776-784.

The Idiopathic Interstitial Pneumonias

Jeffrey R. Galvin, M.D.

Chief, Pulmonary and Mediastinal Radiology

Armed Forces Institute of Pathology and Clinical Professor Department of Radiology

University of Maryland

Learning Objectives

1. Review the current classification of the idiopathic interstitial pneumonias
2. Enumerate the characteristic radiologic patterns and underlying pathology
3. Discuss the postulated pathogenesis for these diseases

Introduction

The idiopathic interstitial pneumonias (IIPs) are a group of nonneoplastic disorders that were originally described by Dr. Averill A. Leibow in the mid 70's. The patients usually present with prolonged symptoms (months) of dyspnea and the lung biopsy usually demonstrates varying patterns of interstitial fibrosis and inflammation. The IIPs are currently separated into the following diagnostic categories:

Idiopathic Pulmonary Fibrosis (Usual Interstitial Pneumonitis)
Respiratory Bronchiolitis-Associated Interstitial Lung Disease
Desquamative Interstitial Pneumonitis
Acute Interstitial Pneumonitis (Hammon Rich)
Cryptogenic Organizing Pneumonia
Nonspecific Interstitial Pneumonia

The plain radiograph usually demonstrates areas of abnormally increased density and the lungs tend to be small. However, the process of describing a chest film with "chronic diffuse lung disease" is often frustrating. These diseases display a limited range of findings on chest radiographs, and the differential diagnosis list often becomes lengthy. In addition, the radiographic concept of "alveolar vs. interstitial" infiltrates has limitations. Dr. Felson, the radiologist who extended the concept of interstitial lung disease to the reading of chest radiographs, recognized that it was difficult to predict the microscopic distribution of lung disease based on the imaging. In fact, there are few lung diseases that involve the interstitium alone. Even Dr. Leibow, recognized that exudation into the alveolar spaces was common. We now accept that cells within the alveoli may be a dominant finding within the alveoli and respiratory bronchioles in diseases such as respiratory bronchiolitis and desquamative interstitial pneumonia.

The information now available from high resolution computed tomographic (HRCT) scans of the lung has changed our approach to the assessment of patients with the idiopathic interstitial pneumonias. The process of improving scanner resolution has blurred the distinction between a gross anatomic lung specimen and the in vivo image of that specimen. As we shall see the anatomic distribution of abnormalities in the IIPs plays an important diagnostic role. This is true at both at the microscopic level and grossly.

The majority of patients who are suspected of having a chronic infiltrative process in the lungs will undergo an HRCT study during the initial investigation. When combined with clinical information the imaging data are often adequate, and no further diagnostic work-up is necessary. When a biopsy is required, images provide key information that helps determine the biopsy site and the type of procedure to be used. This is especially important when the patient is a cigarette smoker, and the symptoms may be related totally or in part to cigarette smoke. The HRCT study has become an integral part of the pre-biopsy workup. The area to biopsy is better delineated, and since these processes do not involve the lung uniformly, multiple biopsies from one lung are preferable. Computed tomography is critical to proper site selection.

Experience with these diseases dictates close cooperation between the pulmonologist, radiologist and pathologist in order to improve diagnostic accuracy. A recent Joint Statement of the American Thoracic Society and the European Respiratory Society was published January 15, 2002. This paper provides a comprehensive review of the current state of our knowledge regarding the idiopathic interstitial pneumonias.

The Idiopathic Interstitial Pneumonias

Idiopathic Pulmonary Fibrosis (IPF) has come to have a more limited definition. This disease currently encompasses a group of patients with progressive fibrosing interstitial pneumonia. The patients usually present in the 5th decade and relate a history of 6 months or more of increasing dyspnea on exertion. The chest radiograph demonstrates low lung volumes with peripheral reticular opacities that are found predominantly in the lower lung fields. The chest CT is characterized by reticular opacities and honeycombing in a strikingly peripheral and lower lobe distribution. These changes are often associated with traction bronchiectasis and architectural distortion. Ground glass may also be found to a lesser extent. When ground glass is associated with reticulation and bronchiectasis then it usually correlates with the presence of fibrosis on biopsy. A confident diagnosis of IPF based on typical clinical features of IPF obviates the need for biopsy. However, typical HRCT features of IPF are found in only 50% of patients with biopsy proven disease.

Respiratory Bronchiolitis-Associated Interstitial Lung Disease (RB-ILD) and Desquamative Interstitial Pneumonia (DIP) are best thought of as a spectrum of smoking related fibrotic and inflammatory reactions. Respiratory bronchiolitis is found in the lung biopsies of essentially all smokers although it rarely causes symptoms. It is characterized by the presence of pigmented macrophages within and around respiratory bronchioles. Mild peribronchiolar fibrosis may occur. A small percentage of the smokers with respiratory bronchiolitis will present with significant dyspnea and hypoxemia. The patients are almost always heavy smokers in their fourth or fifth decade who improve after cessation of smoking. The chest radiograph demonstrates airway thickening in the majority of patients but may be normal. The chest CT reveals centrilobular nodules and ground glass with an upper lobe predilection. Mild upper lobe emphysema is also common. Evidence of air trapping may be present on expiratory CT scans. The differential diagnosis for this appearance includes hypersensitivity pneumonitis and Langerhans Cell Histiocytosis.

DIP is now considered to be a more extensive form of respiratory bronchiolitis in which the macrophages are found within the alveolar spaces in addition to those found in the peribronchiolar region. Rarely, the disease occurs in non-smokers. The patients present with dyspnea and low lung volumes. The chest radiograph is usually characterized by patchy lower lobe ground glass. However, the chest radiograph is normal in up to 25% of cases. The chest CT demonstrates ground glass opacity in a peripheral and lower lobe distribution in the majority of cases. Reticular opacities and irregular lines are usually found in the lung bases and honeycombing is found in less than one third.

Acute Interstitial Pneumonia (AIP) is a rapidly progressive process with a subacute (2-3 weeks) presentation. Most patients relate a history suggestive of a prior viral illness and the histologic pattern is indistinguishable from adult respiratory distress syndrome. The patients develop severe hypoxemia and mechani-

cal ventilation will be required in almost all patients. The chest radiograph reveals patchy bilateral opacities with sparing of the costophrenic angles. The disease may progress to diffuse consolidation of both lungs in the exudative phase. Lung volumes are usually normal early in the disease but may decrease in the organizing phase. The chest CT reveals patchy areas of ground glass and consolidation with focal areas of sparing. The areas of consolidation, however are often dependent suggesting an element of atelectasis. The presence of traction bronchiectasis indicates that the disease has entered the organizing phase. The differential diagnosis is wide and includes: infection, hydrostatic edema, hemorrhage and alveolar proteinosis.

Cryptogenic Organizing Pneumonia (COP) has also been known as bronchiolitis obliterans organizing pneumonia (BOOP). That term may be avoided to prevent confusion with constrictive bronchiolitis which is an airway disease. The patients present with cough fever and weight loss after a suspected pulmonary infection. The duration is short (2-3months) when compared to IPF. Most patients respond to steroids but relapse is common. The chest radiograph is characterized by consolidation which may be unilateral or bilateral. Nodules are present in less than 50% of cases. The chest CT reveals areas of consolidation with a peribronchovascular distribution. Small nodules are usually centrilobular. Some patients present with solitary masses that are difficult to distinguish from a primary lung malignancy or lymphoma. The main differential is infection although eosinophilic pneumonia may be considered when the consolidation is peripheral.

Nonspecific Interstitial Pneumonia (NSIP) remains a controversial diagnosis and represents those patients who have interstitial lung diseases that do not fit cleanly into the above diagnostic categories. Those patients with the cellular form of NSIP have an excellent prognosis, while increasing fibrosis on lung biopsy is associated with a poor survival. NSIP may be the presenting manifestation of collagen vascular disease or hypersensitivity pneumonitis and should prompt an investigation for these diseases. The diagnosis of NSIP may also be made in those patients with inadequately sampled IPF. In that case imaging is important and the finding of typical IPF on computed tomography carries a poor prognosis despite the histologic diagnosis NSIP. There is usually a lower lobe predominance and in some cases only the lower lobes are involved. Peribronchovascular reticulation is a common finding along with traction bronchiectasis. The chest CT may demonstrate ground glass which tends to be bilateral and subpleural. A variety of reports, however, have revealed disparate findings. Consolidation and honeycombing can be found and supports the concept that NSIP is not a uniform diagnosis and probably represents the pulmonary manifestation of a number of diseases. In a recent study with 50 patients carrying the histologic diagnosis of NSIP, experienced radiologists considered the CT pattern indistinguishable from UIP in 32%, hypersensitivity pneumonitis is 20% and organizing pneumonia in 14%. Traction bronchiectasis and reticulation suggest the presence of fibrosis and may portend a poor prognosis.

BIBLIOGRAPHY

- American Thoracic Society/European Respiratory Society International Multidisciplinary Consensus Classification of the Idiopathic Interstitial Pneumonias. This joint statement of the American Thoracic Society (AST), and the European Respiratory Society (ERS) was adopted by the ATS board of directors, June 2001 and by the ERS Executive Committee, June 2001. *American Journal of Respiratory and Critical Care Medicine* 2002; 165(2):227-304.
- Adesina AM, Vallyathan V, McQuillen EN, Weaver SO, Craighead JE. Bronchiolar inflammation and fibrosis associated with smoking. A morphologic cross-sectional population analysis. *American Review of Respiratory Disease* 1991; 143(1):144-9.
- Arakawa H, Kurihara Y, Niimi H, Nakajima Y, Johkno T, Nakamura H. Bronchiolitis obliterans with organizing pneumonia versus chronic eosinophilic pneumonia: high-resolution CT findings in 81 patients. *AJR. American Journal of Roentgenology* 2001; 176(4):1053-8.
- Hartman TE, Primack SL, Swensen SJ, Hansell D, McGuinness G, Muller NL. Desquamative interstitial pneumonia: a thin-section CT findings in 22 patients. *Radiology* 1993; 187(3):787-90.
- Heyneman LE, Ward S, Lynch DA, Remy-Jardin M, Johkoh T, Muller NL. Respiratory bronchiolitis, preparatory bronchiolitis-associated interstitial lung disease, and desquamative interstitial pneumonia: different entities or part of the spectrum of the same disease process? *AJR. American Journal of Roentgenology* 1999; 173(6): 1617-22.
- Hunninghake GW, Zimmerman MB, Schwartz DA, King TE, Jr., Lynch J, Hegele R, et al. Utility of a lung biopsy for the diagnosis of idiopathic pulmonary fibrosis. *American Journal of Respiratory and Critical Care Medicine* 2001; 164(2):193-6.
- Johkoh T, Muller NL, Taniguchi H, Kondoh Y, Akira M, Ichikado K, et al. Acute interstitial pneumonia: thin-section CT findings in 36 patients. *Radiology* 1999; 211(3):859-63.
- Muller NL, Staples CA, Miller RR. Bronchiolitis obliterans organizing pneumonia: CT features in 14 patients. *AJR. American Journal of Roentgenology* 1990; 154(5):983-7
- Nicholson AG, Colby TV, du Bois RM, Hansell MD, Wells AU. The prognostic significance of the histologic pattern of interstitial pneumonia in patients presenting with the clinical entity of cryptogenic fibrosing alveolitis. *American Journal of Respiratory and Critical Care Medicine* 2000; 162(6): 2213-7.
- Remy-Jardin M, Edme JL, Boulenguez C, Remy J, Mastora I, Sobaszek A. Longitudinal follow-up study of smoker's lung with thin-section CT in correlation with pulmonary function tests. *Radiology* 2002; 222(1): 261-70.
- Selman M, King TE, Pardo A. Idiopathic pulmonary fibrosis: prevailing and evolving hypotheses about its pathogenesis and implications for therapy. *Annals of Internal Medicine* 2001; 134(2): 136-51

Imaging of Occupational and Environmental Lung Disease

David Lynch, M.D.

Pneumoconioses

The most common pneumoconioses are coal workers' pneumoconiosis, silicosis, and asbestosis. Although the prevalence of coal workers' pneumoconiosis in the US appears to be declining, silicosis remains a significant problem worldwide requiring continued surveillance of multiple occupational groups, particularly foundry workers and sandblasters, including surveillance for the known complication of silicotuberculosis. In highly exposed workers, silicosis may occur after less than 10 years of exposure. The radiographic and CT features of coal workers' pneumoconiosis and silicosis are similar (1-5). Both conditions present with predominantly upper lobe nodules, which may later coalesce to form mass-like opacities (progressive massive fibrosis). The CT findings in these diseases vary with the size of the opacities seen on the chest radiograph. Opacities classified as type p by the ILO criteria are characterized on HRCT by tiny branching structures or a cluster of small dots (1). Centrilobular emphysema is a frequent association. By contrast, opacities of the q and r type are characterized by sharply demarcated round nodules or irregular contracted nodules (4). The nodules may be centrilobular or subpleural in location, and tend to predominate in the posterior upper lobes. Subpleural micronodules may become confluent to form a "pseudo-plaque". About 20% of coal workers develop irregular opacities suggestive of lung fibrosis, associated with functional impairment (6). In some such patients, CT scanning and biopsy have shown changes identical to those of idiopathic pulmonary fibrosis (7). This type of lung fibrosis appears to predispose to development of lung cancer (8). It is important for the radiologist to be aware that silica exposure predisposes to emphysema and lung cancer, even in nonsmokers.

Progressive massive fibrosis (PMF), sometimes referred to as complicated pneumoconiosis or conglomerate pneumoconiosis, is much more common in silicosis than in coal workers' pneumoconiosis. On the chest radiograph, PMF presents with oval opacities, typically seen in the posterior upper lobes, with associated hilar retraction. Because the masslike fibrosis is usually lenticular rather than spherical in shape, it is often less dense than expected on the frontal radiograph. Sequential evaluation of these masses often shows apparent migration toward the hila, leaving a peripheral rim of cicatricial emphysema. Although usually symmetric, masses may be unilateral. Unilateral PMF may be distinguished from lung cancer by the presence of lobar volume loss and peripheral emphysema. On CT, PMF typically appears as an upper lobe mass (often bilateral) with irregular borders, frequent calcification, and surrounding cicatricial emphysema. Thickening of the adjacent extrapleural fat is common. A central area of low density is often seen in masses which are greater than 4 cm in diameter, and likely represents necrosis. Cavitation is less frequent. The presence of PMF should always raise the suspicion of tuberculous or atypical mycobacterial superinfection. CT may help in the diagnosis of mycobacterial infection by showing occult cavities.

Asbestos-related diseases

In asbestos-related disease, the radiologist must determine the presence or absence of pleural disease as a marker of asbestos exposure, and identify complications of asbestos exposure, including asbestosis, lung cancer, mesothelioma, pleural abnormalities, and benign asbestos-related lung masses. The table provides an illustration of the latency and relative frequen-

cy of the pleural and parenchymal manifestations of asbestos exposure.

There are four distinct types of asbestos-related pleural disease. Benign asbestos-related pleural effusion has the shortest latency (5 to 20 years), but is the least common. Pleural plaques are the most common manifestation of asbestos exposure. Diffuse pleural thickening is less common, and often complicated by rounded atelectasis. Finally, malignant mesothelioma is one of the most feared, though least common, manifestations of asbestos exposure. CT scanning is more sensitive than the chest radiograph for detection of pleural plaques (9), particularly non-calcified pleural plaques. Both diffuse pleural thickening and pleural plaques may be associated with pulmonary restriction (10, 11).

CT is an excellent modality for early detection of asbestosis. Minimal criteria for diagnosis of early asbestosis include the presence of interstitial lines bilaterally at more than one slice level (12).

Occupational/environmental malignancy

Based on epidemiologic studies, approximately 15% of lung cancers in men and 5% of lung cancers in women are due to occupational exposures. Pulmonary carcinogens recognized by the International Agency for Research on Cancer include arsenic, asbestos, beryllium, bis-(chloromethyl) ether, cadmium, chromium (IV), mustard gas, nickel, radon, and silica. The clinical presentation and pathology of lung cancers due to such exposures does not differ from that of cancers due to other causes.

Bronchogenic carcinoma is estimated to develop in 20% to 25% of asbestos workers who are heavily exposed (13). There is typically a latency period of approximately 20 years, and the greater the exposure to asbestos, the higher the risk of lung cancer. Asbestos exposure and cigarette smoking appear to be synergistic in development of cancer (Table 1). There is a strong association between the presence of histologic asbestosis and development of lung cancer (14), but this asbestosis is not always apparent on imaging studies. There is a relative increased incidence of malignancy in lower lobes, compared with the upper lobe predominant distribution of lung cancer in the general population.

Tiitola et al. screened 602 asbestos exposed workers with low-dose CT, and identified 111 patients with noncalcified nodules, of which 5 were malignant (15). However, as with screening for non-occupational lung cancer, the effectiveness of screening for asbestos-related lung cancer has not been demonstrated.

The incidence of mesothelioma in asbestos-exposed individuals is about 10%. Mesothelioma presents radiographically with focal or diffuse pleural thickening or with a pleural effusion. MR may help in staging mesothelioma by identifying transdiaphragmatic spread, or spread into the chest wall. PET scanning may help identify spread into the chest wall and to mediastinal or distant nodes (16).

Hypersensitivity pneumonitis

Hypersensitivity pneumonitis (HP) is an inflammatory interstitial lung disease caused by recurring exposure to a variety of occupational and environmental antigens. Microbial agents are the most common inciting antigens, but other important agents include proteins (particularly from birds) and inorganic agents such as isocyanates (17). HP features widely variable clinical,

radiologic, and histopathologic findings. Because the clinical findings of HP mimic multiple other diseases, a high degree of clinical suspicion and a thorough occupational and environmental history are essential for accurate diagnosis. There is no single pathognomonic feature for HP; rather, diagnosis relies on a constellation of clinical, radiologic, and pathologic findings.

The HRCT findings of HP provide important clues and frequently point clinicians towards the correct diagnosis. In particular the finding of profuse centrilobular nodules of ground glass attenuation is strongly suggestive of this diagnosis. Another strongly suggestive pattern is the combination of ground glass attenuation with air trapping (18, 19).

Although hypersensitivity pneumonitis is commonly classified into acute, subacute and chronic subsets, patients with longstanding symptoms may often be radiologically indistinguishable from those with more acute presentations. However, about 50% of patients with chronic HP present with evidence of reticular abnormality, traction bronchiectasis, or honeycombing suggestive of lung fibrosis. These findings may predominate in the upper, mid or lower zones. The challenge for the imager is to distinguish these patients from patients with other fibrotic lung conditions, particularly idiopathic pulmonary fibrosis (20) and nonspecific interstitial pneumonia. In patients with CT evidence of lung fibrosis, the presence of associated centrilobular nodules or air trapping should suggest HP. Several series have reported that emphysema is a common CT finding on followup of patients with hypersensitivity pneumonitis, even in nonsmokers (18, 21). However, the radiologic characteristics of this type of emphysema remain poorly characterized. Distinction between chronic HP and other conditions can be important, because the CT findings of chronic HP can be reversible with appropriate management including removal of the antigen.

New occupational diseases

With the increasing complexity of occupational exposures, it is not surprising that new occupational diseases continue to be identified. Two recent examples are flock-workers' lung (22) which produces a diffuse ground glass pattern, and flavor-workers lung which produces a pattern of constrictive bronchiolitis (23).

Summary

Challenges for the radiologist in occupational lung disease include detection and characterization of the abnormality, and recognition of new and evolving lung diseases.

REFERENCES

1. Akira M, Higashihara T, Yokoyama K, et al. Radiographic type P pneumoconiosis: High-resolution CT. *Radiology* 1989;171:117-123.
2. Collins LC, Willing S, Bretz R, Harty M, Lane E, Anderson WH. High-resolution CT in simple coal workers' pneumoconiosis. Lack of correlation with pulmonary function tests and arterial blood gas values. *Chest* 1993;104(4):1156-62.
3. Gevenois PA, Pichot E, Dargent F, Dedeire S, Vande Weyer R, De Vuyst P. Low grade coal worker's pneumoconiosis. Comparison of CT and chest radiography. *Acta Radiologica* 1994;35(4):351-6.
4. Remy-Jardin M, Remy J, Farre I, Marquette CH. Computed tomographic evaluation of silicosis and coal workers' pneumoconiosis. *Radiologic Clinics of North America* 1992;30(6):1155-76.
5. Worrell JA, Carroll FJ, Pendergrass HP, O'Donnell D. Coal worker's pneumoconiosis CT assessment in exposed workers in correlation with radiographic findings. *Investigative Radiology* 1992;27(1):98-100.
6. Cockcroft A, Lyons JP, Andersson N, Saunders MJ. Prevalence and relation to underground exposure of radiological irregular opacities in South Wales coal workers with pneumoconiosis. *British Journal of Industrial Medicine* 1983;40(2):169-72.
7. Briche A, Wallaert B, Gosselin B, Remy-Jardin M, Voisin C, Lafitte JJ, et al. "Primary" diffuse interstitial fibrosis in coal miners: a new entity? Study Group on Interstitial Pathology of the Society of Thoracic Pathology of the North. *Revue des Maladies Respiratoires* 1997;14(4):277-85.
8. Katabami M, Dosaka-Akita H, Honma K, Saitoh Y, Kimura K, Uchida Y, et al. Pneumoconiosis-related lung cancers: preferential occurrence from diffuse interstitial fibrosis-type pneumoconiosis. *Am J Respir Crit Care Med* 2000;162:295-300.
9. Im J-G, Webb W, Rosen A, Gamsu G. Costal pleura: Appearances at high-resolution CT. *Radiol* 1989;171:125-131.
10. Schwartz DA, Galvin JR, Dayton CS, Stanford W, Merchant JA, Hunninghake GW. Determinants of restrictive lung function in asbestos-induced pleural fibrosis. *J Appl Physiol* 1990;68(5):1932-7.
11. Kee ST, Gamsu G, Blanc P. Causes of pulmonary impairment in asbestos-exposed individuals with diffuse pleural thickening. *American Journal of Respiratory & Critical Care Medicine* 1996;154:789-793.
12. Gamsu G, Salmon CJ, Warnock ML, Blanc PD. CT quantification of interstitial fibrosis in patients with asbestosis: a comparison of two methods. *Ajr. American Journal of Roentgenology* 1995;164(1):63-8.
13. Selikoff I, Seidman H, Hammond E. Mortality effects of cigarette smoking among amosite asbestos factory workers. *J Natl Cancer Inst* 1980;65:507-513.
14. Kipen HM, Lilis R, Suzuki Y, Valciukas JA, Selikoff IJ. Pulmonary fibrosis in asbestos insulation workers with lung cancer: a radiological and histopathological evaluation. *British Journal of Industrial Medicine* 1987;44:96-100.
15. Tiitola M, Kivisaari L, Huuskonen MS, Mattson K, Koskinen H, Lehtola H, et al. Computed tomography screening for lung cancer in asbestos-exposed workers. *Lung Cancer* 2002;35(1):17-22.
16. Benard F, Sterman D, Smith RJ, Kaiser LR, Albelda SM, Alavi A. Prognostic value of FDG PET imaging in malignant pleural mesothelioma. *J Nucl Med* 1999;40(8):1241-5.
17. Glazer CS, Rose CS, Lynch DA. Clinical and radiologic manifestations of hypersensitivity pneumonitis. *J Thorac Imaging* 2002;17(4):261-72.
18. Remy-Jardin M, Remy J, Wallaert B, Muller NL. Subacute and chronic bird breeder hypersensitivity pneumonitis: sequential evaluation with CT and correlation with lung function tests and bronchoalveolar lavage. *Radiology* 1993;189(1):111-8.
19. Adler BD, Padley SP, Muller NL, Remy JM, Remy J. Chronic hypersensitivity pneumonitis: high-resolution CT and radiographic features in 16 patients. *Radiology* 1992;185(1):91-5.
20. Lynch D, Newell J, Logan P, King T, Muller N. Can CT distinguish idiopathic pulmonary fibrosis from hypersensitivity pneumonitis? *Am J Roentgenol* 1995;165:807-811.
21. Cormier Y, Brown M, Worthy S, Racine G, Muller NL. High-resolution computed tomographic characteristics in acute farmer's lung and in its follow-up. *Eur Respir J* 2000;16(1):56-60.
22. Kern DG, Crausman RS, Durand KT, Nayer A, Kuhn C, 3rd. Flock worker's lung: chronic interstitial lung disease in the nylon flocking industry. *Ann Intern Med* 1998;129(4):261-72.
23. Kreiss K, Goma A, Kullman G, Fedan K, Simoes EJ, Enright PL. Clinical bronchiolitis obliterans in workers at a microwave popcorn plant. *N Engl J Med* 2002;347(5):330-8.

Sarcoidosis

John D. Newell, Jr., M.D.

Background and Epidemiology

The first description of Sarcoid was in 1877, and is credited to the English physician Jonathon Hutchinson, [1]. He first recognized the cutaneous manifestations of this disease. The term Sarcoid arose from the description of cutaneous sarcoid by the Norwegian physician Caesar Boeck who, in 1899 coined the term "Sarkoid," because he felt the skin lesion resembled sarcoma, but was benign, [1]. Later the systemic nature of the disease was made clear, when Caesar Boeck went on to describe sarcoid involving lung, bone, lymph nodes, spleen, nasal mucosa, and conjunctivae, [1]. Sarcoid is often referred to as Boeck's Sarcoid.

Sarcoidosis is a systemic glaucomatous disease with multi-system involvement of unknown cause that usually affects young and middle-aged adults. It primarily involves the lungs and lymphatic regions of the body. Sarcoid frequently presents with bilateral hilar lymphadenopathy, pulmonary infiltration, and with ocular and skin lesions, [1-5]. Multiple other organs may be involved including the liver, spleen, lymph nodes, salivary glands, heart, nervous system, muscles, and bones. Hypercalcemia and hypercalciuria are serious known complications of sarcoid, [5].

Sarcoid occurs world wide with a prevalence of from fewer than 1 to 40 patients per 100,000 people. The lifetime risk in the United States of sarcoidosis is 0.85% for Caucasians and 2.4% for African Americans. In the United States, the age adjusted annual incidence rate is 35.5 per 100,000 for African-Americans and 10.9 per 100,000 for Caucasians, [1]. The most common cause of death is respiratory failure, except in Japan where myocardial involvement is the most common cause of death, [1]. The overall mortality from Sarcoidosis is 5%, [1]. There is significant heterogeneity in disease presentation among different ethnic and racial groups. The disease can affect any age, gender, or race, but typically affects adults less than 40 years of age with those between 20 and 29 years of age most likely to be affected. There is a slightly higher disease rate for women. It is more common in non-smokers than in smokers.

HLA analysis of affected families suggest a polygenic mode of inheritance of risk with the most common genotype frequencies being class I HLA-Ai, HLA-B8 and class II HLA-DR3, [1,6].

Etiology and Pathobiology

Pulmonary sarcoid is usually grouped into the category of non-infectious granulomatous lung disease without significant vasculitis, which includes sarcoid, hypersensitivity pneumonitis, and Berylliosis, [3].

Sarcoid is a systemic immunomediated disease whose etiology is not precisely known. The most accepted cause of Sarcoid, at this point, is the idea that genetically susceptible hosts are exposed to specific environmental agents that trigger the inflammatory response by the hosts own immune system, [1]. The immune response in tissues with sarcoid is characterized by large numbers of activated macrophages and T lymphocytes. These T lymphocytes have the CD4 helper phenotype. The pattern of cytokine production by the activated alveolar macrophages and T lymphocytes is consistent with a Th1-type immune response characteristically triggered by an antigen, [1]. Sarcoid is not thought to be an autoimmune disease at this point. The precise environmental agent or agents that produces sarcoid is still hotly debated. The list of possible infectious agents includes: Viruses (herpes, Epstein-Barr, retrovirus, cox-

sackie B virus, cytomegalovirus), bacteria (Borrelia burgdorferi, Propionibacterium acnes, Mycobacterium tuberculosis, Non-tuberculous mycobacterial disease, Mycoplasma). The organic antigens include Pine tree pollen, clay, and the inorganic antigens include aluminum, zirconium, and talc, [1]. There may be more than one agent responsible for sarcoid. Beryllium provokes a response similar to sarcoid but is considered a separate disease entity, [1].

The pathologic hallmarks of Sarcoid are discrete, compact, noncaseating epithelioid cell granulomas with lymphocytes and fibroblasts in the outer margin of the granuloma, [1,2]. The epithelioid cell granuloma is composed of epithelioid cells and giant cells that represent highly differentiated mononuclear phagocytes. The giant cells may contain cytoplasmic inclusions such as asteroid bodies and Schaumann bodies. The granulomas have a perilymphatic distribution in the lung. Alternative causes of granulomas need to be ruled out including infection, pneumoconiosis, schistosomiasis, leprosy, inflammatory bowel disease, and sarcoid-like reaction in patients with lymphoma and other solid tumors, [7].

Seventy-five percent of the sarcoid granulomas in the lung are near or within the connective tissue sheath of bronchioles, the subpleural space, and the interlobular septal space, [1-5]. These pathologic observations correlate nicely with the HRCT observation of a perilymphatic distribution of nodules in the lung (see below). Intra-thoracic lymph nodes are also a common site of sarcoid granulomas, again correlating nicely with known medical imaging findings in thoracic sarcoidosis. Identically appearing sarcoid granulomas can also involve extra-thoracic lymph nodes in the liver, spleen, and skin. It should be noted that vascular involvement is noted in half of the patients with sarcoid where tissue is available from transbronchial biopsies, [2]. Clinical evidence of vasculitis in sarcoid is unusual.

The sarcoid granulomas either resolve or go on to cause parenchymal lung fibrosis and honeycombing, [1]. The factors that influence which process that will occur in an individual patient are not well understood. There is some evidence that the fibrotic response in the lung may be due to a shift of T cell lymphocyte phenotypes from the Th1 to the Th2 lymphocyte and this later T cell lymphocyte secretes a pattern of cytokines that promote a fibroproliferative response, substantial extracellular matrix deposition, and ultimately pulmonary fibrosis, [1].

Clinical Presentation, Diagnosis and Treatment

The lungs are affected in more than 90% of patients with sarcoidosis, [1,4,5]. Thirty to sixty percent of patients with sarcoid are asymptomatic, but have incidental findings on chest radiographs, [4]. Ten percent of sarcoid patients have normal chest radiographs, but usually present with significant extra-thoracic disease such as uveitis or skin lesions, [5]. The symptomatic patient may have a normal radiographic and CT examination of the lungs, and Gallium 67 scanning may be helpful to detect intra-thoracic disease in this situation, [5]. Dyspnea, dry cough, and chest pain occur in one-third to one-half of all patients, [1]. The chest pain is retrosternal and is described most often as a vague tightness of the thorax, [1]. The chest pain occasionally is severe and is indistinguishable from cardiac pain, [1]. Hemoptysis and clubbing are rare, and lung crackles occur in less than 20% of patients, [1].

Siltzbach developed a radiographic staging system for sarcoid over 40 years ago, and it is still in use today, Table 1, [5]. This radiographic staging system has important prognostic

application. The untreated patient with sarcoid will improve 50 to 90 percent of the time with Radiographic stage 1 disease. The untreated patient with Stage 2 disease will improve 30 to 70 percent of the time. Only 10 to 20 percent of untreated patients with Stage 3 disease will improve, and there is no improvement in those with untreated Stage 4 disease, [5]. It is important to note that there may be considerable discrepancy between the severity of the radiographic abnormalities and the patient's symptoms, [5].

The clinical diagnosis of sarcoid requires a compatible clinical and radiographic presentation, biopsy evidence of sarcoid granulomas, usually from transbronchial biopsies of the lung, and the exclusion of other diseases capable of producing a similar clinical, radiographic, and histological picture, [1-5].

Systemic corticosteroid therapy is clearly indicated for cardiac disease, neurological disease, eye disease that is refractory to topical therapies, and hypercalcemia, [1]. Most physicians feel that progressive symptomatic pulmonary and extrapulmonary disease should be treated with systemic corticosteroids, [1]. Cytotoxic agents, antimalarial agents, and lung transplantation are useful in select patients with advanced sarcoid, [1].

The diagnostic yield of endomyocardial biopsies is low in sarcoid patients. Sarcoid patients with symptomatic cardiac dysfunction, ECG abnormalities, thallium 201 imaging defects, or MR evidence of myocardial disease should be presumed to have cardiac sarcoidosis in the presence of a negative endomyocardial biopsy, [1]. It is important in older sarcoid patients to exclude coronary artery disease as cause of their cardiac illness.

Sarcoid is a multisystem disease and, for this reason, careful clinical evaluation of the entire patient must be done. This clinical review includes the peripheral lymph nodes, skin, spleen, liver, eyes, central nervous system, musculoskeletal system, gastrointestinal tract, bone marrow, parotid glands, reproductive organs, kidneys, and the endocrine system, [1-5].

Physiology

The pulmonary physiology of sarcoid is usually a predominantly restrictive ventilatory process, with reductions in vital capacity (VC) and diffusion capacity (DLCO), [4]. Physiology testing cannot distinguish alveolitis from fibrosis, [4]. Serial physiological testing is quite valuable in monitoring the course of an individual patient's pulmonary sarcoid, [4]. An obstructive component of the lung physiology is detected in one-third or more of sarcoid patients with lung involvement with reductions in FEV1 and expiratory flow rates, [4]. Central and small airway involvement accounts for the obstructive physiology observed in these sarcoid patients.

Typical Radiographic and CT Observations in the Thorax

The most common radiographic presentation is Stage 1 sarcoid with bilateral symmetric hilar lymphadenopathy and mediastinal lymphadenopathy in an asymptomatic patient, [5]. Mediastinal lymph node enlargement usually is seen in the right paratracheal, aortopulmonary window, and subcarinal regions. Anterior mediastinal lymph node enlargement is unusual in sarcoid unlike lymphoma patients, [5]. CT demonstrates lymphadenopathy better than radiography and often demonstrates additional regions of lymph node involvement. CT is more sensitive than radiography for the detection of lymph node calcifications in sarcoid, [5].

The typical radiographic observations in Stage 2 or 3 sarcoid are nodules, linear/reticular opacities and ground glass opacities with a mid and upper lung zone distribution [5]. HRCT examination demonstrates a perilymphatic distribution of irregular, small discrete nodules, 2 to 10 mm in size, that predominate in both the mid and upper lung zones and in the central portion of the lung. This perilymphatic distribution of nodules results in nodules that are associated with the bronchovascular structures,

interlobular septae, and pleural surfaces. Peribronchial wall thickening is common on HRCT, as well as interlobular septal thickening and ground glass opacities. Nodules larger than 10 mm in size may be seen but are less common.

Radiographic Stage 4 sarcoid has marked upper lobe volume loss, architectural distortion of the lung, conglomerant mass formation, cyst formation, honeycombing, traction bronchiectasis, and emphysema, [5]. Pulmonary fibrosis and honeycombing with an upper lobe predominance develops in 20 % of sarcoid patients. HRCT examinations show similar findings but to better advantage than radiography.

Plain radiography and CT may show severe bronchial stenosis or irregularity in patients with endobronchial sarcoid. Central airway observations on CT include regular or irregular bronchial wall thickening, luminal narrowing or occlusion, and displacement of central bronchial structures by adjacent lymphadenopathy, [5]. 3D reconstructions of multidetector spiral CT datasets can show central bronchial stenosis for endobronchial stent placements, [5].

Less Common Radiographic and CT Observations in the Thorax

Radiographic and CT examinations of patients may demonstrate a number of observations that are less commonly associated with pulmonary sarcoidosis. These include a solitary mass, multiple masses, focal consolidation, cavity formation, pleural thickening, pleural effusion, and pleural calcifications, [4,5]. The presence of cavities may indicate a different process than sarcoid including necrotizing sarcoid granulomatosis, superinfection, or vasculitis, [4,5]. Mycetomas may develop in upper lobe bullae and cysts in Stage 4 sarcoid. These mycetomas may present with life threatening hemoptysis. A pattern of pulmonary fibrosis indistinguishable from IPF has also been described in sarcoid, [4,5]. Though unusual, unilateral lung and intrathoracic lymph node disease have also been described in sarcoid and are indistinguishable radiographically from infectious granulomatous disease and intrathoracic malignancies, [4,5]. Pulmonary arterial hypertension is seen in less than 5% of patients and usually in patients with Stage 4 disease, [4,5].

There is an increased rate of sarcoid recurring in a transplanted lung compared to other diseases that undergo lung transplantation therapy, [1,8]. The frequency of recurrency has been reported to be as high as 35%, [8]. Posttransplantation immunosuppression therapy is reported to control the recurring sarcoidosis, [1]. Myocardial imaging is helpful in the 5% of patients suspected of having cardiac sarcoid, [1]. Thallium 201 myocardial imaging is superior to Doppler echocardiography if the detection of segmental wall motion abnormalities of the left ventricle that correspond to sarcoid induced granulomas or fibrosis in the myocardium, [1]. MR imaging of the heart has recently been shown to be effective in the detection of myocardial sarcoid lesions and the MR imaging findings may be helpful in monitoring the response of the myocardium to steroid therapy, [9].

Differential Diagnosis

The differential diagnosis of pulmonary sarcoid includes conditions that have preferential involvement of the perilymphatic space of the lungs and lymph node involvement in the hila of the lungs and in the mediastinum. This includes infectious granulomatous diseases, Berylliosis, lymphoma, leukemia, and lymphangitic carcinomatosis. Asymmetric involvement of the lung and intrathoracic lymph nodes usually excludes malignant and infectious diseases of the thorax. Lymphangitic carcinomatosis has recently been shown to have more involvement of the interlobular septae and subpleural space on HRCT than either lymphoma or sarcoid, [10]. Almost all patients with thoracic malignancies are symptomatic as opposed to asymptomatic.

matic sarcoid patients, and the occurrence of bilateral hilar lymphadenopathy is much more common in sarcoid than in malignant conditions of the thorax, [41].

REFERENCES

- Statement on sarcoidosis. Joint Statement of the American Thoracic Society (ATS), the European Respiratory Society (ERS) and the World Association of Sarcoidosis and Other Granulomatous Disorders (WASOG), adopted by the ATS Board of Directors and by the ERS Executive Committee, February 1999. *Am J Respir Crit Care Med*, 1999. 160(2): p. 736-55.
- Travis, W.D., et al., Chapter 3, Idiopathic Interstitial Pneumonia and other Diffuse Parenchymal Lung Disease, in *Atlas of Nontumor Pathology, First Series, Fascicle 2, Non-Neoplastic Disorders of the Lower Respiratory Tract*, W.D. Travis, et al., Editors. 2002, American Registry of Pathology and the Armed Forces Institute of Pathology: Washington. p. 123-136.
- Zinck, S.E., et al., CT of noninfectious granulomatous lung disease. *Radiol Clin North Am*, 2001. 39(6): p. 1189-209, vi.
- Lynch, J.P., 3rd, E.A. Kazerooni, and S.E. Gay, Pulmonary sarcoidosis. *Clin Chest Med*, 1997. 18(4): p. 755-85.
- Lynch, D.A., et al., Imaging of Diffuse Infiltrative Lung Disease, in *Imaging of Diffuse Lung Disease*, D.A. Lynch, J.D. Newell, and J.S. Lee, Editors. 2000, B.C. Decker Inc.: Hamilton. p. 78-86.
- Semenzato, G., M. Bortoli, and C. Agostini, Applied clinical immunology in sarcoidosis. *Curr Opin Pulm Med*, 2002. 8(5): p. 441-4.
- Hunsaker, A.R., et al., Sarcoidlike reaction in patients with malignancy. *Radiology*, 1996. 200(1): p. 255-61.
- Collins, J., et al., Frequency and CT findings of recurrent disease after lung transplantation. *Radiology*, 2001. 219(2): p. 503-9.
- Shimada, T., et al., Diagnosis of cardiac sarcoidosis and evaluation of the effects of steroid therapy by gadolinium-DTPA-enhanced magnetic resonance imaging. *Am J Med*, 2001. 110(7): p. 520-7.
- Honda, O., et al., Comparison of high resolution CT findings of sarcoidosis, lymphoma, and lymphangitic carcinoma: is there any difference of involved interstitium? *J Comput Assist Tomogr*, 1999. 23(3): p. 374-9.

Table 1
Radiographic Staging of Sarcoid

Stage 0	Normal
Stage 1	Bilateral Hilar Lymphadenopathy (BHL)
Stage 2	BHL and Pulmonary infiltrations
Stage 3	Pulmonary infiltrations (Without BHL)
Stage 4	Pulmonary Fibrosis

The Expanded Spectrum of Smoking-Related Diseases

Rosita M. Shah, M.D.

Thomas Jefferson University Hospital
Philadelphia, PA

The Pathogenicity of Cigarette Smoke

The constituents of cigarette smoke are frequently divided into gas and particulate phases, with greater than 3500 compounds known to exist in cigarette smoke. Over 40 of these compounds are known carcinogens, some of which have been shown to directly interact with plasmid DNA and produce irreversible injury. Many of the gas phase components are extremely short lived and the following discussion is directed at the particulate phase.

The term 'tar' is applied to the particulate components of cigarette smoke of which 50% of inhaled particles are deposited in the lung. Particles less than 5µm easily bypass normal pulmonary defenses and frequently aggregate near respiratory bronchioles where reduced airway diameter results in reduced particle speed. Deposition of these particles is greatest in the lower lobes, paralleling ventilation. However, as with other diseases associated with particle deposition including silicosis, the greatest concentrations of deposited particulate material are recovered in the upper lobes. This may be explained by the relatively reduced lymphatic clearance in the upper lung zones. It follows that smoking-related lung pathology is most common in the upper lung zones.

The accumulation of particulate matter in the lung parenchyma is associated with several physiologic responses. Smokers have significantly elevated systemic and intra-pulmonary neutrophil counts as well as a peribronchiolar accumulation of macrophages. Release of elastase from activated neutrophils is the principal factor in the development of emphysema.

Per gram of TAR, there are greater than 10^{17} radicals. These radicals are likely contributors to the carcinogenicity of cigarette smoke and also result in the oxidation of intra-pulmonary enzymes, including alpha-1-anti-trypsin. Subsequently reduced levels or the presence of non-functioning anti-proteases in the lung augment the effect of elevated elastase levels.

Pathologic and Physiologic Changes in Smoker's Lungs

Consistent pathology identified in smoker's lungs include submucosal gland hypertrophy and goblet cell hyperplasia resulting in an elevated Reid index, smooth muscle hypertrophy, bronchiolar inflammation and respiratory bronchiolitis. Mucus hypersecretion occurs predominantly at a large airway level and is usually reversible. Airway obstruction occurs primarily secondarily to small airway and airspace pathology, and results in irreversible abnormalities.

Neoplastic Smoking-related Disease

Smoking is associated with a 10-25 fold increase in lung cancer deaths and accounts for 75-90% of the lung cancer risk. Twenty percent of smokers will develop bronchogenic carcinoma, indicating the obvious significance of other factors including individual susceptibility. Smoking has also resulted in a 10-30 fold increase in lung cancer deaths in non-smokers and a 50 fold increase in upper respiratory tract and esophageal malignancies.

Non-neoplastic Smoking-related Lung Disease Chronic Obstructive Pulmonary Disease

The association of smoking with COPD is more than convincing. The literature has repeatedly demonstrated a direct relation between the degree of emphysema and reduced FEV1

with the number packs smoked per day. Smoking is associated with an annual reduction in FEV1 of 50ml. Smoking cessation does not improve FEV1 but may slow the rate of decline.

Emphysema is defined by the permanent enlargement of air spaces distal to terminal bronchioles. Destruction of alveolar walls without significant fibrosis results from the elastolytic effect of neutrophilic byproducts, including elastase, following the activation cytokine networks. The development of emphysema is potentiated by low levels of alpha-1-anti-trypsin, with significant emphysema developing in 15-20% of smokers. Previous literature has shown significantly greater degrees of emphysema and air-trapping in smoking vs nonsmoking patients.

Correlative HRCT-pathologic studies have demonstrated that imaging will miss or undercall the extent of emphysema in 50%. Centrilobular emphysema is the form of emphysema most closely associated with smoking. Imaging findings include focal lucencies without visible walls and the visualization of residual centrilobular anatomy.

An upper lung predominance is usual.

Panlobular emphysema may also develop in smokers and coexist with centrilobular emphysema. Imaging features include diffuse areas of reduced attenuation with reduced vessel size in a lower lung zone distribution. Panlobular emphysema is to be differentiated from advanced centrilobular emphysema or air-trapping.

Chronic bronchitis is defined by persistent productive cough for 3 consecutive months over 2 consecutive years. Pathologic findings in the airways of patients with chronic bronchitis and asymptomatic smokers may overlap, including an elevated Reid index with submucosal and goblet gland hyperplasia and an increased mucus volume

Smoking-related Interstitial Lung Disease Langerhans' Cell Histiocytosis

Pulmonary Langerhans' histiocytosis represents approximately 5% of cases of chronic infiltrative interstitial lung disease diagnosed by biopsy. Nearly all patients are smokers and disease progression is characteristic in patients who continue the habit. The Langerhans' cell represents an immunologically functioning histiocyte derived from the monocytes-macrophages. Immune-mediators can be isolated from BAL fluid and the histiocytic lesions, including growth factors, granulocyte colony stimulating factor and tumor necrosis factor.

The lesions of langerhans' histiocytosis are peribronchiolar and characterized by a collection of Langerhans' cells, macrophages and eosinophils. The inflammation typically extends into the adjacent interstitium, including alveolar and interlobular septae. The adjacent lung parenchyma commonly demonstrates an associated organizing pneumonia and respiratory bronchiolitis.

Imaging findings include an upper lung predominant, irregular nodular abnormality. Costophrenic angles are spared. A peribronchiolar distribution is usually readily apparent. Cavitation is common, frequently consisting of unusually shaped lucencies. Earlier in the disease course, nodules dominate the radiographic picture, whereas in later stages, the cystic component is most prominent. An accompanying interstitial abnormality may be observed.

Respiratory Bronchiolitis

Respiratory bronchiolitis and respiratory bronchiolitis-associated interstitial lung disease are causes of chronic bronchiolitis in the smoking patient. As with Langerhans' cell histiocytosis, patients are significantly younger than those presenting with chronic bronchitis and emphysema. The literature reports an age range of 25-55 years. Respiratory bronchiolitis was first described in 1974 as an incidental finding in young, previously healthy patients who had suffered sudden deaths. A strong association with smoking was established. Many patients with respiratory bronchiolitis and associated interstitial lung disease may also be asymptomatic or present with restrictive functional parameters and reduced diffusion capacity.

Pathologically there is a bronchiolar and peribronchiolar accumulation of pigmented, tar laden macrophages. In RB-ILD, mild fibrosis may be evident in the bronchiolar walls with extension into adjacent alveolar septae. Features of desquamative interstitial pneumonitis may also be present. Pathologic features of respiratory bronchiolitis have been identified in past smokers, indicating a lack of complete reversibility.

Imaging findings are dominated by subtle peribronchiolar ground glass opacity and centrilobular nodules. There is considerable overlap with HRCT findings in DIP and hypersensitivity pneumonitis.

Desquamative Interstitial Pneumonitis

Desquamative interstitial pneumonitis was initially described and classified by Liebow in 1965 and subsequently classified as one of the chronic interstitial pneumonias, and a possible precursor of usual interstitial pneumonitis. Since then, the pathologic cell in DIP has been identified as a macrophage, a strong epidemiologic association with smoking has been established, and DIP is considered as a distinct diagnostic entity, with closer ties to RB-ILD than UIP.

Demographic features and clinical manifestations are similar to patients with RB-ILD although a greater degree of functional impairment has been reported.

The most prominent pathologic finding in DIP is the intra-alveolar accumulation of pigmented macrophages. While mild alveolar septal thickening may be present, there is no architectural distortion.

Imaging findings are dominated by patchy or peripheral ground-glass opacity demonstrating a tendency toward lower lung zone involvement. Signs of associated fibrosis are evident in 50%.

DIP-like reactions have been identified in pulmonary drug toxicities, Langerhans' Histiocytosis, and HIV-related infections.

Conclusion

While there is a greater understanding of the pathophysiologic changes associated with smoking, much remains unknown. In addition to the established associations between smoking and thoracic malignancies and obstructive lung disease, it is now clear that smoking is strongly associated with a spectrum of interstitial lung disease. These interstitial diseases share imaging features and optimistic prognoses with potential reversibility noted with smoking cessation.

REFERENCES

- Brauner MW, Grenier P, Tijani K, et al. Pulmonary Langerhans cell histiocytosis: evolution of lesions on CT scans. *Radiology* 1997;204:497-502
- Gurney JW. Pathophysiology of obstructive airways disease. *RCNA* 1998;36:15-27.
- Hartman TE, Primack SL, Kang EY, et al. Disease progression in usual interstitial pneumonitis compared with desquamative interstitial pneumonia: Assessment with serial CT. *Chest* 1996;110:378-382
- Heyneman LE, Ward S, Lynch DA, et al. Respiratory bronchiolitis, respiratory bronchiolitis-associated interstitial lung disease, and desquamative interstitial pneumonia: Different entities or part of the spectrum of the same disease process? *AJR* 1999;173:1617-1622.
- Park J, Brown K, Tuder R, et al. *Radiology* 2002;26:13-20
- Remy-Jardin M, Remy J, Boulenguez C, et al. Morphologic effects of cigarette smoking on airways and pulmonary parenchyma in healthy adult volunteers: CT evaluation and correlation with pulmonary function tests. *Radiology* 1993;186:107-115.
- Smith RA, Glynn TJ. Epidemiology of lung cancer. *RCNA* 2000;38:453-469.
- Stern EJ, Frank MS. CT of the lungs in patients with pulmonary emphysema: diagnosis, quantification, and correlation with pathologic and physiologic findings. *AJR* 1994;162:555-560

Hypersensitivity Pneumonitis (a.k.a. Extrinsic Allergic Alveolitis)

Aine M. Kelly, M.D.

University of Michigan Medical Center, Ann Arbor, Michigan

Overview:

The clinical settings associated with hypersensitivity pneumonitis, its symptoms and the findings on physical examination are initially discussed. Corresponding abnormalities on pulmonary function testing and histologic examination are described. The most common radiographic and HRCT findings of acute, subacute and chronic hypersensitivity pneumonitis are described with differential diagnoses.

Objectives:

To be familiar with the clinical, histological, radiographic and HRCT features of hypersensitivity pneumonitis. To be familiar with the differential diagnosis of the above findings

Pathophysiology:

Hypersensitivity pneumonitis (HP) or extrinsic allergic alveolitis (EAA) represents the body's immunological response to a variety of inhalational particulate antigens. The offending agents are many, with the resulting disorders having names such as farmer's lung, mushroom workers lung, pigeon fancier's lung, humidifier lung, hot tub lung etc. See Table 1 for details. The antigens inhaled range in size from 1 to 5 micrometers and include bacteria, fungi, amoebas, animal and plant proteins, drugs and small molecular weight chemicals. For disease to be induced there must be a high level of exposure. This can either be heavy exposure of short duration or low-grade exposure of long duration. Many exposures relate to particular occupations or hobbies, with exceptions such as humidifier lung. Therefore, an extensive social and occupational history should be sought.

The **immune mechanism** is thought to be mediated by the alternate complement pathway and type III and IV hypersensitivity reactions. Serum precipitins are evidence of exposure, and may also be found in many asymptomatic individuals. False-negative serum precipitins are common, particularly with advanced chronic disease. HP has a higher incidence in non-smokers.

Clinical presentation:

Acute disease occurs within hours of a heavy antigen exposure, and manifests with fever, chills, dry cough, dyspnea, wheeze, malaise, myalgia and malaise. This presentation may simulate an acute viral or bacterial illness; however, repeated exposures should arouse suspicion of HP. Physical examination may yield lower lung crackles. Tachypnea and cyanosis occur in severe cases. Spontaneous recovery in days usually follows removal of the offending antigen from the individual's surroundings. Acute disease is a common mode of presentation in pigeon fancier's lung.

Subacute disease consists of repeated acute episodes on a background of deteriorating lung function. Pulmonary function tests may show an obstructive pattern.

Chronic disease occurs secondary to long-term low-grade antigen exposure. Progressive shortness of breath, malaise, fever and weight loss can occur. These symptoms mimic such diseases as chronic granulomatous infections, idiopathic pulmonary fibrosis and sarcoidosis. Pulmonary function tests show a mixed obstructive and restrictive pattern.

Table 1: Spectrum of hypersensitivity pneumonitis

Syndrome	Antigen	Cause
Farmer's lung	Thermophilic actinomycetes	Moldy hay
Bird fancier's lung ducks,	Avian proteins (droppings, feathers)	Pigeons, parakeets, canaries, geese
Humidifier lung tubs,	Mycobacterium Avium Intracellular complex, fungi, Amebae, Klebsiella oxytoca	Air Conditioners, hot- tubs, humidifiers
Mushroom worker's lung	Saccharopolyspora rectivirgula Micromonospora vulgaris Pleurotus ostreatus Pholiota nameko Thermophilic actinomycetes	Mushroom culture compost
Malt worker's lung	Aspergillus clavatus	Moldy malt / barley
Maple bark disease	Cryptostroma corticale	Tree bark
Japanese summer type HP	Trichosporum asahii (formerly t.cutaneum)	House dust
Suberosis	Penicillium frequentans	Moldy cork
Bagassosis	Thermoactinomyces sacchari	Moldy sugar cane
Occupational	Isocyanates	Adhesives, paints, Polyurethane foam

Histological Features: In the *early or acute stage* there is a temporally uniform interstitial pneumonitis consisting of mononuclear and lymphocytic infiltration of the inter- and intralobular septa. Alveolar spaces may fill with cellular elements and fluid. Bronchiolitis is common and bronchiolitis obliterans has been described. These histological findings have a patchy and peribronchiolar distribution. Acute changes predominate in the lower lungs. In the *subacute stage*, non-caseating granulomas occur surrounding the centrilobular structures. Interstitial pneumonitis, alveolar filling and bronchiolitis also occur at this stage in a peribronchiolar distribution. With the *chronic stage*, granulomas resolve and fibrosis ensues. This occurs more in the upper lungs. Scarring and honeycomb cysts occur with compensatory emphysema, which may later be complicated by pulmonary hypertension and cor pulmonale.

Radiographic Abnormalities: In the *acute stage* the chest radiograph may be normal.

Small well-or ill-defined lung nodules, usually 1 to 3-mm in size are most commonly found in the *acute / subacute stage*. Superimposition leads to a generalized ground glass haze, usually bilateral, in all lung zones, but most severe in the mid lungs, sparing the extreme apices and bases. Occasionally, larger 4 to 8-mm nodules, patchy consolidation or a linear interstitial pattern may be seen. In the *chronic stage*, lung volumes are reduced with the development of fibrosis. This overlap of fibrosis leads to combined reticular and nodular opacities, and usually has an upper lung predominance. Linear parallel opacities may occur due to traction bronchiectasis or bronchial wall thickening. Nodules may persist into the chronic stage.

HRCT Findings

Acute/Subacute: HRCT is more sensitive than chest radiographs in the detection and assessment of HP. Little published data regarding the acute stage exists. Bilateral consolidation with multiple small 1 to 3-mm nodules has been described. In the subacute stage, in *ground glass opacity (GGO)* is found in approximately 70% of cases, diffuse or patchy in distribution,

and often with lobular sparing. GGO predominates in the mid and lower lungs, but may occur in all lung zones. It is thought to represent the interstitial inflammatory infiltrate seen histologically. Ill-defined **centrilobular nodules**, less than 5-mm in diameter, are found in approximately 55% of cases. These are usually ground glass in attenuation, occur in all lung zones, and often spare the extreme apices. GGO and centrilobular nodules correlate with disease activity, and may resolve after cessation of antigen exposure. **Mosaic attenuation** is seen on inspiratory HRCT images representing normal lung parenchyma interspersed with areas of GGO and areas of air-trapping. The latter will become more evident and exaggerated on expiratory HRCT images, and represents a manifestation of bronchiolitis. A combination of ground glass opacity, low attenuation areas and normal lung (*the "head-cheese" sign ala Rick Webb!*) on inspiratory sections is common in HP. Less commonly, consolidation or linear interstitial opacities due to fibrosis are seen.

Differential diagnosis includes atypical / viral pneumonias, desquamate interstitial pneumonia (DIP), non-specific interstitial pneumonitis (NSIP), and less commonly sarcoidosis. Centrilobular nodules are also found in respiratory bronchiolitis but tend to be more patchy, sparse and upper lung predominant. The nodules in sarcoidosis and the pneumoconioses are usually more solid and less ground glass like than in HP.

Chronic: In this stage the findings are a combination of those found in the subacute phase with superimposed fibrosis. Therefore, patchy GGO and centrilobular nodules are common, seen in 66% of cases. Mosaic attenuation and air trapping on expiration are also seen. In addition, there may be **thickened interlobular septa, irregular interfaces and traction bronchiectasis**, found in decreasing order of frequency. **Honeycombing** is less common, occurring in less than 25% of cases. The distribution of the fibrosis is patchy and most often shows a mid- or lower lung predominance. Relative sparing of the costophrenic recesses is seen in a majority of cases. **Emphysema** is reported in up to 50% of cases on HRCT.

Differential diagnosis of these HRCT features includes an overlap with usual interstitial pneumonitis (UIP/IPF), NSIP and DIP. Clinical history, serology, the mosaic patchy distribution, air trapping and sparing of the costophrenic recesses help distinguish HP from these entities.

Summary: HP is an immune-mediated interstitial lung disease caused by recurring or heavy exposure to a variety of antigens. It has non-specific clinical features and physical findings. A detailed occupational and recreational history is essential for diagnosis. The constellation of HRCT findings may be the first to suggest the diagnosis during the patient work-up, and distinguish this disease from interstitial pneumonias like DIP, NSIP and UIP.

REFERENCES

- _Kumar and Clark. Clinical Medicine. 5th edition. WB Saunders. 2002
- Armstrong P, Wilson AG, Dee P, Hansell DM. Imaging of Diseases of the Chest. 3rd edition. Mosby. 2000
- Webb WH, Muller NL, Naidich DP. High Resolution CT of the Lung. Lippincott Williams & Wilkins. 3rd edition. 2001
- Glazier CS, Rose CS, Lynch DA. Clinical and Radiological Manifestations of Hypersensitivity Pneumonitis. Journal of Thoracic Imaging. 2002;17(4):261-272.
- Bourke SJ, Dalphon JC, Boyd G, McSharry C, Baldwin CI, Calvert. Hypersensitivity Pneumonitis: current concepts. European Respiratory Journal 2001;18 suppl.32, 81s-92s.
- Fink JN. Hypersensitivity Pneumonitis. Clinics in Chest Medicine 1992;13(2):303-309.
- Chiu A, Pegram PS, Haponik EF. Hypersensitivity Pneumonitis: A diagnostic dilemma. Journal of Thoracic Imaging. 1993;8(1):69-78.
- Sharma OP, Fujimura N. Hypersensitivity Pneumonitis: A Noninfectious Granulomatosis. Seminars in Respiratory Infections 1995;10(2):96-106.
- Patel RA, Sellami D, Gotway MB, Golden JA, Webb WR. Pictorial Essay. Hypersensitivity Pneumonitis: Patterns on High-Resolution CT. Journal of Computer Assisted Tomography 2000;24(6):965-970.
- Cormier Y, Brown M, Worthy S, Racine G, Muller NL. High-Resolution Computed Tomographic characteristics in acute farmer's lung and in its follow-up. European Respiratory Journal 2000;16, 56-60.
- Hansell DM, Moskovic E. High-Resolution Computed Tomography in Extrinsic Allergic Alveolitis. Clinical Radiology 1991;43:8-12.
- Small JH, Flower CDR, Trail ZC, Gleeson FV. Air-trapping in Extrinsic Allergic Alveolitis on Computed Tomography. Clinical Radiology 1996;51:684-688.
- Adler BD, Padley SPG, Muller NL, Remy-Jardin M, Remy J. Chronic Hypersensitivity Pneumonitis : High-Resolution CT and Radiographic Features in 16 Patients. Radiology 1992;185:91-95.
- Lynch DA, Rose CS, Way D, King TE. Hypersensitivity Pneumonitis: Sensitivity of High-Resolution CT in a Population-Based Study. American Journal of Roentgenology 1991;159:469-472.
- Silver SF, Muller NL, Miller RR, Lefcoe MS. Hypersensitivity Pneumonitis Evaluation with CT. Radiology 1992;173:441-445.
- Buschman DL, Gamsu G, Waldron JA, Klein JS, King TE. Chronic Hypersensitivity Pneumonitis: Use of CT in Diagnosis. American Journal of Roentgenology 1992;159(5):957-960.
- Hansell DM, Wells AU, Padley SPG, Muller NL. Hypersensitivity Pneumonitis: Correlation of Individual CT Patterns with Functional Abnormalities. Radiology 1996;199:123-128.
- Kim KI, Kim CW, Lee MK, Park CK, Choi SJ, Kim JG. Imaging of occupational lung disease. Radiographics 2001;21(6):1371-1391.
- Akira M. HRCT in the evaluation of occupational and environmental disease. Radiological Clinics of North America 2002;40(1):43-59.
- Richerson HB, Bernstein IL, Fink JN et al. Guidelines for the Clinical Evaluation of Hypersensitivity Pneumonitis. J. Allergy Clin. Immunol 1989;84(5)part 2:839-844.
- Patel AM, Ryu JH, Reed CE. Hypersensitivity Pneumonitis: Current Concepts and future questions. J. Allergy Clin. Immunol 2001;108(5)661-670.

Small Airway Diseases

Michael B. Gotway, M.D.

The term small airway refers to airways 3mm or less in diameter (most of which represent bronchioles). Small airways are quite numerous, and thus contribute little to overall airway resistance; this implies that considerable destruction of the small airways must be present before the patient will become symptomatic.

Small Airway Diseases and Pulmonary Pathophysiology

In patients with small airways diseases, obstruction of the bronchiolar lumen results in hypoxia of the underventilated lung and air trapping. This hypoxia results in reflex vasoconstriction, causing blood to be shunted away from the underventilated segments of lung to normal lung areas. Because much of pulmonary parenchymal attenuation is the result of the lung's blood volume, redistribution of blood flow, due to small airway diseases, appears on HRCT as inhomogeneous lung opacity. This inhomogeneous opacity is appreciated as areas of relatively increased and decreased lung parenchymal attenuation, which is accentuated on expiratory imaging. In this circumstance, the vessels within the areas of relatively diminished lung parenchymal attenuation appear abnormally small, representing mosaic perfusion (1).

Approach to Small Airway Diseases

Small airway diseases may be approached in several different ways. The two major approaches to small airway diseases are:

- Classification based on pathologic descriptions
- Classification based on HRCT appearances

Pathologic Classification of Small Airway Diseases

The major small airway disease pathologic categories include cellular bronchiolitis (both acute and chronic bronchiolitis), panbronchiolitis, follicular bronchiolitis, respiratory bronchiolitis, constrictive bronchiolitis (bronchiolitis obliterans), and proliferative bronchiolitis (aka bronchiolitis obliterans organizing pneumonia) (2).

Cellular Bronchiolitis

Cellular bronchiolitis involves inflammation within the bronchiolar lumen and bronchial walls. Diseases that fall within this pathologic category include infections (virus, *Mycoplasma*, airway invasive *Aspergillosis*), hypersensitivity pneumonitis, asthma, chronic bronchitis, and bronchiectasis. The typical appearance of cellular bronchiolitis is small ground-glass opacity, commonly presenting as centrilobular nodules (3), sometimes with coexistent air trapping. More diffuse ground-glass opacity may reflect coexistent alveolitis (2).

Panbronchiolitis

Panbronchiolitis is a rare disease in the United States, although it is common in Asia (especially Japan and Korea). Pathologically it is characterized by macrophage and mononuclear cell infiltration within the respiratory bronchioles and adjacent alveoli. The HRCT correlate of these pathologic findings is centrilobular nodules, with and without tree-in-bud, air trapping, bronchiectasis, and bronchiolectasis (2, 3).

Follicular Bronchiolitis

Follicular bronchiolitis (FB) represents hyperplasia of the bronchus-associated lymphoid tissue (BALT), characterized

histopathologically by hyperplastic lymphoid follicles with reactive germinal centers distributed along bronchioles and, to a lesser extent, bronchi. FB is associated with collagen vascular diseases (especially rheumatoid arthritis and Sjögren's syndrome), immunodeficiencies, chronic inflammatory diseases (such as bronchiectasis), and hypersensitivity reactions. FB may be thought of as a less extensive "version" of lymphocytic interstitial pneumonitis (LIP); both are associated with similar clinical conditions (collagen vascular disease, immunodeficiency). On HRCT, FB usually appears as lower lobe predominant, small (3 mm or less, rarely up to 12 mm) nodules distributed along the bronchioles and subpleural interstitium. These small nodules along the bronchioles are often seen as centrilobular on HRCT. Foci of ground-glass opacity may be present. Associated findings include bronchiolectasis and bronchial wall thickening, mild interlobular septal thickening, and air trapping. In immunocompromised patients, LIP has a similar appearance, but is usually more extensive than FB. In immunocompetent patients, LIP often appears as small, lower lobe centrilobular ground glass nodules (which histologically represent peribronchiolar cellular infiltration), perhaps associated with cysts. Bronchial wall thickening, adenopathy, and thickening of the peribronchovascular interstitium may be associated (4).

Respiratory Bronchiolitis

Respiratory bronchiolitis is due to irritation from cigarette smoke, and results in inflammation associated with alveolar macrophage accumulation. The typical CT appearance is airway thickening associated with centrilobular ground-glass nodules predominantly in the upper lobes. When extensive, the condition is referred to as *respiratory bronchiolitis-interstitial lung disease* (2, 5). On the most extensive end of the spectrum, when alveolar macrophage accumulation is very extensive, the condition is referred to as *desquamative interstitial pneumonia (DIP)*, or *alveolar macrophage pneumonia*.

Constrictive Bronchiolitis (Bronchiolitis Obliterans)

Constrictive bronchiolitis (CB) is characterized pathologically by submucosal and peribronchiolar fibrosis causing extrinsic airway narrowing. There is little bronchiolar inflammation. The major pathophysiologic consequence of this condition is airflow obstruction, manifest as air trapping on HRCT. Associated conditions include: prior childhood infection (Swyer-James syndrome, *Mycoplasma*), toxic fume inhalation, connective tissue diseases, rheumatoid arthritis, certain drugs (especially penicillamine), in association with inflammatory bowel disease, and in association with neuroendocrine cell hyperplasia. BO is the major manifestation of chronic rejection following lung transplantation, and also may represent chronic graft-versus-host disease following bone marrow transplantation (2, 6).

Proliferative Bronchiolitis (Bronchiolitis Obliterans Organizing Pneumonia)

Proliferative bronchiolitis, or bronchiolitis obliterans organizing pneumonia (BOOP), is characterized histologically by granulation tissue polyps within the lumina of bronchioles and alveolar ducts, often associated with foci of organizing pneumonia. BOOP, like BO, may be seen idiopathically (idiopathic BOOP), or it may be seen in association with certain conditions (BOOP reactions), such as infections (viral, bacterial, and fungal pneumonia), chronic eosinophilic pneumonia, collagen vas-

cular diseases, drug reactions, radiation, and following bone marrow and lung transplantation. HRCT commonly reveals foci of lower lobe peripheral (at least 50% of cases) consolidations and peribronchiolar consolidation (3), often recurrent and migratory. Small nodules and ground-glass opacity may also be seen (2, 6).

HRCT Classification of Small Airway Diseases

For the radiologist, an approach to small airway diseases that utilizes HRCT is far more useful than approaching such patients using a pathologic classification system. Major manifestations of small airway diseases on HRCT include **centrilobular nodules with or without tree-in-bud**, bronchial wall thickening, bronchial dilation, **mosaic perfusion**, and **air trapping** (3). The combination of these findings (as well as other findings, such as consolidation), their distribution, and the clinical and laboratory findings may allow a specific diagnosis. When these findings are insufficiently specific, HRCT provides an accurate map to direct tissue-sampling procedures.

Centrilobular Nodules

Centrilobular nodules represent opacities within the center of the secondary pulmonary lobules. These nodules may reflect infected material, bronchial impaction, or alveolitis. Nodules are identified as centrilobular on HRCT by noting their relationship to the secondary lobule. Functionally, such nodules are seen adjacent to, but not touching, the costal and fissural pleura. The distribution is often patchy, but may be diffuse (particularly in the case of hypersensitivity pneumonitis). Once nodules are identified as centrilobular in distribution, the presence or absence of tree-in-bud opacities must be ascertained. Tree-in-bud represents impaction of small bronchioles, almost always due to pyogenic infections or mucous.

The differential diagnosis of centrilobular nodules with tree-in-bud opacity includes (1):

1. bacterial pneumonia
2. tuberculous and non-tuberculous mycobacteria
3. *Aspergillus* infection (especially airway-invasive *Aspergillus*)
4. cystic fibrosis
5. bronchioloalveolar carcinoma (rare)

Once centrilobular nodules with tree-in-bud are identified, the differential diagnosis is sufficiently narrowed to particular infections such that attempts to recover respiratory pathogens for microbiologic diagnosis are indicated.

The differential diagnosis of centrilobular nodules without tree-in-bud is more extensive (1):

everything that causes centrilobular nodules with tree-in-bud
hypersensitivity pneumonitis
respiratory bronchiolitis
Langerhans cell histiocytosis
pneumoconioses
LIP
pulmonary edema
BOOP

Associated findings (for example, bizarre shaped cysts with Langerhans cell histiocytosis) and the distribution of the findings are important for narrowing the differential diagnosis.

Inhomogeneous Lung Opacity

The appearance of areas of increased and decreased lung attenuation on inspiratory HRCT imaging is termed inhomogeneous lung opacity (1). When inhomogeneous opacity is due to increased pulmonary parenchymal attenuation, ground-glass

opacity is present. When the inhomogeneous opacity is due to areas of decreased lung attenuation, mosaic perfusion is present. When inhomogeneous lung opacity is due to the presence of both increased and decreased lung attenuation, the “headcheese” sign is present (1).

Mosaic Perfusion

When decreased opacity on inspiratory images is the predominant finding (as opposed to small nodules), mosaic perfusion may be present. Mosaic perfusion is caused by alterations in perfusion of the lung parenchyma, resulting in areas of relatively increased attenuation (hyperperfused) and areas of relatively decreased attenuation (hypoperfused) (1). Mosaic perfusion may be differentiated from ground-glass opacity by the observation that vessels within the areas of relatively decreased lung attenuation are abnormally small, whereas in the cases of ground-glass opacity, vessels are equal in size throughout all areas of inhomogeneous lung opacity. The small size of the vessels within areas of mosaic perfusion reflects the diminished blood flow within these areas of lung.

There are two major categories of causes of mosaic perfusion: small airway diseases and vascular occlusion (1). Vascular occlusion is commonly the results of chronic thromboembolic disease or capillaritis from vasculitis. The major categories of small airway diseases resulting in mosaic perfusion include bronchiolitis obliterans (constrictive bronchiolitis), asthma, chronic bronchitis, and hypersensitivity pneumonitis. Vascular and small airway causes of mosaic perfusion may be differentiated with expiratory imaging (7). When the cause of mosaic perfusion is vascular, the inhomogeneous opacity seen on the inspiratory image remains roughly similar on the expiratory image. When the cause of the mosaic perfusion on the inspiratory image is related to small airway disease, however, the appearance of the inhomogeneous lung opacity is accentuated (7). This occurs because lung parenchymal attenuation increases with expiratory imaging as air within the lung is exhaled. With vascular causes of mosaic perfusion, air trapping is not present and all areas of lung increase in attenuation in a similar fashion (there are some normal regional differences, however). With airway causes of inhomogeneous opacity, air trapping impedes the expulsion of air from some areas of lung, whereas other areas decompress normally. This results in an accentuation of the inhomogeneous opacity with expiratory imaging. Overall, small airway causes of mosaic perfusion are far more common than vascular etiologies.

Normal Inspiratory Scans with Air Trapping on Expiratory Imaging

Most patients with air trapping seen on expiratory scans have inspiratory scan abnormalities, such as bronchiectasis, mosaic perfusion, airway thickening, nodules, and tree-in-bud, which may suggest the proper diagnosis. Occasionally, air trapping may be the sole abnormal finding on an HRCT study; the inspiratory scan is normal (8). In this situation, expiratory HRCT techniques are valuable for demonstrating the presence of an underlying airway abnormality (8, 9). This situation may reflect less extensive physiologic derangements than conditions in which abnormalities are visible on the inspiratory images. The differential diagnosis of this situation includes constrictive bronchiolitis (bronchiolitis obliterans), asthma, chronic bronchitis, and hypersensitivity pneumonitis (8). When air-trapping conforming to the configuration of individual pulmonary lobules is detected on expiratory HRCT (“lobular low attenuation”), large or small airway diseases may be the cause. In one investigation, bronchiectasis was the most common cause of such a pattern (10). In this case, the bronchiectasis is not always seen exactly in the areas of lobular low attenuation, but the latter reflects the presence of a more widespread abnormality.

The “Head-cheese Sign”

The head-cheese sign represents the simultaneous presence of ground-glass opacity and mosaic perfusion (representing air trapping) on inspiratory HRCT images. This finding represents mixed infiltrative and obstructive disease, and carries the name “head-cheese sign” due to its resemblance to the variegated appearance of sausage made from the parts of the head of a hog (1). The differential diagnosis of this observation includes hypersensitivity pneumonitis (especially chronic), sarcoidosis, and atypical infections (such as *Mycoplasma pneumoniae*) (1). Respiratory bronchiolitis may also result in this sign.

REFERENCES

1. Webb WR, Muller NL, Naidich DP. High-Resolution CT of the Lung. 3rd Edition. Philadelphia: Lippincott Williams and Wilkins, 2000.
2. Worthy SA, Muller NL. Small airway diseases. *Radiol Clin North Am* 1998; 36:163-173.
3. Hwang JH, Kim TS, Lee KS, et al. Bronchiolitis in adults: pathology and imaging. *J Comput Assist Tomogr* 1997; 21:913-919.
4. Howling SJ, Hansell DM, Wells AU, Nicholson AG, Flint JD, Muller NL. Follicular bronchiolitis: thin-section CT and histologic findings. *Radiology* 1999; 212:637-642.
5. Gruden JF, Webb WR. CT findings in a proved case of respiratory bronchiolitis. *AJR Am J Roentgenol* 1993; 161:44-46.
6. Garg K, Lynch DA, Newell JD, King TE, Jr. Proliferative and constrictive bronchiolitis: classification and radiologic features. *AJR Am J Roentgenol* 1994; 162:803-808.
7. Worthy SA, Muller NL, Hartman TE, Swensen SJ, Padley SP, Hansell DM. Mosaic attenuation pattern on thin-section CT scans of the lung: differentiation among infiltrative lung, airway, and vascular diseases as a cause. *Radiology* 1997; 205:465-470.
8. Arakawa H, Webb WR. Air trapping on expiratory high-resolution CT scans in the absence of inspiratory scan abnormalities: correlation with pulmonary function tests and differential diagnosis. *AJR Am J Roentgenol* 1998; 170:1349-1353.
9. Stern EJ, Frank MS. Small-airway diseases of the lungs: findings at expiratory CT. *AJR Am J Roentgenol* 1994; 163:37-41.
10. Im JG, Kim SH, Chung MJ, Koo JM, Han MC. Lobular low attenuation of the lung parenchyma on CT: evaluation of forty-eight patients. *J Comput Assist Tomogr* 1996; 20:756-762.

Asthma: Role of CT

Denis H. Carr, M.D.

Objective

To demonstrate the use of high-resolution computed tomography (HRCT) in defining both anatomical and functional information in patients with asthma

Asthma is a clinical and functional diagnosis. The diagnosis is not made on CT. HRCT has a defined role in determining both anatomical and functional abnormalities in patients with asthma.

HRCT has a particular value in assessing complications in asthma, for example, consolidation, atelectasis and allergic bronchopulmonary aspergillosis.

Subtle changes in segmental and subsegmental airways can be easily visualised with HCRT. The question has been posed – at what stage do abnormal airways in asthmatics become “bronchiectatic”? The other major question is – “what is the difference, if any, between severe asthma and obstructive/constrictive bronchiolitis (OB)?”.

It is simpler to describe the airway abnormalities in asthma as dilated or non-dilated and bronchial wall thickening as present or absent. It avoids abstract discussion as to the definition of bronchiectasis.

With regard to the definitions of asthma and obliterative bronchiolitis. Asthma is a process characterised by airflow obstruction which may be reversible but in late stages may be only partially reversible. OB patients have irreversible airflow obstruction. Various disease processes including asthma and emphysema must be excluded before a diagnosis of OB can be made.

There is a strong overlap in findings in HRCT between asthma and OB. Both may demonstrate bronchial wall thickening, dilatation of bronchi, patchy decreased attenuation on inspiration and expiration (mosaic pattern) scans.

Several studies have shown varying degrees of correlation between HRCT findings and lung function. Our group has noted a correlation between lung function and two different patterns of air trapping, namely global air trapping and patchy “mosaic” air trapping. Lung function correlates with changes in cross section as mapped on inspiration and expiration CT images.

CT not only has a role in defining anatomical abnormalities in asthma, but is able to give accurate regional and global functional information.

REFERENCES

- Paganin F, Trussard V, Seneterre E et al. *Am Rev Respir Dis* 1992;146:1084-1087.
- Carr DH, Hibon S, Rubens MB, Chung KF. *Resp Med* 1998;92:448-453.
- Jenson SP, Lynch DA, Brown KK, Wenzel SE, Newell JD. *Clin Rad* 2002;57:1078-1085.

“Holes” in the Lung: Radiologic-Pathologic Correlations?

Alexander A. Bankier, M.D.

Department of Radiology
University of Vienna, Austria

There is a multitude of different lesions, solitary or multiple, that radiologists perceive as including or consisting of “holes” on either chest radiographs or CT examinations of the lung. Yet, the definition of the term “hole” applies to a two-dimensional context, whereas the three-dimensional correspondence of the hole is termed cavity. Both hole and cavity are often defined indirectly, i.e., by describing the border of the structure to be defined, while the hole or the cavity itself is the more or less empty space within the border used to define it. This conceptual sophistication makes the descriptive approach to “holes” in the lung both difficult and challenging.

This challenge is increased by the many potential origins that “holes” in the lung might have. These origins may well be restricted to the categories congenital, idiopathic, infectious, neoplastic, traumatic, and post-therapeutic. However, each of these categories include individual lesions such diverse as cysts, bullae, granulomas, papillomas, sequestrations, abscesses, emboli, infarctions, pseudotumors, and malignant tumors. They also include such diverse disorders such as Sarcoidosis, Silicosis, Histiocytosis X, Amyloidosis, Carcinomas, Lymphangiomyomatosis, Lymphomas, Infections, and Carcinomas. This suggests that an indirectly descriptive approach to “holes” in the lung might not meet all the needs required for an accurate and effective diagnostic approach to these lesions.

The current presentation will attempt to overcome existing drawbacks in the diagnostic approach of pulmonary “holes” by first analyzing apparent contradictions as to definition and description of pulmonary “holes”. Based on pathologic correlations, it will then propose an alternative diagnostic categories for these lesions.

LITERATURE

Bankier AA, Brunner C, Lomoschitz F, Mallek R. Pyrofluid inhalation in “fire-eaters”: sequential findings on CT. *J Thorac Imaging*. 1999 Oct;14(4):303-6.

Bankier AA, Stauffer F, Fleischmann D, Kreuzer S, Strasser G, Mossbacher U, Mallek R. Radiographic findings in patients with acquired immunodeficiency syndrome, pulmonary infection, and microbiologic evidence of *Mycobacterium xenopi*. *J Thorac Imaging* 1998; 13:282-288

Bankier AA, Stauffer F, Lomoschitz F, Brunner C. *Mycobacterium xenopi* infection of a 50-year-old oil plumbage complicated by bronchopleural and pleurocutaneous fistulas. *J Thorac Imaging*. 1999 Oct;14(4):307-11.

Cleverley JR, Hansell DM. Imaging of patients with severe emphysema considered for lung volume reduction surgery. *Br J Radiol*. 1999 Mar;72(855):227-35.

Crans CA Jr, Boiselle PM. Imaging features of *Pneumocystis carinii* pneumonia. *Crit Rev Diagn Imaging*. 1999 Aug;40(4):251-84.

Erasmus JJ, Connolly JE, McAdams HP, Roggli VL. Solitary pulmonary nodules: Part I. Morphologic evaluation for differentiation of benign and malignant lesions. *Radiographics*. 2000 Jan-Feb;20(1):43-58.

Franquet T, Muller NL, Gimenez A, Guembe P, de La Torre J, Bague S. Spectrum of pulmonary aspergillosis: histologic, clinical, and radiologic findings. *Radiographics*. 2001 Jul-Aug;21(4):825-37.

Franquet T, Serrano F, Gimenez A, Rodriguez-Arias JM, Puzo C. Necrotizing Aspergillosis of large airways: CT findings in eight patients. *J Comput Assist Tomogr*. 2002 May-Jun;26(3):342-5.

Grum CM, Lynch JP 3rd. Chest radiographic findings in cystic fibrosis. *Semin Respir Infect*. 1992 Sep;7(3):193-209.

Herman SJ. Radiologic assessment after lung transplantation. *Radiol Clin North Am*. 1994 Jul;32(4):663-78.

Kubak BM. Fungal infection in lung transplantation. *Transpl Infect Dis*. 2002;4 Suppl 3:24-31.

Kulwicz EL, Lynch DA, Aguayo SM, Schwarz MI, King TE Jr. Imaging of pulmonary histiocytosis X. *Radiographics*. 1992 May;12(3):515-26.

Legmann P. Imaging and lung disease: uses and interpretation. *Tuber Lung Dis*. 1993 Jun;74(3):147-58.

Levin DL, Klein JS. Imaging techniques for pleural space infections. *Semin Respir Infect*. 1999 Mar;14(1):31-8.

Logan PM, Muller NL. CT manifestations of pulmonary aspergillosis. *Crit Rev Diagn Imaging*. 1996 Feb;37(1):1-37.

Lynch DA. High-resolution CT of idiopathic interstitial pneumonias. *Radiol Clin North Am*. 2001 Nov;39(6):1153-70.

Lynch DA. Imaging of asthma and allergic bronchopulmonary mycosis. *Radiol Clin North Am*. 1998 Jan;36(1):129-42.

Lynch DA. Imaging of small airways diseases. *Clin Chest Med*. 1993 Dec;14(4):623-34.

Maschmeyer G. Pneumonia in febrile neutropenic patients: radiologic diagnosis. *Curr Opin Oncol*. 2001 Jul;13(4):229-35.

Mesuroolle B, Qanadli SD, Merad M, Mignon F, Baldeyrou P, Tardivon A, Lacombe P, Vanel D. Unusual radiologic findings in the thorax after radiation therapy. *Radiographics*. 2000 Jan-Feb;20(1):67-81.

North LB, Libshitz HI, Lorigan JG. Thoracic lymphoma. *Radiol Clin North Am*. 1990 Jul;28(4):745-62.

Nuchtern JG, Harberg FJ. Congenital lung cysts. *Semin Pediatr Surg*. 1994 Nov;3(4):233-43.

Pallisa E, Sanz P, Roman A, Majo J, Andreu J, Caceres J. Lymphangiomyomatosis: pulmonary and abdominal findings with pathologic correlations. *Radiographics*. 2002 Oct;22 Spec No:S185-98.

Tanaka N, Matsumoto T, Miura G, Emoto T, Matsunaga N. HRCT findings of chest complications in patients with leukemia. *Eur Radiol*. 2002 Jun;12(6):1512-22.

Thurlbeck WM, Muller NL. Emphysema: definition, imaging, and quantification. *AJR Am J Roentgenol*. 1994 Nov;163(5):1017-25.

Webb WR. Radiology of obstructive pulmonary disease. *AJR Am J Roentgenol*. 1997 Sep;169(3):637-47.

Weisbrod GL. Pulmonary angiitis and granulomatosis: a review. *Can Assoc Radiol J*. 1989 Jun;40(3):127-34.

Zinck SE, Leung AN, Frost M, Berry GJ, Muller NL. Pulmonary cryptococcosis: CT and pathologic findings. *J Comput Assist Tomogr*. 2002 May-Jun;26(3):330-4.

Zylak CJ, Eyler WR, Spizarny DL, Stone CH. Developmental lung anomalies in the adult: radiologic-pathologic correlation. *Radiographics*. 2002 Oct;22 Spec No:S25-43.

Pulmonary Aspiration: You Are What You Eat

Laura E. Heyneman, M.D.

Objectives: To describe the clinical and radiologic manifestations of pulmonary aspiration

The aspiration of foreign material into the tracheobronchial tree results in a myriad of radiologic patterns that depend on the type and amount of material that is aspirated. The presence of dependent pulmonary opacities in a patient with a known risk factor for aspiration suggests the diagnosis. Risk factors include neurologic abnormalities that affect swallowing and coughing, general anesthesia in a nonfasting patient, abnormalities of the esophagus, and debilitation. However, the diagnosis of aspiration may be difficult when the patient has no known risk factors, when the opacities are not in dependent locations, or when the opacities mimic other conditions such as pulmonary edema, tuberculosis, lung cancer, metastatic disease, and bronchiolitis.

Gastric Acid Aspiration: The aspiration of gastric contents with a very low pH (pH<2.5) is known as Mendelson's syndrome. First described in pregnant women, the syndrome also occurs frequently in alcoholics and IV drug abusers. The acidic material incites a chemical pneumonitis, resulting in diffuse alveolar damage, and a radiographic appearance of noncardiogenic edema.

Aspiration of Partially Digested Food: The aspiration of small particles of partially digested food most often results in a focal opacity that clears rapidly; coughing and mucociliary action usually clear the airways within 24-48 hours of an aspiration event. Diffuse alveolar damage is avoided because the gastric acid was neutralized by the food. Occasionally, aspiration of small food particles incites an inflammatory response in the distal airways (aspiration bronchiolitis) that presents with small nodules rather than as focal consolidation. Histologically, aspiration bronchiolitis is characterized by chronic mural inflammation with foreign body reaction in bronchioles. On high-resolution CT, aspiration bronchiolitis demonstrates branching, centrilobular nodules with a "tree-in-bud" pattern. A similar pattern can be seen in patients who aspirate partially digested legumes (lentil aspiration pneumonia). The vegetable material incites a granulomatous pneumonitis that manifests on radiographs as nodules or reticulonodular opacities. On high-resolution CT, lentil aspiration pneumonia presents with branching centrilobular nodules (a "tree-in-bud" appearance). The opacities may not be confined to dependent portions of the lungs because the vegetables are frequently pureed and may be distributed throughout the lungs due to coughing.

Aspiration of Infectious Material: Aspiration of infectious material from the oropharynx may result in pneumonia, lung abscess, empyema, or bronchopleural fistula formation. Patients at risk for infectious aspiration include those with poor dental hygiene and advanced periodontal disease. The infection in non-hospitalized patients is usually due to anaerobes (i.e. *Bacteroides*) and facultative aerobes such as *Actinomyces israelii*. In hospitalized patients, *Staphylococcus aureus* and gram-negative bacteria (ie. *Pseudomonas aeruginosa*) are typically involved. An aspiration pneumonia may not be evident for 24-72 hours after the aspiration event. If left untreated, the consolidation may go on to necrosis. If the inoculum of bacteria is small and the host's immune system is able to mount a defense, a focal lung abscess may form. Abscesses present as a well-marginated lung mass with or without cavitation. Patients typically describe a 1-2 month constellation of constitutional symptoms such as fever, weight loss, and night sweats. The clinical symptoms and the radiographic appearance may mimic tubercu-

losis. Aspiration of anaerobic bacteria may also manifest with empyema and bronchopleural fistula. Infections with *A. israelii* may present as a homogeneous opacity similar to lobar pneumonia. If untreated, however, an infection by *A. israelii* may progress to involvement of the adjacent ribs and chest wall.

Foreign Body Aspiration: Children are more likely to aspirate a foreign body than adults. The radiologic manifestations of foreign body aspiration depends on the size of the object that is aspirated. Large objects may obstruct the trachea and result in asphyxiation and death. Sudden death due to aspiration of large pieces of food may mimic a myocardial infarction, giving rise to the term "café coronary". The aspiration of small objects may result in bronchial obstruction, with resultant air-trapping, atelectasis, or post-obstructive pneumonia. Occasionally, if the object is mobile within the airways, pulmonary opacities may be migratory. Approximately 5-15% of foreign bodies are radio-opaque. An interesting form of a radio-opaque foreign body is that of aspirated sand or gravel; the calcium carbonate in the aspirated material can result in a sand or gravel bronchogram.

Lipid Aspiration: The aspiration of mineral oil, vegetable oil, or oily mist is most often seen when patients ingest mineral oil to treat constipation or chronically use oil-based nose drops. Patients are frequently asymptomatic or have nonspecific complaints such as cough and dyspnea. Radiographic patterns of lipid aspiration include chronic focal masslike opacities, multifocal consolidation, and chronic segmental or lobar consolidation. CT is extremely helpful in establishing the diagnosis, as fat attenuation within the area of interest is characteristic. A "crazy-paving" pattern of ground glass superimposed on interlobular septal thickening has been described on high-resolution CT.

Chronic Aspiration: Patients with hiatal hernias, gastroesophageal reflux, strokes, esophageal pathology, or laryngeal dysfunction are considered at risk for chronic aspiration. These patients may be asymptomatic or may present with chronic cough and dyspnea. If untreated, recurrent aspiration can result in chronic or recurrent pneumonia as well as pulmonary fibrosis. Other specific forms of chronic aspiration include aspiration bronchiolitis, lentil pneumonia, and lipid pneumonia.

REFERENCES

- Fraser RS, Colman N, Muller NL, Pare PD. Diagnosis of Diseases of the Chest, 4th ed. Philadelphia: Saunders, 1999, 2485-2516.
- Marom EM, McAdams HP, Erasmus JJ, Goodman PC. The Many Faces of Pulmonary Aspiration. AJR 1999;172:121-128.
- Matsuse T, et al. Widespread occurrence of diffuse aspiration bronchiolitis in patients with dysphagia, irrespective of age. Chest 1998;114(1):350-351.
- Marom EM, McAdams HP, Sporn TA, Goodman PC. Lentil aspiration pneumonia: radiographic and CT findings. J Comput Assist Tomogr 1998;22:598-600.
- Hargis JL, Hiller FC, Bone RC. Migratory pulmonary infiltrates secondary to aspirated foreign body (letter). JAMA 1978;240:2469.
- Kennedy JD, Costello P, Baliicia JP, Herman PG. Exogenous lipid pneumonia. AJR 1981;136:1145-1149.
- Franquet T, Gimenez A, Bordes R, Rodriguez-Arias JM, Castella J. The crazy-paving pattern in exogenous lipid pneumonia: CT-pathologic correlation. AJR 1998;170:315-317.

Pleural Effusions

Gerald F. Abbott, M.D.

Rhode Island Hospital / Brown Medical School

Pleural effusion is a common manifestation of local and systemic diseases that involve the thorax, affecting an estimated 1.3 million individuals each year. The most commonly associated diseases are (in decreasing order of frequency) congestive heart failure, bacterial pneumonia, malignancy, pulmonary thromboembolic disease, cirrhosis, pancreatitis, collagen vascular disease, and tuberculosis. Other etiologies include trauma, abdominal disease, and iatrogenic causes.

In normal subjects, a small amount of pleural fluid (5-15 ml) is present within the pleural space providing a frictionless surface between the visceral and parietal layers of pleura as lung volume changes during respiration. Normal pleural fluid forms and flows from capillaries in the parietal pleural and is absorbed via the visceral pleura.

A variety of factors can cause an imbalance in the formation and absorption of pleural fluid: increased hydrostatic pressure, decreased oncotic pressure, decreased pressure in the pleural space, increased permeability of the microvascular circulation, and impaired lymphatic drainage. Fluid may also move from the peritoneal space into the pleural space through diaphragmatic lymphatics or anatomic defects in the diaphragm.

Patients with pleural effusion may be asymptomatic (15%) or have dull aching pain, cough, and dyspnea. Large effusions may displace the mediastinum and cause respiratory distress. The history and physical examination are important elements in guiding the evaluation of pleural effusions. Dullness to percussion and decreased or absent breath sounds are characteristic features in many patients with pleural effusion. Other physical findings may suggest the etiology (e.g. distended neck veins and peripheral edema in CHF).

Thoracentesis is usually performed to evaluate pleural effusions of unknown etiology. The extracted fluid is examined for its gross appearance and odor and submitted for biochemical analysis, white blood cell and red blood cell counts, gram and acid-fast stains, and cytologic evaluation. Invasive diagnostic procedures including closed, open, or thoracoscopic biopsy, are sometimes necessary to establish a diagnosis.

Clinically, most pleural effusions are categorized as transudates or exudates using the criteria established by Light. Exudates have one or more of the following characteristics: 1) fluid-to-serum protein ratio > 0.5 ; 2) pleural fluid LDH > 200 IU; and 3) fluid-to-serum LDH ratio > 0.6 . Transudates have none of those characteristics. Such categorization may be combined with clinical and other laboratory findings to establish a differential diagnosis.

Transudative pleural effusions are characteristically caused by systemic factors that alter pleural fluid formation or absorption. The most common causes of transudative effusions are CHF, cirrhosis, and pulmonary embolism. Exudative effusions result from diseases that alter the pleural surfaces. The most common causes are pneumonia, cancer, and pulmonary embolism. If analysis reveals a transudative pleural effusion, the cause of the systemic disorder can be treated and the pleura does not require further investigation. When an exudative effusion is found, further investigation of the pleura is warranted to determine the etiology of the pleural disease.

Malignant pleural effusions occur in patients with primary or metastatic neoplasia involving the thorax, but most frequently in those with a primary tumor that is extrapulmonary. The most common tumors related to malignant effusions are pulmonary, ovarian, and gastric carcinomas and lymphoma.

Pleural effusions associated with pneumonia (parapneumonic) occur in 40% of cases and are usually serous exudates that resolve. Empyema (pus in the pleural space) may develop as a complication of a parapneumonic effusion. Most empyemas are secondary to spread from a pneumonic focus in the adjacent lung or by formation of a bronchopleural fistula. Affected patients are usually febrile and have an elevated white blood cell count.

A variety of other etiologies are associated with pleural effusion. Systemic lupus erythematosus and rheumatoid disease are the most common causes of pleural effusions in connective tissue disease. Benign asbestos-related effusions occur in 3% of asbestos exposed individuals and are dose-related.

Other fluids may accumulate within the pleural space including blood (hemothorax) and chyle (chylothorax). It is important to distinguish between chylothorax and pseudochyloous effusions. Both look milky white on gross inspection, but are different in their composition and in the mechanisms responsible for their formation. The fluid of a chylothorax contains triglycerides whereas pseudochyloous effusions are rich in cholesterol. Chylothorax typically occurs in the setting of trauma or tumor. In approximately 50% of cases, chylothorax is a complication of thoracic or mediastinal tumor. Postoperative chylothorax usually appears within the week following surgery; post-traumatic chylothorax develops over a longer time period, often a month. Pseudochyloous effusions are rare and are associated with long-standing chronic pleural effusion (e.g. tuberculous pleurisy, rheumatoid pleural effusion).

Imaging features

In the upright patient, small pleural effusions manifest as blunting of the costophrenic sulcus, detectable on the lateral chest radiograph with amounts as small as 25-50 ml and on the frontal radiograph with accumulations of 200 ml. The ipsilateral diaphragm is obscured by effusions of approximately 500 ml. Most effusions are freely mobile in the pleural space and decubitus radiographs may detect effusions as small as 5 ml.

Larger effusions manifest as dense opacities that obliterate the costophrenic angle on both PA and lateral chest radiographs. The peripheral aspect of these opacities characteristically extends cephalad in the upright patient and forms a "meniscus".

In supine patients, pleural effusions manifest as a veil-like opacity that does not obscure the pulmonary vascular structures. The margin of the ipsilateral hemidiaphragm may be hazy and indistinct, the affected costophrenic angle is obscured, and with sufficient accumulation (>500 ml) an "apical cap" is formed and fluid may extend into interlobar fissures.

Atypical radiographic manifestations of pleural effusions include subpulmonic (intrapulmonary) effusions, "pseudotumors" formed by fluid accumulating within interlobar fissures, and diaphragmatic inversion by large effusions. Air within a pleural fluid collection should prompt consideration of the following entities: bronchopleural fistula, hydropneumothorax, trauma, esophageal rupture, and the presence of gas-forming organisms.

Pleural effusions may become loculated and form mass-like opacities that appear fixed and nonmobile, often with edges that are better defined than freely mobile effusions. Empyemas cause smooth thickening of the visceral and parietal pleura surrounding the abnormal fluid collection and manifest as the "split pleura" sign on CT imaging.

CT, ultrasound and MRI are highly sensitive for detecting pleural fluid. Ultrasound is particularly useful in demonstrating septations within loculated collections.

SUGGESTED READING

Fridlender ZG, Gotsman I. Pleural Effusion. *N Engl J Med* 2002; 347:1286-1287.

Fraser RG, Muller NL, Colman N, Pare PD. *Diagnosis of diseases of the chest*, 4th ed. Philadelphia: WB Saunders Co., 1999:2739-2779.

Light RW. *Pleural diseases*. 4th ed. Philadelphia: Lippincott Williams & Wilkins, 2001.

Petersen JA. Recognition of intrapulmonary pleural infusion. *Radiology* 1960; 74:34-41.

Sahn, SA. The pleura. *Am Rev Respir Dis* 1988; 138:184-234.

Vix VA. Roentgenographic manifestations of pleural disease. *Semin Roentgenol* 1977; 12:277-286.

Asbestos Related Pleural Disease and Mesothelioma

Francine L. Jacobson, M.D., MPH

Learning Objectives:

- Understand sources of exposure to asbestos.
- Recognize asbestos exposure on radiographs and CT.
- Review current practice for diagnosis, staging and treatment of malignant pleural mesothelioma (MPM).

Exposure to Asbestos

Asbestos is a fibrous silicate that had been widely used in commercial applications for its unique combination of attributes. It is strong, flexible, and will not burn. It resists corrosion and is an effective insulator. The three most common varieties are chrysotile, amosite, and crocidolite. Chrysotile fibers, widely used in commerce, are pliable and most often arranged in bundles of cylinders. Asbestos fibers can be combined with binding materials and used in a variety of construction applications. It is estimated that 3000 commercial products, ranging from older plastics and paper products to brake linings, floor tiles, cement pipe, and insulation, have contained asbestos. Asbestos containing materials were used most extensively for fireproofing, insulation, soundproofing and decorating in the United States for thirty years following World War II.

Amosite and crocidolite fibers (collectively called amphibole fibers) are like tiny needles. When crushed, asbestos fibers are too small to be seen by the human eye and do not become dust particles. Small and light, the fibers can remain in the air, available to be inhaled, for a long time. The EPA estimates asbestos was included in most of the approximately 107,000 primary and secondary schools and 733,000 public and commercial buildings in the United States. It is estimated that between 1940 and 1980, 27 million Americans had occupational exposure to asbestos. Occupational exposure is greatest among those who work in asbestos mines, mills, factories, shipyards that use asbestos, and those who manufacture and install asbestos insulation. Proximity to such facilities and exposure to the laundry of those occupationally exposed to asbestos also provide significant sources of exposure. Two to six million people in the United States are estimated to currently have significant occupational levels of exposure.

Evidence of Exposure to Asbestos

Pleural effusion, the earliest radiographic finding, may not be attributed to asbestos exposure, if a chest radiograph is even obtained when it is present. It generally occurs within ten years of exposure and may or may not be present years later when pleural plaques have developed. Upon testing, the effusion is exudative with non-specific findings. It can be hemorrhagic and therefore resolves with diffuse pleural thickening. Further complications include calcification and development of rounded atelectasis.

Pleural plaques occur after a latent period of 20-40 years. In approximately 80% of cases, asbestos exposure is known. The plaques consist of acellular collagen bundles primarily involving the parietal pleura and may contain asbestos fibers. For many years it was felt that the fibers reached the parietal pleural by penetrating the visceral pleura, however, they may also reach it via the lymphatics where they incite an inflammatory response. Plaques grow slowly and continue to grow in the absence of continued exposure and without malignant potential. Calcification may occur after 10-20 years. Pleural plaques tend to occur without other stigma of asbestos exposure, such as asbestosis.

Pleural plaques may be calcified or not, but chest radiographic criterion of bilateral hemidiaphragmatic calcification remains the radiographic criterion for the diagnosis of asbestos exposure. Pleural plaques may also be seen following middle ribs, and along the spine. These findings are more apparent on CT scans.

Malignant Pleural Mesothelioma (MPM)

Due to the long latency period, the incidence of MPM has continued to increase in the United States despite the removal of asbestos from commercial use. Two to three thousand cases are now seen per year; MPM is not limited to those with occupational exposure but 6-10% of asbestos workers will develop the disease based on tumorigenesis of amphibole fibers after 35-40 years.

The peak years in which patients present are the 6th to 8th decades of life, particularly when due to occupational exposure. The occupations involved have been male dominated resulting in 3-6:1 ratio of men to women patients. The onset of symptoms is usually insidious characterized by dyspnea, chest pain, cough and weight loss. Right-sided disease is more common and SVC syndrome and Horner syndrome may also be seen. Hypertrophic osteoarthropathy, clubbing and hypoglycemia may complicate the differentiation of this disease from metastatic adenocarcinoma. Pathologically, this differentiation remains difficult. VATS is recommended for diagnosis (98% sensitivity) with special histochemical stains or ultrastructural analysis. Due to the tendency of the tumor to seed the incision, incisions are planned with an eye to be resected at the time of more definitive treatment.

Early in its course, the tumor burden may be relatively small with pleural effusion dominant. While the pleural effusion can be large enough to cause shift of the mediastinum to the contralateral side, decreased volume of the affected hemithorax is far more common. Asbestos pleural plaques are present in approximately 20% of patients. Over time, tumor involving both the parietal and visceral pleural surfaces will progress to encase the lung with reduction in lung volume and fixation of the mediastinum. It will eventually lead to lobulation of pleural masses and invade the contiguous structures including the lung, mediastinum, and chest wall. Distant metastases are a very late phenomenon and very uncommon at initial presentation. The prognosis has improved, particularly for patients with epithelial cell type disease who undergo aggressive multimodality therapy, including extra-pleural pneumonectomy with intra-operative chemotherapy.

MPM presenting as a pleural effusion may present for imaging that is routine but not specific to MPM. Once the diagnosis is established, the primary role of imaging is to help select the course of treatment. The decision to perform a procedure such as an extra-pleural pneumonectomy requires confidence that the entire burden of disease can be removed. If the disease cannot be entirely resected, only palliative therapy, such as pleurectomy, will be offered.

Sagittal and coronal image planes are most helpful to assess extent of disease, particularly regarding potential invasion of chest wall, mediastinum, diaphragm and abdomen. The modality of the imaging may actually be less important although MRI has been used to provide this multi-planar imaging for several years. MR easily differentiates the separate solid components of disease from pleural effusion. MR does remain limited

regarding calcification frequently present though not part of the MPM. The spatial resolution of CT is still required, and CT is generally superior to MR for subtle questions regarding chest wall invasion. The functional information of FDG-PET appears to offer an important addition to the selection process for identifying the patients who will most benefit from aggressive surgery. It can detect otherwise unsuspected distant disease and possibly differentiate subgroups of MPM and quantify tumor burden. Echocardiography is also routinely performed to assess potential involvement of the pericardium as well as cardiac function prior to surgery.

Several staging systems are in use, the historical Butchart Staging System, the surgically driven Brigham/DFCI system, and the TNM system embodied in the New International Staging System. The primary consideration for the radiologist in staging remains determining operability. Those with positive resection margins, N2 nodal disease, advanced stage-particularly with sarcomatous or mixed pathology do not achieve prolonged survival.

An extrapleural pneumonectomy is a radical pneumonectomy, a bit like a radical nephrectomy, in that the surgeon endeavors to remove the lung with its parietal pleura and extra-thoracic fascia without seeing the lung. The hemidiaphragm and pericardium are routinely removed; the hemidiaphragm is then reconstructed with either a flap or synthetic material such as Gore-Tex. Chest wall resection can be performed as necessary to a modest to moderate degree. Ligation of vessels is occasionally considered. Very focal invasion of liver may be considered for extended resection although disease within the abdomen is generally a contraindication to the procedure. Invasion of the aorta, pulmonary artery, or superior vena cava will ordinarily become a contraindication for surgery. Reviewing the imaging with the surgeon can make the critical difference in determining the true operability for an individual patient.

REFERENCES

Benard F, Sterman D, Smith RJ, Kaiser LR, Albelda SM, and Alavi A. Prognostic value of FDG PET imaging in malignant pleural mesothelioma. *J Nucl Med* 1999; 40 (8):1241-1245.

Britton M. The epidemiology of mesothelioma. *Semin Oncol* 2002; 29 (1):18-25.

Carbone M, Kratzke RA, Testa JR. The pathogenesis of mesothelioma. *Semin Oncol* 2002; 29(1): 2-17.

Gerbaudo VH; Sugarbaker DJ, Britz-Cunningham S, Di Carlo MF, Mauceri C, and Treves ST. Assessment of malignant pleural mesothelioma with 18F-FDG dual-head gamma-camera coincidence imaging: Comparison with histopathology. *J Nucl Med* 2002; 43(9):1144-1149.

Marom EM, Erasmus JJ, Pass HI, Patz EF. The role of imaging in malignant pleural mesothelioma. *Semin Oncol* 2002; 29 (1): pp 26-35.

Miller BH Rosado-de-Christenson ML, Mason AC, Fleming MV, White CC, Krasna MJ. From the Archives of the AFIP. Malignant pleural mesothelioma: Radiologic-pathologic correlation. *Radiographics* 1996;16: 613-644.

Patz EF, Rusch VW, Heelan R. The proposed new international TNM staging system for malignant pleural mesothelioma: Application to imaging. *AJR* 1996; 166: 323-327.

Steele JPC. Prognostic factors in mesothelioma. *Semin Oncol* 2002; 29(1): 36-40.

Sugarbaker DJ, Flores RM, Jaklitsch MT, Richards WG, Strauss GM, Corson JM, DeCamp MM, Swanson J, Bueno R, Lukanich JM, Baldini EH, Mentzer SJ. Resection margins, extrapleural nodal status, and cell type determine postoperative long-term survival in trimodality therapy of malignant pleural mesothelioma: Results in 183 patients. *J Thorac Cardiovasc Surg* 1999; 117(1):54-65.

Zellos LS and Sugarbaker DJS. Multimodality treatment of diffuse malignant pleural mesothelioma. *Semin Oncol* 2002; 29(1):41-50.

New TNM International Staging System for Diffuse Mesothelioma

T — Primary Tumor

- T1a Tumor limited to ipsilateral parietal pleura, including mediastinal and diaphragmatic pleura
No involvement of visceral pleura
- T1b Tumor involving ipsilateral parietal pleura, including mediastinal and diaphragmatic pleura
Scattered foci of tumor also involving visceral pleura
- T2 Tumor involving each ipsilateral pleural surface with at least one of the following features:
 - Involvement of diaphragmatic muscle
 - Confluent visceral pleural tumor (including fissures) or extension of tumor from visceral pleura into underlying pulmonary parenchyma
- T3 Locally advanced but potentially resectable tumor
Tumor involving all of ipsilateral pleural surfaces with at least one of the following:
 - Involving endothoracic fascia
 - Extension into mediastinal fat
 - Solitary, completely resectable focus of tumor extending into soft tissues of chest wall
 - Nontransmural involvement of pericardium
- T4 Locally advanced technically unresectable tumor
Tumor involving all of ipsilateral pleural surfaces with at least one of the following:
 - Diffuse extension or multifocal masses of tumor in chest wall, with or without associated rib destruction
 - Direct transdiaphragmatic extension of tumor to peritoneum
 - Direct extension of tumor to contralateral pleura
 - Direct extension of tumor to one or more mediastinal organs
 - Direct extension of tumor into spine
 - Tumor extending through to internal surface of pericardium with or without pericardial effusion, or tumor involving myocardium

N — Lymph Nodes

- NX Regional lymph nodes not assessable
- N0 No regional lymph node metastases
- N1 Metastases in ipsilateral bronchopulmonary or hilar lymph nodes
- N2 Metastases in subcarinal or ipsilateral mediastinal lymph nodes, including ipsilateral internal mammary nodes
- N3 Metastases in contralateral mediastinal, contralateral internal mammary, and ipsilateral or contralateral supraclavicular lymph nodes

M — Metastases

- MX Distant metastases
- M0 No distant metastases
- M1 Distant metastases present

Stage	Description
Ia	T1aN0M0
Ib	T1bN0M0
II	T2N0M0
III	Any T3M0 Any N1M0 Any N2M0
IV	Any T4 Any N3 Any M1

Other Pleural Neoplasms

Sujal R Desai, MD, MRCP, FRCR

Consultant Radiologist, King's College Hospital, London, England

Objectives

To appreciate the relative rarity of primary pleural tumours
To understand the radiological features of pleural neoplasms but also acknowledge their non-specificity

Introduction

It is a fact that pleural tumours are rare and only account for a negligible proportion of all intrathoracic neoplasms. Indeed, the view that there are no *primary* pleural tumours was strongly held by many, until relatively recently. Interestingly, such conviction was maintained in the face of evidence which revealed the potential for mesothelial cells to differentiate into epithelial or sarcomatous cell lines (1).

Classification of Pleural Neoplasms (*other than Malignant Pleural Mesothelioma*)

Whilst diffuse malignant pleural mesothelioma is perhaps the commonest and most widely studied tumour, a variety of other pleural neoplasms, may be encountered (albeit rarely) in clinical practice (see *Table*). Primary tumours of the pleura (some bearing enigmatic names), include the so-called *localised fibrous tumour of the pleura*, *calcifying fibrous pseudotumour*, *multicystic mesothelial proliferation* and *adenomatoid tumours*. However, the more common scenario is that of metastatic dissemination to the pleura, from a number of primary sources (but most typically breast or lung). In the vast majority of patients histologic examination of secondary pleural disease will confirm the presence of adenocarcinoma. However, lymphoma, malignant thymoma, a variety of sarcomas and melanoma may also spread to the pleura.

Imaging of Pleural Neoplasms

It will come as little surprise to most readers that the radiologic features (on plain chest radiography or computed tomography [CT]) of pleural masses are non-specific. In itself, this is not the issue. For practical purposes, there are two basic conundrums: firstly, in the case of a localised mass, the radiologist must distinguish between a "true" pleural lesion and a peripheral intrapulmonary or indeed, a chest wall mass. The second question arises in the context of diffuse pleural thickening when the radiologist must discern what is benign and what is likely to represent malignant pleural involvement.

Localised pleural masses:

The plain radiographic appearance of a pleural mass will vary depending on whether it is being viewed *en face* or tangentially. On a frontal radiograph, the interface between the lung and a pleural (or chest wall) mass is usually well demarcated, in contrast to an intrapulmonary neoplasm, in which the margin between a mass and normal lung tends to be less well defined.

Laterally, a pleural lesion will appear to make obtuse angle with the chest wall, again in contrast to an intrapulmonary neoplasm where the angle tends to be acute. Unless there is obvious rib destruction, the distinction between a pleural mass and a chest wall lesion is frequently impossible based on chest radiographic signs alone.

Because of the superior contrast resolution of CT compared to chest radiography and the absence of anatomical superimposition, the evaluation of pleural lesions can be more accurate. Determining whether or not there is an obtuse angle with the lateral wall is rendered more straightforward by CT. Furthermore, subtle variations in density within a lesion (e.g. internal calcification or the predominantly low [fat] density of a lipoma) or the presence of adjacent rib or chest wall involvement will be readily demonstrated.

Diffuse pleural thickening:

When there is widespread pleural thickening, a common question posed to the radiologist is whether or not the process is malignant. In this regard CT may prove particularly valuable. In patients with diffuse pleural thickening, Leung and colleagues have shown that there are four CT signs which strongly suggest the possibility of malignancy: 1) a circumferential pleural thickening (sensitivity 41%, specificity 100%); 2) nodularity (sensitivity 51%, specificity 94%); 3) pleural thickness greater than 1cm (sensitivity 36%, specificity 94%) and 4) mediastinal pleural involvement (sensitivity 56% specificity 88%) (2). The presence of calcification tends to suggest a benignity (92% specificity). It is important to remember that, these CT signs, whilst suggesting pleural malignancy do not distinguish between malignant mesothelioma and other pleural malignancies (particularly as metastatic adenocarcinoma) (2). Furthermore, the data indicate that whilst the positive predictive of the above CT signs for malignancy is high, the negative predictive value (ie the likelihood that there is no malignancy in the absence of these signs is not. Finally, it is salutary to note that even with recent advances in CT technology, there is a vogue among physicians for relying on thoracoscopy, as opposed to imaging, for make the diagnosis (and staging) of pleural malignancy (3-5).

Summary

Primary pleural neoplasms are rare. In many cases, radiological examination is the first to highlight the presence of a pleural mass. Compared to chest radiography, CT allows more accurate analysis. This presentation will some discuss the primary pleural tumours, other than malignant pleural mesothelioma, including a brief discussion of the histopathological characteristics as relevant to imaging. The chest radiographic and CT features of pleural lesions, in general will reviewed.

TABLE: CLASSIFICATION OF PLEURAL NEOPLASMS OTHER THAN MALIGNANT MESOTHELIOMA

PRIMARY

Neoplastic

Localised fibrous tumour of the pleura
Multiple benign fibromas
Calcifying fibrous pseudotumour
Adenomatoid tumour
Desmoplastic small round cell tumour
Pleural lymphoma (*pyothorax-associated /body-cavity based lymphoma*)

Non-neoplastic

Thoracic splenosis
Endometriosis
Fibrin body
Amyloid

SECONDARY

Metastatic adenocarcinoma (breast, lung, ovary, stomach, large bowel, kidney)
Malignant thymoma
Lymphoma
Melanoma
Sarcomas

REFERENCES

- (1) Stout AP, Murray MR. Localized pleural mesothelioma: investigation of its characteristics and histogenesis by the method of tissue culture. Arch Pathol 1942; 34:951-964.
- (2) Leung AN, Müller NL, Miller RR. CT in differential diagnosis of diffuse pleural disease. AJR 1990; 154:487-492.
- (3) Boutin C, Rey F. Thoracoscopy in pleural malignant mesothelioma: a prospective study of 188 consecutive patients. Part 1: diagnosis. Cancer 1993; 72:389-393.
- (4) Menzies R, Charbonneau M. Thoracoscopy for the diagnosis of pleural disease. Ann Intern Med 1991; 114:271-276.
- (5) Mathur P, Martin WJII. Clinical utility of thoracoscopy. Chest 1992; 102(1):2-4.

FURTHER READING:

Desai SR, Wilson AG. Pleural and Pleural Disorders. In: Imaging of Diseases of the Chest. Armstrong P, Wilson AG, Dee P, Hansell DM eds. 3rd Edn. Mosby, St Louis
Corrin B. Pleura and Chest Wall. In: Pathology of the Lung. Churchill Livingstone, London

Image-Guided Therapy of Malignant Pleural Effusions

H. Page McAdams, M.D.

Learning Objectives:

At completion of this lecture, the attendee will be able to:

1. Describe indications for image-guided treatment of malignant pleural effusions.
2. Explain image-guided treatment of malignant pleural effusions.
3. Discuss the use of fibrinolytic and sclerosing agents for management of malignant pleural effusions.

Definition:

Malignant pleural effusions are common in cancer patients with advanced disease. Approximately 50% of patients with breast carcinoma, 25% of patients with lung carcinoma and 35% of patients with lymphoma develop a malignant effusion during the course of their disease. Patients with malignant effusions present with progressive dyspnea, cough, and chest pain that compromises their quality of life.

Treatment Options:

Treatment options depend on the extent of disease, effectiveness of systemic therapy, and patient performance status. Pleural effusions in patients with lymphoma, small cell lung cancer or germ cell malignancies may be controlled by systemic treatment alone. Patients with pleural metastatic disease refractory to systemic therapy may require palliative treatment to improve their quality of life. Therapeutic options include thoracentesis, large bore tube thoracostomy and sclerotherapy, and thoroscopic instillation of sclerosing agents such as talc. Numerous studies have now shown that malignant effusions can be effectively managed by image-guided small bore catheter drainage and sclerotherapy. Imaging guidance is particularly useful in these patients both for localizing pleural abnormalities and for avoiding unnecessary procedures in patients with central obstructing masses, a thick pleural peel, or multiple loculated fluid pockets.

Tube Placement:

We typically place our catheters in the mid-axillary line at the sixth or seventh interspace using either US or fluoroscopic guidance and adequate conscious sedation. The skin entrance site is marked and prepped using aseptic technique. The skin is anesthetized with 1% topical lidocaine and an 18 gauge trocar needle is placed directly into the pleural space. Fluid is aspirated to confirm the intrapleural location of the needle. A 0.38, 100 cm floppy-tip guidewire is then fed through the needle to guide tube placement and to mechanically break up pleural adhesions. With the guidewire in position, progressive dilation of the drainage tract is performed and a 14 French pig tail catheter is inserted. The chest tube is then secured by a catheter retention device and up to 1 liter of fluid is immediately aspirated. If the patient begins to cough or complain of increased shortness of breath during aspiration, we discontinue further aspiration.

A post tube placement radiograph is obtained to assure proper placement of the tube. Up to 30% of patients will have a pneumothorax on the post tube placement films. This is usually due to an 'ex vacuo' phenomenon and will resolve over the next few days. When the patient is returned to the ward, the tube is connected to a Pleur-evac with continuous wall suction at 20 to 25 cm H₂O. Daily tube outputs are recorded and tubes are

flushed with 10 cc of normal saline every 8 -12 hours. Patients are seen each day to assure that the tube is functioning properly. Daily chest radiographs are not obtained when drainage continues without difficulty. When drainage decreases to 150-200 cc in a 24-hour period, a chest radiograph is performed to exclude loculated fluid and to assure complete lung re-expansion. It is important that the pleural fluid is completely drained and that the lung is completely re-expanded prior to instillation of the sclerosing agent.

Sclerotherapy:

Once the pleural space has been drained (usually 2 to 5 days), a sclerosing agent is infused. The most common agents are doxycycline, bleomycin or a sterile talc slurry. The dosage for doxycycline is 500 mg in 100 cc of normal saline. The dosage for Bleomycin is 60 units in 100 cc of D5W. The dosage for talc is 5 grams in 100 cc saline. Although no single sclerosant has been shown to have a clear advantage over the others, we are currently using talc because it is both effective and inexpensive. We usually add 10 cc of a one percent lidocaine solution to the talc slurry for pain control. Most patients require some degree of pain control and sedation during instillation of either talc or doxycycline. Pain is the most common complication of sclerotherapy. A small percentage of patients develop systemic complaints such as fever after bleomycin or talc instillation. There are rare reports of serious reactions, including ARDS and death, following instillation of large amounts of talc, usually 10 grams or greater.

After the sclerosing agent is instilled, the tube is closed to suction and the patient is instructed to change positions every 15 minutes for 2 hours in order to evenly distribute the sclerosant throughout the pleural space. The tube is then reopened to suction until the following day when the tube is removed if overnight drainage is less than 200 cc. Repeat sclerosis is recommended if the overnight drainage is greater than 200 cc.

Complications:

Complications are unusual and include tube malfunction (e.g., clotting or kinking) or malposition, infection, loculation, pneumothorax and re-expansion pulmonary edema (see below). Tubes with decreased drainage are flushed with saline, heparin or streptokinase to determine patency; guide wire insertion is occasionally required to re-establish tube patency. If the tube is severely kinked or clotted, it may have to be replaced.

If the pleural fluid is loculated, multiple drainage catheters may be required. We have also found that fibrinolytic agents such as streptokinase are quite useful for managing complex or loculated collections. We typically instill 250,000 U of streptokinase mixed in 100 cc of normal saline directly into the pleural space. The tube is then closed for 2 hours to allow the fibrinolytic agent to distribute throughout the pleural space and is thereafter reopened to continuous suction. We repeat instillation on a daily basis as needed. The choice of fibrinolytic agent is controversial. While streptokinase is less expensive than either urokinase or tPA, it is antigenic and can cause fever in up to 28% of treated patients. Urokinase is non-antigenic, does not cause fever, and may be slightly more effective than streptokinase. The dosage for Urokinase is 100,000 units in 100 cc of normal saline. Unfortunately, Urokinase is not currently available for intrapleural injection in the United States. Experience with tPA in the pleural space is limited.

Re-expansion Pulmonary Edema:

Re-expansion pulmonary edema is an uncommon, but occasionally life-threatening complication of pleural drainage. Many (perhaps most) patients with re-expansion edema have only minimal symptoms. Fortunately, very few patients develop life-threatening dyspnea. When it occurs, however, re-expansion edema is quite difficult to treat. The best treatment is, in fact, prevention. Risk factors include:

- Rapid re-expansion of lung
- Evacuation of more than 1500 cc of pleural fluid per day
- Prolonged collapse (> 72 hours) of subsequently re-expanded lung
- High negative intrapleural pressure

In order to prevent re-expansion edema, we typically withdraw only one liter of fluid when the catheter is placed. We also stop withdrawing fluid if the patient experiences symptoms such as cough, chest pain or increasing dyspnea. If there is a large volume of residual fluid (two or three liters), we may leave the catheter closed for several hours and then open it to gravity drainage. Suction is applied by Pleur-evac only when most of the fluid has been evacuated by gravity drainage. It should be recognized, however, that symptomatic re-expansion edema can occur despite careful attention to detail. These risks, including the risk of death from re-expansion edema, should be carefully explained to the patient during informed consent.

Ambulatory Drainage:

Selected highly functional patients can be offered ambulatory drainage. We usually place a smaller catheter in these patients (10.3 French APDC) and connect it to a Tru-Close 600 cc bag (UreSil, L.P. Skokie, IL 60077) for gravity drainage. Patients are provided with home care instructions and instructed to return to clinic for sclerotherapy when drainage falls below 200 cc per day. In clinic, a radiograph is obtained to confirm complete fluid drainage, absence of loculations, and complete lung re-expansion. Any remaining fluid is aspirated prior to instillation of the sclerosing agent. Following instillation of the sclerosing agent, the tube is clamped and the patient is instructed to change positions frequently. After 2 hours, the tube is reopened to gravity drainage, the patient is sent home, and is instructed to return the following day for chest tube removal.

The Pleuryx Catheter (Denver Biomedical, Golden, CO) is a further option for ambulatory treatment of malignant effusions. This is a tunneled catheter placed into the pleural space using a trocar, guidewire and a peel-away sheath. The catheter has a Teflon cuff to prevent bacterial contamination of the pleural space. Fluid is removed periodically (every one-two days) using small disposable vacuum bottles (1 liter). Preliminary results suggest that this technique is as efficacious as conventional inpatient therapy, with few complications, and markedly reduced cost.

SELECTED REFERENCES

- Chang YC, Patz EF Jr, Goodman PC. Pneumothorax after small-bore catheter placement for malignant pleural effusions. *AJR* 1996; 166:1049-1051.
- Marom EM, Patz EF Jr, Erasmus JJ, et al. Malignant pleural effusions: treatment with small-bore-catheter thoracostomy and talc pleurodesis. *Radiology* 1999; 210:277-81.
- Marom EM, Erasmus JJ, Herndon JE, Zhang C, McAdams HP. Usefulness of image-guided catheter drainage and talc sclerotherapy in patients with metastatic gynecologic malignancies and symptomatic pleural effusions. *AJR* 2002; 179:105-8.
- Morrison MC, Mueller PR, Lee MJ, et al: Sclerotherapy of malignant pleural effusions through sonographically placed small-bore catheters. *AJR* 1992; 158:41.
- Moulton JS, Moore PT, Mencini RA. Treatment of loculated pleural effusions with transcatheter intracavitary urokinase. *AJR* 1989; 153:941.
- Parulekar W, Di Primio G, Matzinger F, Dennie C, Bociek G. Use of small-bore vs large-bore chest tubes for treatment of malignant pleural effusions. *Chest* 2001; 120:19-25.
- Patz EF Jr, McAdams HP, Goodman PC, et al. Ambulatory sclerotherapy for malignant pleural effusions. *Radiology* 1996; 199:133-135.
- Pollak JS, Burdge CM, Rosenblatt M, Houston JP, Hwu WJ, Murren J. Treatment of malignant pleural effusions with tunneled long-term drainage catheters. *J Vasc Interv Radiol* 2001; 12:201-8.
- Putnam JB Jr, Walsh GL, Swisher SG, et al. Outpatient management of malignant pleural effusion by a chronic indwelling pleural catheter. *Ann Thorac Surg.* 2000; 69:369-75.
- Putnam JB Jr, Light RW, Rodriguez RM, et al.. A randomized comparison of indwelling pleural catheter and doxycycline pleurodesis in the management of malignant pleural effusions. *Cancer* 1999; 86:1992-9.
- Seaton KG, Patz EF Jr, Goodman PC. Palliative treatment of malignant pleural effusions: value of small-bore catheter thoracostomy and doxycycline sclerotherapy. *AJR* 1995; 164:589-591.

Notes

A large empty rectangular area with a black border, intended for taking notes. The border is composed of a vertical line on the left and a horizontal line at the bottom, meeting at a rounded corner at the bottom-left.

Monday

March 3, 2003

General Session

Monday

7:00 - 8:00 am Continental Breakfast Americana 4

8:00 - 11:00 am Guest Hospitality Suite Moon Room

Cardiovascular Imaging: Heart I

Moderator: Curtis Green, MD

Americana 3

8:50 - 9:10 Cardiac MR: Established Indications
Charles White, MD

9:10 - 9:30 Cardiac MR: New Developments
Gautham Reddy, MD

9:30 - 9:50 Session Discussion

9:50 - 10:10 am Coffee Break Americana 4

Cardiovascular Imaging: Aorta and Other

Moderator: Stephen Miller, MD

Americana 3

10:10 - 10:30 CT Angiography of the Thoracic Aorta
Poonam Batra, MD

10:30 - 10:50 Acute Aortic Syndromes
Ernest Scalzetti, MD

11:10 - 11:30 Pulmonary Veins: Imaging for Radiofrequency Ablation Procedures
Michael Sneider, MD

11:30 - 11:50 Imaging of Cardiopulmonary Support Technology
Philip Cascade, MD

11:50 - 12:00 Session Discussion

12:00 - 2:00 pm STR Annual Business Meeting/Lunch Americana 4

March 3, 2003 General Session

Monday

Cardiovascular Imaging: Pulmonary Vascular

Americana 3

Moderator: Lawrence Goodman, MD

2:00 - 2:20 Epidemiology of Venous Thromboembolic Disease
Lacey Washington, MD

2:20 - 2:40 MDCT Pulmonary Angiography
James Gruden, MD

2:40 - 3:00 CT Structural and Functional Imaging of PE
Joseph Schoepf, MD

3:00 - 3:20 Non Thrombotic Pulmonary Embolism
Lawrence Goodman, MD

3:20 - 3:40 Pulmonary Hypertension
Aletta Frazier, MD

3:40 - 4:00 Session Discussion

4:00 - 4:15 pm Coffee Break

Americana 4

Benjamin Felson Memorial Lecture

Americana 3

Moderator: Ella Kazerooni, MD

5:30 - 7:30 PM General Reception

Americana Lawn

Cardiac MRI: Established Indications

Charles S. White, M.D.

University of Maryland
Baltimore, MD

Overview

Role of MRI as Compared with Other Techniques

The traditional imaging techniques used for cardiac imaging are echocardiography, cardiac catheterization and nuclear cardiology. This approach to cardiac imaging in part reflects the earlier development of these techniques as well as the referral patterns of cardiac patients. MRI of the heart was first made possible in the early 1980's by the development of ECG triggering (gating). More recent innovations permit a wide range of cardiac assessment by MRI. Cardiac MRI has major advantages because of the high intrinsic contrast between the blood pool and surrounding structures, the large field-of-view and ability to image in any plane, and versatility of multiple sequences. Nevertheless, cardiac MRI plays a secondary role to the techniques described above and is still used mainly when these techniques fail provide diagnostic information or are ambiguous. There are certain indications for which cardiac MRI provides superior information and these applications will be highlighted.

General Considerations

Cardiac MR imaging requires that the patient remain in the magnet for some length of time. A good examination is difficult in patients who are uncooperative or disoriented. However, if the patient is only mildly uncooperative, it is possible to obtain much useful information with fast imaging techniques, depending on the indication. Similar to MR imaging studies of other parts of the body, cardiac MRI is contraindicated in patients with a variety of foreign devices, including certain aneurysm clips, cochlear implants and penile prostheses. MRI is also contraindicated in patients who have pacemakers or implantable cardioverter defibrillator (ICD) devices. In general, MRI can be performed in patients who have prosthetic cardiac valves. Patients who have undergone recent cardiac surgery (CABG or valve surgery) can probably be studied 1-2 weeks after the procedure although this has not been documented conclusively.

Cardiac MRI Set Up

ECG-gating is mandatory in order to achieve a study of good quality. Gating is triggered to the R-wave and thus image degradation occurs in patients who have irregular cardiac rhythms such as atrial fibrillation in which the R-R interval is highly variable. Because a high quality study depends on effective ECG triggering, it is advisable to ensure that the technologist obtains a good ECG-tracing both outside and inside the machine prior to beginning the examination. The tracing is often somewhat degraded once the patient is moved into the machine bore. To achieve a proper tracing it may be necessary to relocate the ECG leads on the patient several times. If no ECG-tracing can be obtained, a less desirable alternative is to gate from the pulse oximeter (peripheral gating). Respiratory artifact may also substantially degrade the image. Respiratory gating is time consuming and is not widely used. Another strategy employs respiratory compensation, which consists of reordering the sequence information to smooth out respiratory variations. A respiratory bellows is wrapped around the abdomen to perform these techniques. A more recent approach uses "navigator" pulses to track the diaphragm. Only imaging with the diaphragm in a predefined window is accepted.

For many situations, cardiac imaging in adults can be performed using the standard body coil. However, improvement in

signal-to-noise is achieved by using a specialized phased cardiac coil. For infants, a head coil can be used.

Overview of Sequences Used in Cardiac MRI

Cardiac sequences can be divided generically into dark-blood and bright-blood (gradient-echo) sequences. For dark-blood imaging multislice T1-weighted spin-echo sequences are giving way to double inversion sequences that are faster, and can be done in a breath hold. T2-weighted images are infrequently used but may be appropriate in patients with cardiac masses or pericardial disease.

Gradient-echo sequences (bright blood) are useful to supplement spin-echo sequences. They can be used to perform fast imaging and obtain physiologic information. Gated, gradient-echo images can be placed in a cine format that allows visualization of cardiac motion at a single level in any plane throughout the cardiac cycle. When fast gradient techniques are applied, the entire cardiac cycle can be imaged in a single breathhold. Gradient-echo techniques are also sensitive to turbulence which causes loss of signal. Gradient-echo techniques can be phase-encoded so that information about blood flow and velocity can be obtained. Steady state free precession (True FISP, balanced FFE) sequences are now widely used to improve segmentation between myocardium and blood pool.

Selected Topics in Adult Cardiac MRI

- 1) Cardiac and paracardiac lesions
- 2) Pericardial disease
- 3) Valvular and ischemic heart disease
- 4) Cardiomyopathies and dysplasias
- 5) Functional cardiac imaging

1) Cardiac and Paracardiac Lesions

Thrombus is a frequent cause of a cardiac lesion. Thrombus is particularly common in the left atrium in patients with atrial fibrillation and is often located along the back wall or in the atrial appendage. Thrombus may be difficult to distinguish from a cardiac tumor. Enhancement after gadolinium chelate administration is more typical of tumor than thrombus. Metastatic cardiac lesions are about ten to forty times more prevalent than primary cardiac tumors. Common sites of origin of metastatic lesions include lung, breast and skin. Lymphomatous involvement of the heart is also common. Spread of extracardiac tumors may occur through the systemic (renal cell carcinoma, hepatocellular carcinoma) or pulmonary (lung carcinoma) veins.

The most common primary cardiac tumor is the myxoma, which is almost always benign histologically. Seventy-five percent are located in the left atrium where most are attached by a pedicle to the atrial septum near the fossa ovalis. The tumor occurs in the right atrium in about 20% of patients and is found in a ventricle occasionally. Atrial myxomas are usually pedunculated and may prolapse through valves, causing regurgitation. Tumor fragments may embolize and cause systemic or pulmonary symptoms. Rhabdomyomas are less common tumors that typically manifest in infancy and have a strong association with tuberous sclerosis. Another interesting tumor-like condition is called lipomatous hypertrophy of the interatrial septum, which consists of a large quantity of unencapsulated fat that is deposited in and widens the atrial septum, and may even project into the right atrium. Malignant primary tumors of the heart are

rare, and consist largely of sarcomatous lesions, particularly angiosarcoma.

2) Pericardial Disease

The pericardium is well-visualized on spin-echo images as a dark-signal intensity structure that is highlighted by the bright signal intensity of the surrounding epicardial and mediastinal fat. The normal pericardium measures no more than 3 mm in width. A simple (transudative) pericardial effusion appears as widening of the pericardium with maintenance of the low signal intensity on T1-weighted images. It is particularly well-seen anterior to the heart and lateral to the left ventricle. Pericardial fluid usually appears bright on T2-weighted gradient-echo images. Hemorrhagic or exudative fluid may show medium or high signal intensity on T1-weighted images.

Echocardiography is the primary technique used to detect pericardial effusions but is less optimal in defining pericardial thickening due to constriction. Pericardial constriction has a similar clinical and hemodynamic profile to restrictive cardiomyopathy. Moreover, therapeutically there is an important distinction between restrictive cardiomyopathy, in which medical treatment is directed at the underlying cause, and pericardial constriction, in which surgical stripping is often performed. MR imaging is the technique of choice to make this distinction. The finding of a thickened pericardium confirms the diagnosis of pericardial constriction. MR imaging is also useful to diagnose congenital absence of the pericardium.

3) Valvular and Ischemic Heart Disease

Echocardiography remains the principal technique to evaluate valvular disease. Both the valve diameter and estimate of the gradient across the valve can be measured with echocardiography. On MRI, it is also possible to detect valvular stenosis or regurgitation on gated gradient-echo images (cine MRI). Using this bright blood sequence, stenosis or regurgitation is identified as a plume of low-signal intensity that emanates from the valve in the direction of blood flow during the appropriate part of the cardiac cycle. The low-signal intensity is caused by dephasing that occurs in the turbulent jet. Some physiologic low signal intensity may be observed in otherwise normal patients but it is usually less extensive and of shorter duration. Valvular vegetations are difficult to identify but perivalvular abscess or septic pseudoaneurysm is more readily shown on MRI.

Most ischemic heart disease is evaluated by echocardiography, angiocardiology and nuclear cardiology, although the role of MRI is increasing rapidly. From the standpoint of morphology, MRI is occasionally used to distinguish between true and false aneurysms. True aneurysms involve all three layers of the heart, and are typically apicolateral. False aneurysms traverse all three layers with containment by the pericardium or mediastinal structures. A posteroinferior location is most common. A false aneurysm requires urgent surgical repair to prevent free rupture. The key to differentiation of the two entities on MRI is evaluation of the neck of the aneurysm. True aneurysms are wide-mouthed whereas false aneurysms are narrow-mouthed.

4) Cardiomyopathies and Dysplasias

Three major types of cardiomyopathy are recognized: hypertrophic, dilated and restrictive. Most patients with cardiomyopathy undergo echocardiography and/or angiocardiology and MR imaging is used in a secondary role. The most common type of hypertrophic cardiomyopathy is characterized by asymmetric thickening of the septum in comparison with the lateral wall of the left ventricle. There is (paradoxical) systolic anterior motion (SAM) of the mitral valve that may contribute to the outflow obstruction in the subaortic region. MRI findings show striking thickening of the septum and, often, lateral wall of the

left ventricle with nearly complete obliteration of the ventricular cavity during systole. MRI can also demonstrate the turbulent flow in left ventricular outflow track and SAM of the mitral valve.

Dilated cardiomyopathy is caused by ischemia and a variety of toxic and infectious agents that lead to severe compromise of the left ventricular ejection fraction. MRI typically shows a markedly dilated left ventricle that is hypokinetic. Restrictive cardiomyopathy is due to several infiltrative diseases (amyloidosis, sarcoidosis, hemochromatosis) that impair diastolic filling. On MRI, it appears as slight myocardial thickening with relatively preserved myocardial function. The main role of MRI is to distinguish it from pericardial constriction.

A condition for which MR imaging has proved to be a primary technique is arrhythmogenic right ventricular dysplasia (ARVD). ARVD is an abnormality that occurs predominantly in adolescents and young and may cause ventricular tachycardia or sudden death. Pathologically, it is caused by replacement of the right ventricular free wall myocardium by fat or fibrosis. MRI findings in this condition include areas of fatty replacement and marked thinning of the free wall. Cine imaging may reveal abnormalities of wall motion.

5) Functional Cardiac Imaging

A further indication of the versatility of cardiac MR imaging is its ability to provide functional information about cardiac status. Using cine imaging, wall motion abnormalities due to ischemia or primary myocardial disorders can be assessed. Left ventricular ejection fraction (end diastolic volume - end systolic volume/end diastolic volume) can be calculated by acquiring multiphase images contiguously through the heart along its short axis. The end-diastolic and end-systolic volumes can be determined for each section allowing determination of a global left ventricular ejection. Alternatively, the ejection fraction can be estimated from a single long axis image. As noted above, valvular disease can be detected with gradient-echo imaging. The severity of the lesion correlates qualitatively with the extent of loss of signal that emanates from the valve. Another capability of MR imaging is to calculate shunting in patients with septal lesions. This measurement is obtained using a phase encoded gradient echo sequence to measure blood flow in the aorta and pulmonary artery. The proportion of flow in the two vessels indicates the amount of shunting (i.e. a left-to-right shunt demonstrates more flow in the pulmonary artery).

SUGGESTED READING

- Earls JP, Ho VB, Foo TK, Castillo E, Flamm SD. Cardiac MRI: recent progress and continued challenges. *J Magn Reson Imaging* 2002 Aug;16(2):111-27.
- Grebenc ML, Rosado-de-Christenson ML, Green CE, Burke AP, Galvin JR. Cardiac myxoma: imaging features in 83 patients. *Radiographics* 2002 May-Jun;22(3):673-89.
- Araoz PA, Eklund HE, Welch TJ, Breen JF. CT and MR imaging of primary cardiac malignancies. *Radiographics* 1999 Nov-Dec;19(6):1421-34.
- Frank H, Globits S. Magnetic resonance imaging evaluation of myocardial and pericardial disease. *J Magn Reson Imaging* 1999 Nov;10(5):617-26.
- Rozenshtein A, Buxt LM. Computed tomography and magnetic resonance imaging of patients with valvular heart disease. *J Thorac Imaging* 2000 Oct;15(4):252-64.
- Kayser HW, van der Wall EE, Sivananthan MU, Plein S, Bloomer TN, de Roos A. Diagnosis of arrhythmogenic right ventricular dysplasia: a review. *Radiographics* 2002 May-Jun;22(3):639-48; discussion 649-50.

Cardiac MRI: New Developments

Gautham Reddy, M.D.

Coronary artery disease (CAD) is the leading cause of death in the United States and other industrialized countries. Although a reduction in the prevalence of CAD has been noted over the past 2 decades, the increasing age of the population will result in more patients developing coronary artery disease. The number of Americans older than 65 years is approximately 25 million and over the next 50 years is expected to exceed 65 million. Cardiac MRI is a rapidly evolving modality that can be applied to the evaluation of ischemic heart disease, including the appraisal of perfusion, left ventricular function (wall motion), viability, and coronary obstruction.

Perfusion. Myocardial perfusion imaging can be assessed by MRI, which offers several advantages over other imaging methods. MRI uses no ionizing radiation, offers high spatial resolution (which allows delineation of the subendocardial layer) and good temporal resolution, and allows assessment of left ventricular function during the same examination. A recent study has shown that MRI perfusion examination can detect coronary lesions with a sensitivity of 90% and a specificity of 83%.

Left ventricular function / Wall motion. Pharmacological stress MRI with high-dose dobutamine can be used to detect areas of ischemic myocardium. Stress MRI is safe and has greater diagnostic accuracy than dobutamine stress echocardiography. A recent study has shown that stress MRI has greater sensitivity (86% vs 74%), specificity (86% vs 70%), and accuracy (86% vs 73%) than stress echocardiography. The most important clinical indication is the assessment of stress-induced wall-motion abnormalities in patients whose stress echocardiography examination is of moderate or poor quality.

Viability. In patients with ischemic heart disease, it is important to differentiate between viable and non-viable myocardium, independent of ventricular function in response to stress. Contrast-enhanced MRI can differentiate between viable and non-viable myocardium independent of the age of infarction, and without regard to ventricular function. MRI viability studies can detect acute and chronic infarcts with high sensitivity (100% acute, 91% chronic) and can precisely localize the area of infarction.

Coronary MRA. Invasive x-ray coronary angiography remains the gold standard for the identification of clinically significant CAD. Although numerous noninvasive tests have been

developed to assist in the identification of patients with coronary artery disease, a substantial minority of patients referred for elective diagnostic x-ray coronary angiography are found not to have clinically significant coronary stenosis (defined as a reduction in the luminal diameter of at least 50 percent).

Recently, Kim et al performed a prospective, multicenter study to determine the clinical usefulness of free-breathing coronary MR angiography in the diagnosis of native-vessel coronary artery disease. A total of 636 of 759 proximal and middle segments of coronary arteries (84%) were interpretable on MR angiography. In these segments, 78 (83%) of 94 clinically significant lesions (>50 luminal stenosis on x-ray angiography) were detected by MR angiography. Overall, coronary MR angiography had an accuracy of 72% for diagnosing coronary artery disease. The sensitivity, specificity, and accuracy for patients with disease of the left main coronary artery or three-vessel disease were 100%, 85%, and 87%, respectively. The negative predictive values for any coronary artery disease and for left main artery or three-vessel disease were 81% and 100%, respectively. In effect, free-breathing MR angiography can reliably identify or rule out left main coronary artery or three-vessel disease.

REFERENCES:

1. Al-Saadi N, Nagel E, Gross M, et al. Noninvasive detection of myocardial ischemia from perfusion reserve based on cardiovascular magnetic resonance. *Circulation* 2000; 101:1379-1383.
2. Nagel E, Lehmkuhl HB, Bocksch W, et al. Noninvasive diagnosis of ischemia-induced wall motion abnormalities with the use of high-dose dobutamine stress MRI: comparison with dobutamine stress echocardiography. *Circulation* 1999; 99:763-770.
3. Simonetti OP, Kim RJ, Fieno DS, et al. An improved MR imaging technique for the visualization of myocardial infarction. *Radiology* 2001;218:215-223.
4. Wu E, Judd RM, Vargas JD, et al. Visualization of presence, location, and transmural extent of healed Q-wave and non-Q-wave myocardial infarction. *Lancet* 2001;357:21-28.
5. Kim WY, Danias PG, Stuber M, et al. Coronary magnetic resonance angiography for the detection of coronary stenoses. *N Engl J Med* 2001; 345:1863-1869.

CT Angiography of the Thoracic Aorta

Poonam Batra, M.D.

CT aortic angiography (CTA) consists of acquiring volumetric helical CT images of thoracic aorta at peak contrast enhancement during the rapid intravenous injection of contrast material, within a breath hold period. This presentation will focus on the technical aspects of CTA, will describe the current protocol of CTA at UCLA and will discuss the pitfalls encountered in the interpretation of CTA.

In spiral CT by slip ring interfaces, a volume of data is acquired by continuously rotating x-ray tube and detector array to cover the target volume as the patient is moved simultaneously through the gantry. In the decade since the introduction of single-slice spiral CT, the improvement in technology has led to the development of 4-slice multidetector array CT (MDCT) with a 360° gantry rotation in sub second. UCLA has just installed a 16-slice machine (Siemens SOMATOM Sensation 16) with a gantry rotation speed of 0.5 sec. for 360° revolution. The multi-detector CT provides faster scanning time and enhanced image quality and is ideally suited for angiography.

With multi-detector CT one can acquire more slices, retrospectively reconstruct overlapping images and acquire a better data set for a single study. However, this has produced a major challenge for data storage requirement, transferring data across intranet and for viewing images, which may run into hundreds and thousands for a single study on multi-detector CT. This number of images make printing on the films almost impractical. Viewing of these many images requires picture archiving and communication system (PACS) workstations. Even with PACS workstations, it is difficult to scroll through hundreds of images per study. Although no ideal solution has been proposed, conversion to 3-D volume data set offers potential to solve the problem of slow loading and storage. Additionally, it has been suggested that instead of storing raw data per study, one may store only the image data, but this will allow only limited ability to manipulate the electronic data. For example, it will not allow decrease of slice thickness or change in the reconstruction algorithm.

Spiral CT Scan Parameters

In helical (spiral) CT the x-ray traces a helix on the patient's body surface resulting in a helix of raw projection data from which planar images are generated. Each rotation of the x-ray tube generates data specific to an angle plane of the section. To acquire an axial image the data points above and below the desired plane of section are interpolated. The technique allows retrospective and arbitrary selection of anatomic levels. In General Electric Lightspeed Qxi multidetector CT four interweaving helices are traced. It has 16 rows of detector. The information from these detectors is combined into 4 channels providing nominal section thickness of 1.25, 2.5, 3.75, 5.0, 7.5 and 10 mm.

The parameters that need to be considered for performing a good quality CT angiography include slice thickness, table feed speed in mm/gantry rotation, contrast administration, reconstruction interval and post processing of data. When slice thickness (mm) is equal to table feed speed (mm per gantry rotation), the technique is considered to have a pitch of 1. When the table speed is double the slice thickness, the pitch equals 2.

Increasing pitch generates increasing noise. In single slice CT scanner the time required for 360° gantry rotation was 1 sec., while in newer scans it is sub second (0.8 and 0.5 sec. respectively for our two scanners). In multi-slice CT scanner the pitch refers to the ratio of table speed (mm/rotation) to total beam collimation (number of detector channels x width of each channel).

Although the transverse plane resolution of spiral CT is equivalent to the conventional CT, the longitudinal plane or Z-axis resolution is degraded because of increased volume-averaging effect produced by broadening of the section sensitivity profile (SSP). The effective section thickness is defined as a full width at half maximum of the SSP. Most current scanners use 180° linear interpolation algorithms so that SSP is minimized. But this is achieved at the expense of increasing noise. In a single slice CT at a pitch of 1, effective slice thickness is equal to collimator setting, while at a pitch of 2, effective slice thickness is 30% greater than designated collimation. In lightspeed multi-detector CT there is much less broadening of SSP. It uses different interpolation algorithms based on acquisition mode and it is difficult to determine the effective slice thickness based on pitch, collimation and interpolation.

Reconstruction of images and Field of View

In spiral CT images can be reconstructed anywhere along the volume and at arbitrary intervals to produce overlapping images. Overlapping images produce smooth 3-D renderings and decrease partial volume artifacts. Longitudinal resolution improves when reconstruction interval is less than slice thickness. To improve spatial resolution, the field of view should be decreased, thus decreasing pixel size. A field of view of 20-25 cm is often used for CTA.

Post Processing of Data

The post processing methods include multiplanar and curved planar reformations, shaded surface display, maximum intensity projection (MIP) and volume rendering.

Current CTA Protocol at UCLA

In order to optimize CTA, intravenous contrast medium administration must be synchronized with the image acquisition. The current protocol for performing CTA on 4-slice helical CT scanner (General Electric Lightspeed OXi) is described below:

1. Obtain a scout view. (This determines the scan length.)
2. Initial non-contrast CT examination is performed with 3.75 mm slice thickness, 120 kV, and low mAS (80) from lung apices to diaphragmatic hiatus at suspended inspiration whenever possible.
3. Intravenous contrast medium is administered preferably via right antecubital vein to avoid streak artifacts. If the contrast medium is administered via left antecubital vein streak artifacts originate from dense contrast medium in the left brachiocephalic vein across the aortic arch.
4. Non-ionic contrast medium with 350 mg I/ml (iohexol [omnipaque 350; Nycomed, Princeton, NJ]) is administered to reduce nausea, vomiting or motion during rapid injection of contrast.

5. The volume of contrast medium required is equivalent to the injection rate (ml/sec.) multiplied by scan duration (sec.). A bolus of 120-150 ml of the contrast medium is administered by power injector if scanning only the thoracic aorta, but it is increased to 200 ml if scanning both thoracic and abdominal aorta.
6. The injection rate is 3 ml/sec. via a 22 gauge intravenous angio-catheter.
7. A 30 second delay time is used between the start of injection and onset of scanning. Although timing scan is not routinely obtained at our institution, it may be acquired in patients with cardiac dysfunction to determine time delay for peak aortic enhancement. In this procedure, a bolus of 20 ml of contrast material is injected via a peripheral vein at a rate of 3 ml/sec. Beginning 10 seconds after the start of injection, 20 dynamic images are obtained at the level of aortic arch at 2-second intervals (i.e., 1 sec./section scan acquisition time, 1 second interscan delay). A time attenuation curve is generated at the arch level by placing a region of interest (ROI) and delay time is calculated from the start of injection to peak aortic enhancement. Alternatively, the manufacturer's automated technique such as "Smart Prep" (General Electric Medical Systems, Milwaukee, WI) or "Care Bolus" (Siemens, Erlangen, Germany) can be used where a series of low milliamperage (mA) single scans are obtained until the desired threshold density is reached and the high mA spiral aortic scan is performed.
8. 120kV, 180-280 mAS, 0.8-second time per gantry rotation.
9. The patient is hyperventilated 3 times prior to scanning and the scan is acquired in suspended inspiration.
10. The field of view for the CT Angiogram is approximately 20-25 cm, detector collimation is 2.5 mm, slice thickness is 2.5 mm and the table speed is 15mm per gantry rotation (high speed HS mode). The images are acquired caudo-cranial from the aortic hiatus in the diaphragm to 2 cm above the arch.
11. The images are reconstructed at 1.5 mm interval with standard reconstruction filter.
12. Sagittal oblique reformations (MPR) are performed through aortic arch at the scanner. Data is transferred to PACS workstation for interpretation. In selected cases, data is also transferred to clinical 3D laboratory for performing shaded surface display, curved planar reformations or maximum intensity projection. Every other image is printed on film as 20:1 format, axial contrast sequence at vascular window. Additionally the oblique sagittal reformation images of aorta are also printed. (Although reformations do not improve sensitivity for the disease detection, they do better display the anatomic relationships and extent of disease in a format that is familiar to most clinicians.)

UCLA has just installed a 16 channel Siemens Sensation 16 scanner. The protocols for the clinical applications are being developed currently.

Pitfalls in interpretation of Thoracic Aortic Angiography

A variety of pitfalls are encountered when interpreting CTA, particularly for aortic dissection and aneurysms. These are

attributed to technical factors, streak artifacts, periaortic structures, aortic wall motion, aortic variations such as congenital ductus diverticulum or acquired aortic aneurysm, and penetrating atherosclerotic ulcer.

Technical factors: Optimal contrast enhancement is critical to the diagnosis of aortic pathology, for example aortic dissection. Improper timing of contrast material administration relative to image acquisition or slow rate of injection may fail to opacify the lumen sufficiently to demonstrate intimal flap resulting in false - negative diagnosis.

Streak artifacts: High attenuation material within or outside the patient may generate streak artifacts on both non-contrast and contrast enhanced images. These appear as straight parallel lines that radiate from a single point and generally exceed the confines of aorta. Conversely, intimal flaps are thin and smooth, slightly curved and restricted to aortic lumen. Strategies to reduce these artifacts include the use of diluted contrast material, injection of contrast material in right antecubital vein and acquiring scan in caudo-cranial direction.

Periaortic Structures: Several vessels such as origins of arch vessels, left brachiocephalic, left superior intercostal and left pulmonary veins may simulate double lumen or intimal flap. Residual thymus, superior pericardial recess, atelectasis, pleural thickening or effusion, periaortic fibrosis or lymphoma can also simulate aortic dissection. These structures can be identified on reviewing contiguous images, and by the knowledge of normal anatomy.

Aortic wall motion and normal aortic sinuses

The pendular motion of ascending aorta produces curvilinear artifacts in the left anterior and right posterior aspect of aortic root. The combined pendular and circular motion of the aorta on the other hand produces a circumferential artifact over the ascending aorta. The motion artifact is restricted to only one or two adjacent scans. The artifact can be minimized by reconstructed images generated with 180° linear interpolation algorithm or by electrocardiographic gating of the scan.

Normal aortic sinuses are recognized by their characteristic location at the same level as the proximal left coronary artery.

Congenital aortic diverticulum and acquired aortic aneurysm

Congenital aortic diverticulum appears as a smooth focal bulge with obtuse angles with the aortic wall. It is located at the aortic isthmus.

A fusiform aneurysm with intraluminal thrombus may simulate aortic dissection with thrombosed false lumen. However, on non-contrast images high attenuation thrombosed false lumen and internal displacement of intimal calcification is seen in dissection. Calcification occurring on the surface of an intraluminal thrombus in an aneurysm is difficult to distinguish from aortic dissection.

Penetrating atherosclerotic ulcer

It is an atheromatous lesion where the ulcer, a focal contrast material filled out-pouch protrudes from the intima into the media and produces intramural hemorrhage. It generally occurs in descending aorta and an intimal flap is absent.

REFERENCES

- Kalender WA, Seissler W, Klotz E, Vock P. Spiral volumetric CT with single-breath-hold technique, continuous transport, and continuous scanner rotation. *Radiology* 1990; 176:181-183.
- Brink JA. Technical aspects of helical (spiral) CT. *Radiol Clin North Am.* 1995; 33(5):825-41.
- Polacin A, Kalender WA, Marchal G. Evaluation of section sensitivity profiles and image noise in spiral CT. *Radiology* 1992; 185(1):29-35.
- Klingenbeck-Regn K, Schaller S, Flohr T, Ohnesorge B, Kopp AF, Baum U. Subsecond multi-slice computed tomography: basics and applications. *Eur J Radiol.* 1999; 31(2):110-24.
- Rubin GD. Techniques for performing multidetector-row computed tomographic angiography. *Tech Vasc Interv Radiol.* 2001; 4(1):2-14.
- Rankin SC. CT angiography. *Eur Radiol.* 1999; 9(2):297-310.
- Rubin GD. Data explosion: the challenge of multidetector-row CT. *Eur J Radiol.* 2000; 36(2):74-80.
- Batra P, Bigoni B, Manning J, Aberle DR, Brown K, Hart E, Goldin J. Pitfalls in the diagnosis of thoracic aortic dissection at CT angiography. *Radiographics.* 2000; 20(2):309-20.
- Kazerooni EA, Bree RL, Williams DM. Penetrating atherosclerotic ulcers of the descending thoracic aorta: evaluation with CT and distinction from aortic dissection. *Radiology.* 1992; 183(3):759-65.

Acute Aortic Syndrome

Ernest M. Scalzetti, M.D.

January 2003

Four conceptually distinct but clinically interrelated conditions of the thoracic aorta.

Aortic Dissection

Pathogenesis

Usually, intimal disruption with dissection of blood in the aortic media

It is thought that the aortic wall is weakened by medial degeneration

Clinical features

Risk factors

Males>females, at least 2:1

Most patients also have systemic hypertension

Other predisposing factors: Marfan syndrome, pregnancy, pre-existing aneurysm, cocaine use, etc.

Presentation

Typical age at presentation:50-70 years

Pain (chest pain, intrascapular back pain)

Hypertension

Unequal extremity blood pressures

"Acute dissection" presents within 2 weeks of onset of symptoms

Classification based on location, correlates with prognosis

Type A involves ascending aorta

Type B is limited to descending aorta

Treatment

Type A usually managed surgically

Type B usually managed medically

Although the type A dissections are more lethal in the acute phase, type B dissections can be life-threatening as well.

Diagnosis: CT and MR features

Intimal flap separating true and false lumen

Extent of involvement

Aortic insufficiency

Patency or involvement of branch vessels

Hemopericardium

Intramural Hematoma

Pathogenesis

Hemorrhage into the aortic media, without an intimal tear

Source of hemorrhage: vasa vasorum

Clinical features

Presentation similar to aortic dissection

Classification similar to aortic dissection

Treatment is controversial; for now, recommendations are similar to those for aortic dissection

Diagnosis: CT and MR features

Appearance of acute blood in aortic wall

Extent of involvement

Penetrating Atherosclerotic Ulcer

Pathogenesis

Atherosclerosis with ulceration that penetrates the intima

Blood from the aortic lumen has access to the aortic media

May lead to IMH, aortic dissection, pseudoaneurysm or rupture

Aortic dissection, when it occurs, usually is limited in extent

Clinical features

Presents with severe chest/back pain of sudden onset

Uncommon presentation: atheroembolism

May be asymptomatic

Pleural effusion may be present

Occurs in elderly hypertensive men

Can involve any portion of the aorta

Most common in mid- and distal descending thoracic aorta

Often involves an ectatic or aneurysmal segment of aorta

May be multiple

Range in diameter from 5-25 mm.

Range in depth from 4-30 mm.

Most can be managed medically

Surgery versus endovascular (stent-graft) therapy

Diagnosis: CT and MR features

Crater-like outpouching from the aortic lumen

Thickened aortic wall

Severe atherosclerosis of the surrounding aorta

Aortic Rupture

Pathogenesis

Traumatic transection

Pre-existing aneurysm, dissection, IMH or penetrating ulcer

Spontaneous?

Clinical features

Presents with chest/back pain

Usually presents with hemodynamic instability

Site of rupture may be anywhere in thoracic aorta, but in trauma it usually is in the proximal descending aorta

High mortality without surgical intervention

Diagnosis: CT and MR features

Mediastinal hematoma

Abnormal contours of aortic lumen

Hemothorax may be present

Signs of instability in a partially thrombosed pre-existing aneurysm

REFERENCES :

- Hartnell GG. Imaging of aortic aneurysms and dissection: CT and MRI. *J Thoracic Imag* 2001;16:35-46.
- Khan IA, Nair CK. Clinical, diagnostic and management perspectives of aortic dissection. *Chest* 2002;122:311-28.
- Levy JR, Heiken JP, Gutierrez FR. Imaging of penetrating atherosclerotic ulcers of the aorta. *AJR* 1999;173:151-4.
- Prete R, Von Segesser LK. Aortic dissection. *Lancet* 1997;349:1461-64.
- Sawhney NS, DeMaria AN, Blanchard DG. Aortic intramural hematoma: an increasingly recognized and potentially fatal entity. *Chest* 2001;120:1340-6.
- Troxler M, Mavor AID, Homer-Vanniasinkam S. Penetrating atherosclerotic ulcers of the aorta. *Br J Surg* 2001;88:1169-77.
- Yokoyama H, et al. Spontaneous rupture of the thoracic aorta. *Ann Thorac Surg* 2000;70:683-9.

Valvular Heart Disease

Lynn S. Broderick, M.D.

Objectives

At the completion of this course, the attendee should be able to:

1. Describe major causes of valvular heart disease
2. Describe the typical radiographic appearance of valvular heart disease including chest radiography, CT and MR
3. Describe the physiology of valvular heart disease and how it affects patients' symptoms

Basic Principles of Valvular Heart Disease

When a cardiac valve is stenotic, the proximal chamber hypertrophies in order to overcome the increased pressure necessary to pump blood through the valve. The receiving chamber is unaffected by the stenotic valve. When a cardiac valve is regurgitant, both the proximal and receiving chambers dilate; the delivering chamber because it is receiving additional blood volume through the regurgitant valve, and the receiving chamber as it receives this additional blood volume during its filling phase. Echocardiography is the study of choice in evaluation of valvular heart disease. However, the diagnosis may be first suggested on chest radiograph. Patients with known valvular heart disease may also demonstrate typical findings on cross-sectional imaging. MR imaging may be performed in cases where echocardiography is unable to fully evaluate the heart. Gated 2D *fiesta* images will demonstrate the signal void of the jet of blood being forced through a stenotic valve or the retrograde jet of blood through a regurgitant valve. Phase contrast sequences can be performed to quantitate the peak velocity.

Aortic Stenosis

Aortic stenosis may result from a congenital abnormality, a sequela of rheumatic heart disease or may be due to age-related degeneration. The stenotic aortic valve results in pressure overload for the left ventricle, which must hypertrophy in order to maintain cardiac output. The hypertrophied left ventricle requires an increased supply of oxygen due to the increased muscle mass as well as the increased work that is being performed. This can result in an oxygen imbalance that leads to angina, even in the presence of normal coronary arteries. During periods of exercise, there is increase in peripheral capacitance. In the normal person, the left ventricle responds to this by increasing the cardiac output. In aortic stenosis, the left ventricle may be responding maximally at rest and will be unable to increase cardiac output. This can lead to decreased blood flow to the brain resulting in syncope. Decreased blood flow to the left ventricle can also result in ventricular arrhythmias leading to syncope or sudden death. If the left ventricle fails, dyspnea and signs of heart failure may be the dominant symptoms.

Congenital bicuspid aortic valve occurs in 1-2% of the population. The two cusps can be oriented in an anterior and posterior position, with the right and left coronary arteries arising from the anterior leaflet or they may be oriented in a left and right position with one coronary artery arising from each leaflet. The anterior or right leaflets have a raphe, the site where the commissure should have formed. Complications of bicuspid aortic

valve include valvular stenosis, valvular regurgitation and bacterial endocarditis. Patients with aortic malformations have a high incidence of bicuspid aortic valve. For example, approximately 50% of patients with aortic coarctation will also have a bicuspid aortic valve. Turbulent blood being ejected through the abnormal valve is thought to result in wear and tear causing thickening of the leaflets. Calcification of the valve begins during the 4th decade of life. As with all causes of aortic stenosis, the amount of valvular calcification correlates with the severity of the stenosis. The diagnosis of a bicuspid aortic valve can be made on chest radiograph when the valve and raphe are calcified. As the valve becomes stenotic, the blood is pumped through at increased pressure and forms a jet. This jet of blood can, over time, cause dilatation of the ascending aorta. Patients with aortic stenosis secondary to a bicuspid aortic valve tend to present earlier in life than patients with aortic stenosis from other causes.

Rheumatic fever occurs following beta-hemolytic streptococcal pharyngitis. Valvular disease secondary to rheumatic fever almost always involves the mitral valve. Mitral valve disease occurs 7-10 years following rheumatic endocarditis with aortic stenosis developing approximately seven years following the onset of mitral valve disease. As the endocarditis heals, the commissures thicken and fuse resulting in stenosis. Asymmetry of the fused commissures may result in the appearance of a bicuspid valve. However, there is greater asymmetry of the leaflet size in rheumatic aortic stenosis than in congenital bicuspid aortic valve.

Age-related degeneration of the aortic valve can occur in patients over the age of 65 and affects women more than men. The leaflets thicken and eventually calcify, resulting in a stenotic valve. In contrast to rheumatic aortic stenosis, the commissures are not fused in age-related degenerative aortic stenosis.

The chest radiograph and cross-sectional imaging will show normal vascularity and may show evidence of left ventricular hypertrophy. Calcification of the aortic valve may be present and is seen best on the lateral view as it is obscured by the spine on the PA radiograph. It should be noted that patients might have aortic stenosis without evidence of valvular calcification on the chest radiograph. However, visible calcification of the aortic valve on the chest radiograph implies aortic stenosis. In patients with bicuspid aortic stenosis, prominence of the ascending aorta secondary to post-stenotic dilatation may be identified. This is due to the jet effect of blood being pumped through the narrowed valve, which is directed toward the lateral wall of the aorta. The aortic arch and descending aorta will be normal.

Aortic Regurgitation

Aortic regurgitation can occur secondary to an abnormal aortic valve or from an abnormality of the aortic root. Congenital bicuspid aortic valve can result in aortic regurgitation if the larger of the two cusps does not appose the smaller cusp. Degenerative and rheumatic aortic stenosis may result in aortic regurgitation due to shortening of the leaflets as they thicken. Bacterial endocarditis can cause perforation of the valve leaflets

as well as separation of the cusps due to involvement of the annulus. Dilatation of the aortic root can occur in patients with aortitis, aortic dissection, systemic hypertension, cystic medial necrosis and connective tissue disease.

When the aortic valve is regurgitant, the left ventricle receives the normal blood volume from the left atrium as well as the regurgitant volume from the aorta. To compensate for this increased blood volume, the left ventricle enlarges in order to maintain cardiac output. However, over time, the increased stroke volume leads to decreased systolic function. The left ventricle requires an increased oxygen demand due to the increased stroke volume and increased wall tension as a result of dilatation. This may result in angina. Left ventricular enlargement might be identified on chest radiograph. However, the ventricle must enlarge almost twice its size before this is reliably seen. Cross-sectional imaging will show dilatation of the left ventricle and aorta.

Mitral Stenosis

Rheumatic heart disease accounts for nearly all cases of mitral stenosis. Women are affected much more frequently than men. Mitral stenosis occurs several years after the initial endocarditis and is a result of fibrotic thickening of the valve and scarring and retraction of the chordae tendinae. The stenotic valve increases the left atrial pressure, which is transmitted to the pulmonary vasculature resulting in pulmonary venous hypertension. The left atrium also dilates with dilatation of the left atrial appendage. If the left atrial appendage is not dilated, it may represent a preavalvular lesion such as atrial myxoma or mobile thrombus or may represent chronic clot that has retracted the appendage. The left ventricle, which is distal to the site of stenosis, will be normal in size. With progression of mitral stenosis, patients will develop interstitial edema. With continued elevated venous pressure, pulmonary arterial hypertension develops with increase in size of the main pulmonary artery. With longstanding mitral stenosis, pulmonary valve regurgitation, right ventricular failure and tricuspid regurgitation may occur.

The chest radiograph and cross-sectional imaging will show redistribution of the pulmonary vasculature, mild left atrial enlargement, with enlargement of the left atrial appendage and may show prominence of the main pulmonary artery. Calcification of the left atrium is a late sequelae of rheumatic endocarditis.

Patients with mitral stenosis may initially be asymptomatic. As the left atrial pressure increases, the patient experiences dyspnea on exertion. Dyspnea is also a symptom when pulmonary arterial hypertension develops. Once the right ventricle fails, symptoms include peripheral edema and ascites. Right heart failure also leads to decreased left ventricular cardiac output leading to fatigue.

Mitral Regurgitation

Although mitral regurgitation can result from rheumatic heart disease, unlike mitral stenosis, there are multiple additional causes of mitral regurgitation. Abnormality of the mitral valve leaflets (fusion, calcification, retraction) is frequently seen in patients with rheumatic heart disease. Calcific or myxomatous degeneration of the valve, and endocarditis can also result in a regurgitant mitral valve. If the left ventricle, and therefore the mitral annulus are dilated, the mitral valve leaflets may fail to close. Usually the left ventricle is dilated secondary to ischemic heart disease or cardiomyopathy. Abnormality of the tensor

apparatus can result in mitral valve regurgitation. This can occur with rupture of the papillary muscle following myocardial infarction or papillary muscle dysfunction secondary to ischemia. Rupture of the chordae tendinae can occur in patients with endocarditis and mitral valve prolapse. Rheumatic heart disease can result in shortening and thickening of the chordae tendinae resulting in mitral valve regurgitation. Occasionally, exuberant calcification of the mitral annulus may adhere to and immobilize the posterior mitral leaflet resulting in regurgitation.

The chest radiograph and cross-sectional imaging will show evidence of left atrial enlargement, which is usually more pronounced than in patients with isolated mitral stenosis. Enlargement of the left atrial appendage can be seen in patients with mitral regurgitation secondary to rheumatic heart disease. Because the left ventricle also sees the increased stroke volume, left ventricular enlargement will be present although this is not as reliably demonstrated on chest radiographs as left atrial enlargement. Redistribution of the pulmonary vasculature and mild interstitial edema will also be present. If mitral regurgitation occurs acutely, such as in papillary muscle rupture, cardiac decomposition occurs. However, the chest radiograph may not show evidence of left atrial and left ventricular enlargement as in patients with slowly developing mitral regurgitation, since the cardiac chambers do not have time to adapt. Patients with left atrial enlargement may develop atrial fibrillation. Occasionally, patients with mitral regurgitation may show evidence of edema localized to the right upper lobe. This is thought to be secondary to the regurgitant blood being directed toward the right superior pulmonary vein.

Pulmonary Stenosis

Pulmonary stenosis usually results from a congenital lesion in which there is thickening of the leaflets with or without fusion of the commissures, or there is a congenitally bicuspid pulmonary valve. Abnormalities associated with congenital pulmonary stenosis include ASD, VSD, TOGV, single ventricle and tetralogy of Fallot. Rare causes of pulmonary stenosis include rheumatic heart disease and carcinoid tumor, metastatic to the liver. In the setting of carcinoid, vasoactive amines result in thickened valve leaflets. Pulmonary valve stenosis results in increased right ventricular systolic pressure. The right ventricle responds by hypertrophying. The right atrial pressure increases due to the elevated right ventricular filling pressures. With elevation of the right atrial pressure, the foramen ovale can become patent resulting in a right-to-left shunt. In the setting of right ventricular failure secondary to pressure overload, the right ventricle dilates which can lead to stretching of the tricuspid annulus and resultant tricuspid regurgitation. In the absence of right-to-left shunt and right ventricular failure, patients may be asymptomatic.

In patients with congenital pulmonary stenosis, the chest radiograph and cross-sectional imaging shows enlargement of the main pulmonary artery and left pulmonary artery. This is due to a high velocity jet directed at the anterior wall of the main pulmonary artery with turbulence extending into the left pulmonary artery. The right pulmonary artery, which takes off at a more acute angle to the main pulmonary artery, is unaffected. Right ventricular hypertrophy may be identified on the lateral view, with filling of the retrosternal space. Subpulmonary narrowing may occur due to hypertrophy of the crista supraventricularis. This may cause outflow obstruction that can persist after valve replacement.

Pulmonary Regurgitation

Pulmonary valvular regurgitation usually results from severe pulmonary arterial hypertension. Less common causes include infectious endocarditis, carcinoid and syphilis. Chest radiograph and cross-sectional imaging shows findings of pulmonary arterial hypertension with enlargement of the central pulmonary arteries and dilatation of the right ventricle.

Tricuspid Stenosis

An uncommon lesion, tricuspid stenosis is usually associated with rheumatic heart disease and mitral stenosis. Carcinoid syndrome can cause tricuspid stenosis, in which case the pulmonary valve is usually involved, and typically there is a degree of tricuspid insufficiency. Prevalvular lesions such as right atrial myxoma and extension of renal cell carcinoma into the inferior vena cava and right atrium can also cause right atrial outflow obstruction. Patients typically present with fatigue due to decreased cardiac output, and symptoms of systemic venous hypertension such as hepatomegaly, ascites and peripheral edema. Chest radiograph and cross-sectional images will show signs of elevated systemic venous pressure with enlargement of the vena cavae, azygos vein and dilatation of the right atrium.

Tricuspid Regurgitation

In the majority of cases, tricuspid regurgitation is a result of right ventricular failure with dilatation of the tricuspid annulus. Less common causes include carcinoid tumor, infectious endocarditis, particularly in drug abusers, and rupture of the papillary muscle. If pulmonary venous hypertension is not present, tricuspid regurgitation may be well tolerated. If pulmonary

venous hypertension is present, such as in patients with mitral valve disease, patients with tricuspid regurgitation develop symptoms of systemic venous hypertension. The chest radiograph and cross-sectional imaging will show right heart enlargement and dilatation of the azygos vein and vena cavae. CT scan with intravenous contrast may show reflux of contrast into the hepatic veins.

REFERENCES

- Elliott LP. Cardiac imaging in infants, children and adults. Philadelphia, 1991, JB Lippincott
- Lester SJ, Heilbron B, Gin K, et al. The natural history and rate of progression of aortic stenosis. *Chest* 1998; 113:1109-1114
- Lippert JA, White CS, Mason AC, Plotnick GD. Calcification of aortic valve detected incidentally on CT scans: Prevalence and clinical significance. *Am J Roentgenol* 1995; 164:73-77
- Lipton MJ, Coulden R. Valvular heart disease. *Radiol Clin N Am* 1999; 37:319-339
- Miller SW. Cardiac Radiology. St. Louis, 1996, Mosby-Year Book
- Sabet HY, Edwards WD, Tazelaar HD, Daly RC. Congenitally bicuspid aortic valves: A surgical pathology study of 542 cases and a literature review of 2,715 additional cases. *Mayo Clin Proc* 1999; 74:14-26
- Schnyder PA, Sarraj AM, Duvoisin BE, et al. Pulmonary edema associated with mitral regurgitation: Prevalence of predominant involvement of the right upper lobe. *Am J Roentgenol* 1993; 161:33-36
- Sorgato A, Faggiano P, Aurigemma GP, et al. Ventricular arrhythmias in adult aortic stenosis: Prevalence, mechanisms and clinical relevance. *Chest* 1998; 113:482-491

Pulmonary Veins: Imaging for Radiofrequency Ablation Procedures

Michael B. Sneider, M.D.

Atrial fibrillation is the most common sustained supraventricular arrhythmias and a major cause of stroke [1]. Abnormalities involving the pulmonary veins, such as arrhythmogenic foci within the vein walls from myocardial rests and venous dilatation, are frequent triggers of atrial fibrillation [1-3] and segmental ostial ablation of the pulmonary veins has been shown to be an effective treatment to prevent recurrences of atrial fibrillation [4, 5]. However, ablation with radiofrequency (RF) energy has been shown to be associated with risk of pulmonary vein stenosis [4, 6-9]. As catheter-directed pulmonary venography can potentially result in sub-optimal visualization of the pulmonary veins, pre-procedural mapping of the pulmonary venous anatomy is useful to define the position of the left atrial ostia, as well as defining the position and size of small accessory pulmonary veins which may be potentially arrhythmogenic [10]. While both magnetic resonance imaging and transesophageal ultrasound have been used to image the left atrium and pulmonary veins [8, 10], computed tomography (CT) is an excellent tool to define the pulmonary venous anatomy prior to ablation. CT can also be used as a sensitive tool with which to follow patients for post-procedural pulmonary vein stenosis [11, 12].

INDICATIONS AND TECHNIQUES OF RF ABLATION

Indications: Typical indications for the use of RF ostial ablation are the presence of either paroxysmal or persistent atrial fibrillation, though the efficacy is lower in patients with persistent atrial fibrillation [5]. Atrial fibrillation is defined as persistent when present for greater than 30 days duration and requires cardioversion for termination.

Techniques: While there are several different techniques for electrically isolating the pulmonary veins from the left atrium, they all involve placing electrode catheters under fluoroscopic guidance into the left atrium through a transseptal approach [13, 14]. Catheters are placed via the femoral vein in to the right atrium. The interatrial septum is then probed for a patent foramen ovale. If there is none, a needle septostomy is performed. Catheters are then extended into the left atrium. Selective pulmonary venography is used to road-map the individual pulmonary veins. Typically, as each individual pulmonary vein is probed, an electrical map is produced using a decapolar catheter with a distal ring configuration (Lasso™ catheter, Biosense Webster). When electrically conductive fascicles are identified, the pulmonary vein is electrically isolated by placing a catheter tipped with an RF thermistor into the vein, within 5 mm of the ostium. The wall of the pulmonary vein is then heated to 52°C with multiple applications of 30-35 watts of energy, for up to 45 seconds duration per application [5]. There is a direct relationship between the ostial diameter and the duration of RF energy needed to achieve electrical isolation. Most patients will have multiple pulmonary veins treated. Isolation is best performed as close to the venoatrial junction as possible to avoid inducing venous stenosis and limit fibrillation recurrence from ostial remnants [15]. Patients are then maintained on anticoagulants for at least one month following the procedure. Some patients will undergo a repeat procedure should they continue to have fibril-

lation episodes. Techniques using cryoablation, rather than radiofrequency energy, are currently under investigation.

CT PULMONARY VENOGRAPHY

At our institution, all patients scheduled for pulmonary vein isolation undergo pre-procedural helical CT exams. Pulmonary vein anatomy and dimensions allow the electrophysiologist to select appropriately sized catheters and anticipate any anatomic variations or accessory veins. Three month follow-up CT exams are also performed to monitor for the development of pulmonary venous stenosis.

Technique: CT examinations were initially performed on a GE LightSpeed QX/i (GE Medical Imaging, Milwaukee, WI) four-row multidetector CT scanner. 150 cc (or 120 cc in patients under 120 lbs.) of Omnipaque 300 (Nycomed, Inc., Princeton, NJ) non-ionic intravenous contrast is power-injected at a rate of 4 cc/sec via a right antecubital vein. The scan is initiated with a delay of 30 seconds after beginning contrast injection. A collimation of 1.25 mm is used, reconstructed with a 0.6 mm interval. Currently, we use a GE LightSpeed16 (GE Medical Imaging) 16-row multidetector CT scanner with prospective ECG gating for reduced motion artifact. Scanning is performed from lung bases to the apices during a single breath-hold. This bottom-up direction minimizes respiratory motion should the patient inhale or exhale toward the end of the scan. For an average-sized adult male patient, the effective radiation dose per pulmonary vein scan, assuming 320 mA tube current, is approximately 10 mSv (1 rem). The dose is proportional to mAs, which is adjusted for the patient's size (i.e., for the same time per rotation and 300 mA, the effective dose would be $10 \text{ mSv} \times (300/320) = 9.4 \text{ mSv}$).

Three-dimensional pulmonary vein models: 3D models are constructed using volume analysis software from GE Medical Imaging on an Advantage Windows (GE Medical Imaging) workstation. Models are constructed to exclude surrounding structures such as the descending thoracic aorta, ribs, vertebral column and peripheral pulmonary arteries and veins. The models are best viewed from a posterior position with variable RPO and LPO angulations and dorsocranial tilt to avoid overlap with adjacent structures. Pulmonary vein diameters can be obtained in orthogonal planes.

PULMONARY VEIN ANATOMY

Normally, the right superior pulmonary vein drains the RUL and RML and the left superior pulmonary vein drains the LUL and lingula. The lower lobes are drained by their respective inferior pulmonary vein. In a recent series of 58 patients with atrial fibrillation [11], there were 4 separate pulmonary vein ostia in 47 patients (81%), three separate ostia in 2 patients (3%) due to a common origin of left superior and inferior pulmonary veins, and five separate ostia in 9 patients (16%) due to an accessory right middle pulmonary vein. The ostia of the inferior pulmonary veins tend to be more posterior and medial relative to the superior pulmonary veins. As measured by CT, the superior pulmonary veins tend to have a longer trunk ($21.6 \pm$

7.5 mm) than the inferior pulmonary veins (14.0 ± 6.2 mm). There is no significant difference between the average diameters of the right and left pulmonary vein ostia, (mean of 18.0 ± 3.7 mm). The superior pulmonary veins are typically larger than the inferior pulmonary veins [3, 16, 17]. The most common anatomic variant, the right middle pulmonary vein, has an ostial diameter significantly smaller than the other pulmonary veins (9.9 ± 1.9 mm). When present, a common left pulmonary vein trunk will have a diameter significantly larger than the other pulmonary veins (32.5 ± 0.5 mm). In studies by Scharf, Sneider, et al., and Tsau, Wu, et al., the pulmonary veins in patients with atrial fibrillation were significantly larger than those of patients without atrial fibrillation. There was no difference between the size of veins in patients with paroxysmal versus persistent fibrillation. Atrial fibrillation patients also had a left atrial surface area greater than normal individuals [10, 11].

EFFECTS OF ABLATION ON OSTIAL DIAMETER

Several studies have shown that 40 – 100% of patients will develop some degree of pulmonary vein stenosis following RF ablation [6, 11, 12]. The vast majority have less than 10% stenosis, and are completely asymptomatic with up to 68% luminal stenosis. Severe stenosis is very rare, and to date there have been only two reported cases of significant sequela from severely symptomatic veno-occlusive disease and hemorrhagic pulmonary venous infarction [7, 12].

SUMMARY

Radiofrequency ablation of arrhythmogenic foci within the proximal veins has been repeatedly shown to be highly effective for the treatment of paroxysmal and persistent atrial fibrillation. Knowledge of the size and number of pulmonary veins is important in planning a successful ablation procedure, since as many as 20% of patients will display anatomic variations. Imaging with multi-row CT is an effective and rapid method providing this information. Although pulmonary venous stenosis is a frequent complication of RF ablation, it is most usually asymptomatic, even with stenosis of up to 68%. Complications from severe stenosis are extremely rare. CT imaging facilitates effective follow-up screening for pulmonary vein stenosis and assessment of severity and progression.

REFERENCES

1. Haissaguerre M, Jais P, Shah DC, et al. Spontaneous initiation of atrial fibrillation by ectopic beats originating in the pulmonary veins. *N Engl J Med* 1998;339:659-666
2. Chen SA, Hsieh MH, Tai CT, et al. Initiation of atrial fibrillation by ectopic beats originating from the pulmonary veins: electrophysiological characteristics, pharmacological responses, and effects of radiofrequency ablation. *Circulation* 1999;100:1879-1886
3. Lin WS, Prakash VS, Tai CT, et al. Pulmonary vein morphology in patients with paroxysmal atrial fibrillation initiated by ectopic beats originating from the pulmonary veins: implications for catheter ablation. *Circulation* 2000;101:1274-1281
4. Haissaguerre M, Jais P, Shah DC, et al. Electrophysiological end point for catheter ablation of atrial fibrillation initiated from multiple pulmonary venous foci. *Circulation* 2000;101:1409-1417
5. Oral H, Knight BP, Tada H, et al. Pulmonary vein isolation for paroxysmal and persistent atrial fibrillation. *Circulation* 2002;105:1077-1081
6. Robbins IM, Colvin EV, Doyle TP, et al. Pulmonary vein stenosis after catheter ablation of atrial fibrillation. *Circulation* 1998;98:1769-1775
7. Scanavacca MI, Kajita LJ, Vieira M, Sosa EA. Pulmonary vein stenosis complicating catheter ablation of focal atrial fibrillation. *J Cardiovasc Electrophysiol* 2000;11:677-681
8. Yu WC, Hsu TL, Tai CT, et al. Acquired pulmonary vein stenosis after radiofrequency catheter ablation of paroxysmal atrial fibrillation. *J Cardiovasc Electrophysiol* 2001;12:887-892
9. Seshadri N, Novaro GM, Prieto L, et al. Images in cardiovascular medicine. Pulmonary vein stenosis after catheter ablation of atrial arrhythmias. *Circulation* 2002;105:2571-2572
10. Tsao HM, Wu MH, Yu WC, et al. Role of right middle pulmonary vein in patients with paroxysmal atrial fibrillation. *J Cardiovasc Electrophysiol* 2001;12:1353-1357
11. Scharf C, Sneider MB, Case I, et al. Anatomy of the Pulmonary Veins in Patients With Atrial Fibrillation and Effects of Segmental Ostial Ablation Analyzed by Computed Tomography. *J Cardiovasc Electrophysiol* 2003;In Press
12. Ravenel JG, McAdams HP. Pulmonary venous infarction after radiofrequency ablation for atrial fibrillation. *AJR Am J Roentgenol* 2002;178:664-666
13. Jais P, Shah DC, Hocini M, Yamane T, Haissaguerre M, Clementy J. Radiofrequency catheter ablation for atrial fibrillation. *J Cardiovasc Electrophysiol* 2000;11:758-761
14. Lickfett LM, Calkins HG, Berger RD. Radiofrequency Ablation for Atrial Fibrillation. 2002;4:295-306
15. Oral H, Knight BP, Ozaydin M, et al. Segmental ostial ablation to isolate the pulmonary veins during atrial fibrillation: feasibility and mechanistic insights. *Circulation* 2002;106:1256-1262
16. Nathan H, Eliakim M. The junction between the left atrium and the pulmonary veins. An anatomic study of human hearts. *Circulation* 1966;34:412-422
17. Ho SY, Sanchez-Quintana D, Cabrera JA, Anderson RH. Anatomy of the left atrium: implications for radiofrequency ablation of atrial fibrillation. *J Cardiovasc Electrophysiol* 1999;10:1525-1533

Imaging of Cardiopulmonary Support Technology

Philip N. Cascade, M.D.

Department of Radiology, University of Michigan

Objectives and Need for Presentation:

To inform radiologists of the clinical use and imaging characteristics of cardiopulmonary support technology.

Presentation:

Circulatory Support Technology

The first open-heart surgical procedure was performed in 1953 using an extracorporeal pump system that had taken 20 years to develop. During the 1950's this technology gained widespread acceptance and open-heart surgery became a routine procedure. This was the beginning of artificial cardiovascular support.

Other clinical needs for temporary and even permanent circulatory assist have since become evident. Up to 4% of patients undergoing open-heart surgery cannot be weaned from cardiopulmonary bypass. While the majority of these patients can be salvaged with modern drug therapy, others require mechanical cardiopulmonary assist. Cardiogenic shock following acute myocardial infarction is a more common problem occurring in approximately 7.5% of patients admitted to hospitals with acute myocardial infarction. This condition has an 85% or greater mortality rate. Some of these patients survive with combined pharmacologic therapy and short-term cardiopulmonary assist; others require circulatory assist during cardiac catheterization and subsequent coronary artery angioplasty or coronary bypass surgery. Assist devices can also be used as a temporary bridge to transplant in patients with overwhelming acute and irreversible cardiac failure following myocardial infarction or acute myocarditis. More than 16,000 patients in the United States become candidates for heart transplant each year. When patients 55-65 years of age are included the figure rises to >40,000. Many die before donor hearts become available (5,200 donor hearts available) (1).

There have been many configurations of circulatory support devices. Some remain in clinical use, while others have been abandoned because of unacceptable complication rates. New technologies are in various stages of development. Following is a discussion of a variety of cardiopulmonary assist technologies, their modes of action and their radiographic appearance.

Short Term Circulatory Assist

Intraaortic Balloon Pump (IABP)

The IABP provides partial cardiovascular assist, supplementing cardiac output by 20 - 30%. This is currently the primary tool for partial, temporary cardiovascular assist. The IABP is often in place for days, occasionally for a few weeks and in experimental situations it has been used for months at a time. This sausage shaped flexible balloon pumping chamber works by counterpulsation, inflating and then decompressing out of phase with the cardiac cycle. By increasing blood pressure during diastole, the balloon pump increases blood flow to the coronary arteries and other core organs. By deflating when the aortic valve opens in systole, there is a significant decrease in oxygen consumption as myocardial work diminishes with the decrease

in afterload. Placed percutaneously by femoral artery approach, the IABP is ideally positioned with its tip overlying the aortic knob on frontal chest radiographs (2). If placed too proximal, the tip will extend into the left subclavian, or even left vertebral artery. If placed too distal, the balloon will lie adjacent to the orifices of the visceral arteries with the potential for microembolism.

Roller Pumps and Centrifugal Pumps

Cardiovascular pumps are simple; relatively inexpensive left ventricular assist devices. These systems consist of a drainage cannula, usually placed in the left atrium, the pump itself and a catheter to return blood to the arterial system either to the aorta or via a femoral artery (3). The *roller pump* repeatedly compresses a narrow tubing filled with blood, creating the force to propel blood into the arterial system. The action is relatively traumatic to the blood resulting in a high incidence of hemolysis. *Centrifugal pumps* spin blood to create flow by a forced vortex pumping action. These pumps are less traumatic to blood and have had greater clinical success than the roller type. Fibrin deposits and thrombus formation in the pumping chamber limit duration of use to approximately 5 to 7 days. Centrifugal pumps generate flow rates of 5 - 6 liters per minute and can thus completely support the circulation. Both roller and centrifugal pumps yield continuous, non-pulsatile flow. Most experts believe that pulsatile flow is clinically superior and for this reason intraaortic balloon pumps are often placed simultaneously. The Thoratec device is an example of a pulsatile pumping apparatus that can be used for short-term assist for one or both ventricular chambers simultaneously.

Hemopump

The Hemopump is a left ventricular assist device that works on the Archimedean principle (3). This concept has been known for centuries, that a rapidly rotating screw confined within a tube will propel fluid. With rotational speeds of 25,000 per minute, the pump withdraws a stream of oxygenated blood from the left ventricle and pumps it into the aorta. Flow rates can supplement up to 80% of resting cardiac output. Thrombocytopenia, footdrop and peripheral embolism are the most frequent complications. Hemolysis occurs but has not been reported to be clinically significant.

Permanent/Long term Circulatory Assist

There are two basic functional types of pulsatile ventricular assist devices (VAD). Those driven pneumatically and those that use electromagnetic power. Air powered assist devices work by pulsing bursts of compressed air into a ridged chamber, inflating and deflating a polyurethane sack to produce pulsatile blood flow. Electromechanically driven assist devices use opposing pusher plates to compress a seamless polyurethane sack, propelling blood in a pulsatile fashion.

The HeartMate Device

The Heart-Mate device is a pump that can be implanted in the left upper quadrant of a patient with cannulation of the left

ventricular apex to access blood and with cannulation into the ascending aorta to return blood to the circulation (4). The HeartMate was the first implantable heart pump to gain Federal and Drug Administration approval to bridge patients to transplantation.

The CardioVad

In the early 1970's, Adrian Kantrowitz implanted a pumping chamber similar to the intraaortic balloon into the wall of the descending aorta in three patients. Pneumatically driven by an external pump, the prosthesis was called the "dynamic aortic patch." The clinical trial was terminated because of the problem of infection. Redesign and further animal studies have apparently solved the problem of sepsis caused by migration of bacteria along external tube tracts. A modified version of the Kantrowitz implantable pumping chamber, the CardioVad (LVAD Technology, Detroit, Mich.), is under development and clinical assessment has begun.

Jarvik 2000

The Jarvik 2000 is a relatively new small axial continuous flow pump that is inserted into the left ventricle. A conduit carries the pumped blood to the descending thoracic aorta. Early trials show promise for long term assist with a low complication rate. The small size of the pump will be very helpful in children and smaller adults.

Cardiomyoplasty

The long-standing idea of using skeletal muscle to augment cardiac function has been tested clinically. Dynamic cardiomyoplasty is a surgical technique involving wrapping of the latissimus dorsi muscle around the heart to augment contractility. Electrodes powered by an implantable pulse generator induce cyclical contraction of the pedicled muscle (5). Alternatively, the muscle can be sewn into the left ventricular wall as a replacement for extensively damaged muscle. Dynamic aortoplasty, wrapping latissimus dorsi around the ascending aorta, has also shown promise in animals. An additional innovative experimental technique utilizes skeletal muscle wrapped around a pumping chamber implanted adjacent to the thoracic aorta. Muscle contraction is induced during cardiac diastole, the chamber is compressed, and diastolic pressure and flow are augmented as blood is squeezed out of the device.

Biventricular Pacing

Patients with moderate to severe heart failure with prolonged intraventricular conduction delay may have asynchronous ventricular contraction and a reduction in cardiac output. Prolonged PR intervals can also contribute to significant atrial-ventricular valve regurgitation. Pacing both right and left ventricles, biventricular pacing can significantly improve forward output, and atrioventricular pacing can reduce tricuspid and mitral valve regurgitation. Left ventricular pacing can be accomplished by mini-thoracotomy or thoroscopic placement of left ventricular electrodes. A recent technologic development using a retrograde approach through the coronary sinus facilitates placement of electrodes in epicardial veins on the surface of the left ventricle (6).

Total Artificial Heart (TAH)

As of 1992, 116 TAH implants had been reported using at least eight different models, most commonly using the Symbion Jarvik-7 device (3). The Jarvik-7 incorporates two artificial ventricles that are attached to the native atria, the pulmonary artery

and the aorta. Four disk-type artificial valves control blood flow direction. Each ventricle consists of a ridged housing separated into blood and air containing spaces by a polyurethane membrane. An external pneumatic pump connects to the airspace of each chamber by transthoracic polyurethane tubes. Pressurized air, cyclically driven into the pumping chamber, pumps the blood with sufficient cardiac output to totally support circulatory requirements. Radiographs show a radiolucent crescent inside each chamber during diastolic filling, whereas during systole, each air-containing chamber is completely filled producing two lucent globe-like structures (7). Total permanent replacement has not been successful because of complications including mechanical malfunction, thromboembolism, bleeding secondary to anticoagulation, infection from bacterial seeding along external tube tracts, and physical compression of adjacent anatomic structures, particularly pulmonary veins and inferior vena cava. Successful implantation of a permanent TAH remains a future goal. Recently, clinical trial of a new total artificial heart built by Abiomed was begun, although the results are too early to reach any conclusions.

Respiratory Support Technology

The need for technology to assist pulmonary gas exchange is another issue, particularly for patients with the adult respiratory distress syndrome (ARDS). ARDS has a reported mortality rate of 50 - 90% depending on group selection. Despite vigorous intensive care, the chances of survival have not significantly improved since the syndrome was first described. Patients with severe ARDS can be treated with artificial gas exchange devices while damaged lung recovers. Extracorporeal membrane oxygenation (ECMO) technology uses a synthetic semi-permeable membrane as a blood/gas interface for exchange of oxygen and carbon dioxide. Investigation of an implantable artificial lung for long term or even permanent respiratory support is underway.

Extracorporeal Membrane Oxygenation (ECMO)

Neonates with respiratory failure have been successfully managed with ECMO since 1975, reducing mortality rates from 85% to approximately 15%. This procedure has been modified and used for the treatment of adults (8). Using selection criteria which would predict a 90% risk of death, early trials report a reduction in mortality of approximately 50%. ECMO removes blood, perfuses it with oxygen and eliminates carbon dioxide, and returns blood to the patient. Two types of ECMO are used: veno-venous (VV) and veno-arterial (VA) (26). VV is used for pure respiratory support. Venous blood is drained from the right atrium by a cannula introduced into the right internal jugular vein or occasionally other large systemic veins. Oxygenated blood is reintroduced into a large peripheral vein, usually a femoral vein, or directly back into the right atrium by a double channel catheter. In VA bypass, venous blood is removed as in VV methods. Blood is returned to the arterial system by a cannula placed in the right internal carotid artery with the tip in the aortic arch. Sometimes the blood is returned to the femoral artery. VA ECMO is physiologically similar to cardiopulmonary bypass, providing both cardiovascular and pulmonary assist.

Intravenous Oxygenator (IVOX)

The IVOX device is a membrane oxygenator system configured as a complex of thin hollow fibers mounted on a catheter. The device is placed in the vena cava and venous blood circulates through the porous oxygenator while pure oxygen is sup-

plied to the hollow fibers by an external pump. A radiographic opaque stripe surrounded by gas lucency indicates its position on radiographs (9). Gas exchange capacity is limited compared to ECMO. The use of this device was discontinued after a short clinical trial. Future models are in development.

Liquid Ventilation

ARDS can be treated by perflouorocarbon (PFC) liquid ventilation in two different ways: 1) Total liquid ventilation using a "liquid ventilator and 2) Partial liquid ventilation using a conventional mechanical gas ventilator. PFC liquid permits free exchange of oxygen and carbon dioxide while simultaneously expanding the lungs, eliminating atelectasis and washing debris from alveoli. The liquid is eliminated from the lungs by evaporation. The radiographic appearance of patients undergoing liquid ventilation is quite striking as the liquid is radiopaque (10).

The Future

The need for new effective methods of treatment for the thousands of patients with severe chronic intractable heart and lung failure is clear. New technological innovations may make permanent cardiopulmonary assist possible. Advances in miniaturization and transcutaneous energy systems will eventually completely eliminate the need for external connections. A different solution may evolve through research aimed at the development of genetically altered tissue surfaces of animal organs, thus providing an unlimited supply of hearts and/or lungs for transplantation. Stem cell research may yield methods of regenerating new myocardium, and research in organogenesis is showing early promise.

REFERENCES

- O'Connell JB, Gunnar RM, Evans RW, et al. Task Force 1: Organization of heart transplantation in the U.S. *JACC* 1993; 22:8-64
- Cascade PN, Rubenfire M, et al. Radiographic aspects of the phase-shift balloon pump. *Radiology* 1972;103:299-302
- Locke T, McGregor C. Ventricular assist devices. In: Kay PH, ed. *Techniques in Extracorporeal Circulation*. Third edition. Oxford, England. Butterworth-Heinemann LTD. 1992:268-81
- Emery RW, Joyce LD. Directions in cardiac assistance. *Journal of Cardiac Surgery* 1991;6:400-14
- Nguyen TH, Hoang T-A, Dash N, et al. Latissimus dorsi cardiomyoplasty: radiographic findings. *AJR* 1988; 150:545-547
- Cascade PN, Sneider MB, Koelling TM, Knight BP. The radiographic appearance of biventricular pacing for the treatment of heart failure. *AJR* 2001; 144:7-1450
- Fajardo LL, Standen JR, et al. Radiologic appearance of the Jarvik artificial heart implant and its thoracic complications. *AJR* 1988;151:667-71
- Anderson III HL, Delius RE, et al. Early experience with adult extracorporeal membrane oxygenation in the modern era. *Ann Thorac Surg* 1992;53:553-63
- Shukla PR, Snider MT, et al. Radiologic evaluation of the intravenous oxygenator. *Radiology* 1993;187:783-86
- Kazerooni EA, Pranikoff T, Cascade PN. Partial liquid ventilation with perflubron during extracorporeal life support in adults: radiographic appearance. *Radiology* 1996; 198:137-142

Venous Thromboembolism: Epidemiology

Lacey Washington, M.D.

Medical College of Wisconsin
Milwaukee, Wisconsin

The epidemiology of venous thromboembolism (VTE) is a difficult and poorly understood field of study, because of inherent flaws in all available approaches to its study. Nevertheless, it is important to have an understanding of what is and is not known about this disease. The radiologist should remember that the positive predictive value of any test is dependent on the pretest probability of disease. As we go about the process of diagnosing pulmonary embolism (PE) and deep venous thrombosis (DVT), it is helpful to know as much as we can about which patients are at risk. An improved awareness of the epidemiology of this disease will help the radiologist and thus the clinician assess the true probability that any given patient may have VTE.

First, it is important to recall that, as Virchow first recognized, PE and DVT represent a dual manifestation of a single disease, which may be manifested by symptoms in the vein in which DVT originates or by symptoms in the pulmonary circulation to which DVT embolizes.

Risk factors for the development of VTE include malignancy, other hypercoagulable states, immobility, and venous injury. (The historic Virchow triad of causes of deep venous thrombosis is made up of changes in the properties of the blood, changes in blood flow, and changes in the vessel wall.) Nearly all commonly accepted risk factors for VTE still fall into one or more of these categories. However, the first of Virchow's categories, the hypercoagulable state, is an expanding one, as increasing numbers of inherited and acquired causes of hypercoagulability are discovered.

Approaches to the Epidemiology of VTE

Before discussing the risk factors for PE, it is important to review the limitations of epidemiologic data on VTE. There are two major types of studies: those that rely on autopsy data and those that rely on clinical diagnosis.

While autopsy data are considered "the gold standard," there are important limitations to these data. In particular, the sensitivity and the rate of detection of PE at autopsy is largely dependent on the aggressiveness with which PE is sought and varying levels of attention given to small, peripheral vessels. Autopsy rates of PE range from 1.5% to almost 30%, and with careful microscopic analysis rates as high as 90% have been reported, with chronic appearing lesions included.¹ Autopsy patients are, of course, a selected subgroup, and one explanation for these high rates of PE would be that PE carries a very high mortality. However, at autopsy, the contribution of emboli to patient mortality is also frequently unclear.

Another approach to the epidemiology of VTE is that of large, population-based studies. While these are of interest in assessing for risk factors for VTE, they have serious limitations because of extremely variable diagnostic tests and criteria used to make the diagnosis. For example, the large series drawn from public health records of Olmsted County, Minnesota, showed a decline in the rate of VTE by approximately 35% from 1977 to 1979. This is thought to be because new noninvasive diagnostic tests caused a decrease in false positive clinical diagnoses of VTE. This kind of variability should increase our caution in interpreting data from this type of study with respect to the incidence of VTE—yet there may be few alternative sources to consider.

Risk Factors for VTE

Recognizing the uncertainty of any approach to the epidemiology of this disease, what is known about its incidence and prevalence?

VTE is not an uncommon disease. The incidence rates of VTE in two recent, large population-based studies were 1.17 and 1.83 per 1000 population annually.^{2,3} Autopsy data have shown that PE is an underdiagnosed clinical entity, with a recent series showing only a slight improvement in the pre-mortem detection of PE in comparison with the 1/3 detection rate shown in a 1988 study.⁴ Some cases of PE will lead to circulatory collapse so rapidly that treatment cannot be initiated, however this is probably a minority of fatal PE. It is estimated that PE is the major cause of death in 100,000 cases per year in the United States, and that it contributes to an additional 100,000 deaths in patients with serious coexisting diseases such as heart disease and cancer.

Risk factors for VTE seen in the Olmsted County study included increased patient age, with a slightly higher incidence in males, particularly over the age of 45 (reflecting a somewhat higher incidence in women during childbearing years). With increasing age, PE becomes more common compared with DVT as the manifestation of VTE. This suggests that, absent better identification of risk factors and better prophylaxis, an aging population will lead to a higher incidence of PE.

Congestive heart failure did not show a significant correlation with VTE in this study, unlike in some autopsy series. Similarly, in PLOPED patients, pulmonary edema occurred less commonly in patients with pulmonary embolism as compared with those with no pulmonary embolism (13% as opposed to 4%). The strongest risk factors for PE in this series were hospitalization for surgery, confinement to chronic care facilities, trauma, and malignancy.⁵

Clinical presentations of patients with PE are notoriously nonspecific, and are reviewed by Dalen.⁶ Patients may present with symptoms caused by pulmonary infarction or hemorrhage, with massive pulmonary embolism and acute cor pulmonale, or with acute unexplained dyspnea. The first group of patients have clinical manifestations including hemoptysis, pleuritic chest pain, pleural friction rub, and chest radiographic consolidation, sometimes with pleural effusions. Those with massive embolism and acute cor pulmonale present with shock and collapse. The third group often have no physical findings other than tachycardia and tachypnea.

Diagnosis of DVT has historically often depended on physical examination findings, including calf measurements and the presence of a Homan's sign (calf pain on dorsiflexion.) However, these findings have been shown to be unreliable predictors of the presence of DVT. Reported sensitivity for DVT of physical examination findings, when compared with venography, ranges from 60 to 96%, and reported specificity ranges from 20 to 72%.

Nevertheless, clinical factors can be used to stratify risk for DVT. One published scoring method gives one point for any of a list of clinical parameters, while subtracting two points for any alternative diagnosis. Parameters related to clinical history are active cancer (or within previous six months), paralysis, paresis, or lower extremity immobilization, or a history of being bedridden for more than three days for major surgery within a four-week time period. Physical examination parameters are

swelling of the entire leg, calf swelling with the symptomatic leg measuring more than 3 cm greater than asymptomatic leg (10 cm below the tibial tuberosity), pitting edema, and collateral (nonvaricose) superficial veins.⁷

Relationship between PE and DVT

Although a causal relationship between DVT and PE is accepted, the temporal relationship between these entities is less well established. Depending on patient population and method of investigation, widely variable percentages of patients with proven PE have DVT. For this reason, evaluation of the venous system is not an appropriate first-line test for patients who present with clinical syndromes suggesting PE rather than DVT. For example, in 89 patients with suspected PE and no risk factors or symptoms of DVT, Sheiman et al found no DVT.⁸ However if patients who are suspected of having PE also have risk factors for or symptoms of DVT, an assessment of the deep venous system may allow for a diagnosis of VTE; these same authors found a 14 to 25% rate of DVT in patients with risk factors for and/or symptoms of venous disease. Additionally, an increased risk of DVT at ultrasound has been shown in one study in patients with larger perfusion defects on lung scintigraphy, so lower extremity investigation may be warranted in patients without lower extremity symptoms but with demonstrated large embolic burdens.

DVT by location

DVT is frequently isolated to one of two areas within the lower extremity deep venous system: it may be iliofemoral or calf-popliteal. Isolated superficial vein thrombosis occurs with varying frequency, but has been seen in as large a percentage as 22.3 % of patients. Within the lower extremities, calf vein thrombosis is associated with a relatively low risk of PE. However, calf vein thrombosis may extend and involve the popliteal and femoral veins, and the need for imaging of the calf veins therefore remains controversial.

The risk of isolated pelvic vein thrombus is an even more important area of inquiry, since pelvic vein thrombus is clearly associated with a risk of PE. Isolated pelvic vein DVT has been historically thought to be rare, approximately 2% of total DVT.⁹ Some recent MR literature has reported much higher rates of isolated pelvic DVT, with some CTV studies showing intermediate results. As with so many other factors in VTE, the prevalence of this particular manifestation probably depends on patient risk factors.

Upper extremity DVT is a small minority of DVT, estimated to represent 1-4% of total DVT. The overall incidence may be increasing as a consequence of increased use of central venous catheters, a major risk factor for the development of upper extremity DVT.⁵ The relative risk of PE in these patients compared with the risk in patients with lower extremity DVT is not known, but high-probability scans were found, in one series, in five of 19 asymptomatic patients with upper extremity DVT.

Hypercoagulable States

Of the traditional risk factors for VTE, hypercoagulable states represent an expanding category. Three inherited conditions, antithrombin III, protein C, and protein S deficiencies, were discovered early but account for a only a small percentage of cases of VTE. These are seen in from 0.1 to 0.5 % of the population and from 2 to 5 % of patients with VTE. However, several more recently discovered conditions are associated with a much larger percentage of VTE cases. These include Factor V Leiden mutation, prothrombin G-A gene variant, elevated Factor XI and Factor VIII, and hyperhomocystinemia.⁶ Including all of these conditions, hypercoagulable states now may be identified in more than 25% of patients with VTE. It may be that, as more of these conditions are recognized, it will be possible to find a

predisposing hypercoagulable state in the majority of patients with VTE, which may allow for prophylaxis tailored to patients who are truly at very high risk for disease.

Mortality of PE

PE was a significant cause of mortality in the Olmsted County study, and even excluding patients initially diagnosed with PE at autopsy, only 71.1% of patients with PE survived 7 days. PE was an independent predictor of reduced survival for up to 3 months after onset. Other series show better survival in treated patients (92%), and it is generally accepted that the majority of deaths due to PE occur in patients who are not treated because the diagnosis is not made.⁶ However, some authors have questioned whether PE is always the highly lethal event that these data suggest.¹⁰

In autopsy series, it is difficult to ascertain the contribution of PE to patient death, and the possibility that PE is sometimes clinically unimportant is reinforced by the fact that some studies have shown that PE may be asymptomatic, even relatively frequently. For example, studies of patients with DVT with no respiratory symptoms show a high, 40-60%, rate of PE. Perfusion scans may be used to quantitate the extent of physiologic abnormalities secondary to PE. One study showed that the severity of clinical signs increased with increasing perfusion abnormalities, so many of these asymptomatic PE may have smaller physiological consequences. The idea that some PE is clinically insignificant is reinforced by the use of declotting procedures for dialysis access grafts. In these procedures, thrombus is often pushed into the lungs, with very rare negative consequences in patients of whom many have very poor cardiopulmonary reserve.¹⁰

Nevertheless, it is still widely accepted that PE causes significant mortality in patients in whom a pre-mortem diagnosis is not made, and that treatment reduces this mortality. It has been estimated that less than 10% of PE deaths occur in patients in whom treatment is initiated, and that while a minority of these patients will die too soon to be treated, the missed diagnoses remain a major opportunity for improvement in patient outcomes.⁶

Natural History of VTE

One of the most significant risk factors for VTE is a history of prior VTE, with particularly high rates of recurrence, compared with other studies, documented in the Olmsted County, Minnesota, study.⁵ There is no well established protocol for imaging followup of patients with a history of VTE, although some authors have suggested that attention should be given to establishing the degree of lysis that occurs following an episode of PE, to help prevent misdiagnosis of chronic clot as recurrent acute clot, and to facilitate identification of patients at risk for chronic thromboembolic pulmonary hypertension.

The natural history of PE is for the native thrombolytic system to dissolve clots over time. In some patients, however, this does not completely occur, with chronic PE as a result.¹¹ Some of these patients will develop the syndrome of chronic thromboembolic pulmonary hypertension. This condition is thought to occur in 0.1 to 0.5 % of patients who survive after acute PE. Approximately 10% of patients with this disorder have anticardiolipin antibodies, however the remainder have no discernible underlying predisposition. Many present late in the course of the disease without any history of diagnosed acute PE.¹²

CONCLUSIONS

Unlike the other major acute cardiovascular events, heart attack and stroke, the difficulties of diagnosis in VTE have led to persistent uncertainty about its prevalence and natural history. This uncertainty adds to the difficulty of making educated judgments about which patients are at risk for this disease. Nevertheless, an awareness of at least the limited information

available about the epidemiology of VTE may help the radiologist to guide clinicians in interpreting results of any study for PE or DVT. It is hoped that continued improvement in the non-invasive diagnosis of VTE will lead to better understanding of the range of presentations of VTE and its epidemiology, and will eventually result in better prevention and lower morbidity and mortality.

REFERENCES :

1. Wagenvoort CA. Pathology of pulmonary thromboembolism. *Chest* 1995;107(1 Suppl):10S-17S.
2. Heit JA, Silverstein MD, Mohr DN, Petterson TM, Lohse CM, O'Fallon WM, et al. The epidemiology of venous thromboembolism in the community. *Thrombosis & Haemostasis*. 2001;86(1):452-63.
3. Oger E. Incidence of venous thromboembolism: a community-based study in Western France. EPI-GETBP Study Group. Groupe d'Etude de la Thrombose de Bretagne Occidentale. *Thrombosis & Haemostasis*. 2000;83(5):657-60.
4. Pineda LA, Hathwar VS, Grant BJB. Clinical suspicion of fatal pulmonary embolism. *Chest* 2001;120(3):791-795.
5. Heit JA. Venous thromboembolism epidemiology: implications for prevention and management. *Seminars in Thrombosis & Hemostasis* 2002;2:3-14.
6. Dalen JE. Pulmonary embolism: What have we learned since Virchow? *Chest* 2002;122:1440-1456.
7. Wells PS, Anderson DR, Bormanis J, Guy F, Mitchell M, Gray L, et al. Value of assessment of pretest probability of deep-vein thrombosis in clinical management. *Lancet* 1997;350(9094):1795-8.
8. Sheiman RG, McArdle CR. Clinically suspected pulmonary embolism: use of bilateral lower extremity US as the initial examination--a prospective study. *Radiology* 1999;212(1):75-8.
9. Nicolaides AN, Kakkar W, Field ES, Renney JT. The origin of deep vein thrombosis: a venographic study. *Br J Radiol* 1971;44(525):653-63.
10. Smith TP. Pulmonary embolism: what's wrong with this diagnosis? *AJR. American Journal of Roentgenology* 2000;174(6):1489-97.
11. Gotthardt M, Schipper M, Franzius C, Behe M, Barth A, Schurrat T, et al. Follow-up of perfusion defects in pulmonary perfusion scanning after pulmonary embolism: are we too careless? *Nuclear Medicine Communications* 2002;23(5):447-52.
12. Fedullo PF, Auger WR, Kerr KM, Rubin LJ. Current concepts: chronic thromboembolic pulmonary hypertension. *N Engl J Med* 2001;345(20):1465-1472.

Multi-channel Pulmonary CTA: New Techniques, Observations, and Concepts

James F. Gruden, M.D. FCCP

Associate Professor of Radiology and Internal Medicine, Emory University School of Medicine, Adjunct Professor of Biomedical Engineering, Georgia Institute of Technology Director, Cardiothoracic Imaging Division, Emory Healthcare, Medical Director, Biomedical Imaging Laboratory, Emory University Hospital and Clinic

OBJECTIVES

1. Understand the fundamental differences and similarities between single and multi-channel helical CT angiography and the advantages each has over conventional angiography and scintigraphy and to know the scientific basis for these advantages.
2. Identify current areas of research in image display and processing of large volumetric data sets that may enhance our ability to diagnose thromboembolic disease.
3. Understand the concept of the accuracy of a diagnostic test and the limitations of accuracy as a measure of true test utility.
4. Reconsider the current understanding of venous thromboembolism and its recommended therapy.
5. Understand the recent clinical literature and its limitations.

BACKGROUND

During the period 1984-1991, an average of 50,000 cases of pulmonary embolism were diagnosed each year in the hospitalized Medicare population alone with a mortality rate of at least 10% [1]. Definitive diagnosis is of paramount importance because of both the seriousness of the condition itself and because complications of anticoagulant therapy are frequent and can be severe.

The definitive diagnosis or exclusion of venous thromboembolic disease (PE and DVT) remains problematic, and there are few areas of medicine with such a significant level of uncertainty and confusion with regard to accurate diagnosis and therapy. One autopsy study found that only 10% of patients 70 years of age and older with PE had a correct diagnosis before death [2]. Missed diagnosis is not the only problem; of all patients with an ICD-9 discharge diagnosis of PE in one series, 28% had no objective evidence of either PE or deep venous thrombosis (DVT) [3].

These diagnostic inaccuracies exist for two major reasons. First, the clinical signs and symptoms associated with PE are nonspecific, as are laboratory investigations, electrocardiograms, and chest radiographs. Clinical studies show a high prevalence of symptoms in patients with PE because diagnostic testing is initiated by the clinical scenario; however, 26-38% of patients with high-probability ventilation-perfusion (VQ) scans in the setting of known DVT are asymptomatic [4, 5]. Clinical estimates of the probability of PE are clearly not sufficient for individual patient management decisions.

The second reason for imprecision is that the widely used tests and algorithms for suspected venous thromboembolism (which includes both DVT and PE) are limited in accuracy and inconsistently applied. The ideal diagnostic test should be accurate, direct (objective), rapid, safe, readily available, and of reasonable cost. Only approximately 30% of patients (probably much less in the current medicolegal climate) with clinically suspected PE have the disease [6]. A diagnostic test able to provide information regarding the presence and significance of other chest disease would also be desirable. None of the common tests in use (other than CT) meet all or even most of these criteria.

The use of CT angiography (CTA) in the assessment of patients with possible thromboembolic disease has coincided with the development of rapid helical (spiral) scanners, which enable angiogram-like images of the pulmonary circulation in a single breath-hold. This technique has revolutionized the approach to the patient with possible PE and offers significant

and important improvements over the traditional diagnostic approach (chest radiograph and VQ scan) in the initial assessment of these patients. New "multi-channel" or "multi-detector" scanners acquire 4 or even 8 channels of data simultaneously and faster (16, 32 channels) scanners are in development. These multi-channel scanners have significant advantages over single channel helical CT; these will be outlined and illustrated after a brief review of pertinent issues in pulmonary CTA. There is no question that multi-channel CT (MCCT) is the new gold standard in the diagnosis of PE and it is unethical to perform randomized trials that exclude some patients from MCCT or force conventional angiography to be performed after clearly negative or positive MCCT studies.

SINGLE CHANNEL HELICAL CT ANGIOGRAPHY

Nearly all of the published literature in CT pulmonary angiography refers to studies obtained with single channel helical CT, and a basic understanding of this information is essential to an understanding of the significant impact of MCCT in this setting. All helical data sets are volumetric and permit image reconstructions at overlapping intervals, improving density discrimination between small adjacent structures of different attenuation (such as thrombi within enhancing arteries). The central thorax can also be scanned in a single breath hold (no respiratory motion) on these scanners; these features in concert enable high quality multiplanar reconstructions. Helical pulmonary CT angiography has become the method of choice in the assessment of patients with suspected venous thromboembolism even prior to the development of multi-channel technology. Images should be reviewed on a workstation, in cine mode, and multiplanar reconstructions performed in difficult cases at commercially available workstations. Examples will be shown.

With single channel scanners, we use a collimation of 3 mm and a pitch of 2 with a reconstruction interval of 2 mm after acquiring data from the diaphragm up during a single 20-25 second breath-hold. If necessary, scans can be performed during either quiet respiration or two distinct breath-holds separated by a short (5-10 seconds) interval although this introduces motion and limits assessment of smaller, peripheral vessels. Few patients have difficulty tolerating the examination. We use 100-150 cc of low osmolar, nonionic contrast (30-48% iodine) injected at a rate of 2.5-3 cc/sec. Although we formerly achieved optimal opacification of the pulmonary vasculature through the use of a "timing run" or by using the Smart Prep (General Electric Medical Systems, Milwaukee) program, we now use a fixed delay of 20 seconds from the start of the injection to imaging. This is easier to reproduce, introduces less potential for error during the exam, and enables more predictable timing of the leg vein image acquisition (see below).

The thinly-collimated overlapping images permit detailed assessment of the central airways, hilar and mediastinal lymph nodes, and of the lungs and pleural surfaces. This ancillary information is not provided by any other diagnostic test commonly used in the assessment of patients with suspected venous thromboembolism and is of importance in the symptomatic patient with an unknown diagnosis. We perform a half-mA scan of the entire chest prior to contrast injection as well since the entire thorax cannot be scanned with single channel helical machines using the above parameters.

CT, like pulmonary angiography, directly depicts thrombi within the opacified arterial lumen as intravascular filling

defects surrounded by a rim of contrast material or as meniscus-like filling defects with contrast extending around the edges of the clot. A nonopacified artery is nondiagnostic unless the diameter of the vessel is clearly expanded. Lack of filling of small arteries is nondiagnostic at angiography as well; the ability of CT to depict and assess vascular diameter is an advantage of CT over angiography. Arteries peripheral to a central thrombus may or may not opacify; central clot does not necessarily completely obstruct the distal flow of contrast. Although nonocclusive clot is depicted by CT, false negative scintigraphy in this setting is well-known. The CT findings diagnostic of chronic PE are also modified from angiographic criteria and include mural thrombus (adherent to the arterial wall), webs, stenoses, or strictures of the arteries, and a central "dot" of contrast surrounded by circumferential thrombus indicative of recanalization. CT, like angiography, usually enables distinction between acute and chronic PE; this is not possible with scintigraphy.

Technical pitfalls in CT interpretation relate to the physical properties of contrast material, mechanics of contrast injection, image reconstruction algorithm, and miscellaneous factors such as respiratory motion. These are readily recognized by the experienced observer. However, even with a high quality examination, several common errors must be avoided. Pulmonary arterial vasoconstriction, which often occurs in areas of pleural or parenchymal disease, can result in vascular nonopacification due to slow blood flow in the area of abnormality. Pulmonary veins may also fail to opacify because scanning is performed during the arterial enhancement phase. Veins and arteries can be readily differentiated by experienced observers, but nonopacified vessels without caliber expansion should never be considered diagnostic of PE regardless of their nature. Periarterial abnormalities, such as lymph node enlargement or infiltration of the axial interstitium by edema fluid, inflammation, or neoplasm, can mimic eccentric or mural thrombus. Multiplanar reconstructions, easily performed in 1-5 minutes on standard workstations, are of particular diagnostic value in problematic cases. However, reformations cannot produce results better than the initial axial images from which they are generated; again, meticulous CT technique is essential.

"ACCURACY" OF SINGLE CHANNEL HELICAL CT ANGIOGRAPHY

Studies of accuracy usually compare CT to pulmonary angiography, the favored "gold standard" in PE diagnosis. CT and angiography are both direct tests for PE which depict actual endovascular thrombi. The accuracy of CT, like that of angiography, depends on many variables, including the technical adequacy of the examination, the number and location of thrombi (extent of disease), prevalence of PE in the population, reader experience, and the criteria used for a positive or negative test result. CT accuracy also depends upon the actual accuracy of the "gold standard" and can therefore not exceed 100%. This is intuitive; however, clear CT diagnoses of PE can occur in the setting of normal or nondiagnostic angiograms [7]. A simple quotation of the published sensitivity and specificity of CT is simplistic yet is routinely incorporated into discussions of all types on this topic. The accuracy of even single channel CT for PE is probably over 100%, but that of MCCT is certainly so. This will be discussed in some detail.

More relevant is the fact that properly performed CTA (even single channel) and angiography depict identical information, but in different ways. Remy-Jardin and colleagues showed that the number of arteries depicted with properly performed CT through the segmental level is equivalent to that of angiography and that perfect anatomic correlation between the two modalities was present in 188 central emboli in 39 patients [7]. Given the superior contrast resolution of CT and the elimination of

overlapping structures due to the nature of cross sectional imaging, it is not surprising that single channel CTA is at least as good as and should be better than cut-film-based pulmonary angiography in most cases. Both studies are limited in the display of subsegmental arteries due to their small size. Conventional angiographic dual observer agreement is only slightly better than random guessing at the subsegmental level (66%) and falls to 13% with three readers [6, 8].

Fortunately, isolated subsegmental emboli are of controversial significance, however, for in patients without concomitant cardiopulmonary disease, no difference in the incidence of recurrent PE between treated and untreated patients with these small clots has been noted [9]. However, in patients with limited cardiopulmonary reserve, such small emboli may be fatal. The residual DVT burden is of major importance in this setting, as this determines the risk of continued or recurrent thromboembolism. Assessment of the deep venous system can be performed at the same sitting as the single channel chest CT. MCCT is the gold standard for the diagnosis of isolated subsegmental (and smaller) clots, as will be shown. In the inpatient setting using single channel CTA, the author has never read an isolated subsegmental clot- the risk of anticoagulation may exceed the risk of morbidity and mortality from the suspected clot in this setting. This may change, however, with MCCT- for the first time, the issue of the incidence and significance of isolated subsegmental clot may be resolved- we can actually see them.

SCINTIGRAPHY: AN INDIRECT TEST (OR EDUCATED GUESS)

The VQ scan depicts neither thrombus nor the actual pulmonary circulation; it is an indirect test, and the presence or absence of PE is based on inference. In a study of 185 perfusion defects in 68 patients, only 16% corresponded to visible angiographic abnormalities; only 10 of 35 segmental or larger scintigraphic mismatches corresponded to angiographically-proven emboli, while 43 segmental thrombi identified at angiography had no evident ventilation-perfusion mismatches [10]. What are we looking at?

Patients with proven PE in the setting of low- probability scans do not necessarily have subsegmental or a few small emboli; central thrombus involving main or lobar arteries is more frequent than isolated subsegmental thrombi (31% to 17%) in these patients [11]. False positive scintigraphy (high probability scans in the absence of PE) also occur; 12% of such patients may have normal angiograms [6]. Clearly, low- or indeterminate probability scans do not constitute sufficient evidence upon which to base treatment decisions, particularly in patients with other cardiopulmonary disease.

Recent studies have directly compared single channel CTA to scintigraphy in the setting of possible PE. Cross and colleagues found that CTA enabled confident diagnosis (positive, negative, or alternative) in 90% of patients compared to 54% for scintigraphy [12]. CTA also detected thrombi missed or considered indeterminate at scintigraphy, although the opposite did not occur. A unique study conducted by van Rossum and colleagues evaluated 123 patients who underwent both VQ and CT within a 48 hour period; each patient was assessed twice by a radiologist and a pulmonologist with associated clinical information, chest radiographs, and either the VQ scan or the CTA [13]. There was a significant difference in the number of inconclusive evaluations with scintigraphy (28%) in comparison to CT (8%). CT also had a higher sensitivity (75% to 49%) and specificity (90% to 74%) for PE than did scintigraphy, and enabled twice the number of alternative diagnoses (93% to 51%). Of note, these alternative diagnoses excluded conditions evident on the chest radiograph, but included entities such as aortic dissection, mediastinitis, and malignancy. In the 35 inde-

terminate scintigrams, CT correctly identified the final diagnosis in 29 (13 PE, 11 alternative, 5 normal). These authors suggested that CTA replace the VQ scan.

MULTI-CHANNEL CT: THE DEFINITIVE TEST

The advantage of multi-channel CT is speed. Thus, much larger volumes can be covered with the same or even thinner collimation than possible with a single slice scanner. In practice, we use 1.25 mm collimation, single breath hold, HS mode (pitch=6), and cover the entire chest in one breath hold. Images are reconstructed at 1 mm intervals. Therefore, we get both thinner sections (better resolution) and a larger coverage area than with single channel scanning. This facilitates depiction of smaller peripheral vessels, increases the resolution and quality of multiplanar reformations, and leads to potential applications of dynamic repeated acquisitions through questionable areas if necessary. We assess the pelvic and upper leg veins routinely with 5 or 10 mm collimation 2-3 minutes after the start of the contrast injection. Tube cooling, often problematic in single channel scanning, does not limit multi-channel acquisitions.

Image processing is an area of active research. Cardiac gating software is now available for multi-channel scanners that facilitates data acquisition only during quiescent phases of the cardiac cycle as well. Huge data sets, gated, with 1.25 mm overlapping reconstructions can be sent to powerful computers; software engineers in concert with radiologists are only beginning to develop new means of processing this information to extract pertinent diagnostic value with the click of a mouse. Axial images will probably be only a small or nonexistent part of CT display in the not-so-distant future. Examples of color-based threshold techniques and pulmonary perfusion maps will be shown.

More "conventional" image processing tools, including maximum intensity projection (MIP) angiography, can also be used as needed. These images project the brightest pixel at a given location in a preselected slab of images onto a final summation image- we often perform 3.5-5 mm MIP angiography using our CTA data set- this reduces the number of images for review and increases the degree of apparent vascular enhancement. Examples and pitfalls will be illustrated.

In sum, multi-channel CT represents a major advance in our ability to scan large volumes rapidly with collimation sufficiently small to resolve small vessels. Processing volumetric data in novel ways is the key to use of the full potential of this exciting technological advance.

CLINICAL LITERATURE: CONTROVERSIES

Despite the above, much clinical literature continues to question the use of CTA in comparison to old (old, not gold) standards (scintigraphy, conventional angiography, and even best clinical guess). In part, this is due to an incomprehensible simple "meta-analysis" of the CT "accuracy" literature despite its clear limitations. Other problematic factors relate to the specialty-of-origin of the authors of recent major publications: in many cases, judgments on CT angiography are rendered without any input from radiologists. Editorial boards in many cases appear to be impressed by patient numbers and have little expertise in radiologic techniques. We must be aware of these studies and must be very clear and pointed in our criticism as needed.

It is vital for radiologists to peruse the major clinical journals for such "reviews" or "panels" and especially for the trendy "meta-analysis"- such are often the basis for physician test-ordering patterns. It is our job to maintain diligence in the appropriate education of nonradiologist physicians and physician extenders- technology changes are quite rapid and will continue to be so.

ACCP Consensus Committee on PE, 1998

Based on pooled "CT accuracy" data, the panel concluded that CTA "still under investigation" and that a normal CTA "does not exclude PE." (In fairness, these recommendations preceded recent CTA outcomes studies.) The expert panel concluded that "further studies are necessary to delineate the diagnostic role" of CTA. There were no CT/CTA specialists on the panel, but the recommendations are now familiar to most practicing pulmonary physicians and have not yet been updated [14]. Still, simple combination of reported accuracy values without a consideration of the variables that explain these quoted ranges seems superficial for such an expert group.

Annals of Internal Medicine CTA Accuracy Meta-analysis, 2000

Rathbun and colleagues concluded that no sound methodologic studies prove that CTA should be used clinically, and cite the "wide range of accuracy values" as well as an "interobserver variability problem" (as if this is not problematic with scintigraphy or best clinical guess or even conventional angiography). Stuningly, this Oklahoma group of nonradiologists concludes that "scintigraphy combined with best clinical guess" is still the best way to diagnose or exclude pulmonary embolism. Maybe in Oklahoma [15].

Annals of Internal Medicine Repeats Controversial CTA Manuscript, 2001

Perrier and colleagues published a disastrous review of 299 ER patients who had abnormal d-dimer levels and CTA [16]. Gold standards for PE included a positive conventional angiogram, DVT on ultrasound with clinical symptoms of PE, or a high probability VQ scan. The gold standard for "no PE" was a negative angiogram (in few patients), a normal or low probability VQ scan, or a low clinical suspicion of PE with negative leg ultrasound and an indeterminate VQ scan. Any event (DVT or PE) in a 3-month follow-up period (diagnosed in the same ways as above) indicated that the initial CTA was a false negative.

In other words, clot noted on CTA was wrong if the VQ was low probability. A negative CTA was wrong if the patient had a DVT within 3 months of follow-up or had a DVT and symptoms of possible PE at initial diagnosis.

The authors' unavoidable conclusion: the sensitivity of CTA (70%) is too low to exclude PE. Worse, "false positives" occur "even in the lobar (15%) and segmental (38%) levels." Again- in other words- 15% of the lobar clots and 38% of all the segmental clots identified at CTA were reported as false positives of CTA rather than false negatives of the other testing combinations. Alternative explanation: the VQ scan and best clinical guess can miss clots, even big ones.

Archives of Surgery CTA Condemnation, 2001

Velmahos and colleagues (no radiologists) assessed CTA results in 22 SICU patients who also underwent pulmonary angiography. CTA techniques were limited, with a single slice machine, 3 mm collimation, only 100cc of intravenous contrast- worse, there was no induced apnea in these intubated patients [17].

CT sensitivity values in comparison to the angiography gold standard were low, but angiography showed isolated segmental or subsegmental in clots in 6 of the 11 patients with "proven" PE. The authors conclude that "CTA has not stood up to the challenge" and cannot be relied upon in ICU patients.

What can we as radiologists say? It is not surprising that technically bad CTA exams performed in moving patients miss tiny clots diagnosed with great certainty by angiography readers in tiny vessels where the interobserver variability is similar that of predicting the results of a coin flip. This cannot, however, rationally lead to the conclusion that CTA is not accurate.

AJRCCM Prospective CTA Validation, 2002

Fortunately, there are some well-constructed and logical studies that confirm the clinical role of CTA- even single slice CTA- and document the accuracy of a negative CTA during follow-up intervals. **Lorut** et al. reported results in a prospective (n=247) cohort of patients suspected of PE and studied with CTA, V/Q, and d-dimer levels all within 24 hours [18]. Gold standards for diagnosis included:

Positive PE: CTA positive or DVT US positive (US was performed only if the if CTA was negative or inconclusive and the VQ was nondiagnostic)

Negative PE: CTA negative and one of other stated criteria met

The prevalence PE in the cohort was 42%; CT diagnosed 73% of these cases; US 23%; VQ 4% (VQ diagnoses were only in patients who did not undergo CT, US diagnosed DVT, not PE). The mortality rates in patients with (treated) and without (not treated) PE were comparable; recurrent PE /DVT rate was 1-2% in each group. The authors conclude that CTA positive diagnoses are reliable, negative CTA results were never overturned unless by leg ultrasound showing DVT, and that the VQ is superfluous.

Outcomes After Negative CTA: European Journal of Radiology, 2001

Several outcomes studies are also now available documenting negligible PE or DVT rates in patients 3-6 months after negative CTA. **Gottsater** et al. reported 3-month outcomes in 305 patients studied with CTA for possible PE; 61 (20%) had a CTA diagnosis of PE, and 215 of the negative CTA group were followed and not treated. Three (1.4%) of these patients developed DVT or PE; 2 had underlying advanced malignancy and one had COPD [19]. The authors conclude that patient outcomes after negative CTA are no different than outcomes reported after normal VQ or conventional angiography.

Outcomes After Negative CTA in High risk Patients, 2001

Ost et al. studied 103 patients who had intermediate or low probability VQ scans and a high clinical suspicion for PE with CTA: 22 were positive, 71 negative, and 10 indeterminate. Only 3 of the 71 patients with negative CTA had a PE in a 6 month follow-up period [20]. Thus, even in these symptomatic patients with non-normal scintigraphy, negative CTA appears to be safe. This has been our clinical experience as well.

CONCLUSIONS

- CTA has all the desired attributes of a test for PE/DVT
- Multi-channel CTA is an angiogram- but better
- The accuracy, particularly of multi-channel CTA, exceeds 100% for PE
- Multi-channel CTA is the best test for subsegmental (and smaller) clot
- CTA allows rapid estimate of clot age and extent
- CTA facilitates other diagnoses in the chest and allows leg vein assessment
- Perfusion analysis and color volumetric images possible in the near future
- Not all CTA is the same: beware simplistic accuracy quotes and meta-analyses
- Be suspect of the literature: especially if no radiologist is involved
- New research directions: redo all aspects of PE from physiology to treatment

REFERENCES

1. Siddique RM, Siddique MI, Rimm AA. Trends in pulmonary embolism mortality in the US elderly population: 1984 through 1991. *Am J Public Health* 1998; 88(3):478-480.

2. Goldhaber SZ, Hennekens CH, Evans DA, et al. Factors associated with the correct antemortem diagnosis of major pulmonary embolism. *Am J Med* 1982; 73:822-826.
3. Proctor MC, Greenfield LJ. Pulmonary embolism: diagnosis, incidence, and implications. *Cardiovasc Surg* 1997; 5(1):77-81.
4. Monreal M, Ruiz J, Olazabal A, Arias A, Roca J. Deep venous thrombosis and the risk of pulmonary embolism: a systematic study. *Chest* 1992; 102:667-681.
5. Decousus H, Leizorovicz A, Parent F, et al. A clinical trial of vena cava filters in the prevention of pulmonary embolism in patients with proximal deep venous thrombosis. *N Engl J Med* 1998; 338:409-415.
6. The PIOPED investigators. Value of the ventilation/perfusion scan in acute pulmonary embolism: results of the Prospective Investigation of Pulmonary Embolism Diagnosis (PIOPED). *JAMA* 1990; 263:2753-2759.
7. Remy-Jardin M, Remy J, Deschildre F. Diagnosis of pulmonary embolism with spiral CT: comparison with pulmonary angiography and scintigraphy. *Radiology* 1996; 200:699-706.
8. Quinn MF, Lundell CJ, Klotz TA, et al. Reliability of selective pulmonary arteriography in the diagnosis of pulmonary embolism. *AJR* 1987; 149:469-471.
9. Stein PD, Henry JW, Relyea B. Untreated patients with pulmonary embolism: outcome, clinical, and laboratory assessment. *Chest* 1995; 107:931-935.
10. Breslaw BH, Dorfman GS. Ventilation/perfusion scanning for prediction of the location of pulmonary emboli: correlation with pulmonary angiographic findings. *Radiology* 1992; 185:180-185.
11. Stein PD, Henry JW. Prevalence of acute pulmonary embolism in central and subsegmental pulmonary arteries and relation to probability interpretation of ventilation/perfusion lung scans. *Chest* 1997; 111:1246-1248.
12. Cross JLL, Kemp PM, Walsh CG, Flower CDR, Dixon AK. A randomized trial of spiral CT and ventilation perfusion scintigraphy for the diagnosis of pulmonary embolism. *Clin Radiol* 1998; 53:177-182.
13. van Rossum AB, Pattynama PMT, Mallens WMC, Hermans J, Heijerman HGM. Can helical CT replace scintigraphy in the diagnostic process in suspected pulmonary embolism? A retrospective-prospective cohort study focusing on total diagnostic yield. *Eur Radiol* 1998; 8:90-96.
14. ACCP Consensus Committee on Pulmonary Embolism. Opinions regarding the diagnosis and management of venous thromboembolic disease. *Chest* 1998; 113:499-504.
15. Rathbun SW, Raskob GE, Whitsett TL. Sensitivity and specificity of helical computed tomography in the diagnosis of pulmonary embolism: a systematic review. *Ann Intern Med* 2000; 132:227-232.
16. Perrier A, Howarth N, Didier D, Loubeyre P, Unger PF, de Moerloose P, Slosman D, Junod A, Bounameaux H. Performance of helical computed tomography in unselected outpatients with suspected pulmonary embolism. *Ann Intern Med* 2001; 135(17):88-97.
17. Velmahos GC, Vassiliu P, Wilcox A, Hanks SE, Salim A, Harrel D, Palmer S, Demetriades D. Spiral computed tomography for the diagnosis of pulmonary embolism in critically ill surgical patients: a comparison with pulmonary angiography. *Arch Surg* 2001; 136(5):505-11.
18. Lorut C, Ghossains M, Horellou MH, Achkar A, Fretault J, Laaban JP. A noninvasive diagnostic strategy including spiral computed tomography in patients with suspected pulmonary embolism. *Am J Respir Crit Care Med* 2000 Oct;162:1413-8.
19. Gottsater A, Berg A, Centergard J, Frennby B, Nirhov N, Nyman U. Clinically suspected pulmonary embolism: is it safe to withhold anticoagulation after a negative spiral CT? *Eur Radiol* 2001;11(1):65-72.
20. Ost D, Rozenshtein A, Saffran L, Snider A. The negative predictive value of spiral computed tomography for the diagnosis of pulmonary embolism in patients with nondiagnostic ventilation-perfusion scans. *Am J Med* 2001;110(1):16-21.

CT Structural and Functional Imaging of PE

U. Joseph Schoepf, M.D.

Department of Radiology, Brigham and Women's Hospital, Harvard Medical School

CT Imaging of Pulmonary Embolism: General Considerations

Although increasingly sophisticated clinical algorithms for "bed-side" exclusion of Pulmonary Embolism (PE) are being developed, mainly based on a negative d-dimer test¹⁻⁴ there is a high and seemingly increasing demand for imaging tests for suspected PE.

Some still regard invasive pulmonary angiography as the "gold standard" technique for PE diagnosis, but in reality it is infrequently performed⁵⁻⁸. It is perceived as an invasive procedure, although the incidence of complications with contemporary technique is low^{9, 10}. More importantly there is accumulating evidence describing the limitations of this technique for the unequivocal diagnosis of isolated peripheral pulmonary emboli: Two recent analyses of the inter-observer agreement rates for detection of subsegmental emboli by selective pulmonary angiography ranged between only 45% and 66%^{11, 12}. Given such limitations, use of this test as an objective and readily reproducible tool for the verification of findings at competing imaging modalities as to the presence or absence of PE seems questionable and the status of pulmonary angiography as the standard of reference for diagnosis of PE is in doubt^{11, 12}.

Use of nuclear medicine imaging, once the first study in the diagnostic algorithm of PE, is in decline^{13, 14} due to the high percentage of indeterminate studies (73% of all performed¹⁵) and poor inter-observer correlation¹⁶. Revised criteria for the interpretation of ventilation-perfusion scans^{17, 18} and novel technologies in nuclear medicine such as single photon emission tomography (SPECT)^{19, 20} can decrease the ratio of indeterminate scintigraphic studies, but cannot offset the limitations inherent to a functional imaging test²¹.

Contrast enhanced magnetic resonance (MR) angiography has been evaluated for the diagnosis of acute PE²²⁻²³. However, the acquisition protocols that are currently available for MR pulmonary angiography lack sufficient spatial resolution for reliable evaluation of peripheral pulmonary arteries^{23, 24}. More importantly, this modality has not seen widespread use in the acutely ill patient with suspected PE due to lack of general availability, relatively long examination times and difficulties in patient monitoring.

This leaves us with computed tomography (CT), which for most practical purposes has become the first line imaging test after lower extremity ultrasound for the assessment of patients with suspected PE in daily clinical routine. The most important advantage of CT over other imaging modalities is that both mediastinal and parenchymal structures are evaluated, and thrombus is directly visualized^{25, 26}. Studies have shown that up to two thirds of patients with an initial suspicion of PE receive another diagnosis²⁷, some with potentially life-threatening diseases, such as aortic dissection, pneumonia, lung cancer, and pneumothorax²⁸. Most of these diagnoses are amenable to CT visualization, so that in many cases a specific etiology for the patients' symptoms and important additional diagnoses can be established²¹. The inter-observer agreement for CT is better than for scintigraphy²⁹; in a recent study the inter-observer agreement for the diagnosis of PE was excellent for spiral CT angiography ($k=0.72$) and only moderate for ventilation-perfusion lung scanning ($k=0.22$)¹⁶. CT also appears to be the most cost-effective modality in the diagnostic algorithm of PE compared to algorithms that do not include CT, but are based on other imaging modalities (ultrasound, scintigraphy,

pulmonary angiography)³⁰. Additionally, there are some indications that CT may not only be used for evaluating thoracic anatomy in suspected PE but could also to some degree allow derivation of physiologic parameters on lung perfusion at single-slice, electron-beam and multidetector-row CT³¹⁻³³.

The main impediment for the unanimous acceptance of computed tomography as the new modality of choice for the diagnosis of acute PE have been limitations of this modality for the accurate detection of small peripheral emboli. Early studies comparing single-slice CT to selective pulmonary angiography demonstrated CT's high accuracy for the detection of PE to the segmental arterial level³⁴⁻³⁷ but suggested that subsegmental pulmonary emboli may be overlooked by CT scanning. The degree of accuracy that can be achieved for the visualization of subsegmental pulmonary arteries and for the detection of emboli in these vessels with single-slice, dual-slice and electron-beam CT scanners was found to range between 61% and 79%^{36, 38-40}, limitations that are overcome by novel developments in CT technology.

Advantages of Multidetector-Row CT for PE Imaging

In the last few years CT has seen decisive dynamic developments, mainly brought about by the advent of multidetector-row CT technology^{41, 42}. The current generation of 4-slice, 8-slice and 16-slice CT scanners now allows for acquisition of the entire chest with 1-mm or sub-millimeter resolution within a short single breath-hold of now less than 10 seconds in the case of 16-slice CT. The ability to cover substantial anatomic volumes with high in-plane and through-plane spatial resolution has brought with it a number of clear advantages. Shorter breath-hold times were shown to benefit imaging of patients with suspected PE and underlying lung disease reducing the percentage of non-diagnostic CT pulmonary angiography investigations⁴³. The near isotropic nature of high-resolution multidetector-row CT data lends itself to 2-D and 3-D visualization. This may, in some instances, improve PE diagnosis⁴⁴ but is generally of greater importance for conveying information on localization and extent of embolic disease to referring clinicians in a more intuitive display format. Probably the most important advantage is improved diagnosis of small peripheral emboli. Single-slice CT has shown that superior visualization of segmental and subsegmental pulmonary arteries can be accomplished with thinner slice widths (e.g. 2-mm versus 3-mm)³⁸. However, with single-slice CT the range of coverage with thin slice widths within one breath-hold was limited^{38, 40}. The high spatial resolution of 1-mm or sub-millimeter collimation data sets now allows evaluation of pulmonary vessels down to 6th order branches⁴⁵ and significantly increases the detection rate of segmental and subsegmental pulmonary emboli⁴⁶. This improved detection rate is likely due to reduced volume averaging and the accurate analysis of progressively smaller vessels by use of thinner sections. These results are most striking in peripheral arteries with an anatomic course parallel to the scan plane; such vessels tend to be most affected by volume averaging when thicker slices are used⁴⁶. The high spatial resolution along the scan axis of a thin-collimation multidetector-row CT data set, however, allows an accurate evaluation of the full course of such vessels. The inter-observer correlation for confident diagnosis of subsegmental emboli with high-resolution multidetector-row CT by far exceeds the reproducibility of selective pulmonary angiography^{11, 12, 46}.

Imaging the Subsegmental Embolus

While traditional technical limitations of CT in the diagnosis of pulmonary emboli appear successfully overcome by multidetector-row CT, we are now facing new challenges that are a direct result of our high-resolution imaging capabilities. Small peripheral clots that might have gone unnoticed in the past are now frequently detected, often in patients with minor symptoms.

While, based on a good quality multidetector-row CT scan, there may be no doubt in the mind of the interpreting radiologists as to the presence of a small isolated clot, such findings will be increasingly difficult to prove in a correlative manner. Animal experiments that use artificial emboli as an independent gold standard indicate that high-resolution 4-slice multidetector-row CT is at least as accurate as invasive pulmonary angiography for the detection of small peripheral emboli⁴⁷. However, it appears highly unlikely that pulmonary angiography will be performed on a patient merely to prove the presence of a small (2-3 mm) isolated embolus. Additionally, given the limited inter-observer correlation of pulmonary angiography discussed earlier^{11, 12} it appears doubtful that this test, even if performed, would provide as useful and conclusive proof as high-resolution multidetector-row CT. Broad based studies such as PLOPED II, which set out to establish the efficacy of multidetector-row CT in suspected PE, account for this latter fact by using a composite reference test based on ventilation/perfusion scanning, ultrasound of the lower extremities, pulmonary angiography, and contrast venography to establish the PE status of the patient⁴⁸.

Perhaps more importantly there is a growing sense of insecurity within the clinical community how to manage patients in whom a diagnosis of isolated peripheral embolism has been established. It has been shown that 6%¹⁵ to 30%⁴⁹ of patients with documented PE present with clots only in subsegmental and smaller arteries, but the clinical significance of small peripheral emboli in subsegmental pulmonary arteries in the absence of central emboli is uncertain. It is assumed that one important function of the lung is to prevent small emboli from entering the arterial circulation²⁵. Such emboli are thought to form even in healthy individuals although this notion has never been substantiated⁵⁰. Controversy also exists, whether the treatment of small emboli, once detected, may result in a better clinical outcome for patients^{37, 51, 52}. There is little disagreement though, that the presence of peripheral emboli may be an indicator for current deep vein thrombosis thus potentially heralding more severe embolic events^{27,49,53}. A burden of small peripheral emboli may also have prognostic relevance in individuals with cardio-pulmonary restrictions^{25,49,52} and for the development of chronic pulmonary hypertension in patients with thromboembolic disease⁴⁹.

Perhaps the most practical and realistic scenario for studying the efficacy of computed tomography for the evaluation of patients with suspected PE is to assess patient outcome. There is a growing body of experience concerning the negative predictive value of a normal CT study and patient outcome if anticoagulation is subsequently withheld^{16, 43, 52, 54-58}. According to these retrospective studies the negative predictive value of a normal CT study is high, approaching 98%, regardless whether multidetector-row technology is used⁴³ or whether underlying lung disease is present⁵⁷. The frequency of a subsequent clinical diagnoses of PE or DVT after a negative CT pulmonary angiogram is low and lower than that after a negative or low-probability V-Q scan⁵². Thus even single-slice CT appears to be a reliable imaging tool for excluding clinically relevant PE so that it appears that anticoagulation can be safely withheld when the CT scan is normal and of good diagnostic quality^{52, 58}.

CT Functional Imaging of PE

To date, CT has not permitted the functional evaluation of

pulmonary microcirculation during pulmonary embolism. Yet, the choice of the adequate therapeutic regimen critically hinges on an accurate evaluation of the functional effect of the embolic event on lung perfusion. If large percentages of the lung parenchyma are affected by embolic occlusion, imminent right heart failure warrants a more aggressive regimen, such as thrombolysis that carry a small but definite risk^{59 60}. Thus the quantitative assessment of the effect of PE on tissue perfusion may bear more important information for patient management than the direct visualization of emboli by CT angiography alone.

It has been shown that with the advent of fast CT scanning techniques functional parameters of lung perfusion can be non-invasively assessed by means of CT imaging^{31, 32, 61, 62}. In the following we would like to discuss different experimental approaches for visualization and quantification of pulmonary perfusion, based on various CT techniques. We anticipate these methods to evolve in a valuable adjunct to CT pulmonary angiography by providing both structural and functional information using the same modality. The well-established accuracy of CT for the depiction of emboli and thoracic anatomy is thus supplemented by an effective means to quantitatively assess the functional effect of the embolic event on lung perfusion. This way, a comprehensive diagnosis is feasible within few minutes, without having to subject a patient to multiple expensive and time-consuming tests requiring transportation and advanced logistics.

Electron-Beam CT:

Functional EBCT Scan Protocol:

A unique feature of Electron Beam CT (EBCT) is that it can be used both for volume scanning for the depiction of structure⁶³ and for functional analyses by acquiring high temporal resolution data sets simultaneously on multiple sections of an organ. EBCT has successfully been used for perfusion measurements in the heart^{64 65 66}, the brain⁶⁷ and the kidneys⁶⁸. The feasibility of pulmonary blood flow measurements with EBCT has been validated in a number of controlled animal studies^{69 70}. However the value of this method in the diagnostic work-up of patients with suspected PE has never been assessed. In a prospective study we were able to demonstrate the usefulness of EBCT as a single modality to image both thoracic structure and function in patients with suspected acute PE.

The technical design of the electron beam scanner is described in detail elsewhere^{71 72}. In the multidetector-row mode of the scanner eight slices in a 7.6-cm volume at 20 consecutive time-points can be acquired without patient table movement to monitor the passage of a contrast material bolus through the lung parenchyma. To improve the quality of the data, scans can be ECG triggered to the quiet diastolic phase of the heart cycle. For measuring pulmonary perfusion, contrast material is intravenously injected with a flow rate of 10 cc/s for 4 s.

Functional EBCT analysis:

For dynamic blood flow evaluation we use an approach that comprises a qualitative analysis by selectively coding lung pixel attenuation in a color-coded cold-to-hot spectrum. This way maps can be generated for visualization of parameters such as peak Hounsfield Unit (HU) change, time to peak or mean transit time of contrast material. In our experience peak HU change is most suitable for identification of flow deficits. Using this parameter a qualitative analysis of lung perfusion can be performed by generating a color-coded map for the eight scan levels that are simultaneously acquired by EBCT. On color-coded maps flow deficits are defined by predominance of cold-spectrum colors with segmental distribution. Guided by color-coded maps, a quantitative analysis for the assessment of regional pulmonary blood flow can be performed. To this end, time-density

curves (TDCs) are generated by manually tracing regions of interest (ROIs) over lung segments showing flow-deficits. A ROI over the main pulmonary artery or the right ventricle can be used as input function. Regional pulmonary blood-flow in each segment can then be assessed according to the indicator dilution theory^{73 74} using a basic flow equation^{64, 69} where $PBF/V = DPul / \int_{RCdt}$ (PBF/V = pulmonary blood flow per unit volume of lung tissue; $DPul$ = peak HU change during contrast injection; \int_{RCdt} = area under a g variate-fit of a TDC of the right side of the circulation).

Advantages and Disadvantages of Functional EBCT Perfusion Imaging of the Lung:

Once a suspicion of pulmonary embolism arises, crucial questions need to be answered: Is it indeed PE that causes the patient's symptoms, or are there other reasons for the patient's discomfort? If it is PE, where are the emboli located and how extensive is the disease? Does anticoagulation suffice, or are thrombolysis or invasive measures warranted? And are there conditions that prohibit thrombolysis? Where does the disease originate? Contrast enhanced CT provides high spatial resolution and allows the objective, non-invasive visualization of thoracic anatomy. Sources of chest pain other than PE can be identified. The location of pulmonary emboli and the extent of the disease can be assessed to determine the need for and feasibility of anticoagulation, thrombolysis or more invasive measures. However, to date, computed tomography has not permitted the functional evaluation of pulmonary microcirculation during pulmonary embolism. CT perfusion measurements as described in this chapter may represent a valuable adjunct to CT pulmonary angiography by providing both structural and functional information using the same modality. The well-established accuracy of CT for the depiction of emboli and thoracic anatomy is thus supplemented by an effective means to quantitatively assess the functional effect of thromboemboli on lung perfusion. This way, a comprehensive diagnosis is feasible within few minutes, without having to subject a patient to multiple expensive and time-consuming tests requiring transportation and advanced logistics. In a recent study³² we were able to show that EBCT can successfully be used for the functional analysis of pulmonary blood flow and therefore allows to differentiate between segments with normal and reduced capillary perfusion. This allows to estimate the percentage of lung parenchyma with impaired microcirculation. Thus, a decision whether anticoagulation or thrombolysis is warranted is facilitated. During the course of treatment, the effect of therapy may be monitored by comparing pre- and post-therapy blood-flow values by repetitive scanning. Up to two thirds of patients with initially suspected PE receive other diagnoses including unknown malignancies or life-threatening conditions such as aortic rupture or dissection. By initially performing a contrast enhanced thin-slice volume study, the presence of pulmonary embolism can be verified and other or additional underlying diseases are readily recognized. The patient with previously unknown small-cell lung cancer in our patient group illustrates the importance of a thorough analysis of thoracic structure. A major limitation is that the 7.6 cm scan volume of the dynamic study does not cover the entire chest. The additional radiation dose for the dynamic study amounts to an effective dose equivalent of 7.2 mSv, which about equals the radiation exposure usually applied during nuclear scanning⁷⁵.

While there is good correlation between volume and functional scans for the detection of segmental emboli, a potential limitation of this technique arises from partial occlusion of vessels with maintained blood flow on a capillary level despite of the presence of thrombi. Such findings may be regarded as "false negative" results. However, valuable information can be gained by assessing the actual effect of small emboli on lung microcirculation. Completely or partially maintained perfusion

despite of the presence of emboli revealed by functional scanning may influence the decision whether or not to start thrombolytic therapy in a patient, the latter carrying a small but definite risk^{59 60}. Thus the quantitative assessment of the effect of PE on tissue perfusion may bear more important information for patient management than the direct visualization of emboli by CT angiography alone. Non-occluding emboli are also a well-known problem in lung scintigraphy, where even extensive central emboli frequently go undiagnosed if they are only partially occluding and do not cause localized perfusion defects. Similar pitfalls can be avoided by the combined use of both CT angiography and CT perfusion measurement for a comprehensive diagnosis. Our model for the assessment of pulmonary blood flow in patients with suspected PE has been previously described^{64 69 73}. However, numerous different models have been developed in the past for the derivation of different blood flow parameters from non-invasive imaging modalities.

Functional Multidetector-Row CT Imaging of Lung Perfusion:

Dedicated image processing tools are currently being developed for use with high-resolution Multidetector-row CT. Based on EBCT experiences we currently pursue several approaches to non-invasively visualize blood-flow parameters in the lung with a dedicated software platform (LungLab™, Siemens). LungLab™ is an image processing tool for diagnosis of pulmonary embolism using high-resolution Multidetector-row CT protocols. For visualization of lung attenuation "Perfusion weighted display" allows color encoded display of lung parenchyma enhancement. This kind of display is generated by acquiring a high resolution Multidetector-row CT data set of the entire thorax with 500 msec gantry rotation, pitch of 6 at 120 kV and 120 mAs. Contrast enhancement is achieved with a sharp (5 cc/s) bolus of 120 cc low-viscosity, non-ionic contrast material with 16 s delay via a cubital vein. Images are reconstructed with 1-mm sections with a soft body kernel. The lung parenchyma is segmented from the enhanced thin slice reconstructions using threshold based contour finding to extract the lung volume and HU range selection to suppress major vascular structures. The segmented images are low pass filtered with an adaptive 3D filter. The filter can be selected out of a range of dedicated image filters. The resulting images are interactively mapped on a spectral color scale in order to optimally display differences in enhancement. Additional overlay of the parenchymal color map onto the original CT-image is used to enhance visualization of spatial relationships. Due to the isotropic nature of high resolution Multidetector-row CT data set, color-coded images can be viewed in arbitrary imaging planes. This allows for semi-quantitative evaluation of blood flow in the lung parenchyma. We anticipate these methods to evolve in a valuable adjunct to CT pulmonary angiography by providing both structural and functional information using the same modality. The well-established accuracy of CT for the depiction of emboli and thoracic anatomy is thus supplemented by an effective means to quantitatively assess the functional effect of thromboemboli on lung perfusion. This way, a comprehensive diagnosis is feasible within few minutes, without having to subject a patient to multiple expensive and time-consuming tests requiring transportation and advanced logistics.

Problems and Limitations of Computed Tomography for PE Diagnosis

Contrast Media Injection and Artifacts:

Despite advances in CT technology, there are still several factors that can render CT pulmonary angiography inconclusive. The most common reasons for non-diagnostic CT studies are poor contrast opacification of pulmonary vessels, patient motion and increased image noise due to excessive patient obesity.

The advent of multidetector-row CT necessitates an exten-

sive revision of contrast material injection protocols. Faster scan acquisition times allow scan acquisition during maximal contrast opacification of pulmonary vessels⁴⁰ but pose an increased challenge for precise timing of the contrast bolus. Strategies that have the potential to improve the delivery of contrast media for high and consistent vascular enhancement during CT pulmonary angiography include use of a test bolus or automated bolus triggering techniques⁷⁶. Saline chasing^{77, 78} has been used for effective utilization of contrast media and for reduction of streak artifacts arising from dense contrast material in the superior vena cava. Use of multi-phasic injection protocols has proven beneficial for general CT angiography^{79, 80} but has not been scientifically evaluated for the pulmonary circulation.

Another limitation that in some instances results in suboptimal diagnostic quality of CT pulmonary angiography are motion artifacts due to patient respiration or transmitted cardiac pulsation. Shorter breath-hold times that are feasible with multidetector-row CT should facilitate investigation of dyspneic patients⁴³ and reduce occurrence of respiratory motion artifacts. Similarly, artifacts arising from transmitted cardiac pulsation appear amenable to decreased temporal resolution with fast CT acquisition techniques⁴⁰. ECG-synchronization of CT scan acquisition allows for effective reduction of cardiac pulsation artifacts that might interfere with the unambiguous evaluation of cardiac structures, the thoracic aorta and pulmonary structures^{81, 82}. However, the spatial resolution that could be achieved e.g. with retrospectively ECG gated technique using the previous generation of 4-slice multidetector-row CT scanners was limited by the relatively long scan duration inherent to data oversampling⁸². Thus, high-resolution acquisition could only be achieved for relatively small volumes, e.g. the coronary arterial tree, but not for extended coverage of the entire chest. The advent of 16-slice scanners now effectively eliminates these previous tradeoffs. With 16-slice multidetector-row CT it is now possible to cover the entire thorax with sub-millimeter resolution in a single breath-hold with retrospective ECG gating, effectively reducing transmitted pulsation artefacts. This way, potential sources of diagnostic pitfalls arising from cardiac motion can be effectively avoided.

Radiation Dose:

Use of high resolution multidetector-CT protocols was shown to improve visualization of pulmonary arteries⁴⁵ and the detection of small subsegmental emboli⁴⁶. In suspected PE, establishing an unequivocal diagnosis as to the presence or absence of emboli or other disease based on a high-quality multidetector-row CT examination may reduce the overall radiation burden of patients, since further work-up with other tests that involve ionizing radiation may be less frequently required. However, if a 4-slice multidetector-row CT protocol with 4x1-mm collimation is chosen to replace a single-detector CT protocol based on a 1x5-mm collimation, the increase in radiation dose ranges between 30%⁸³ and 100%⁴¹. Similar increases in radiation dose, however, are not to be expected with the introduction of 16-slice multidetector-CT technology with sub-millimeter resolution capabilities. The addition of detector elements should improve tube output utilization compared to current 4-slice CT scanners and reduce the ratio of excess radiation dose that does not contribute to actual image generation⁸⁴. As sophisticated technical devices move into clinical practice, that modulate and adapt tube output relative to the geometry and x-ray attenuation of the scanned object, i.e. the patient⁸⁵⁻⁸⁷, substantial dose savings can be realized without compromising diagnostic quality⁸⁸. The most important factor, however, for ensuring responsible utilization of multidetector-row CT's technical prowess is the increased awareness of protocols used by technologists and radiologists. It has been shown that diagnostic

quality of chest CT is not compromised, if tube output is adjusted to the body type of the individual patient⁸⁹. Also, with multidetector-row CT radiologists are more and more adapting to the concept of volume imaging. There is a trade-off between increased spatial resolution and image noise, when thinner and thinner sections are acquired with fast CT techniques. Given the great flexibility and diagnostic benefit that a high-resolution, near-isotropic multidetector-row CT data set provides radiologists are increasingly willing to compromise on the degree of image noise in an individual axial thin-section image that they are willing to accept in order to keep radiation dose within reasonable limits.

Data Management:

Multidetector-row CT increases our diagnostic capabilities, however, the massive amount of data, which is generated by this technique puts significant strain on any image analysis and archiving system. A high-resolution 16-slice multidetector-row CT study in a patient with suspected pulmonary embolism routinely results in 500 – 600 individual axial images. 3D visualization of multidetector-row CT data in suspected PE may aid diagnosis in some instances and help avoid diagnostic pitfalls for example for the correct interpretation of hilar lymphatic tissue adjacent to central pulmonary arteries⁹⁰. However, in contrast to focal lung disease, which can be accurately diagnosed by use of maximum intensity projection reconstructions that beneficially “condense” large volume multidetector-row CT data sets⁹¹, a diagnosis of pulmonary embolism is usually most beneficially established based on individual axial sections. Interpretation of such a study is only feasible by use of digital workstations that allow viewing in “scroll-through” or “cine” mode. Development of dedicated computer aided detection algorithms⁹² may be helpful in the future for the identification of pulmonary emboli in large volume multidetector-row CT data sets. Large and accessible storage capacities are an essential requirement for successful routine performance of multidetector-row CT in a busy clinical environment. Adapting this environment to the new demands which are generated by the introduction of ever-faster scanning techniques is not a trivial task. New modalities for data transfer, data archiving and image interpretation will have to be devised in order to make full use of the vast potential of multidetector-row CT imaging.

REFERENCES

1. Wells PS, Anderson DR, Rodger M, et al. Excluding pulmonary embolism at the bedside without diagnostic imaging: management of patients with suspected pulmonary embolism presenting to the emergency department by using a simple clinical model and d-dimer. *Ann Intern Med* 2001; 135:98-107.
2. Kruip MJ, Slob MJ, Schijen JH, et al. Use of a clinical decision rule in combination with D-dimer concentration in diagnostic workup of patients with suspected pulmonary embolism: a prospective management study. *Arch Intern Med* 2002; 162:1631-5.
3. Dunn KL, Wolf JP, Dorfman DM, et al. Normal D-dimer levels in emergency department patients suspected of acute pulmonary embolism. *J Am Coll Cardiol* 2002; 40:1475.
4. Brown MD, Rowe BH, Reeves MJ, et al. The accuracy of the enzyme-linked immunosorbent assay D-dimer test in the diagnosis of pulmonary embolism: a meta-analysis. *Ann Emerg Med* 2002; 40:133-44.
5. Schluger N, Henschke C, King T, et al. Diagnosis of pulmonary embolism at a large teaching hospital. *J Thorac Imaging* 1994; 9:180-4.
6. Khorasani R, Gudas TF, Nikpoor N, Polak JF. Treatment of patients with suspected pulmonary embolism and intermediate-probability lung scans: is diagnostic imaging underused? *AJR Am J Roentgenol* 1997; 169:1355-7.

7. Crawford T, Yoon C, Wolfson K, et al. The effect of imaging modality on patient management in the evaluation of pulmonary thromboembolism. *J Thorac Imaging* 2001; 16:163-9.
8. Prologo JD, Glauser J. Variable diagnostic approach to suspected pulmonary embolism in the ED of a major academic tertiary care center. *Am J Emerg Med* 2002; 20:5-9.
9. Stein PD AC, Alavi A et al. Complications and Validity of Pulmonary Angiography in Acute Pulmonary Embolus. *Circulation* 1992; 85:462-468.
10. Zuckerman DA, Sterling KM, Oser RF. Safety of pulmonary angiography in the 1990s. *J Vasc Interv Radiol* 1996; 7:199-205.
11. Diffin D, Leyendecker JR, Johnson SP, Zucker RJ, Grebe PJ. Effect of Anatomic Distribution of Pulmonary Emboli on Interobserver Agreement in the Interpretation of Pulmonary Angiography. *AJR Am J Roentgenol* 1998; 171:1085-1089.
12. Stein PD, Henry JW, Gottschalk A. Reassessment of pulmonary angiography for the diagnosis of pulmonary embolism: relation of interpreter agreement to the order of the involved pulmonary arterial branch. *Radiology* 1999; 210:689-91.
13. Schibany N, Fleischmann D, Thallinger C, et al. Equipment availability and diagnostic strategies for suspected pulmonary embolism in Austria. *Eur Radiol* 2001; 11:2287-94.
14. Leveau P. [Diagnostic strategy in pulmonary embolism. National French survey]. *Presse Med* 2002; 31:929-32.
15. PIOPED-Investigators. Value of the Ventilation / Perfusion Scan in Acute Pulmonary Embolism. *JAMA* 1990; 95:498-502.
16. Blachere H, Latrabe V, Montaudon M, et al. Pulmonary embolism revealed on helical CT angiography: comparison with ventilation-perfusion radionuclide lung scanning. *AJR Am J Roentgenol* 2000; 174:1041-7.
17. Stein PD, Relyea B, Gottschalk A. Evaluation of individual criteria for low probability interpretation of ventilation-perfusion lung scans. *J Nucl Med* 1996; 37:577-81.
18. Stein PD, Gottschalk A. Review of criteria appropriate for a very low probability of pulmonary embolism on ventilation-perfusion lung scans: a position paper. *Radiographics* 2000; 20:99-105.
19. Palmer J, Bitzen U, Jonson B, Bajc M. Comprehensive ventilation/perfusion SPECT. *J Nucl Med* 2001; 42:1288-94.
20. Bajc M, Bitzen U, Olsson B, et al. Lung ventilation/perfusion SPECT in the artificially embolized pig. *J Nucl Med* 2002; 43:640-7.
21. Garg K, Welsh CH, Feyerabend AJ, et al. Pulmonary embolism: diagnosis with spiral CT and ventilation-perfusion scanning--correlation with pulmonary angiographic results or clinical outcome. *Radiology* 1998; 208:201-8.
22. Meaney J, Weg JG, Chenevert TL, Stafford-Johnson D, Hamilton BH, Prince MR. Diagnosis of Pulmonary Embolism with Magnetic Resonance Angiography. *N Engl J Med* 1997; 336:1422-1427.
23. Oudkerk M, van Beek EJ, Wielopolski P, et al. Comparison of contrast-enhanced magnetic resonance angiography and conventional pulmonary angiography for the diagnosis of pulmonary embolism: a prospective study. *Lancet* 2002; 359:1643-7.
24. Gupta A, Frazer CK, Ferguson JM, et al. Acute pulmonary embolism: diagnosis with MR angiography. *Radiology* 1999; 210:353-9.
25. Gurney JW. No Fooling Around: Direct Visualization of Pulmonary Embolism. *Radiology* 1993; 188:618-619.
26. Woodard PK. Pulmonary arteries must be seen before they can be assessed. *Radiology* 1997; 204:11-2.
27. Hull R, Raskob GE, Ginsberg JS, Panju AA, Brill-Edwards P, Coates G, Pineo GF. A noninvasive strategy for the treatment of patients with suspected pulmonary embolism. *Arch Intern Med* 1994; 154:289-297.
28. van Rossum AB, Pattynama PM, Mallens WM, et al. Can helical CT replace scintigraphy in the diagnostic process in suspected pulmonary embolism? A retrospective-prospective cohort study focusing on total diagnostic yield. *Eur Radiol* 1998; 8:90-6.
29. van Rossum AB, van Erkel AR, van Persijn van Meerten EL, et al. Accuracy of helical CT for acute pulmonary embolism: ROC analysis of observer performance related to clinical experience. *Eur Radiol* 1998; 8:1160-4.
30. van Erkel AR, van Rossum AB, Bloem JL, Kievit J, Pattynama PNT. Spiral CT Angiography for Suspected Pulmonary Embolism: A Cost-Effectiveness Analysis. *Radiology* 1996; 201:29-36.
31. Groell R, Peichel KH, Uggowitz MM, et al. Computed tomography densitometry of the lung: a method to assess perfusion defects in acute pulmonary embolism. *Eur J Radiol* 1999; 32:192-6.
32. Schoepf U, Bruening R, Konschitzky H, Becker CR, Knez A, Weber J, Muehling O, Herzog P, Huber A, Haberl R, Reiser M. Pulmonary Embolism: Comprehensive Diagnosis Using Electron-Beam Computed Tomography for Detection of Emboli and Assessment of Pulmonary Blood Flow. *Radiology* 2000; 217:693-700.
33. Wildberger JE, Niethammer MU, Klotz E, et al. Multi-slice CT for visualization of pulmonary embolism using perfusion weighted color maps. *Rofo Fortschr Geb Rontgenstr Neuen Bildgeb Verfahr* 2001; 173:289-94.
34. Remy-Jardin M, Remy J, Watinne L, Giraud F. Central pulmonary thromboembolism: diagnosis with spiral volumetric CT with the single-breath-hold technique--comparison with pulmonary angiography. *Radiology* 1992; 185:381-7.
35. Teigen CL, Maus TP, Sheedy PF II, Stanson AW, Johnson CM, Breen JF, McKusick MA. Pulmonary Embolism: Diagnosis with Contrast-Enhanced Electron Beam CT and Comparison with Pulmonary Angiography. *Radiology* 1995; 194:313-319.
36. Goodman LR, Curtin JJ, Mewissen MW, et al. Detection of pulmonary embolism in patients with unresolved clinical and scintigraphic diagnosis: helical CT versus angiography. *AJR Am J Roentgenol* 1995; 164:1369-74.
37. Remy-Jardin M, Remy J, Deschildre F, et al. Diagnosis of pulmonary embolism with spiral CT: comparison with pulmonary angiography and scintigraphy. *Radiology* 1996; 200:699-706.
38. Remy-Jardin M, Remy J, Artaud D, et al. Peripheral pulmonary arteries: optimization of the spiral CT acquisition protocol [see comments]. *Radiology* 1997; 204:157-63.
39. Qanadli SD, Hajjam ME, Mesurole B, et al. Pulmonary embolism detection: prospective evaluation of dual-section helical CT versus selective pulmonary arteriography in 157 patients. *Radiology* 2000; 217:447-55.
40. Schoepf UJ, Helmberger T, Holzknicht N, et al. Segmental and Subsegmental Pulmonary Arteries: Evaluation with Electron-Beam versus Spiral CT. *Radiology* 2000; 214:433-439.
41. McCollough CH, Zink FE. Performance evaluation of a multislice CT system. *Med Phys* 1999; 26:2223-30.
42. Hu H, He HD, Foley WD, Fox SH. Four multidetector-Row helical CT: image quality and volume coverage speed [In Process Citation]. *Radiology* 2000; 215:55-62.
43. Remy-Jardin M, Tillie-Leblond I, Szapiro D, et al. CT angiography of pulmonary embolism in patients with underlying respiratory disease: impact of multislice CT on image quality and negative predictive value. *Eur Radiol* 2002; 12:1971-8.
44. Remy-Jardin M, Remy J, Cauvain O, et al. Diagnosis of central pulmonary embolism with helical CT: role of two-dimensional multiplanar reformations. *AJR Am J Roentgenol* 1995; 165:1131-8.
45. Ghaye B, Szapiro D, Mastora I, et al. Peripheral pulmonary arteries: how far in the lung does multi-detector row spiral CT allow analysis? *Radiology* 2001; 219:629-36.

46. Schoepf U, Holzknicht N, Helmberger TK, Crispin A, Hong C, Becker CR, Reiser MF. Subsegmental Pulmonary Emboli: Improved Detection with Thin-Collimation Multidetector-Row Spiral CT. *Radiology* 2002; 222:483-490.
47. Baile E, King GG, Muller NL, D'Yachkova Y, Coche EE, Pare PD, Mayo JR. Spiral computed tomography is comparable to angiography for the diagnosis of pulmonary embolism. *Am J Respir Crit Care Med* 2000; 161:1010-1015.
48. Gottschalk A, Stein PD, Goodman LR, Sostman HD. Overview of Prospective Investigation of Pulmonary Embolism Diagnosis II. *Semin Nucl Med* 2002; 32:173-82.
49. Oser RF, Zuckerman DA, Gutierrez FR, Brink JA. Anatomic Distribution of Pulmonary Emboli at Pulmonary Angiography: Implications for Cross Sectional Imaging. *Radiology* 1996; 199:31-35.
50. Tetelman MR, Hoffer PB, Heck LL, Kunzmann A, Gottschalk A. Perfusion Lung Scan in Normal Volunteers. *Radiology* 1973; 106:593-594.
51. Novelline R, Baltarowich O, Athanasoulis C, Greenfield A, McKusick K. The Clinical Course of Patients with Suspected Pulmonary Embolism and a Negative Pulmonary Angiogram. *Radiology* 1978; 126:561-567.
52. Goodman LR, Lipchik RJ, Kuzo RS, et al. Subsequent pulmonary embolism: risk after a negative helical CT pulmonary angiogram--prospective comparison with scintigraphy [see comments]. *Radiology* 2000; 215:535-42.
53. Patriquin L, Khorasani R, Polak JF. Correlation of Diagnostic Imaging and Subsequent Autopsy Findings in Patients with Pulmonary Embolism. *AJR* 1998; 171:347-349.
54. Garg K, Sieler H, Welsh CH, et al. Clinical validity of helical CT being interpreted as negative for pulmonary embolism: implications for patient treatment. *AJR Am J Roentgenol* 1999; 172:1627-31.
55. Gottsater A, Berg A, Centergard J, et al. Clinically suspected pulmonary embolism: is it safe to withhold anticoagulation after a negative spiral CT? *Eur Radiol* 2001; 11:65-72.
56. Ost D, Rozenshtein A, Saffran A, Snider A. The negative predictive value of spiral computed tomography for the diagnosis of pulmonary embolism in patients with nondiagnostic ventilation-perfusion scans. *Am J Med* 2001; 110:16-21.
57. Tillie-Leblond I, Mastora I, Radenne F, et al. Risk of pulmonary embolism after a negative spiral CT angiogram in patients with pulmonary disease: 1-year clinical follow-up study. *Radiology* 2002; 223:461-7.
58. Swensen SJ, Sheedy PF, 2nd, Ryu JH, et al. Outcomes after withholding anticoagulation from patients with suspected acute pulmonary embolism and negative computed tomographic findings: a cohort study. *Mayo Clin Proc* 2002; 77:130-8.
59. Goldhaber S. Pulmonary Embolism Thrombolysis. Broadening the Paradigm for its Application. *Circulation* 1997; 96:716-718.
60. Konstantinides S GA, Olschewski M, Heinrich F, Grosser K, Rauber K, Iversen S, Redecker M, Kienast J, Just H, Kasper W. Association Between Thrombolytic Treatment and the Prognosis of Hemodynamically Stable Patients With Major Pulmonary Embolism. Results of a Multicenter Registry. *Circulation* 1997; 96:882-888.
61. Hoffman E, Tajik JK, Petersen G, Reiners TJ, Thompson BH, Stanford W. Perfusion Deficit Versus Anatomic Visualization in Detection of Pulmonary Emboli Via Electron-Beam CT: Validation in Swine. In Hoffman E, ed. *Medical Imaging 1995: Physiology and Function from Multidimensional Images*, Proc. SPIE 2433, 1995. pp. 26-36.
62. Hoffman E, McLennan G. Assessment of the Pulmonary Structure-Function Relationship and Clinical Outcome Measures: Quantitative Volumetric CT of the Lung. *Acad Radiol* 1997; 4:758-776.
63. Stanford W, Rooholamini SA, Galvin JR. Ultrafast Computed Tomography in the Detection of Intracardiac Masses and Pulmonary Artery Thrombembolism. In Stanford W RJ, ed. *Ultrafast Computed Tomography in Cardiac Imaging: Principles and Practice*. Mount Kisco, NY: Futura Publishing Co., Inc., 1992.
64. Wolfkiel C, Ferguson JL, Chomka EV, Law WR, Labin IN, Tenzer ML, Booker M, Brundage BH. Measurement of Myocardial Blood Flow by Ultrafast Computed Tomography. *Circulation* 1987; 76:1262-1273.
65. Rumberger J, Feiring AJ, Lipton MJ, Higgins CB, Eil SR, Marcus ML. Use of ultrafast computed tomography to quantitate regional myocardial perfusion: a preliminary report. *J Am Coll Cardiol* 1987; 9:59-69.
66. Brundage B. Beyond Perfusion with Ultrafast Computed Tomography. *Am J Cardiol* 1995; 75:69D-73D.
67. Gobbel G, Cann CE, Iwamoto HS, Fike JR. Measurement of Regional Cerebral Blood Flow in the Dog Using Ultrafast Computed Tomography, Experimental Validation. *Stroke* 1991; 22:772-779.
68. Lerman L, Taler SJ, Textor SC, Sheedy PF II, Stanson AW, Romero JC. Computed Tomography-Derived Intrarenal Blood Flow in Renovascular and Essential Hypertension. *Kidney International* 1995; 49:846-854.
69. Wolfkiel C, Rich S. Analysis of Regional Pulmonary Enhancement in Dogs by Ultrafast Computed Tomography. *Invest Radiol* 1992; 27:211-216.
70. Hoffman E, Tajik JK, Kugelmass SD. Matching Pulmonary Structure and Perfusion Via Combined Dynamic Multislice CT and Thin-Slice High-Resolution CT. *Comput Med Imaging Graph* 1995; 19:101-112.
71. Rumberger J. Ultrafast Computed Tomography Scanning Modes, Scanning Planes and Practical Aspects of Contrast Administration. In Stanford W RJ, ed. *Ultrafast Computed Tomography in Cardiac Imaging: Principles and Practice*. Mount Kisco, NY: Futura Publishing Co., Inc., 1992. pp. 17-24.
72. McCollough C, Morin RL. The Technical Design and Performance of Ultrafast Computed Tomography. *Radiol Clin North Am* 1994; 32:521-536.
73. Rumberger J, Bell MR, Feiring AJ, Behrenbeck T, Marcus ML, Ritman EL. Measurement of Myocardial Perfusion Using Fast Computed Tomography. In Marcus M, Schelbert HL, Skorton DJ, Wolf GL, ed. *Cardiac Imaging. A companion to Braunwald's Heart Disease*. Philadelphia: W.B. Saunders Co, 1991. pp. 688-702.
74. Thompson H, Starmer CF, Whalen RE, McIntosh HD. Indicator Transit Time Considered as a Gamma Variate. *Circulation Research* 1964; 14:502-512.
75. Rhodes C, Valind SO, Brudin LH, Wollmer PE, Jones T, Buckingham PD, Hughes JMB. Quantification of Regional V/Q Ratios in Humans by Use of PET. II Procedure and Normal Values. *J Appl Physiol* 1989; 66:1905-1913.
76. Kirchner J, Kickuth R, Laufer U, et al. Optimized enhancement in helical CT: experiences with a real-time bolus tracking system in 628 patients. *Clin Radiol* 2000; 55:368-73.
77. Hopper KD, Mosher TJ, Kasales CJ, et al. Thoracic spiral CT: delivery of contrast material pushed with injectable saline solution in a power injector. *Radiology* 1997; 205:269-71.
78. Haage P, Schmitz-Rode T, Hubner D, et al. Reduction of contrast material dose and artifacts by a saline flush using a double power injector in helical CT of the thorax. *AJR Am J Roentgenol* 2000; 174:1049-53.
79. Bae K, Heiken JP, Brink JA. Aortic and hepatic peak enhancement at CT: effect of contrast medium injection rate--pharmacokinetic analysis and experimental porcine model. *Radiology* 1998; 206:455-464.

80. Fleischmann D, Rubin GD, Bankier AA, Hittmair K. Improved uniformity of aortic enhancement with customized contrast medium injection protocols at CT angiography. *Radiology* 2000; 214:363-71.
81. Schoepf UJ, Becker CR, Bruening RD, et al. Electrocardiographically gated thin-section CT of the lung. *Radiology* 1999; 212:649-54.
82. Flohr T, Prokop M, Becker C, et al. A retrospectively ECG-gated multislice spiral CT scan and reconstruction technique with suppression of heart pulsation artifacts for cardio-thoracic imaging with extended volume coverage. *Eur Radiol* 2002; 12:1497-503.
83. Schoepf U, Bruening RD, Hong C, Eibel R, Aydemir S, Crispin A, Becker CR, Reiser MF. Multislice Helical CT Imaging of Focal and Diffuse Lung Disease: Comprehensive Diagnosis with Reconstruction of Contiguous and High-Resolution CT Sections from a Single Thin-Collimation Scan. *AJR Am J Roentgenol* 2001; 177:179-184.
84. Flohr T, Stierstorfer K, Bruder H, et al. New technical developments in multislice CT--Part 1: Approaching isotropic resolution with sub-millimeter 16-slice scanning. *Rofu Fortschr Geb Rontgenstr Neuen Bildgeb Verfahr* 2002; 174:839- 45.
85. Kalender WA, Wolf H, Suess C, et al. Dose reduction in CT by on-line tube current control: principles and validation on phantoms and cadavers. *Eur Radiol* 1999; 9:323-28.
86. Gies M, Kalender WA, Wolf H, Suess C. Dose reduction in CT by anatomically adapted tube current modulation. I. Simulation studies. *Med Phys* 1999; 26:2235-47.
87. Kalender WA, Wolf H, Suess C. Dose reduction in CT by anatomically adapted tube current modulation. II. Phantom measurements. *Med Phys* 1999; 26:2248-53.
88. Greess H, Nomayr A, Wolf H, et al. Dose reduction in CT examination of children by an attenuation-based on-line modulation of tube current (CARE Dose). *Eur Radiol* 2002; 12:1571-6.
89. Wildberger JE, Mahnken AH, Schmitz-Rode T, et al. Individually adapted examination protocols for reduction of radiation exposure in chest CT. *Invest Radiol* 2001; 36:604-11.
90. Remy J, Remy-Jardin M, Artaud D, Fribourg M. Multiplanar and three-dimensional reconstruction techniques in CT: impact on chest diseases. *Eur Radiol* 1998; 8:335-51.
91. Gruden JF, Ouanounou S, Tigges S, et al. Incremental benefit of maximum-intensity-projection images on observer detection of small pulmonary nodules revealed by multidetector CT. *AJR Am J Roentgenol* 2002; 179:149-57.
92. Schoepf U, Das M, Schneider AC, Anderson A, Wood SA, Costello P. Computer Aided Detection (CAD) of Segmental and Subsegmental Pulmonary Emboli on 1-mm Multidetector-Row CT (MDCT) Studies. *Radiology* 2002; 225 (suppl):384.

Non Thrombotic Pulmonary Embolism

Lawrence Goodman, M.D.

MONDAY

Not Pulmonary Embolism

Lawrence R. Goodman, MD, FACR
 Department of Diagnostic Radiology
 Milwaukee, Wisconsin USA



Emboli to the Lung

Venous Thromboembolism

Intrinsic Emboli

Septic
 Fat
 Amniotic fluid
 Air
 Tumor – 1^o or 2^o
 Parasites

Iatrogenic Emboli

Oil
 Catheters
 Coils, glue, etc.
 Silicone

Self-Injected

Talc
 Cotton
 Mercury
 Bullet

Emboli to the Lung

Venous Thromboembolism

Intrinsic Emboli

Septic
 Fat
 Amniotic fluid
 Air
 Tumor – 1^o or 2^o
 Parasites

Iatrogenic Emboli

Oil
 Catheters
 Coils, glue, etc.
 Silicone

Self-Injected

Talc
 Cotton
 Mercury
 Bullet

Septic Emboli

Source: catheters, valves, abscesses

Clinical: cough, fever, hemoptysis

Imaging: focal nodules, usually basilar, often cavities, feeding vessels

Lemierre's Syndrome

Source: mouth or dental infection, int. jugular vein puncture,

Clinical: dental or mouth infection
 >neck >mediastinum,
 osteomyelitis, hemoptysis
 (fusobacterium, bacteroides)

Imaging: septic emboli,
 mouth and neck inflammation,
 int. jugular thrombosis

Fat Emboli

Source: orthopedic trauma or surgery, severe soft-tissue injury,

Clinical: very variable, resp. insufficiency, neurologic, skin

Imaging: delayed patchy infiltrates, edema, emboli (?)

Etiology

External Trauma

Major trauma
Isolated long bone fracture
External cardiac massage

Underlying Disease

Pancreatitis
Diabetes mellitus
Acute osteomyelitis
Osteoporosis
Sickle cell disease
Thalassemia
Hepatic steatosis
Epilepsy
Burns
Decompression sickness
Teratoma

Surgery or Medical Procedures

Orthopedic procedures
Intraosseous venography
Liposuction
Bone marrow Tx
Venous hyperalimentation
Lung transplantation
Drug therapy

Amniotic Fluid Embolism

Source: placenta

Clinical: early labor to 48 hr. p. p.,
dyspnea, cyanosis, shock,
mental changes, coagulopathy, 50%
mortality

Imaging: edema, ARDS, emboli (?)

Venous Air Embolism

Source: trauma, surgery, catheters,
needle bx, barotrauma, asthma

Clinical: RV or pulmonary capillary
obstruction, sudden dyspnea,
cough, pain, tachycardia, mental
changes

Imaging: air (PA, hepatic veins), edema

Pulmonary Artery Sarcoma – CT

- Central
- (Unilateral)
- Expansile
- Distal thrombosis
- No emboli contralateral
- Out of proportion to Sx
- May “respond” to anticoagulation

Tumor Emboli

Source: melanoma, kidney, liver,
breast, choriocarcinoma

Clinical: gradual dyspnea, pulmonary
hypertension

Imaging: small, heterogenous opacities,
nodules, CT= beaded,
irregular vessels

Parasites

Source: ascaris, hookworm, filaria

Clinical: pulmonary infiltrates with
eosinophilia

Imaging: fleeting, peripheral
infiltrates

Parasites

Source: *Schistosoma* via portal or systemic veins

Clinical: acute = pneumonia, subacute = allergies, chronic = P.A.H.

Imaging: reticulonodular, patchy, P.A.H.

Emboli to the Lung

Venous Thromboembolism

Intrinsic Emboli

Septic
Fat
Amniotic fluid
Air
Tumor - 1° or 2°
Parasites

Iatrogenic Emboli

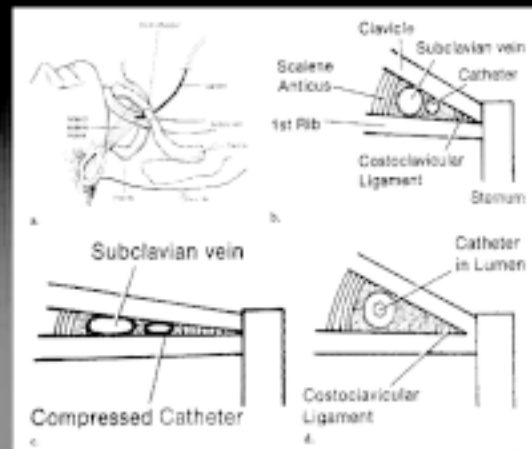
Oil
Catheters
Coils, glue, etc.
Silicone
Self-Injected
Talc
Cotton
Mercury
Bullet

Oil Embolism (Lymphangiogram)

Source: lymphatics > systemic veins > pulmonary capillaries

Clinical: Asx, fever, cough, hypotension

Imaging: fine reticular/nodular infiltrates



Silicone

Source: breast augmentation, dialysis

Clinical: progressive dyspnea

Imaging: patchy, ARDS

Emboli to the Lung

Venous Thromboembolism

Intrinsic Emboli

Septic
Fat
Amniotic fluid
Air
Tumor - 1° or 2°
Parasites

Iatrogenic Emboli

Oil
Catheters
Coils, glue, etc.
Silicone
Self-Injected
Talc
Cotton
Mercury
Bullets

Talc, Cellulose, Starch Emboli

Source: I.V. drug abuse

Clinical: Asx, fever, cough,

Imaging: fine reticular/nodular infiltrates, P.A.H.

Mercury Emboli

Source: Injection of metallic mercury

Clinical: cough, dyspnea, salivation, tremor

Imaging: tiny, dense spheres, (linear)

Emboli to the Lung

Venous Thromboembolism

Intrinsic Emboli	Iatrogenic Emboli
Septic	Oil
Fat	Catheters
Amniotic fluid	Coils, glue, etc.
Air	Silicone
Tumor – 1 ⁺ or 2 ⁺	<u>Self-Injected</u>
Parasites	Talc
	Cotton
	Mercury
	Bullet

References

- Chan OK, et al. Pulmonary tumor embolism: a critical review of clinical, imaging and hemodynamic features. *J Thorac Imaging* 1987; 2:4
- Dudney EM, Elliott CG. Pulmonary embolism from amniotic fluid, fat, and air. *Progress Cardiovascular Dis* 1996;447
- Engelke C, et al. High-resolution CT and CT angiography of peripheral pulmonary vascular disorders. *Radiographics* 2002; 22:739
- Franquet T, et al. Hydatid pulmonary embolism from a ruptured mediastinal cyst: high resolution computed tomography, angiography, angiography and pathologic features. *J Thorac Imaging* 1999;4:130
- Galpe B, et al. Lemierre's syndrome (cervicofacial abscess). *Pediatrics* 1999; 75:881
- Groell B, et al. Vascular air embolism: location, frequency and cause on electron beam CT studies of the chest. *Radiology* 1994; 202:439
- Hinke BH, et al. Pinch-off syndrome: a complication of implantable subclavian venous access devices. *Radiology* 1990; 177:353
- Kahlan JE, et al. Pulmonary septic embolic diagnosis with CT. *Radiology* 1990; 174:211
- Johnson MJ, Lucas GL. Fat embolism syndrome (review). *Orthopedics* 1999; 19:41.
- Peréz AG, et al. Deliberate, repeated self-administration of metallic mercury injection: case report and review of the literature. *Eur Radiol* 2000; 11: 1351
- Rossi SE, et al. Nonthrombotic pulmonary emboli. *AJR* 2000; 174:1499

Pulmonary Hypertension

Aletta Frazier, M.D.

Pulmonary hypertension is an extensively investigated but complex spectrum of diseases with insidious clinical onset and often devastating cardiorespiratory consequences. The condition is defined as a mean pulmonary artery pressure greater than 25 mm Hg at rest, or greater than 30 mm Hg during exercise. These hemodynamic parameters, combined with appropriate clinical history and histologic findings, confirm the diagnosis. The profoundly altered hemodynamics reflect underlying vascular remodeling, intravascular thrombosis, and/or extravascular constriction within the pulmonary circulation. In the case of severe, chronic pulmonary arterial hypertension, the sustained pressure or volume overload leads to changes in right heart mass and function. Additional notable complications of longstanding pulmonary hypertension include aneurysmal dilatation of the central pulmonary arteries, pulmonary elastic arterial thrombosis or dissection, and premature pulmonary arterial atherosclerosis.

In accordance with the established approach at the Armed Forces Institute of Pathology, the spectrum of pulmonary hypertension may be categorized for optimal clarification as either “precapillary” (with histologic changes limited to the arterial side of the pulmonary circulation) or “postcapillary” (with primary vascular changes within the pulmonary venous circulation, between the capillary bed and the left atrium). The histologic changes may be the ultimate consequence – and final common pathway – of an identifiable cause or a coexistent disease state. When no clear etiology is identified, the condition may be termed “idiopathic”.

SPECTRUM OF DISEASES

Well-recognized causes of precapillary pulmonary hypertension include Eisenmenger syndrome, chronic thromboembolic disease, chronic hypoxic states, collagen vascular disease, mediastinal fibrosis or tumor, and widespread pulmonary embolism secondary to agents such as circulating tumor cells, talc injection, and parasitic infestation. Associated conditions include human immunodeficiency virus (HIV) infection, pregnancy, portal hypertension, anorexigenic drug use, hyperthyroidism, and obstructive sleep apnea. Primary pulmonary hypertension (PPH) is a diagnosis reached when no clear etiology is identified and specific histologic features are observed. In the rare familial form of PPH, a gene mutation has been identified. Etiologies of postcapillary pulmonary hypertension include mediastinal fibrosis or tumor, left atrial mass, left ventricular failure, left-sided cardiac valvular disease, and more rarely, pul-

monary venous occlusion, congenital venous stenosis, and anomalous pulmonary venous return. The postcapillary counterpart to PPH is pulmonary veno-occlusive disease (PVOD), a rare idiopathic condition that widely affects the small pulmonary veins. Conditions associated with PVOD include HIV infection, pregnancy, bone marrow transplantation, and chemotherapeutic drug toxicity.

HISTOLOGIC FEATURES

The muscular arteries are predominantly affected in precapillary pulmonary hypertension with histologic changes of intimal cellular proliferation and medial smooth muscle hypertrophy. Features of necrotizing arteritis and plexiform lesions are observed exclusively in patients with PPH or Eisenmenger syndrome. A plexiform lesion is the hallmark of sustained and irreversible pulmonary arterial hypertension, recognized by pathologists as the focal disruption of the internal elastic lamina of small muscular arteries by a proliferative plexus of endothelial channels. Venous medial hypertrophy and intimal proliferation, with secondary findings of capillary congestion and interlobular septal edema and fibrosis, characterize postcapillary hypertension. Recanalized channels and webs within the pulmonary veins are features specific to PVOD and suggest that thrombosis is the central pathogenic factor.

RADIOLOGIC MANIFESTATIONS

The radiologic manifestations of pulmonary arterial hypertension reflect central pulmonary arterial dilatation, sharply diminished peripheral vascular markings, and right-sided hypertrophy with or without chamber dilatation. In cases of chronic thromboembolism or mediastinal fibrosis, findings may be limited to a few segmental or subsegmental vessels. Mosaic perfusion, dilated bronchial arteries and collateral vessels, subpleural pulmonary infarcts, calcified plaques lining larger pulmonary arteries, and arterial thrombosis may be evident on computed tomography. Magnetic resonance imaging is well-suited to demonstrate abnormalities in right ventricular configuration, as well as ventricular and valvular dysfunction. Postcapillary pulmonary hypertension classically reveals the features of interstitial edema, including Kerley B lines, thickened pleural fissures, and small pleural effusions. In addition, the radiologic evaluation of longstanding postcapillary pulmonary hypertension may demonstrate evidence of secondary pulmonary arterial hypertension, due to retrograde transmission of elevated pressures across the capillary bed.

REFERENCES

- Bergin CJ, Rios G, King MA, Belezzuoli E, Luna J, Auger WR. Accuracy of high-resolution CT in identifying chronic thromboembolic disease. *AJR* 1996; 166:1371-1377.
- Botney MD. Role of hemodynamics in pulmonary vascular remodeling. *Am J Respir Crit Care Med* 1999; 159:361-364.
- Burke A, Virmani R. Mini-symposium: pulmonary pathology – evaluation of pulmonary hypertension in biopsies of the lung. *Curr Diagn Pathol* 1996; 3:14-26.
- Burke AP, Farb A, Virmani R. The pathology of primary pulmonary hypertension. *Mod Pathol* 1991; 4:269-282.
- Dalen JE, Haffajee CI, Alpert JSIII, Howe JP, Ockene IS, Paraskos JA. Pulmonary embolism, pulmonary hemorrhage, and pulmonary infarction. *N Engl J Med* 1977; 296:1431-1435.
- Frazier AA, Galvin JR, Franks TJ, Rosado de Christenson M. From the archives of the AFIP: Pulmonary vasculature: hypertension and infarction. *RadioGraphics* 2000; 20:491-524.
- Primack SL, Muller NL, Mayo JR, Remy-Jardin M, Remy J. Pulmonary parenchymal abnormalities of vascular origin: high-resolution CT findings. *RadioGraphics* 1994; 14:739-746.
- Rubin LJ. Approach to the diagnosis and treatment of pulmonary hypertension (clinical conference). *Chest* 1989; 96:659-664.
- Wagenvoort CA. Vasoconstrictive primary pulmonary hypertension and pulmonary veno-occlusive disease. In: Brest AN, ed. *Cardiovascular clinics*. Philadelphia, Pa: Davis, 1972; 98-113.
- Worthy SA, Muller NL, Hartman TE, Swensen SJ, Padley SPG, Hansell DM. Mosaic attenuation pattern on thin-section CT scans of the lung: differentiation among infiltrative lung, airway, and vascular diseases as a cause. *Radiology* 1997; 205:465-470.

A large empty rectangular area with a black border, intended for writing notes. The border is composed of a vertical line on the right side and a horizontal line at the bottom, meeting at a rounded corner in the bottom right.

Notes

Tuesday

March 4, 2003 General Session

Tuesday

7:00 - 8:00 am Continental Breakfast Americana Foyer

8:00 - 11:00 am Guest Hospitality Suite Moon Room

Session 1-A Concurrent Session Cardiovascular Imaging: Heart II
Moderator: Pamela Woodard, MD Americana 3

7:50 - 8:10 Adult Manifestations of Congenital Heart Disease: CT& MR
Gregory Pearson, MD, PhD

8:10 - 8:30 Imaging of the Pericardium
Paul Molina, MD

8:30 - 8:50 Cardiomyopathy
Martin Lipton, MD

9:10 - 9:30 Nuclear Cardiology Update
David Shelton, Jr., MD

9:30 - 9:50 Session Discussion

Session 1-B Concurrent Session
Clinical & Academic Workplace Issues I Americana 4
Moderator: Robert Tarver, MD

8:15 - 8:40 Manpower Shortage in Radiology: Solutions
Kay Vydareny, MD

8:40 - 9:05 NCI Update for Thoracic Radiology
Edward Staab, MD

9:05 - 9:30 NIBIB Update for Thoracic Radiology
Richard Swaja, PhD

9:30 - 9:50 Session Discussion

9:50 - 10:10 am Coffee Break Americana Foyer

Session 2-A Concurrent Session Pediatric Imaging
Moderator: Sandra Kramer, MD Americana 3

10:10 - 10:30 Thoracic Vascular Abnormalities in Children
Sandra Kramer, MD

10:30 - 10:50 Multidetector Pediatric Chest CT: Practical Approach
Donald Frush, MD

10:50 - 11:10 Pulmonary Disease in the Immunocompromised Child
Richard Markowitz, MD

11:30 - 11:50 Session Discussion

March 4, 2003

General Session

Tuesday

Session 2-B Concurrent Session

Clinical & Academic Workplace Issues II

Americana 4

Moderator: Jud Gurney, MD

- 10:50 - 11:10 Voice Recognition
Theresa McCloud, MD
- 11:10 - 11:30 The Internet & the Practice of Radiology: A New Educational Paradigm
Jud Gurney, MD
- 11:30 - 11:50 Session Discussion
- 11:50 - 1:00 pm Lunch (on your own)

Workshops (choose 1)

- 1:00 - 1:45 A1: Lymphoma: Spectrum of Disease Americana 3
Kitt Shaffer, MD, PhD
- 1:00 - 1:45 A2: Digital Images: Camera to Powerpoint Americana 4
Eric Stern, MD
- 1:45 - 2:30 B1: Analysis of Mediastinal Contours Americana 3
James Reed, MD
- 2:30 - 3:15 C2: Unusual Manifestations of Lung Cancer Americana 4
Michelle Ginsberg, MD
- 3:15 - 3:30 pm Coffee Break Americana Foyer

Scientific Session I

(non-CME Session)

Moderators: Jeremy Erasmus, MD and Joel Fishman, MD, PhD

- 5:30 - 7:00 pm Fellow/Resident/Student Reception Venus Room

Adult Manifestations of Congenital Heart Disease

Gregory Pearson, M.D., Ph.D.

Objectives:

- 1) To review the MR and CT manifestations of congenital heart disease commonly seen in adult patients, including those that present in adulthood and those seen in adulthood after pediatric repair.
- 2) To familiarize radiologists with the relevant clinical questions for which adult congenital heart disease patients are referred.
- 3) To describe typical MR and CT protocols for the rapid and efficient evaluation of adult congenital patients.

Introduction

With recent advances in pediatric cardiac surgery, patients with severe congenital heart disease that would previously not have survived past infancy are now surviving into adulthood, necessitating that adult thoracic radiologists familiarize themselves with common postoperative appearances. In addition, less severe congenital cardiac defects may remain occult during infancy and present de novo in adulthood. It is thus important for the thoracic radiologist to have a familiarity with the common presentations of congenital heart disease in the adult patient.

CT and MR imaging of the adult congenital patient has several advantages over the imaging of pediatric patients. Structures are larger and thus easier to see. Adult patients are more able to perform breath hold images, which greatly improves the resolution of small structures. In an infant or small child breath hold images require general anesthesia with intubation and timed pauses of the respirator. In addition, a postoperative adult patient will usually come with a history. A detailed history and review of previous imaging studies (MRI, echo, and catheterization) can allow the radiologist to specifically focus on the relevant clinical questions, thus greatly facilitating the performance of an exam. As many patients with complex congenital heart disease have undergone multiple surgical procedures, it is best to learn as much as possible about the expected anatomy before the patient goes on the table. This can save considerable "head-scratching" while the patient is in the scanner. Thus coordination with our colleagues in Cardiology is essential. I have divided congenital heart disease in the adult patient into three broad categories: the (usually) nonpathologic entities, pathologic entities with de novo adult presentation, and pathologic entities seen in the adult after pediatric palliation or correction. As my presentation is limited to 20 minutes, these will not all be covered in detail.

(Usually) non-pathologic entities

These lesions mostly fall into the category of vascular anomalies. **Right sided aortic arch** is usually discovered incidentally on review of chest films performed for unrelated reasons, seen as a right-sided indentation on the trachea and the lack of a visible left sided aortic arch. Most patients found incidentally will have an **aberrant left subclavian artery**, as most patients with mirror image branching will have associated congenital heart disease. Left arch with an **aberrant right subclavian artery** is

also a common anomaly found in asymptomatic individuals. Occasionally, patients with aberrant subclavian arteries may present with dysphagia due to esophageal compression from the anomalous vessel or from an aortic diverticulum, but this is the exception rather than the rule. Other anomalies such as **bovine arch** (common origin of the brachiocephalic artery and the left common carotid) are perhaps better thought of as normal variants. These often show up as the last line in a CT report prefaced by the phrase "incidental note is made of..." Vascular anomalies may require no further evaluation, or can usually be well demonstrated in adults on CT, spin echo, and gradient echo MRI images.

Venous anomalies are also occasionally seen within the chest. These include **persistent left SVC**, with or without a right SVC or a vein bridging the two brachiocephalic veins, an entity perhaps most commonly diagnosed after noting the anomalous course of a central venous catheter or pacemaker. This is also a common associated anomaly in complex congenital heart disease. **Azygous continuation of the IVC** also deserves mention, for although it most commonly occurs as an isolated incidental finding it is also highly associated with **polysplenia syndrome**, one of the **heterotaxy syndromes**, which in its mild forms can present in adulthood. As with arterial anomalies, venous anomalies are usually well demonstrated on CT and MR images.

Abnormalities with de novo adult presentation

Although most patients with **VSD** will present in infancy, small VSDs will sometimes present in adulthood, as do many patients with an **ASD**. The role of MR imaging is to attempt to define the size and location of the defect and the size and direction of the associated shunt. The high-pressure jet from a VSD can usually be easily visualized on double oblique short axis or 4 chamber ECG gated bright blood cine cardiac images. The size of the jet is highly dependent on the repetition times, with shorter TE leaving less time for spins to dephase and thus lower sensitivity for turbulent flow and a smaller jet. Thus standard (non-breath hold) cine images will demonstrate a larger jet than breath hold segmented k-space cine images, which are more sensitive than the newer steady state cine sequences (true FISP, balanced FFE, or FIESTA, depending on the MR manufacturer.)

Since atrial pressure is much lower than ventricular pressure, and the interatrial septum is much thinner than the ventricular septum, the visualization of an ASD can be more problematic. Turbulent jets are not typically seen, and the interatrial septum may not be visualized in its entirety in normal individuals. An ASD can sometimes be revealed by eddy currents within the atria on cine sequences that traverse the expected location of the interatrial septum. In addition, shunts can be quantified by the use of velocity-encoded MR imaging. In velocity-encoded imaging, two cine images are generated at the same level, one of which shows the magnitude of blood flow (magnitude image) and the other the direction (phase image). By quantifying the flow in the aorta and the main PA, the shunt fraction can be calculated using commercially available software packages.

Coarctation of the aorta can be seen in adult patients both before and after repair. In the preoperative patient, the role of the thoracic radiologist is to determine the location, severity, and length of the narrowed segment as well as involvement of the great vessels. As with VSDs, the size of the turbulent jet arising from the narrowed segment on bright blood cine sequences is dependent on the echo time, and yields only a rough estimate of the severity of the narrowing. Gadolinium enhanced 3-D MRA (Gd-MRA) yields a 3-D dataset that can be sectioned perpendicular to the plane of the aorta to better demonstrate the true size of the narrowed segment and may demonstrate a web-like narrowing that can be missed on axial images. The presence of enlarged collateral vessels is also well demonstrated on Gd-MRA, although care must be taken to include the chest wall in the field of view. As with turbulent jets, the presence of collaterals does not always correlate with the severity of the narrowing.

Surgical repair may involve balloon dilation with or without stent placement, resection and reanastomosis of a short narrowed segment, or in rare cases the placement of a jump graft. In the postoperative patient, imaging is often performed to assess for restenosis or for complications such as aneurysm formation. MR imaging can be complicated by the presence of intravascular stents, which cause varying degrees of susceptibility artifact depending on their composition. CT may be a better choice if the composition of the stent is unknown.

Anomalous coronary arteries may be discovered incidentally in patients undergoing cardiac catheterization or be suspected on the basis of symptoms. The most common question for the cardiac radiologist is the course of an aberrant left main or LAD arising from the right coronary cusp. If the aberrant coronary extends between the aorta and the main PA there is a high risk of sudden cardiac death and the vessel will usually be reimplanted. On the other hand, if the aberrant vessel extends in front of the main PA, a benign clinical course can be expected and the vessel will be left alone. The course of aberrant coronary arteries can usually be displayed on thin section ECG gated spin echo MR images, breath hold double IR black blood images, or on bright blood true FISP images. Gd-MRA is not usually helpful as the commonly used sequences cannot be cardiac gated, a key component in the imaging of small structures running on the surface of the heart. As the vessels in question are often smaller than the slice thickness practically obtainable on an MRI scanner, it can be difficult to display the vessel adequately on axial slices when the vessel is running in plane. Often it is advisable to image with the vessel perpendicular the plane of section: for example, a left coronary extending between the aorta and main PA can be seen on sagittal images as a small circle between the two larger vessels. Not to be overlooked, contrast enhanced CT scan, especially if performed with one of the newer multirow detector scanners and ECG gating, can often display the course of aberrant coronaries as well or better to that achievable with MRI.

Partial anomalous pulmonary venous connection can present in adulthood as an isolated finding or as part of the hypogenetic lung or **scimitar syndrome**. Anomalous veins are more common on the right than the left, and if only draining a single lobe usually do not cause enough of a left to right shunt to warrant surgical repair. The usual repair for an anomalous vein is an intravenous tunnel which baffles the oxygenated blood through the right atrium to an ASD and thus back to the systemic circulation. Variables of clinical interest in the preoper-

ative patient include right ventricular size, hypertrophy, and function, as well as the shunt fraction.

Lesions seen in adults after pediatric repair

Imaging of postoperative patients with complex congenital heart disease strikes fear into many thoracic radiologist, and perhaps rightly so. These can be among the most difficult exams for radiologists to protocol. The field of congenital heart disease has a language all its own which does not often cross over into the mainstream of radiology. Eponyms abound—Blalock-Hanlon, Blalock-Taussig, Taussig-Bing—who can remember what is what if not dealing with these terms on a daily basis? Activities that are relatively trivial on a “normal” heart, such as determining the long and short axes, become more of an art than a science. One must deal not only with the complex congenital anatomy, but also with the results of multiple surgical procedures which may or may not be documented: shunts placed, then taken down; rudimentary structures left behind; surgical clips causing artifact just where you need to see the most. There is no “one-size-fits-all” adult congenital protocol that can be used on all or even most patients. Exams are lengthy, and the radiologist will usually need to be there to monitor the entire procedure, using an image from one series as a scout for the next. Below I have tried to review some of the more common congenital heart diseases that present postoperatively in adults, as well as the relevant clinical questions that need to be answered and how to approach doing so. The last page includes an appendix of common (mostly eponymous) surgical procedures, including descriptions and indications.

It is important to remember that cardiac MR is usually only one of a variety of tests that are used to follow these patients, including nuclear medicine studies, echocardiography, and cardiac catheterization. The MR exam should be focused on answering the clinical questions at hand, not just reproducing information from other modalities. For example, echocardiography may elegantly display a subpulmonic stenosis, but cannot visualize the peripheral pulmonary arteries. One may thus wish to forgo cine images through the pulmonary outflow in favor of a 3-D MRA, which will display peripheral stenosis occult to the echocardiographer.

D-Transposition of the great arteries (synonyms, complete transposition, D-TGA or TGA) is an anomaly in which the aorta arises from the right ventricle and the pulmonary artery from the left ventricle, resulting in two parallel circulations which must be connected by one or more shunts (ASD, VSD, or PDA) in order for the infant to survive. Infants are typically treated palliatively in the neonatal period with the creation of an ASD to increase the admixture of blood (**Blalock-Hanlon** or **Rashkind** procedure) followed by corrective repair. In prior years, this was usually a **Mustard** or **Senning** procedure, in which the interatrial septum was removed, with creation of an intraatrial baffle to channel blood from the SVC and IVC to the mitral valve and the systemic blood to the tricuspid valve. This results in separation of the systemic and pulmonic circulations, with deoxygenated blood traveling from the SVC and IVC through the atrial baffle to the left ventricle and then out the main PA, and with the oxygenated blood traveling from the pulmonary veins into the left atrium, then through the ASD to the right atrium to the right ventricle and then out the aorta.

Postoperative imaging after Mustard repair typically focuses on the atrial baffle, looking for leaks or for obstruction to either the SVC or IVC limbs. Axial and oblique coronal cine images

will usually display the limbs of the baffle well. In addition, it is important to assess right ventricular function, as the right ventricle is not designed for the job of pumping blood against systemic pressures. Right ventricular size, function, and mass can be measured using double oblique short axis cine images. A failing right ventricle is an indication for cardiac transplantation.

More recently, the Mustard and Senning repairs have mostly been replaced with the **Jatene** or arterial switch procedure. In the Jatene procedure, the great vessels are divided above the semilunar valves, with reattachment of the aorta to the left ventricle and the main PA to the right ventricle. Coronary arteries are reimplemented onto the ascending aorta. Complications include obstruction of the proximal pulmonary arteries, narrowing of the RV outflow, enlargement of the aortic root, and supralvalvar AS.

L-Transposition of the great arteries (synonyms L-TGA, corrected transposition, or congenitally corrected transposition) results from an abnormal L-loop of the heart embryologically, leading to a ventricular switch, with the systemic veins connecting to the right atrium, the anatomic left ventricle, and the main PA, with the pulmonic venous blood draining to the left atrium, the anatomic right ventricle, and the aorta. Associated septal defects and valvular stenoses are common. Physiologically, the connections are the same as those seen in D-TGA after Mustard repair, and as such patients may present in adulthood as the right ventricle begins to fail. Multiplanar spin echo and cine images are of use in evaluation of ventricular size, ventricular mass, valvular function, and presence of septal defects.

Tetralogy of Fallot (TOF) and TOF-pulmonary atresia account for about 10% of congenital heart disease. The classic “Tetralogy” consists of pulmonary stenosis, VSD, overriding aorta, and RV hypertrophy. Repair depends on the severity of the pulmonary stenosis and involves closure of the VSD with enlargement of the pulmonary outflow, usually with an extracardiac patch. Sagittal spin echo and cine MR images can demonstrate complications in the RV outflow and PA patch, including stenoses, aneurysms, and regurgitation. Right ventricular mass and function can be assessed on short axis cine images. Peripheral pulmonic stenoses and systemic collateral vessels are well demonstrated on Gd-MRA.

In cases of severe stenosis or atresia, a conduit must be placed from the right ventricle to the pulmonary artery, which until repair receives blood from the requisite PDA. If the pulmonary arteries are too small to allow definitive repair in one stage, the patient must first undergo a palliative PA shunt to supply increased pulmonary flow and allow for pulmonary arterial growth. These shunts are listed in the appendix. The most common shunt performed currently is a modified **Blalock-Taussig (BT)** shunt involving a graft from the subclavian artery opposite from the side of the aortic arch to the pulmonary artery. Complications include stenosis or thrombosis of the shunt, which can be demonstrated on axial and coronal cine MR images, as well as through lack of visualization on Gd-MRA.

Single ventricle repairs. The classification of single ventricles is a topic that by itself could easily cover this entire ses-

sion. Lesions necessitating a single ventricle repair include tricuspid atresia and hypoplastic left heart syndrome. No child with a single ventricle will survive past infancy without palliative surgery, thus all adults presenting for MR evaluation with single ventricle will be post-op, often after multiple staged surgeries and revisions. Regardless of the origin of the ventricle (left, right, or monoventricle), the ventricle must be connected to the systemic circulation to act as the systemic pumping chamber. Pulmonic flow returns to the lungs either without a pumping chamber or with the right atrium as the pumping chamber.

In the **Glenn** shunt, the SVC is connected to the right PA, with the IVC remaining admixed with the pulmonary venous return. Later, the IVC can be anastomosed with either the right or the left pulmonary artery, separating the pulmonic and systemic circulations. In the classic **Fontan** operation, the right atrial appendage is anastomosed with the pulmonary artery. There are several variations. Two of the more common are the lateral tunnel Fontan, in which the IVC is baffled through the atrium, and a fenestrated Fontan, in which a hole is left in the baffle to allow for decompression of the systemic venous circuit.

The Fontan pathway is often well demonstrated on axial and coronal spin echo and cine MR images. Complications include systemic venous hypertension, with right atrial enlargement, which can then secondarily compress the right inferior pulmonary vein. This is most common in the classic Fontan, as the right atrium is not designed to pump against pulmonary arterial pressure. Obstruction or stenosis of the conduit may also develop, and residual atrial septal defects may be present. MR is superior to echocardiography for demonstrating pulmonary artery anastomoses. Several different obliquities angled to the plane of the anastomosis may be necessary for a complete evaluation. In addition, cine MR images through the ventricle can determine size, mass, and function. Precise delineation of cardiac anatomy and associated anomalies can be of use in preoperative planning for cardiac transplantation.

Conclusions

The CT and MR evaluation of adult patients with congenital heart disease is a complex topic that defies easy summary. A few of the entities I have not even touched upon include truncus arteriosus, double outlet ventricles, patent ductus arteriosus, and Ebstein’s anomaly. Patients vary in their anatomy, mental status, and stamina, yielding wide variation in ability to cooperate with the breath hold images required for ideal evaluation. Examinations must be tailored to the individual patient based on the clinical questions to be answered and the patient’s ability to cooperate. The radiologist must usually personally monitor each case. I urge all thoracic radiologists to develop a familiarity with cardiac MR imaging. If radiologists are not willing to undertake this challenging but rewarding task, there are many cardiologists who are willing to fill the void.

Appendix: Common operations performed for congenital heart disease

Palliative PA shunts

Eponym	Connection	Indication
Waterson-Cooley	Ascending aorta to Right PA	Lesions with decreased Pulmonary flow: TOF, Pulmonic stenosis/atresia
Blalock-Taussig (BT)	Subclavian artery to PA	
Potts	Descending aorta to PA	
Glenn	SVC to PA	

Creation/Enlargement of ASD

Eponym	Procedure	Indication
Blalock-Hanlon	Surgical creation of an ASD	D-transposition
Rashkind	Balloon atrial septostomy	

Corrective procedures

Eponym	Procedure	Indication
Mustard Senning	Creation of a common atrium, with intraatrial baffle directing systemic venous blood to the left ventricle (mitral valve) and the pulmonary venous blood to the right ventricle (tricuspid valve)	D-transposition
Jatene	Division of the great vessels with reattachment of the aorta to the left ventricle and the main PA to the right ventricle. Reimplantation of the coronary arteries on the ascending aorta	D-transposition
Rastelli	Creation of an intraventricular tunnel shunting blood from the left ventricle via a VSD to the transposed ascending aorta combined with an extracardiac conduit connecting the right ventricle to the pulmonary trunk	D-transposition with PS and VSD. DORV with PS. TOF with pulmonary atresia Truncus arteriosus types I and II
Fontan	Conduit from right atrium to PA	Tricuspid atresia Single ventricles
Ross	Pulmonic valve reimplanted in aortic position, combined with pulmonic homograft	Aortic valve disease requiring valve replacement
Norwood	Norwood I: PA transected, used to create neo-aorta; Blalock-Taussig (BT) shunt; Atrial septectomy. Norwood II: Bidirectional Glenn with takedown of BT shunt. Norwood III: Completion of Fontan.	Hypoplastic left heart

Imaging of the Pericardium

Paul L. Molina, M.D.

Professor of Radiology, Director, Radiology Residency Training Program, Vice Chairman of Education, University of North Carolina, Chapel Hill, North Carolina

Objectives

1. Review the normal appearance of the pericardium, including the pericardial recesses, on both CT and MRI.
2. Learn the major clinical applications of CT and MRI in the evaluation of patients with suspected pericardial disease.
3. Review the CT and MRI findings in a variety of pericardial disease processes.

Introduction

Computed tomography (CT) is an established technique for evaluation of the pericardium and is generally considered complementary to echocardiography in the assessment of complicated pericardial effusions, pericardial thickening, calcific pericarditis, pericardial masses and congenital anomalies. Magnetic resonance imaging (MRI) is also useful in the evaluation of pericardial disease. Advantages of MRI include its potential for tissue characterization, absence of ionizing radiation and need for intravenous contrast medium, and its ability to scan in any plane. These potential advantages, however, are at times outweighed by the disadvantages of higher cost, longer examination time, and inability to accurately identify calcification. Also, it may be difficult to adequately examine patients with arrhythmias because of the need for cardiac gating of MR studies of the pericardium.

Normal Anatomy

At least a portion of the normal pericardium, a double-layered fibroserous sac enveloping the heart and origin of the great vessels, is visible on CT and MRI in almost all patients. The normal thickness of the pericardium on CT or MRI is 1-2 mm. On CT it appears as a thin curvilinear density and on MR as a low signal intensity line. The decreased signal intensity of the pericardium is probably due to fluid flow during the cardiac cycle. The caudal half of the pericardium is commonly imaged, especially those portions overlying the anterolateral cardiac surface where the pericardium is surrounded by fat in the mediastinum and in the subepicardial region of the heart. The most distal portion of the pericardium, just before its insertion into the central tendon of the diaphragm and in front of the inferior surface of the right ventricle, may measure up to 3-4 mm in thickness due to accumulation of small physiological amounts of pericardial fluid. The dorsal aspect and the cephalad portion of the pericardium are infrequently seen because of the lack of sufficient surrounding fat in these areas.

The pericardial cavity contains several recesses around the heart where normally small amounts of fluid can collect. An understanding of these recesses is important in order not to confuse fluid within them with mediastinal masses or enlarged lymph nodes.

Pericardial Effusion

Echocardiography currently remains the primary means of evaluating a patient for pericardial effusion. Its major advantages include the ease of the examination and the portability of the equipment, along with the absence of exposure to ionizing

radiation. Both CT and MRI are also useful for establishing the diagnosis of pericardial effusion and are usually reserved for those patients who have technically inadequate sonographic studies or in whom there is a discrepancy between clinical and echocardiographic findings.

A pericardial effusion generally is recognizable on CT as an increase in thickness of the normal band-like pericardium. Most commonly, the fluid has a near-water density value and represents a transudate. Near soft-tissue density collections may occur with an exudative or purulent effusion or a hemopericardium. Blood in the pericardium may be isodense with the cardiac muscle and therefore administration of intravenous contrast media may be required for diagnosis, demonstrating enhancement of the myocardium with no alteration of the surrounding hemopericardium. On MRI a simple pericardial effusion usually is characterized by low signal intensity on short TR/TE images; its signal intensity increases on longer TR or longer TE images. Hemorrhagic pericardial effusions often contain areas of mixed, medium and high signal intensity that may vary with the age of the effusion.

On supine CT and MRI scans, small pericardial effusions usually collect dorsal to the left ventricle and behind the left lateral aspect of the left atrium. Larger effusions extend ventrally in front of the right ventricle and right atrium. In massive pericardial effusions, the heart appears to float within the distended pericardial sac and fluid extends cephalad to surround the origin of the great vessels. The over-distended pericardium may project caudally and compress the diaphragm and upper abdominal organs. Encapsulated pericardial effusions can occur when fibrous adhesions seal off portions of the pericardial space; dorsal and right anterolateral loculations are most common. Occasionally the encapsulated fluid will bulge toward the heart and can result in the hemodynamics of cardiac tamponade or constrictive pericarditis. With inflammatory pericarditis and effusion, the pericardium itself may enhance following the intravenous administration of contrast media.

Pericardial Thickening

The pericardium can respond to injury by fibrin production and cellular proliferation in addition to fluid output. All three mechanisms can occur concomitantly or independently. Pericardial thickening may result from proliferation of fibrin deposits or organized blood products or through neoplastic invasion. Pericardial thickening from 0.5 to 2.0 cm or greater can occur and may be focal or involve the entire pericardium. Generally, the maximal thickening occurs ventrally. The thickened pericardium usually is smooth but can be nodular in neoplastic disease. Distinction from a small exudative or bloody pericardial effusion may be difficult.

Constrictive Pericarditis Versus Restrictive Cardiomyopathy

CT and MRI have shown value in differentiating constrictive pericarditis from restrictive or infiltrative cardiomyopathy (e.g., amyloidosis). This distinction is often quite difficult clinically,

as both entities may have identical clinical manifestations and hemodynamic characteristics. The finding of a normal pericardium on CT or MRI practically excludes the diagnosis of constrictive pericarditis. CT and MRI findings in constrictive pericarditis include pericardial thickening, external compression and deformity of the right atrial or ventricular borders, and straightening of the interventricular septum. Thickening of the pericardium may or may not produce hemodynamic abnormalities and this finding alone is insufficient to diagnose constrictive pericarditis. Additional imaging findings that suggest hemodynamically significant pericardial constriction include systemic vein dilatation, hepatomegaly, ascites, and pleural effusions. It should be emphasized that focal pericardial thickening or calcification, sometimes quite large, may be present without clinical findings of constrictive pericarditis. Encasement of large portions of both ventricles is usually necessary to produce hemodynamic consequences.

Neoplastic Pericardial Disease

Neoplastic cells can reach the pericardium by direct invasion from an adjacent origin (carcinomas of the lung and breast are the most frequent neoplasms involving the pericardium) and via hematogenous or lymphatic spread. Associated mediastinal lymph node enlargement may be present. Both CT and MRI are useful in evaluating neoplastic involvement of the pericardium, which most commonly manifests as an exudative effusion although plaque-like thickening or nodular masses can also occur along the pericardium.

Congenital Pericardial Cyst

Pericardial cysts are most often found in the cardiophrenic angles and are usually thin-walled and sharply defined. On CT

they are typically of water attenuation, although high attenuation cysts have been reported. They do not enhance after the injection of contrast media. On MRI, these lesions are of low signal intensity on short TR/TE images and of high signal intensity on long TR/TE images.

REFERENCES

- Aronberg DJ, Peterson RR, Glazer HS, Sagel SS. The superior sinus of the pericardium: CT appearance. *Radiology* 1984; 153:489-492.
- Im J-G, Rosen A, Webb WR, Gamsu G. MR imaging of the transverse sinus of the pericardium. *AJR* 1988; 150:79-84.
- Levy-Ravetch M, Auh YH, Rubenstein WA, Whalen JP, Kazam E. CT of the pericardial recesses. *AJR* 1985; 144:707-714.
- Masui T, Finck S, Higgins CB. Constrictive pericarditis and restrictive cardiomyopathy: evaluation with MR imaging. *Radiology* 1992; 182:369-373.
- Olson MC, Posniak HV, McDonald V, Wisniewski R, Moncada R. Computed tomography and magnetic resonance imaging of the pericardium. *RadioGraphics* 1989; 9:633-649.
- Rienmuller R, Gurgan M, Erdmann E, et al. CT and MR evaluation of pericardial constriction: a new diagnostic and therapeutic concept. *J Thorac Imag* 1993; 8:108-121.
- Silverman PM, Harell GS. Computed tomography of the normal pericardium. *Invest Radiol* 1983; 18:141-144.
- Silverman PM, Harell GS, Korobkin M. Computed tomography of the abnormal pericardium. *AJR* 1983; 140:1125-1129.
- Stark DD, Higgins CB, Lanzer P, et al. Magnetic resonance imaging of the pericardium: normal and pathologic findings. *Radiology* 1984; 150:469-474.
- Suchet IB, Horwitz TA. CT in tuberculous constrictive pericarditis. *JCAT* 1992; 16:391-400.

Cardiomyopathy

Martin J. Lipton, M.D.

Objectives

- Define cardiomyopathy
- Describe the classification
- Discuss etiology & pathophysiology
- Summarize the diagnostic approaches
- Describe the CT & MR Imaging characteristics

Cardiomyopathy is a difficult and confusing topic. There is a great need to simplify the entity and explain the important role, which cardiac CT and MRI can play in diagnosing and managing this complex group of disorders. Once thought to be rare, there is evidence that the incidence is greater than 1 in 500.

Cardiomyopathy was first used to describe a group of diseases of the myocardium of unknown etiology [1]. The term excludes patients with coronary atherosclerosis, valvular heart disease, and arterial hypertension[2]. Three basic types of cardiomyopathy have been described by the World Health Organization (WHO) as illustrated in Table I.

Table I
Cardiomyopathy – Clinical Classification

- Hypertrophic or obstruction (HCM) – resembling aortic valve stenosis
- Dilated (congestive) (DCM) – often resembling severe coronary artery disease
- Restrictive (RCM) – resembling constrictive pericarditis

More recently arrhythmogenic right ventricular dysplasia (ARVD) is regarded as a fourth type. Each cardiomyopathy corresponds to a basic type of functional abnormality, although ARVD is difficult to fit into this classification.

Hypertrophic Cardiomyopathy

This disorder is characterized by an inappropriate myocardial hypertrophy without any obvious cause, such as aortic valve stenosis or hypertension.

The disease has been widely publicized as a cause of sudden death in athletes[3, 4]. The disease is genetically linked in about 50% and it may skip generations. Histologically in HCM there is severe disorganization of the myofibrils and the disorder classically involves the superior part of the interventricular septum. The left ventricle is not dilated, and may even be small. The hypertrophy (LVH) is due to increased wall thickness above and beyond the upper normal limit of 12 mm in diastole in adults. Although a symmetric (concentric) pattern of LVH may occur, the distribution of the hypertrophy is almost always asymmetric, i.e. segments of LV wall are thickened to different degrees. The ventricular septum usually shows the greatest magnitude of hypertrophy, furthermore the disease has been well documented at nearly all ages from infancy to the elderly[5].

Asymmetric septal HCM, previously called, idiopathic hypertrophic subaortic stenosis (IHSS), is the most common subtype. LV outflow obstruction occurs due to the apposition of the anterior mitral valve leaflet to the septum during systole, but

this varies in degree, and does not occur in all patients.

An apical variety of HCM also occurs and is seen most commonly in Japan. The LV cavity has a ‘spade like’ appearance.

Diagnosis requires a detailed family history of cardiac illness, chest radiographs, ECG, and echocardiography, which is usually diagnostic. CT and MRI can demonstrate both morphology and function. However, the majority of patients still undergo cardiac catheterization with hemodynamic measurements with angiography. This also remains true for the other types of cardiomyopathy, dilated and restrictive.

Pressure gradients occur in some patients, and can be severe. These occur either in the outflow tract of the LV, or near the LV apex during systole, when the cavity is obliterated at the mid ventricular level.

A distorted LV cavity may be seen on left ventriculography and has been described as resembling a ballerina’s shoe. This appearance is due to the greatly thickened LV septum which splints the chamber and produces angulation of the LV cavity. LV wall thickness can be estimated from the distance between the coronary vessels and LV cavity during coronary angiography.

Patient evaluation includes accurate measurements of the degree of hemodynamic obstruction together with global and regional LV wall mass and function. A major advantage of MRI is its ability to select angled planes for more precise quantitation. In some patients, abnormal LV diastolic dysfunction is the dominant feature. MRI myocardial tagging has also been used to study wall motion and strain patterns[6].

Gadolinium (Gd) – DTPA has value in two groups, those patients suspected of a myocardial neoplasm which can mimic myocardial hypertrophy, and patients with HCM in whom ischemia or infarction is questioned. The later group demonstrates increased MRI signal in ischemic areas. This does not occur in non-hypertrophied normal myocardium[7].

Dilated Cardiomyopathy (DCM)

This syndrome involves dilatation of either the LV alone or both ventricles. It is associated with myocardial hypertrophy and severely depressed LV function. The degree of wall hypertrophy is disproportionate for the degree of dilatation. Causes include immunological, familial, toxic, metabolic, and infective or it may be idiopathic. The final common pathway for all these entities is often myocardial failure.

The symptoms are variable, often left heart failure is a presenting feature, but some patients are minimally symptomatic or have no symptoms. The chest radiograph reflects LVF often with a normal sized heart. Imaging techniques may be non-specific or demonstrate RV failure. LV thrombi may be present and commonly there is global rather than regional impaired contractility. This is an important feature, which distinguishes DCM from coronary arterial occlusive disease.

MRI is an excellent technique to identify the morphological and functional indices of both ventricles. RV mass is usually normal while the LV mass is increased. The coronary arteries are normal in all cardiomyopathies unless there is concomitant

coronary atherosclerosis. MRI provides the necessary detailed measurements without contrast agents and is able to provide non-invasive serial studies to monitor change and therapeutic response. ECG gated MDCT and Electron Beam CT can also provide much of the same information[8].

Restrictive Cardiomyopathy (RCM)

This is the least common type, in which the major abnormality is impaired diastolic function. Hemodynamically there is increased biventricular filling pressures. The underlying problem is increased myocardial compliance, which impairs diastolic filling[9]. Systolic function in contrast is usually normal. This is why RCM resembles constrictive pericarditis[10]. In both conditions the ventricles look small or normal in size, but the right atrial and inferior vena cava are enlarged. MRI and CT can demonstrate the pericardial thickness. The normal upper limit of which is 4 mm in adults. Constrictive pericarditis can be identified in over 90% of cases with both these cross-sectional non-invasive techniques, however, many patients still undergo cardiac catheterization. RCM may be caused by various infiltrative diseases of the myocardium as listed in Table II, which is based on an etiological classification. Infiltrative causes of cardiomyopathy are also referred to as secondary cardiomyopathies[11].

Table II
Etiological Classification

- Primary types
 - Enzyme deficiencies, genetic influences
- Secondary causes
 - Viral infection
 - Neurogenic: Friedreich's ataxia
 - Infiltrative: amyloidosis, sarcoidosis, hemochromatosis, glycogen storage disease, neoplastic
 - Toxic: alcohol
 - Metabolic: diabetes mellitias
 - Connective tissue disease: lupus, scleroderma

Amyloidosis is a common cause of secondary RCM, and in up to 50% there is asymmetric hypertrophy (ASH) of the inter-ventricular septum, with anterior systolic motion of the mitral valve. Biopsy of liver or other organ is usually the method of diagnosis and this may raise suspicion of involvement of the heart.

Cardiac sarcoidosis occurs in less than 5% patients seen clinically yet it occurs in 25% of autopsy of myocardium by sarcoidosis and usually involves multiple sites leading to post-inflammatory scarring. Sudden death is not an uncommon presentation. MRI demonstrates increased signal from sarcoid infiltrates and is more pronounced on T2 weighted images. Steroid therapy can resolve some of these lesions, MRI can monitor these changes, and can be used to guide biopsy.

Iron overload CM produces depressed cardiac function due to deposits of iron in the heart. It can result from primary or secondary hemochromatosis. The primary type is an autosomal

recessive disease and usually presents late in life. The secondary type is much commoner and associated with hereditary anemias, which is a common cause of mortality in the young adult population in the developed world.

ARVD is a disease which frequently causes arrhythmias during exercise and predominantly afflicts young males. It primarily involves the right ventricle and outflow tract and has become recognized with increasing frequency during the past 1-2 decades. ARVD requires further detailed consideration and therefore will not be discussed at this time.

Acknowledgement

The work was supported in part by the ARRS and ACR through a visiting scientist award to the AFIP, Bethesda, MD.

REFERENCES

1. Brigden W, The noncoronary cardiomyopathies. *Lancet*, 1957. II: p. 1179-1243.
2. Mason J, Classification of Cardiomyopathies, In Hurst's The Heart, Alexander R, Schlant R, and Fuster V, Editors. 1998, Mc-Graw-Hill. p. 2031-2038.
3. Maron BJ, Kragel AH, and Roberts WC, Sudden death in hypertrophic cardiomyopathy with normal left ventricular mass. *Br Heart J*, 1990. 63(5): p. 308-10.
4. Spirito P and Maron BJ, Relation between extent of left ventricular hypertrophy and occurrence of sudden cardiac death in hypertrophic cardiomyopathy. *J Am Coll Cardiol*, 1990. 15(7): p. 1521-6.
5. Maron BJ, Hypertrophic cardiomyopathy: a systematic review. *Jama*, 2002. 287(10): p. 1308-20.
6. Rademakers F and Bogaert J, Myocardial Diseases, In Magnetic Resonance of the Heart and Great Vessels: Clinical Applications, Bogaert J, Duerinckx A, and Rademakers F, Editors. 1999, Springer.
7. Sipola P, Lauerma K, Husso-Saastamoinen M, Kuikka J, Vanninen E, Laitinen T, Manninen H, Niemi P, Peuhkurinen K, Jaaskelainen P, Laakso M, Kuusisto J, and Aronen H, First-pass MR imaging in the assessment of perfusion impairment in patients with hypertrophic cardiomyopathy and the Asp175Asn mutation of the α -tropomyosin gene. *Radiology*, 2002. 226(1): p. 129-137.
8. Skioldebrand CG, Ovenfors CO, Mavroudis C, and Lipton MJ, Assessment of ventricular wall thickness in vivo by computed transmission tomography. *Circulation*, 1980. 61(5): p. 960-5.
9. Diethelm L, Simonson JS, Dery R, Gould RG, Schiller NB, and Lipton MJ, Determination of left ventricular mass with ultrafast CT and two-dimensional echocardiography. *Radiology*, 1989. 171(1): p. 213-7.
10. Refsum H, Junemann M, Lipton MJ, Skioldebrand C, Carlsson E, and Tyberg JV, Ventricular diastolic pressure-volume relations and the pericardium. Effects of changes in blood volume and pericardial effusion in dogs. *Circulation*, 1981. 64(5): p. 997-1004.
11. Sechtem U, Higgins CB, Sommerhoff BA, Lipton MJ, and Huycke EC, Magnetic resonance imaging of restrictive cardiomyopathy. *Am J Cardiol*, 1987. 59(5): p. 480-2.

Nuclear Cardiology Update

David K. Shelton, M.D.

Professor, University of California Davis, Medical Center

Cardiovascular radiotracers were first utilized in the 1927 by Blumgart and Weiss to measure cardiovascular transit times. Then in 1948 the first clinical success for scintigraphic evaluation of cardiac pump function was accomplished by Prinzmetal who introduced the "radiocardiograph". Radioactive potassium was introduced for myocardial perfusion at rest and under stress in the 1970's. This was followed by numerous studies involving the key potassium analogue, thallium-201 as a myocardial perfusion agent. The 1980's brought the development of several new technetium based radiopharmaceuticals for myocardial perfusion. There were also new tracers for the evaluation of myocardial metabolism, myocardial innervation and acute myocardial necrosis. During this decade, there was also the development of tomographic imaging techniques utilizing single photon emission computed tomography (SPECT) and positron emission tomography (PET). The 1990's saw the development of additional technetium based radiotracers, new PET radiotracers and multiheaded SPECT cameras. The subsequent development of ECG gated SPECT techniques allowed the evaluation of cardiac function and wall motion in addition to myocardial perfusion imaging.

Now at the beginning of the new millenium, most nuclear cardiology studies are performed for the assessment of myocardial perfusion imaging utilizing thallium-201, Tc-99m sestamibi or Tc-99m tetrofosmin in association with ECG gated SPECT. The utilization of gated blood pool radionuclide ventriculography (MUGA) and first pass imaging has dramatically decreased. Infarct imaging with technetium 99m pyrophosphate or antimyosin antibodies, innervation studies utilizing I-123 MIBG and fatty acid metabolism utilizing I-123 BMIPP are limited in numbers and are primarily being utilized at research centers.

RADIOTRACERS:

Thallium-201 remains a highly utilized and highly effective radiotracer which is a potassium analogue transported across the cell membrane by the sodium/potassium pump system. It has a high initial myocardial uptake, proportional to blood flow which is increased during stress conditions approximately 5 times that of rest conditions. After its initial myocardial uptake, thallium begins to wash out and will reach equilibrium with the blood pool effect. The stress study can demonstrate hypoperfusion of myocardium distal to a significant coronary stenosis. This can be followed by 4 hour delayed imaging with thallium redistribution. Reversible defects indicate ischemic and viable myocardi-

um. Thallium's long half life of 73 hours can be advantageous for further delayed imaging at 24 hours to differentiate areas of critical stenosis with associated hibernating myocardium. Disadvantages of thallium include its lower energies at 73-81 keV as well as its longer half life which requires a lower prescription dose at 3-4 mCi. The introduction of technetium based radiotracers has offered the advantages of the monoenergetic 140 keV higher energy which is associated with fewer problems due to attenuation, as well as improved imaging properties for modern SPECT cameras. The shorter half life of 6 hours for technetium also allows for higher doses to be administered safely in the 10-30 mCi range. Technetium tetrofosmin (Cardiolite) is a highly lipophilic cation which has the highest myocardial extraction rate of all the technetium radiotracers. However, because of its fast washout rate, its clinical utility for post stress imaging has been very limited. Technetium sestamibi (Cardiolite) was approved for clinical use in 1989 and has had widespread clinical utility. It is a monovalent cation with hydrophilic properties and is also very lipophilic, facilitating entry into myocardial cells. Once sestamibi has entered the myocyte, it remains trapped with very little washout over 4 hours. Technetium tetrofosmin (Myoview) is a monovalent, highly lipophilic cation. Its uptake is also bloodflow dependent and like sestamibi its greatest concentration is in the mitochondria. Also like sestamibi, once in the myocyte there is very little washout. One advantage of tetrofosmin is that there is rapid clearance from non-cardiac structures, especially the liver.

Two new technetium based radiotracers are currently undergoing clinical trials. Tc-furifosmin has properties that are similar to Tc-tetrofosmin. Tc-NOET is a neutral lipophilic myocardial perfusion agent with a very high extraction fraction over a wide range of flow. It appears that Tc-NOET has many kinetic and imaging properties similar to thallium-201 but with the advantage of high photon flux and higher energy. Tc-NOET does have significant washout and redistribution over time due to the absence of intracellular binding and to the high circulating blood levels of this radiotracer.

Table 1 provides a listing of most of the commonly utilized cardiac radiotracers and those radiotracers being utilized in research. There is strong interest in the neuroreceptor imaging agents, the fatty acid metabolism agents and the ability to image myocardial hypoxia directly, as well as myocytes undergoing apoptosis. Research interest is also strong in imaging developing arterial plaque and vulnerable plaque.

Table 1 Radiotracers:MPI-SPECT

Thallium-201:	very good uptake, washout, redistribution, viability
Tc-sestamibi (Cardiolite):	good uptake, very little washout
Tc-tetrofosmin (Myoview):	good uptake, very little washout, rapid background clearance.
Tc-teboroxime (Cardiotech):	very high myocardial extraction fraction, very fast washout, no redistribution.
Tc-furofosmin:	new agent, similar to tetrofosmin.
Tc-NOET:	high extraction fraction, washes out and redistributes, suboptimal background clearance.

MPI-PET:

Rubidium-82:	portable generator myocardial PET perfusion agent.
¹³ N-ammonia (¹³ NH ₃):	good utility PET perfusion agent.
¹⁵ O-water (¹⁵ O-H ₂ O):	short half life perfusion agent.
F-18-FDG:	glucose metabolism and important viability agent.

Blood Pool:

Technetium-RBC:	general nuclear medicine blood pool agent, radionuclide ventriculography (first pass, accurate ejection fraction and wall motion study)
¹⁵ O-Carbon Monoxide (C ¹⁵ O):	PET blood pool agent.

Infarct/Injury Avid:

Tc-PYP:	SPECT agent, recently infarcted myocardium.
Indium-111 antimyosin antibody:	recently infarcted myocardium and chronic injuries.
Tc-annexia:	apoptosis SPECT imaging.

Hypoxia:

Tc-HL-91:	directly labels hypoxic myocardium.
F-18-misonidazole:	PET agent for hypoxic myocardium.

Neuroreceptor:

I-123 MIBG:	presynaptic sympathetic agent.
¹¹ C hydroxyephedrine (HED):	presynaptic sympathetic PET agent.
¹¹ C-CGP12177:	beta adrenoreceptor PET agent.
F-18 dopamine:	presynaptic noradrenaline precursor.
F-18 carazol:	post-synaptic beta adrenoreceptor.

Fatty Acid Metabolism:

I-123-BMIPP:	fatty acid metabolism SPECT agent.
¹¹ C palmitate:	fatty acid metabolism PET agent .
¹¹ C acetate:	oxidative metabolism PET agent.

Thrombosis:

Tc-peptides for GPIIb/IIIa receptors:	activated platelet imaging.
---------------------------------------	-----------------------------

Atherosclerotic Plaque:

Indium-111 C2D3 antibody:	antibody to proliferating smooth muscle cells in arterial walls.
F-18-FDG:	metabolic imaging of developing atheromatous plaque.

METHODOLOGY:

Planar imaging utilizes standard gamma cameras with collimation to acquire static or dynamic imaging. Planar Imaging is used for first pass studies to evaluate right and left ventricular function, with or without active stress. Planar imaging is also utilized for left to right shunt quantification with gamma variate analysis. Planar imaging can also be utilized to quantify right to left shunts utilizing Tc-MAA to quantify the amount of systemic uptake versus pulmonary uptake. Planar imaging is also utilized in the anterior, LAO and left lateral positions for evaluation of radionuclide ventriculography. This remains a highly viable technique for accurate follow-up of left ventricular ejection

fraction and wall motion analysis when following myocardial function while patients are on cardiotoxic drugs or new cardiac agents under development. ECG gated planar studies can also be utilized for myocardial perfusion imaging of patients too obese for SPECT tables or for portable imaging to I.C.U. areas.

Single photon emission computed tomography (SPECT) has become the tomographic standard for imaging myocardial perfusion. Multi-headed gamma cameras have been introduced which improved count statistics and helped to reduce acquisition time. Most protocols utilize 180° acquisitions rather than 360° acquisition, since the heart is asymmetric within the chest and posterior viewing has low count rate and attenuation abnormali-

ties. The predominant 180° acquisition orbit has become the right anterior oblique to left posterior oblique orbit. Because of this, fixed angle two-headed camera systems offer little advantage in cardiac imaging. Triple-headed camera systems do offer improved photon sensitivity and even better is the variable angle two-headed system with the cardiac imaging angle set to 90-100 degrees.

Similar to electrocardiographically gated radionuclide ventriculography for wall motion and LVEF, ECG gated SPECT provides a powerful tool to augment perfusion data with additional functional information. Very little or no increased imaging time is required, and the binned images can be summated to provide excellent static myocardial perfusion tomographic images. The gated images can be reviewed in a cine loop to evaluate rest and post stress wall motion, wall thickening, and left ventricular ejection fraction data. Rest and post stress end diastolic and systolic volumes, also provide accurate functional and prognostic information about left ventricular function.

PET imaging, albeit more expensive, offers several advantages over SPECT imaging. A number of PET radiotracers offer biological and metabolic advantages over standard nuclear radiotracers. In addition, because the annihilation photons are always essentially 180° opposed, the line of coincidence calculations offer improved spacial resolution over standard SPECT imaging. The higher energy 511 keV photons offer fewer attenuation abnormalities and the standardized attenuation correction maps also improve image quality as well as sensitivity. Because of these properties, PET also has the ability to provide accurate quantification. Higher speed computer systems and improved reconstruction algorithms have resulted in improved acquisition times, and improved image quality. Improved techniques for attenuation correction have also led to improved image quality and the most recent PET/CT scanners provide accurate attenuation maps and image co-registration in the same patient visit. The standard BGO detectors are now being replaced by newer LSO and GSO detectors which offer improved imaging properties and energy discrimination.

CLINICAL APPLICATIONS:

Ventricular Function:

Nuclear Medicine offers several clinically effective tests for evaluation of left ventricular function despite strong competition from left ventricular angiography, echocardiography, and ECG gated MRI. First pass studies can be utilized for accurate determination of right ventricular ejection fraction (RVEF) as well as left ventricular ejection fraction (LVEF). These studies can be accomplished at rest as well as with stress techniques. Gated blood pool radionuclide ventriculography has long been an accurate mainstay to evaluate left ventricular function. Most recently, ECG gated blood pool SPECT has been utilized to evaluate chamber volumes, evaluating subtle wall motion abnormalities. Shunt quantification with radiotracer techniques is still occasionally utilized for left to right shunts. The technique involves a first pass protocol with regions of interest placed over the lung to detect left to right recirculation peaks utilizing gamma variate analysis. Right to left shunts are calculated utilizing Tc-MAA to determine the percentage of shunt particles reaching the whole body systemic circulation and organs, versus the percentage trapped in the lungs.

Most recently ECG gated SPECT techniques applied during myocardial perfusion imaging have provided 3-dimensional evaluation of left ventricular function. The ECG gated images

can be viewed as tomographic or 3-dimensional cine-loop images to evaluate wall motion, wall thickening, wall brightening, LVEF, end diastolic and end systolic volumes. The addition of this functional information to the myocardial perfusion data has resulted in improved interpretation (with reference to motion and attenuation artifact) as well as to prognostic and risk stratification information.

Neurocardiology:

Cardiac innervation is important for biological control of cardiac rhythm, rate, conduction, and repolarization. It is estimated that there are approximately 500,000 cardiac deaths per year in Europe with 19% showing no evidence of coronary artery disease. It is felt that a significant percentage of cardiac sudden deaths is due to abnormalities in the cardiac neuroconduction and neuroreceptor system. Sympathetic fibers leave the spinal cord from T-1 to L-3 with those traversing the left stellate ganglion providing innervation to the right ventricle and the posteroseptal left ventricle. The sympathetic innervation traversing the right stellate ganglion provides innervation to the anterior and lateral walls of the left ventricle. The sympathetic nerves travel with the coronary arteries in the subendocardium. Presynaptic neurocardiac imaging agents include I-123 MIBG, F-18 dopamine, and C-11 hydroxyephedrine. Postsynaptic agents to image beta receptors on the myocyte include C-11-CGP12177 and F18 carazol.

The cardioneuropathies can be classified as primary or idiopathic and secondary cardioneuropathies. The primary cardioneuropathies are divided into (a) idiopathic ventricular tachycardia and fibrillation, (b) dysautonomia, and (c) heart transplantation. Patients with idiopathic ventricular tachycardia and fibrillation have no structural or functional abnormalities detectable in the myocardium. Ventricular fibrillation is the most common arrhythmia and often results in sudden cardiac death. In these patients physical or mental stress, as well as catecholamine release can result in the dangerous arrhythmias. Recent studies demonstrate the presynaptic myocardial catecholamine re-uptake and the postsynaptic myocardial beta adrenoceptor densities are reduced. The dysautonomias are derangements of the sympathetic and parasympathetic nervous system which are seen fairly often in neurology as well as cardiology. These diseases can result in dangerous arrhythmias as well as loss of sympathetic neurocirculatory control resulting in orthostatic hypotension and abnormal blood pressure responsiveness. Cardiac transplantation results in complete denervation of the myocardium with the loss of sympathetic control. The donor AV node remains as the primary pacemaker source for the transplanted heart. I-123 MIBG imaging has documented that reinnervation can begin later than 1 year after transplantation, however. Patients who develop vasculopathy after a transplant often experience "silent myocardial angina" due to the absence of functioning autonomic nerves. However, after reinnervation occurs these patients can develop chest pain.

Types of secondary cardioneuropathies include (a) coronary artery disease, (b) dilated cardiomyopathy, (c) hypertrophic cardiomyopathy (d) diabetes mellitus, and (e) arrhythmogenic right ventricular dysplasia. It has been well demonstrated with experimental studies and imaging studies that the sympathetic neurons are more sensitive to prolonged ischemic episodes than are the myocytes. Patients with non wave infarction may demonstrate no loss of myocytes or myocyte function on gated SPECT imaging, however neuronal imaging has demonstrated larger

neuronal damage to the myocardium. The resultant myocardial denervation could result in functional abnormalities, arrhythmias or silent anginal episodes. Patients with diabetes have an increased incidence of coronary artery disease, as well as diabetic neuropathy, resulting in one of the major causes of silent myocardial ischemia. This has been demonstrated with decreased I-123 MIBG uptake which occurs mainly in the inferior wall. Myocardial denervation also results in a hyperreaction to dobutamine stress which may explain the higher incidence of sudden death in advance stage diabetics. Patients with hypertrophic cardiomyopathy demonstrate autonomic dysfunction, which is thought to be directly related to disease progression and heart failure. Quantitative PET studies with C-11 HED and C-11 CGP have shown that the cardiac pre-synaptic catecholamine reuptake is impaired in hypertrophic cardiomyopathy, resulting in reduced postsynaptic beta adrenoreceptor density. Patients with arrhythmogenic right ventricular dysplasia have a form of fibroplomatous degeneration of the right ventricular myocardium and are predisposed to dangerous arrhythmias and sudden cardiac death. It is believed that the abnormal sympathetic innervation is responsible for the arrhythmogenesis. I-123 MIBG imaging and C-11 HED PET Imaging have shown a reduction in the postsynaptic beta adrenoreceptor density in the right ventricle as well as the left ventricle.

Infarct/Injury Avid:

Imaging of acute myocardial necrosis has been accomplished in the past with Tc-pyrophosphate (PYP) utilizing planar and SPECT imaging. It is reported to have a 90% sensitivity and is generally imaged at least 12-24 hours post infarction. The peak level of uptake occurs at 48-72 hours and will slowly revert to negative within 4 weeks post injury. Most recently Tc-glucurate has also been reported for imaging acute myocardial infarction. Indium-111 antimyosin antibody also is utilized for "hot spot" imaging of acute myocardial infarction. This occurs directly after exposure of the myocytes allowing a sensitive and specific antibody to label the area of injury. Indium-111 antimyosin has also been used to detect myocarditis, transplant rejection, and doxyrubicin cardiotoxicity. Myocardial apoptosis has also been imaged utilizing technetium annexin, which is still being evaluated.

Myocardial Perfusion Imaging:

Most nuclear cardiology studies are currently being accomplished with SPECT imaging utilizing thallium or technetium agents. Perfusion tracers are utilized to detect coronary artery stenosis. Lesions less than 50% stenosis demonstrate no flow limitations at rest or stress and are generally not identified with myocardial perfusion imaging. Lesions greater than 50% stenosis will be flow limiting at high flow rates during exercise or pharmacologic stress testing. Critical stenosis or lesions with greater than 85-90% stenosis may result in decreased perfusion even under rest conditions. With slow progression of stenosis, myocardium may remain viable even with lesions up to 100% stenosis, due to development of collateral blood flow. With ECG gating, myocardial SPECT imaging can also now provide information concerning left ventricular function, wall thickening, wall motion, and left ventricular ejection fraction. Most recently, it is felt that prognostic assessment and risk stratification utilizing myocardial perfusion imaging may be just as important as evaluating coronary artery disease itself.

Exercise Tolerance Testing:

Non-imaging exercise tolerance testing is noted to have poor sensitivity and specificity of approximately 60-65% respectively. Utilizing radiotracers delivered at peak stress, ETT SPECT imaging has demonstrated an average sensitivity of 87% and specificity of 73%. Most physicians would prefer MPI-SPECT be accomplished in association with exercise tolerance testing, since this provides additional functional and physiological information over pharmacological stress testing. However, many patients are not able to complete the exercise stress testing due to physical limitations or due to inability to reach 85% of maximum predicted heart rate.

Pharmacological Stress Testing:

Most pharmacological stress testing is currently accomplished utilizing dipyridamole, adenosine, or dobutamine. Dipyridamole and adenosine are potent coronary vasodilators which increase myocardial blood flow by approximately 5 times, thus allowing detection of myocardial perfusion abnormalities resulting from fixed stenosis. For stress imaging, 0.56 mg/kg/min of dipyridamole is injected intravenously over 4 minutes to a maximum total dose of 60 mg. The radiotracer for stress imaging is administered at 7 minutes (3 minutes after completion of infusion). Dipyridamole blocks the reuptake of adenosine which is the direct coronary vasodilator. The dipyridamole therefore increases the extracellular concentration of endogenously produced adenosine. The effects of the dipyridamole can be reversed at 11 minutes with aminophylline. In 18 studies utilizing 1,272 patients with thallium-201, the overall sensitivity was 87% and specificity was 81% for detecting CAD, similar to those studies accomplished with exercise stress testing.

Adenosine can be directly infused at a rate of 140 mcg/kg/min over 6 minutes with the radiotracer injected at 3 minutes. The flow rate must be carefully controlled utilizing a computerized pump to achieve a consistent rate of infusion and pharmacologic effect. Shorter adenosine infusion protocols have also been utilized. In general, the adenosine protocol produces more symptoms than the dipyridamole protocol, however due to its ultra short half life (less than 10 seconds) the effects are quickly reversed when the infusion is terminated. The patients should also be screened 2nd degree and 3rd degree AV nodal block, because of the known AV node blocking effects of adenosine.

Caffeine and food products or beverages containing caffeine should be withheld for 12-24 hours prior to dipyridamole or adenosine testing. Beta blockers, anti-hypertensive medications, and other cardiac medications should not be withheld for adenosine or dipyridamole stress testing. However, beta blockers do need to be withheld for exercise tolerance testing. Dobutamine infusions have also been utilized for pharmacologic stress testing and are used most frequently with echocardiography and infrequently for MPI SPECT imaging. Dobutamine's main mechanism of action is stimulation of beta 1 receptors, thus increasing contractility, workload, heart rate, and myocardial blood flow. One commonly used protocol is a step approach beginning with low dose infusion at 5 mcg/kg/min over 3 minutes and increasing in steps up to 40 mcg/kg/min. Some centers inject a higher dose rate at 50 mcg/kg/min and administer atropine if the 85% maximum predicted heart rate is not achieved.

Imaging protocols:

Utilizing the physical and physiologic properties of thallium and technetium radiotracers allows the physician to establish several different MPI SPECT protocols. For a one day protocol, thallium can be injected at peak stress followed by imaging within 15 minutes. Due to its washout, blood pool, and redistribution effects, the redistribution imaging can be accomplished at 3-4 hours. This amount of time may not be enough for critical stenosis and thus further delayed imaging at 12-24 hours can be accomplished to detect viable myocardium, even in those patients with 100% stenosis. Alternatively a 1-1.5 mCi thallium booster dose can be given prior to the 4 hour redistribution imaging, thus eliminating the necessity for most of the more delayed imaging.

An alternative one-day dual isotope study can be accomplished with a resting thallium scan (3-3.5 mCi) followed almost immediately by a stress technetium radiotracer scan. This protocol matches the best properties of thallium and technetium and allows for the shortest delay time between rest and stress imaging. It also allows 24 hour delayed redistribution images in those cases requiring viability assessment. The main drawback to this protocol is that it does involve 2 different radiotracers with different imaging characteristics.

For technetium sestamibi and technetium tetrofosmin, one can utilize a two-day protocol or a one-day protocol. The two-day protocol would usually involve stress testing with the technetium radiotracer injection, and imaging which is usually accomplished at 30 minutes for tetrofosmin and 60 minutes for sestamibi. The patient returns a second day if necessary for the same 25 mCi technetium dose and rest scan imaging.

For a one-day protocol with sestamibi or tetrofosmin, a 10 mCi rest injection, followed by SPECT imaging is usually accomplished. This is followed by a 3-5 hour delay before stress testing and radiotracer infusion with 25-30 mCi of technetium agent. The lower resting dose, lower myocardial blood flow and decay time delay allow for the most accurate 1 day protocol with the least influence of the rest or stress imaging on each other.

Viability:

The detection of viable myocardium is of extreme importance in prognostic assessment and in choosing the appropriate therapy for a given patient. "Hibernating myocardium" usually refers to myocardium with high grade stenosis with resulting chronic hypoperfusion, altered metabolism from free fatty acid metabolism to glucose metabolism and hypokinesia or akinesia of that myocardial segment. "Stunned myocardium" usually refers to myocardium which has experienced prolonged ischemia/recovery with resulting hypokinesia or akinesia. Prolonged, stunned, myocardium can occur after myocardial infarction with remaining viable myocardium. In the post injury setting, so called "reverse redistribution" can indicate higher uptake of thallium post stress with worsening of the perfusion abnormality on delayed imaging. This usually occurs in those patients with viable myocardium which has experienced prolonged ischemia and damage to the sodium potassium pump and thus an inability to maintain the myocardial thallium concentration levels over the redistribution time period. In the setting of recent injury, reverse redistribution can be a good prognostic sign demonstrating reestablishment of blood flow and viable myocardium.

With sestamibi or tetrofosmin, visible wall motion and more importantly, visible wall thickening and brightening indicate viability. Because there is no significant redistribution however, critical stenosis with resulting hibernating myocardium, may demonstrate fixed defects during rest and stress. This may make detection of viable myocardium difficult for these agents. Administration of nitroglycerin prior to the infusion of the technetium radiotracer has been shown to improve the resting uptake, and thus improve detection of viable myocardium. The standard thallium protocol to detect viable myocardium is best accomplished with a 3.5 mCi resting injection followed by 12-24 hour redistribution imaging. The resting SPECT images can be ECG gated, although the delayed ECG gated imaging is more difficult to obtain. PET imaging with perfusion radiotracers, such as ^{13}N -ammonia or Rubidium-82 can be followed by F-18 fluorodeoxyglucose. The perfusion tracers will demonstrate hypoperfusion secondary to stenosis where as the FDG images will demonstrate normal or increased FDG uptake in those hypoperfused segments. The combined use of a PET flow tracer and FDG metabolic tracer is considered the gold standard for viability assessment. The amount of viable myocardium detected is predictive for functional improvement after revascularization and is also coupled with reduced peri-operative risk and improved long term outcome.

Acute Ischemic Syndrome:

Sestamibi and tetrofosmin given as a resting injection may show regionally reduced perfusion which is a sensitive marker of jeopardized myocardium. Recent studies on chest pain patients in the E.R. have demonstrated the efficacy of MPI SPECT imaging to detect those patients with acute ischemic syndromes. If the patient's MPI SPECT imaging is normal it has been shown that the patient may be safely discharged for further evaluation of their chest pain on an outpatient basis. If the MPI SPECT imaging demonstrates hypokinesia or reduced perfusion, the patient is admitted for observation to rule out myocardial infarction. This form of triage on E.R. chest pain patients has been shown to be highly efficacious as well as cost effective.

Pre-Operative Risk Assessment:

MPI SPECT imaging has been utilized effectively to predict those patients at high risk for cardiac events during major non-cardiac surgery. These patients are typically diabetics, patients with prior CABG, or known CAD who are being evaluated for non-cardiac vascular surgery. A positive MPI SPECT scan indicates significant underlying CAD and high risk, whereas a negative scan is predictive of low risk. In general, a negative myocardial perfusion SPECT scan is associated with less than 1% risk for cardiac event or cardiac death per year.

CONCLUSION:

Nuclear imaging techniques for the heart provide a highly efficacious and cost effective technique for detecting CAD, evaluating the significance of known CAD, detecting viable myocardium and triaging patients with suspected ischemic cardiomyopathy for medical therapy, reperfusion techniques, CABG or cardiac transplantation. Further evaluation of metabolic agents for fatty acid metabolism, direct ischemic labeling, apoptosis and neurocardiac imaging should bring promising results. Direct imaging of developing atheromatous arterial plaque is also an exciting development.

REFERENCES

- Bavelaar-Croon CDL, Atsma DE, Van Der Wall EE, et al. The additive value of Gated SPECT Myocardial Perfusion Imaging on Patients with Known and Suspected Coronary Artery Disease. *Nucl Med Commun.* 2001;22:45-55.
- Bengel FM, Schwaiger M. Nuclear Medicine Studies of the Heart. *Eur Radiol.* 1998;8:1698-1706.
- Cacciabando JM, Szulc M. Gated Cardiac SPECT: Has the Addition of Function to Perfusion Strengthened the Value of Myocardial Perfusion Imaging?. *J Nucl Med.* 2001; 42 (7):1050-2.
- Cerqueira MD, Lawrence A. Nuclear Cardiology Update. *Radiol Clin North Am* 2001; 39(5): 931-46.
- Cuocolo A, Acampa W. Nuclear Cardiology in the New Millenium. *Rev Esp Med Nucl* 2001; 20: 305-308.
- De Puey EG, Garcia EV, Berman DS. Cardiac SPECT Imaging. 2nd Edition. Lippincott, Williams & Wilkins. 2001.
- Matte GG, Barnes DC, Abrams DN. Pharmacological Interventions in Nuclear Medicine Assessment of Cardiac Perfusion. *J Pharm Pharmaceut Sci.* 2001; 4(3): 255-62.
- Schafers M, Schober O, Lerch H. Cardiac Sympathetic Neurotransmission Scintigraphy. *Eur J Nucl Med.* 1998; 25: 435-41.
- Schinkel AF, Bax JJ, Sozzi FB, et al. Prevalence of Myocardial Viability Assessed by Single Photon Emission Computed Tomography in Patients with Chronic Ischaemic Left Ventricular Dysfunction. *Heart.* 2002; 88(2): 125-30.
- Schwaiger M, Melin J. Cardiological Applications of Nuclear Medicine. *Lancet.* 1999; 354(6): 61-66.

Manpower Shortage in Radiology: Solutions

Kay Vydareny, M.D.

The Manpower Crisis in Academic Radiology: Problems and Solutions

Kay H. Vydareny, M.D.
Society of Thoracic Radiologists
March 4, 2003

- What is the problem?
- Are the issues unique to Radiology?
- What are possible solutions?

Is there a problem?

“We are truly in a crisis mode in academic radiology and frankly as long as the job market stays the way it is I believe we are going to continue to see erosion in our faculties. The money, hours and perks in ‘private practice’ are just too hard to overcome with the promise of being involved in research and education”.

© David Maxwell 2002

What’s the problem?

- Increasing clinical workload
- Demands for more timely service (24x7x365)
- Need for closer supervision of residents (IL372, malpractice climate)
- MORE faculty needed to do clinical work – but there are FEWER...

Shortage of faculty–2001 Survey of Academic Chairs

- Survey of medical school departments
- 106/124 responses
- Avg. of 5.5 faculty vacancies/program
- Approx. 600 openings overall
- Most in demand:
 - Neuro and Abd. Imaging @ 84.5 each
 - Vascular/interventional 78

Department Vacancies 106/124 Responding

<u>Type of Position Vacancies</u>	<u>Number of</u>
General Radiology	55.0
Pediatric Radiology	43.8
Chest	36.5
Musculoskeletal	32.0

Department Vacancies 106/124 Responding

<u>Type of Position Vacancies</u>	<u>Number of</u>
Nuclear Radiology	31.5
Research	25.0
Ultrasound	17.0
Other	13.0
Total Vacancies	570.3

Why do radiologists choose academics?

- Enjoyment/aptitude for type of work
- Desire to subspecialize
- Belief in value of research and own skills to do research

• Hillman, *Radiology*, 1990

Why choose private practice?

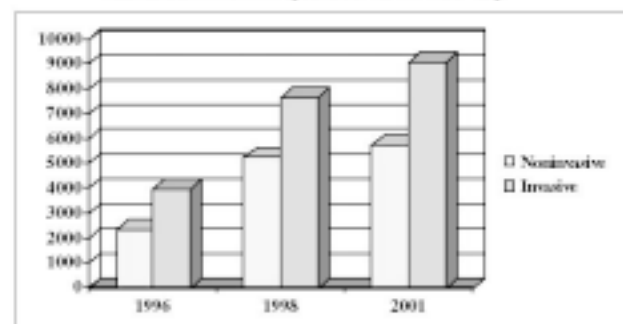
- Family obligations
- Personal income and amt of leisure time significantly more important than in those who chose academics

• Hillman, *Radiology*, 1990

Why are they leaving?

- Increasing clinical workload
- Less time for research
- Less time for teaching med students and residents
- Disparity between private practice and academic income
- Lack of control over practice

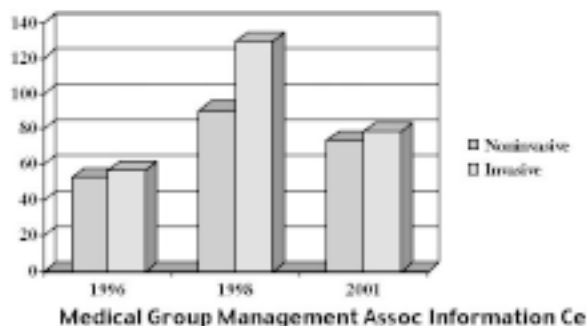
Increasing clinical workload, academic (work RVU's)



Medical Group Management Assoc Information Cent

- Confusion over conflicting missions
 - Deans - "do more research, do more teaching, get more grants" (Holy Grail=NIH grants)
 - Department chair - "do more cases"
 - Faculty - "I can't do it all"

Work RVU's, % Academic cf. Private practice



Academic cf. private practice

- 1996
 - Noninvasive 56%
 - Invasive 57%
- 2001
 - Noninvasive 74%
 - Invasive 79%

- Increasing clinical work load + fewer faculty means:
 - Less time for research
 - Less time for teaching medical students and residents
- Suboptimal training of residents and fellows

Survey of AUR members, 2000

- 521/1200 returned
- 188 institutions
- Clinical work days
 - 64% - 5 days a week
 - 28% - no non-clinical time

» Hunter, Acad Radiol, 2001

What's happening to research by clinical faculty?

- Hunter survey - 68% "less productive" than 5 yrs ago
- Increase in funded research primarily by Ph.D.'s attached to rad departments

Clinical workload effect on research

- 33 FT clinical faculty, 1994-5, 1995-6
- Inverse relationship between RVU's and academic productivity (peer-reviewed articles, published abstracts, presentations)
- Age, rank, administrative jobs no relationship to productivity

Teaching med students

- Anecdotal data only
Emory experience
- Medical students of today are the radiologists, referring clinicians of tomorrow

Why does private practice look so good?

- Disparity between salaries
- Lifestyle choices
- Influenced by increased indebtedness of residents



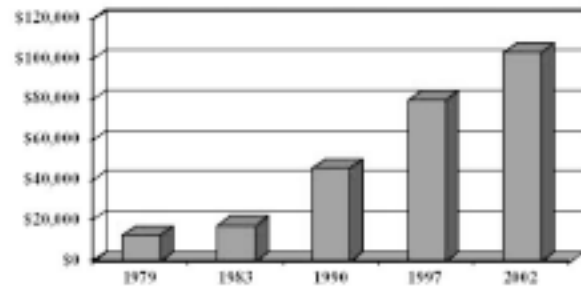
Resident indebtedness

- Influences career decisions
- Increasing medical student debt
 - 1979 - \$13,300
 - 1983 - \$18,000
 - 1990 - \$46,224
 - 1997 - \$80,462
 - 2002 - \$103,855

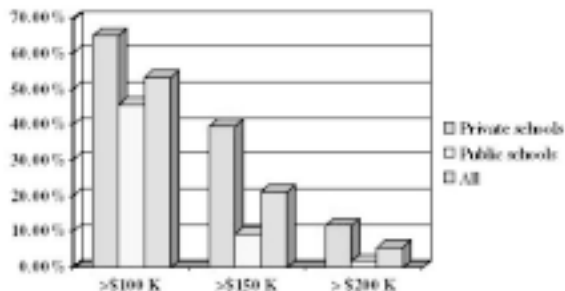
Naradzay, JAMA, 1998, AAMC

2002

Av. Debt of Med Student



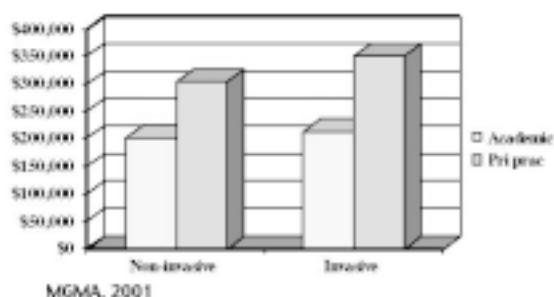
2002 med student debt



www.aamc.org/data

How do they repay this debt?

Median income, 2000



Why are salaries lower in academics?

- Less clinical work performed
- Higher overhead (Dean's tax, more academic support, etc.)
- More indigent care
- More complex cases
- Teaching and research not reimbursable
- Residents take time, influencing productivity
- Rigid sub-specialization, less cross-

Not just radiology's problem

"Despite scientific progress and popular support, academic medicine is in serious danger."

Pardes, The perilous state of academic medicine, JAMA 2000

- Faculty losses worse in highly compensated specialties (surgery, CT surgery, anesthesiology, rad) where salary differentials are greatest
- Less problem in peds, int med., fam practice

What are solutions?

- Academic departments and med schools
- Industry
- Government policies
- Private practice

Academic departments

- Need to value research and teaching, not just clinical productivity
 - Needs to be a "culture change"
 - Re-vitalize the academic enterprise

WILL TAKE DOLLARS AND MANPOWER
WHERE DO THEY COME FROM?

- Increase efficiency (look at private practice models)
 - Need more generalists/cross coverage (unpopular)
 - Increased use of paraprofessionals - radiology assistants, supertechs, etc.
 - Conversion to PACS

- Recruit new faculty among international grads, retired, part-time.
 - Need to be thought of as equals
- Increase number of residents as much as possible within RRC guidelines (1:1 faculty/res. ratio, number of exams)
- Increased support of academic mission by medical school

Industry

- Investment in research programs, departments
 - Dotter Institute (U of Oregon)
 - Frederick Philips MR Lab (Emory)
- Investment in teaching (fellowships, techs, residency programs)

Government

- Increase the number of funded resident slots in specialties with workforce shortages
- Stop extra payment for primary care slots
- New initiatives to pay for indigent care (disproportionate burden on AMC's)

Private practice

- Permit residents to change specialties without funding penalty (CMS)
- Change reimbursement by generic CPT codes (abdomen CT for stomach pain vs. post liver transplant)
 - Academic - RVU's/procedure=0.56
 - Non-academic - RVU's/procedure=0.48

- Sunshine, *Radiology*, 2000 (1996-7 data)

- Need to invest in the future
- Use of days off to help with clinical work
- Increased philanthropy to departments by alumni, local groups
- Sponsorship of resident positions
 - ISC 2002 - tax of \$1000 thru society membership to fund residency positions

- Sponsorship of fellowship positions
 - Informal
 - Formal

ACR Task Force on Financial Support for Fellowship Training

- Presented at ACR annual meeting, 2001
- Chaired by Neil Messinger, members from academic and private practice

Recommendation

- “The Task Force believes that the potential to increase and/or maintain critical disciplines within our specialty by supporting fellowships, which are not traditionally funded, is a worthwhile and responsible commitment by the ACR leadership and its members.”

Conclusion

- The Problem –Academic mission CANNOT be sustained from clinical revenues alone
 - Salaries can’t be competitive
 - Retention and recruitment of faculty are compromised
 - Training of residents and fellows suffers

REMEMBER...

- There is NO simple remedy
 - Need philanthropy (industry, pri prac)
 - Need more support from government
 - Need more support from Schools of Med
 - Need more efficient clinical practices
- HELP is needed!

TODAY'S RESEARCH IS TOMORROW'S
TURF

AND

TODAYS RESIDENTS ARE TOMORROW'S
RADIOLOGISTS

NCI Update for Thoracic Radiology

Edward V. Staab, M.D.

Chief, Diagnostic Imaging Branch
BIP/DCTD/NCI

The objectives of this lecture are to:

1. Describe the overall strategic plan for diagnostic imaging and interventional radiology in cancer research.
2. Explain the importance of imaging and radiologists in the advancement of our knowledge in cancer biology and in the care of cancer patients.
3. Provide an update on the current targeted areas for imaging research in Preclinical studies.
4. Explain the advances in clinical imaging trial research and the growing awareness and participation by radiologists in clinical trials
5. Promote participation in the development of new knowledge by the attendees.
6. Review current trials in imaging of cancer and image guided therapy of cancer specifically related to the thorax.

The National Cancer Institute has recognized imaging of cancer as an extraordinary opportunity for several years. The development of imaging assessment to tumor biology in animal systems and human cancers in parallel with our advancing molecular understanding of the malignant state is an important priority for the National Cancer Institute. To meet the challenges of this extraordinary opportunity the Biomedical Imaging Program was developed five years ago and has had a remarkable growth rate.

The challenge to imaging is to make earlier and more accurate diagnoses for cancer patients that will reduce the number of required invasive therapies, enhance a physicians ability to monitor patient response to treatment and ultimately make a positive affect on the quality of life of cancer patients. Imaging potentially can be used for developing new drugs and other therapeutics because it provides physiological, morphological and molecular information non-invasively. This means that measurements can be made regarding the time-related distribution of drugs and tissue responses without disturbing the milieu. This is the unique information that can be garnered from imaging and what makes it an extraordinary opportunity for cancer research. In addition, imaging is being promoted for targeting tissue for various interventional treatments. This includes image guided radiation therapy and surgery, delivery of specific therapies to focused areas and application of a number of other technologies for eradicating cancerous tissue.

The American College of Radiology Imaging Network (ACRIN) is one of nine cooperative groups in the National Cancer Institute established to conduct clinical trials in cancer patients. It was funded in March of 1999 and is currently undergoing review for renewal of its grant. It has received additional support via supplements for two very large screening trials, the

National Lung Screening Trial (NLST) and the Digital Mammography Imaging Screening Trial (DMIST). Relevant to this conference, NLST is a randomized control trial of 50,000 high-risk patients with smoking history to determine the value of low-dose CT screening for lung cancer. ACRIN has combined its resources with the PLCO contract investigators to conduct this trial. Each entity will enroll 25,000 participants by April 2004. These patients will be followed for eight years to determine the primary endpoint, overall mortality. In addition, 10,000 of the ACRIN participants will undergo extensive evaluation addressing the effect of screening on smoking cessation, quality of life issues, cost effectiveness and the collection of body fluids and tissues for future biomarker research.

Cancer Imaging is being developed for pre-clinical studies directed at the development of new therapeutic methods. To this end the Biomedical Imaging Program has developed initiatives to identify new imaging agents, test these in pre-clinical models and foster their acceptance by regulatory agencies. The BIP has invested in several areas of infrastructure needs to accomplish these tasks. These include:

- Centers for Molecular Imaging which bring together a variety of different scientists and imaging technologies
- Small animal imaging research programs (SAIRP's) to develop the field of animal imaging
- Development of contrast agents and enhancers (DCIDE) to help bring the new agents through the regulatory system
- Imaging agent databases
- Cancer imaging trials
- Clinical Imaging databases
- Imaging informatics
- Optimization and standardization of technological platforms
- Image guided tools and methods

The practicing radiologist should have an understanding of the research that is currently going on that will change the way patients are diagnosed and treated in the future. This talk will present the current framework for the development of new ways to diagnose and treat patients with cancer.

For further information please contact us at the numbers below or access the relevant websites.

Biomedical Imaging Program/DCTD/NCI
6130 Executive Blvd. EPN. Suite 6000
Rockville, MD 20892-7440
Tel: 301-496-9531
FAX: 301-4803507
BIP Web Site: cancer.gov/bip/
NIH Web Site: www.nih.gov

NIBIB Update for Thoracic Radiology

Richard E. Swaja, Ph.D.

National Institute of Biomedical Imaging and Bioengineering
National Institutes of Health

The mission of the National Institute of Biomedical Imaging and Bioengineering (NIBIB) at the National Institutes of Health (NIH) is to support research and training that will advance the fields of biomedical imaging and bioengineering with the objective of improving human health and addressing healthcare issues. The NIBIB offers a variety of biomedical imaging research funding opportunities that are based on input from the biomedical community and can be applied to thoracic radiology. This presentation will review the history and status of the Institute and will describe the bases of current NIBIB biomed-

ical imaging research programs, technical focus areas, current funding opportunities, and near-future plans. Bases of the programs include recent workshops aimed at obtaining community input for bioimaging research needs and larger symposia conducted in conjunction with other NIH institutes and centers. Current funding opportunities include solicitations related to optical technologies, biomedical imaging technologies and systems, imaging informatics, image-guided interventions, and low-cost imaging equipment and techniques. Near-future directions of NIBIB imaging programs will be briefly discussed.

Thoracic Vascular Abnormalities in Children

Sandra Kramer, M.D.

Department of Radiology,

The Children's Hospital of Philadelphia and The University of Pennsylvania School of Medicine

INTRODUCTION

Pediatric vascular abnormalities range from inconsequential normal variants to life threatening lesions with profound effects on the airway and pulmonary parenchyma. Some congenital thoracic lesions such as sequestration may be detected in utero on prenatal sonograms and fetal MRI. Infants with significant vascular abnormalities often present in the neonatal period with respiratory or cardiovascular symptoms. Some anomalies become evident later in childhood, and other congenital lesions are discovered incidentally in adults. Acquired vascular lesions in children may be iatrogenic or result from trauma or underlying genetic or systemic diseases. Imaging plays a key role in evaluating the thoracic vasculature and its pathology.

CONGENITAL ANOMALIES

Vascular Rings

In the first 5 weeks of fetal life, six pairs of aortic arches form and then regress segmentally or entirely. The paired 4th aortic arches connect the ascending aorta (primitive ventral aortic sac) to the descending aorta (embryonic left dorsal aorta). Most of the embryonic right 4th aortic arch regresses, leaving the normal left aortic arch with a left-sided descending aorta. Vascular rings result from interruptions in development of these primitive arches. Severity of symptoms such as expiratory stridor, wheezing, and dyspnea depends on the degree of tracheal compression by the vascular structures.

Careful evaluation of chest radiographs may reveal a "right aortic arch" on the AP view and anterior bowing and narrowing of the trachea on the lateral projection. Since it is impossible to determine the exact anatomy of the vascular ring using plain radiographs and barium swallow alone, MR imaging is used for this purpose. The two common vascular rings are:

1. Double aortic arch. The most complete type of vascular ring occurs when both embryonic fourth aortic arches remain patent and surround and compress the esophagus and trachea. Multiplanar MR images show both components of the double arch and their compressive effects on the airway. The right arch is typically larger and more cephalad than the left.
2. Right aortic arch with an aberrant left subclavian artery. The most common vascular ring, although in some cases it may be asymptomatic. The vascular ring surrounds the trachea and esophagus, closed by the ductus or ligamentum arteriosum, which is almost always left-sided. MR imaging shows the right arch, the course of the descending aorta and the segmental impression on the trachea by the aberrant left subclavian artery. An "aortic diverticulum of Kumerol", a focal enlargement at the origin of the aberrant left subclavian artery, may also be seen.

Pulmonary Sling (Aberrant Origin of the Left Pulmonary Artery)

The pulmonary "sling" is an unusual vascular anomaly in which the aberrant left pulmonary artery originates from the posterior aspect of the right pulmonary artery and passes between the trachea and esophagus to reach the left hilum.

Underlying tracheobronchial abnormalities are associated with pulmonary sling including tracheomalacia and "complete" cartilaginous rings causing tracheal and bronchial stenosis. The lateral chest radiograph may show a small mass between the trachea and esophagus. Bilateral or unilateral hyperinflation may be present depending on the degree of tracheal or bronchial stenosis. On barium swallow an impression caused by the aberrant left pulmonary artery is visible on the posterior wall of the trachea and the anterior wall of the barium filled esophagus. CT and MRI demonstrate the complete anatomy of the pulmonary sling and the airway narrowing.

Pulmonary Lesions with Anomalous Vasculature: Sequestration

Bronchopulmonary sequestrations are foci of pulmonary tissue that lack normal communication with the tracheobronchial tree and have a systemic arterial blood supply. Most of these lesions are discovered incidentally on chest films. Further evaluation usually involves contrast enhanced CT. The contrast bolus is timed to show optimal enhancement of the feeding artery and lung parenchyma. On MRI, sequestrations are well-defined lesions with bright T2 signal intensity, with the feeding artery and draining veins identified. Sequestration may also be diagnosed in utero on prenatal ultrasound and MRI examinations. Two forms of sequestration have been described:

1. Extralobar sequestrations are enclosed in their own pleural layer, with an arterial supply via small branches off the aorta and venous drainage into the azygous or hemiazygous system. They are most commonly found in the posterior costophrenic sulcus, primarily on the left, and less commonly in the mediastinum and upper abdomen. More than half of patients with extralobar sequestrations have other congenital anomalies.
2. Intralobar sequestrations are enclosed within the pleura of the adjacent normal lobe. Their arterial supply is variable, but usually from aortic branches that lie in the inferior pulmonary ligament, and drainage occurs into the pulmonary veins. These lesions may be found in older children with no other congenital anomalies.

Hypogenetic Lung Syndrome

In scimitar syndrome one lung is hypoplastic and is drained by an anomalous pulmonary vein. Its feeding artery is usually a hypoplastic pulmonary artery, but may be of systemic origin. There may be abnormal bronchial branching or bronchial hypoplasia. Pulmonary segmentation anomalies may coexist. This anomaly is found predominantly on the right and is associated with congenital heart disease in approximately 25% of patients, most commonly atrial septal defect. Since the scimitar vessel usually drains into the junction of the inferior vena cava with the right atrium, a left-to-right shunt occurs. When scimitar syndrome presents in infancy, it is usually in the setting of congestive failure. These lesions are, however, often asymptomatic, found incidentally on chest radiographs. The typical radiographic feature is the anomalous pulmonary venous trunk coursing

vertically along the right atrium toward the right cardiophrenic angle with the appearance of a "scimitar". CT shows the course of the "scimitar" vein through the hypoplastic right lung to the inferior vena cava as well as the pulmonary artery and airway anomalies.

HEREDITARY HEMORRHAGIC TELANGECTASIA

Rendu-Osler-Weber (ROW) is an autosomal dominant vascular disorder. It remains unclear whether the vascular lesions are true congenital malformations or acquired lesions occurring in abnormal vessels. Pulmonary arteriovenous malformations (PAVM) occur in about 20% of patients with ROW and include vascular abnormalities ranging from telangiectatic lesions to large arteriovenous channels. Most PAVM are found during adolescence and young adulthood, although symptoms may occur in childhood and infancy. Complications include hemorrhage into the bronchi or pleural cavity, hypoxemia due to right-to-left shunting, and embolization across the vascular lesion into the systemic circulation, especially to the CNS. PAVM may be seen on a chest radiograph depending on their size and location, however, they are better assessed by CT and pulmonary angiography. The size, number, location and architecture of the lesions can be defined prior to angiographic embolization.

MARFAN SYNDROME

Marfan syndrome is an autosomal dominant disorder of connective tissue with variable penetrance. The most serious cardiovascular complications include aortic root dilatation, aortic dissection and aortic valve insufficiency. MR imaging can define these complications involving the ascending aorta and aortic valve. Aneurysms of the pulmonary vasculature, dilatation of the abdominal aorta, and aneurysms at the origin of peripheral aortic branch vessels are also encountered in Marfan syndrome. MR imaging is also valuable in the post-operative evaluation of complications following composite graft placement and in screening of family members of Marfan patients.

VASCULITIS

Vasculitis involving the pulmonary arteries is rare in children, but occurs in Wegener's granulomatosis and Churg-Strauss vasculitis. It may accompany systemic connective tissue diseases such as systemic lupus erythematosus and dermatomyositis. Although imaging findings are helpful, lung biopsy is required for the definitive diagnosis.

Wegener's granulomatosis

Wegener's granulomatosis, a necrotizing vasculitis with granuloma formation, involves the respiratory tract and kidneys. Although nodules and cavities occur frequently in adults, these features are found less often in children. The most common radiographic findings in children include diffuse interstitial and alveolar opacities. High-resolution CT scans may portray a pattern of perivascular, centrilobular hazy opacities, which correlate with biopsy findings of perivascular inflammation and surrounding hemorrhage.

Takayasu arteritis

Takayasu arteritis is a chronic inflammatory arteritis of unknown etiology that results in thrombosis, stenosis, dilatation and aneurysm formation in the aorta, aortic branch vessels and pulmonary arteries. Concentric mural calcification and mural

thickening in the aorta and pulmonary arteries may occur. Early symptoms may have an insidious onset and include dyspnea and hemoptysis. The disease may progress to vascular dissection, cerebrovascular accident and heart failure resulting from aortic insufficiency.

MR and contrast enhanced CT are helpful in the initial diagnosis, follow-up of progression, and assessment of response to treatment. CT shows the thickened vascular wall, contour changes of stenosis or dilatation and mural calcification. MR imaging may depict the size and extent of contour abnormalities, as well as the thickened wall and mural thrombi, but mural calcification may not be visible. Cine gradient echo MR sequences may show pulmonary and aortic valvular insufficiency. Contrast enhanced MR images have been reported to demonstrate increased signal in the thickened vascular walls and surrounding periaortic tissues due to intramural neovascularity in cases with acute and chronic active arteritis.

OTHER ACQUIRED VASCULAR ABNORMALITIES

Thoracic aneurysms

Thoracic aortic and pulmonary artery aneurysms are very rare in infants and children, but may be seen in patients with connective tissue disease, such as Marfan and Ehlers-Danlos syndromes. They are more frequently the sequela of surgery or prior vascular intervention such as umbilical arterial catheterization in the neonatal period. In these settings, a mycotic aneurysm may go unrecognized clinically during the course of treatment for fever of unknown origin or endocarditis. Depending on the location of the lesion, it may or may not be visible on chest radiograph and echocardiography. CT or MRI may demonstrate an unsuspected mycotic aneurysm and provide the details of location and extent of the aneurysm necessary for surgical management. In addition cine gradient echo sequences may show turbulent flow into an aneurysm as well as valvular insufficiency in the case of valvular-based aneurysms.

Traumatic aortic injuries

Traumatic aortic injuries are uncommon in children and are most often the result of motor vehicle accidents. The aortic isthmus is the most commonly injured site and most of these patients have additional severe injuries. Common radiographic findings in aortic injury include mediastinal widening, apical capping, poorly defined aortic contour, and displacement of the course of the NG tube. Enhanced spiral CT is a valuable screening tool for aortic injury in stable patients. Typical CT features of aortic injury include intimal flap and pseudoaneurysm formation, as well as mediastinal hematoma, pleural fluid and pulmonary parenchymal injury. Angiography also has an important diagnostic role.

CONCLUSION:

Pediatric thoracic vascular abnormalities range from benign anatomic variants discovered incidentally to potentially life-threatening lesions. Many lesions come to clinical attention because of their effects on the airway, pulmonary parenchyma or cardiovascular system. Diagnostic imaging frequently begins with plain film radiography and may progress to cross-sectional imaging with CT and MRI. These imaging modalities have largely replaced more invasive techniques such as angiography and provide valuable data contributing to patient management.

ACKNOWLEDGEMENT: Thanks to Dr. Pat Harty for her contributions to this work.

SUGGESTED READING

1. Choe YH, Kim DK, Koh EM, Do YS, Lee WR: Takayasu arteritis: diagnosis with MR imaging and MR angiography in acute and chronic active stages. *J Magnetic Reson Imag* 1999,10:751-757.
2. Connolly B, Manson D, Eberhard A, Laxer RM, Smith C: CT appearance of pulmonary vasculitis in children. *AJR* 1996,167:901-904.
3. Donnelly LF, Strife JL, Bailey WW: Extrinsic airway compression secondary to pulmonary arterial conduits: MR findings. *Pediatr Radiol* 1997,27:268-270.
4. Frazier AA, Rosado-de-Christenson ML, Stocker JT, Templeton PA: Intralobar sequestration: radiologic-pathologic correlation. *RadioGraphics* 1997,17:725-745.
5. Harty MP, Kramer SS, Fellows KE: Current concepts on imaging of thoracic vascular abnormalities. *Curr Opinions in Pediatrics* 2000, 12:194-202.
6. Hubbard AM, Adzick NS, Crombleholme TM, et al.: Congenital chest lesions: diagnosis and characterization with prenatal MR imaging. *Radiology* 1999,21:43-48.
7. Panicek DM, Heitzman ER, Randall PA, et al.: The continuum of pulmonary developmental anomalies. *RadioGraphics* 1987,7:747-772.
8. Park JH, Chung JW, Im JG, Kim SK, Park YB, Han MC: Takayasu arteritis: evaluation of mural changes in the aorta and pulmonary artery with CT angiography. *Radiology* 1995,196:89-93.
9. Pickhardt PJ, Siegel MJ, Gutierrez FR: Vascular rings in symptomatic children: frequency of chest radiographic findings. *Radiology* 1997,203:423-426.
10. Newman B, Meza MP, Towbin RB, Del Nido P: Left pulmonary artery sling: diagnosis and delineation of associated tracheobronchial anomalies with MR. *Pediatr Radiol* 1996,26:666-668.
11. Rosado-de-Christenson ML, Frazier AA, Stocker JT, Templeton PA: Extralobar sequestration: radiologic-pathologic correlation. *RadioGraphics* 1993,13:425-441.
12. Shovlin CL, Letarte M: Hereditary haemorrhagic telangiectasia and pulmonary arteriovenous malformations: issues in clinical management and review of pathogenic mechanisms. *Thorax* 1999,54:714-729.
13. Soulen RL, Fishman EK, Pyeritz RE, Zerhouni EA, Pessar ML: Marfan syndrome: evaluation with MR imaging versus CT. *Radiology* 1987,165:697-701.
14. Spouge AR, Burrows PE, Armstrong D, Daneman A: Traumatic aortic rupture in the pediatric population. *Pediatric Radiology* 1991,21:324-328.
15. Wadsworth DT, Siegel MJ, Day DL: Wegener's granulomatosis in children: chest radiographic manifestations. *AJR* 1994,163:901-904.

Multidetector Pediatric Chest CT: Practical Approach

Donald P. Frush, M.D.

Duke University Medical Center

Introduction

- Multidetector CT (MDCT) is an invaluable imaging modality for thoracic evaluation.
- MDCT provides:
 - unique benefits. For example,
 - scanning completed during limited breath-holding in children
 - improved IV contrast enhanced scanning, especially CT angiography
 - Thin slices (improving z-axis resolution) with improved multiplanar and 3D depictions unique challenges
- Objectives for this material on pediatric chest MDCT:
 - summarize the importance of topic
 - review the technical considerations for children,
 - discuss applications

Importance of Pediatric Chest MDCT

- Pediatric chest MDCT is important for the following reasons:
 - CT use is increasing: 600% increase recently *predates* MDCT.
 - CT is a widely used modality.
 - Estimated that currently 30-65 million CT examinations are performed in the US
 - 600,000 - 1.6 million CT examinations are performed in children or 4-5% of the total.
 - 33% in children ≤ 10 years; 18% under 5 years
 - Pediatric CT has increased from 4% to 11% of all CT 11%
 - After radiography, CT is the most frequently used chest imaging modality
 - CT provides the best combination of parenchymal, mediastinal, cardiovascular, and chest wall assessment

Technical Considerations for Pediatric Chest MDCT

- Patient preparation
 - Sedation is rarely needed for non contrast evaluation
 - If cannot reliably breath hold, scan during quiet breathing.
- Unique considerations for IV contrast media
 - There are many variables in contrast-enhanced pediatric CT
 - small contrast volumes
 - small gauge angiocatheters
 - unusual angiocatheter locations
 - manual IV contrast administration
 - Dose: general chest CT and CT angio 1.5 mL/kg.
 - Rate:
 - mL/sec method: 24-gauge 1.0-1.5 mL/sec, 22-gauge 1.5-2.0 mL/sec, 20-gauge and 2.0-4.0 mL/sec.
 - Another method is a single fixed duration (or a few durations) of injection for all children, such as 60 seconds, with scanning starting just after injection is completed.

- Injection technique: hand (manual) bolus or power injector.
 - Power injection through central venous catheters is also becoming more prevalent. Complication rate similar to manual injection.
- Timing of scan onset:
 - Empiric delays: 0-10 seconds after completion of contrast. I use this routinely
 - Bolus tracking: following enhancement and scan at arbitrary level of enhancement. I use for CT angiography.
- CT parameters: see table 1
 - In general, slice thickness and interval should be selected for the examination that result in about 25-30 images
 - Use fastest gantry rotation time
 - Tube currents in the range of about 25-100 mAs are generally acceptable
 - High-resolution chest CT: I use axial (non-helical) acquisition. 1-1.25 mm thick images at 5-10 mm intervals, tube currents 33-50% from those recommended for helical CT of the chest.

Table 1:
Guidelines for Chest MDCT Parameters in Children*

Weight (lb)	kVp	mAs**		Slice Thickness mm	Pitch: ***			Thickness of Detector mm		Increment mm
		SDCT	MDCT		4	8	16	4-8	16	
10-19	80-100	70	60	1.25	1.52	1.35	1.375	1.25	.625/1.25	5-1x slice
20-39	80-100	80	70	1.25	1.52	1.35	1.375	1.25	.625/1.25	5-1x slice
40-59	100	90	80	1.25	1.52	1.35	1.375	1.25	.625/1.25	5-1x slice
60-79	100	120	100	1.25	1.52	1.35	1.375	1.25	.625/1.25	5-1x slice
80-99	120	140	120	1.25/2.5	1.52	1.35	1.375	1.25/2.5	1.25	5-1x slice
100-150	120	160-180	140-160	1.25/2.5	1.52	1.35	1.375	1.25/2.5	1.25	5-1x slice
>150	120	≥ 200	≥ 170	1.25/2.5	1.52	1.35	1.375	1.25/2.5	1.25	5-1x slice

- * Parameters are based on GE single and multi-detector scanners
- ** Use 0.5 sec gantry time when an option; mA are for 4-, and 8-slice MDCT; 16-slice weight-based color-coded mA are loaded on scanner. 16-slice also has automatic exposure control--max mA based on color-coded mA.
Low dose, standard dose and high detail options (based on image noise) are also available for 16-slice scanner
- *** Suggested pitch for SDCT 1.5
- CT Angiography: see table 2
 - Advantages: CTA vs echo and MR
 - global assessment of more distal pulmonary arteries, and the ascending and descending aorta
 - information on airway and lung
 - CT examinations are cheaper, often easier to schedule, sedation less frequent, completed quicker
 - Bolus tracking is helpful for onset of scanning

Table 2: Pediatric CT Angiography

Weight (lb)	kVp	mAs**		Slice Thickness mm	Pitch: ***			Thickness of Detector mm			Increment mm
		SDCT	MDCT		4	8	16	4	8	16	
10-19	100-120	40	30	2.5-5	0.75	0.875	0.975	2.5	1.25	1.25	5
20-39	100-120	80	30-40	5	0.75	0.875	0.975	2.5	1.25	1.25	5
40-59	120	60	40	5	0.75	0.875	0.975	2.5	1.25	1.25	5
60-79	120	70	50	5-7.5	0.75	1.5	1.35	1.375	2.5	1.25	5
80-99	120	80	60	5-7.5	1.5	1.35	1.375	3.75	2.5	1.25	5-7.5
100-150	120	100-120	70-90	5-7.5	1.5	1.35	1.375	3.75	2.5	1.25	5-7.5
>150	120	120-140	≥110	5-7.5	1.5	1.35	1.375	3.75	2.5	1.25	5-7.5

* mAs slightly higher than body CT protocols

** use 0.5 second rotation time when an option

Consider using bolus tracking vs empiric delay of 10-15 seconds after start of injection

Applications for Pediatric Chest MDCT

- Similar applications for chest MDCT in children and adults:
 - Evaluation of infection, and cancer.
- Different applications in children
 - Less evaluation of chronic lung disease (eg fibrosis), trauma, pulmonary embolism, and evolving use in lung cancer and CAD screening
 - Evaluation of congenital abnormalities of the lung, mediastinum and heart are more typical in children.
- Applications can be divided into lung, airway, mediastinum, cardiovascular system, and chest wall.
 - *Lung parenchyma*:
 - Applications of MDCT are identical to those of SDCT.
 - overlapping reconstructions can be obtained for assessment of small or subtle abnormalities such as a pulmonary nodule.
 - Multiplanar and 3D depictions: can be helpful for clinical services
 - MDCT provides opportunity for evaluation of bronchopulmonary foregut malformations, especially sequestration
 - *Airway*: both functional and anatomic.
 - Anatomic evaluation is established:
 - congenital abnormalities
 - endobronchial or extrinsic processes
 - postoperative stenosis or dehiscence
 - trauma.
 - If only airway evaluation, consider thin slices (e.g. sub mm thickness), 80-110 kVp, and 20-40 mAs., limiting scan to airway and not the whole chest and upper abdomen.
 - Functional evaluation:
 - dynamic assessment of airway narrowing
 - CT data can be segmented and to display dynamic changes in airway caliber related to respiratory cycle displayed, or adjacent structures such as masses or cardiac abnormalities.

- *Mediastinum*:
 - MDCT offers improved contrast enhancement of adjacent structures, and multiplanar and 3D depiction of abnormalities
- *Cardiovascular System*:
 - Improved assessment with MDCT due to CT angiography.
 - Evaluation of aorta (including vascular rings, post operative changes), and pulmonary arteries, as well as problem solving tool for complex cardiac assessment not sufficiently addressed by echo
- *Chest wall*:
 - Assessment of structures that may be arise from or secondarily involve the chest wall

Recent Developments for Pediatric MDCT

- Pediatric protocols
- Automatic exposure controls
- Innovative filters
- More applicable phantom information (CTDI_w and DLP).

REFERENCES

Frush DP, Donnelly LF. Helical CT in children: technical considerations and body applications. *Radiology*. 1998; 209:37-48.

Hollingsworth CL, Frush DP, Cross M, Lucaya J. Helical CT of the body: survey of pediatric techniques. *AJR*. 2002; In press.

Donnelly LF, Emery KH, Brody AS, et al. Minimizing radiation dose for pediatric body applications of single-detector helical CT. *AJR* 2001; 176:303-306.

Frush DP. Pediatric CT: practical approach to diminish radiation dose. *Pediatr Radiol*. 2002; 32 (10):714-717.

Donnelly LF, Frush DP. Pediatric Multidetector CT. *Radiographic Clin N Amer*. In press 2003.

Lucaya J, Piqueras J, Garcia-Peña P, et al. Low-dose high-resolution CT of the chest in children and young adults: dose, cooperation, artifact incidence, and image quality. *AJR* 2000; 175:985-992.

Frush DP, Donnelly LF, Chotas HG. Contemporary pediatric thoracic imaging. *AJR* 2000; 175(3):841-51.

Cohen RA, Frush DP, Donnelly LF. Data acquisition for pediatric CT angiography: problems and solutions. *Pediatr Radiol*. 2000; 30:813-822.

Frush DP, Donnelly LF. Pulmonary sequestration spectrum: a new spin with helical CT. *AJR* 1997; 169(3):679-682.

Denecke T, Frush DP, Li J. Eight-channel multidetector CT: unique potential for pediatric chest CT. *J Thorac Imaging*. 2002;17(4):306-309.

The Spectrum of Pulmonary Infection in the Immunocompromised Child

Richard I. Markowitz, M.D.

The Children's Hospital of Philadelphia & University of Pennsylvania School of Medicine

Although respiratory infection is one of the most common childhood illnesses, it can be a signal of an underlying abnormality of the immune system. A high frequency of infection, an infection of unusual severity, or an infection by an organism usually not pathogenic in a healthy individual should arouse suspicion of an immunodeficiency.¹

However, the radiologic and pathologic patterns of disease in immunodeficient children are not different from the patterns of infection found in normal individuals.² These pathologic patterns differ according to the distribution and extent of pulmonary infection and include bronchopneumonia, interstitial pneumonia, lobar pneumonia, lung abscess, empyema, bronchiectasis, and overwhelming pneumonia. Examples of these patterns will be shown demonstrating the wide and variable spectrum of pulmonary infection in the immunocompromised child.

The most common immune defects in children are not due to rare genetic mutations, but are secondary to common systemic problems such as severe malnutrition,³ debilitating chronic illness, or immaturity of the immune system. Iatrogenic immunodeficiency is a common side effect of steroids, chemotherapy, and radiation predisposing these children to serious infection. Infants are especially vulnerable to infection because of the immaturity of their immune system, although they do obtain passive immunity from their mothers.

Host Defenses

Much has been learned concerning the factors and mechanisms that comprise the immune system. Cellular, humoral, and mechanical factors work in concert to prevent microorganisms from literally "eating us alive." T-lymphocytes, B-lymphocytes, natural killer cells, granulocytes, complement, and antibodies as well as a wide variety of receptors and polypeptide mediators known as cytokines interact in complex ways. The first barrier to infection is the skin and mucous membranes which afford mechanical protection. When these mechanical defenses are impaired as in cystic fibrosis or immotile cilia syndrome, chronic infection can lead to irreversible tissue destruction, i.e. bronchiectasis.

Primary Immunodeficiency Disorders

Primary immunodeficiency disorders are inherited diseases which affect one or more specific parts of the immune system. Although they have been classified by which cell type is predominantly affected, there is a large overlap in the ways these disorders cause disease.⁴ First, we will consider T-cell (cellular) immune deficiency, then B-cell (humoral) immune deficiency, and then combined T and B cell deficiency syndromes. Finally, we will discuss some disorders of phagocytic function and complement deficiencies. Although all of these disorders result in increased susceptibility to pathogens, humoral defects, such as Bruton's agammaglobulinemia, predispose patients to bacterial infections, while cellular or T-cell defects make the individual more prone to viral, fungal, and parasitic diseases.

Disorders of cellular immunity

The prototype genetic defect of T-cell immunity is DiGeorge syndrome or congenital thymic hypoplasia. This disease derives from a deletion at the chromosome 22q11 site which inhibits normal development of structures derived from the third and fourth pharyngeal pouches. Partial or complete absence of thymic lymphoid tissue results in varying degrees of T-cell deficiency; absence of the parathyroid glands causes hypocalcemia which can lead to tetany; and cardiac and aortic arch anomalies are frequent.⁵ These patients present in early infancy, and their course is often complicated by severe viral and fungal infections. Radiologic recognition of the absent thymus is a valuable clue in the first day or two of life, but becomes more difficult thereafter because severe stress in infants with other illnesses can cause rapid thymic involution.

Disorders of humoral immunity

X-linked agammaglobulinemia (Bruton) is a prime example of a defect in humoral immunity caused by a failure of development of B-cell precursors into mature B-cells. This genetic defect of B-cell maturation results from a mutation on the long arm of the X chromosome responsible for the production of a specific tyrosine kinase (Bruton tyrosine kinase or btk) which is necessary for pro B-cells and pre-B-cells to properly develop into mature B-cells capable of producing biologically active gamma-globulin.⁶ Because of the location on the X chromosome, this X-linked recessive disease presents only in the sons of maternal carriers. Clinical manifestations include absent germinal centers of lymph nodes; underdeveloped tonsils, adenoids, and hilar lymph nodes; absent plasma cells; and severely diminished serum gamma-globulin. Recurrent bacterial infections of the respiratory tract due to *Streptococcus pneumoniae*, *Staphylococcus aureus*, and *Haemophilus influenzae* are common and may lead to bronchitis, pneumonia, bronchiectasis, and empyema. Radiologic signs of this disease include a paucity of the normal lymphoid structures surrounding the upper airway, i.e. absent tonsils and adenoids, as well as recognition of an increased frequency and severity of infections with common pyogenic organisms. Immunoglobulin replacement is standard treatment.

Selective or isolated IgA deficiency is common occurring in approximately 1 in 600 people.⁷ Both serum and secretory IgA are absent due to a failure of maturation of IgA-positive B-cells. It can be a familial defect or acquired following a viral infection. Most individuals are asymptomatic, but are prone to variable bacterial infections of the sinuses, respiratory tract, and gastrointestinal tract.

The term "common variable agammaglobulinemia" denotes a heterogeneous group of disorders characterized by defective B-cell function and frequent bacterial sinus and pulmonary infections. Bronchitis and bronchiectasis may lead to chronic respiratory failure.⁷ Non-caseating granulomas are often found as well. Gastrointestinal infections are also common.

Hyperimmunoglobulin E syndrome, sometimes referred to as Job's syndrome, is a rare inherited disorder which manifests

clinically as recurrent skin and pulmonary abscesses and extremely high levels of serum IgE.⁸ Severe staphylococcal infections are common, but these children are also susceptible to *Candida*, *H. influenza*, *Strep. pneumoniae*, as well as other organisms. Lung abscesses leading to large, chronic pneumatoceles are typical.⁹ Non-infectious features of this syndrome include delay in shedding of primary teeth, fractures, hyperextensible joints, and scoliosis. A single-locus autosomal dominant defect on chromosome 4 has been implicated as the cause, although there is probably variable expressivity of the disease.¹⁰ The immunologic deficiency is complicated and involves a T-cell imbalance which leads to excessive IgE production, but decreased IgG antibodies.

Combined humoral and cellular immune deficiencies

Severe combined immunodeficiency (SCID) is heterogeneous group of disorders caused by defects in stem cell maturation and resulting in serious infections beginning in infancy.⁷ Mortality is high, and most patients do not survive beyond early childhood. T-cell and B-cell functions are affected, and patients usually demonstrate generalized systemic and circulating lymphopenia. X-linked and autosomal recessive types of SCID have been discovered, but the X-linked recessive type is slightly more common, resulting in the higher incidence of SCID in males. 50% of the patients with the autosomal recessive type lack the enzyme adenosine deaminase (ADA) leading to a build-up of deoxyadenosine which is toxic to lymphocytes.⁶ These patients can be identified by measuring ADA activity in red blood cells. Infants with SCID usually fail to thrive and become infected with a variety of pathogens including fungi, viruses, and *Pneumocystis carinii* which can cause overwhelming pneumonia. Bone marrow transplantation offers variable success. Gene therapy trials are in progress.

Partial combined immunodeficiency disorders

Wiskott-Aldrich syndrome is an inherited x-linked recessive disease (chromosome Xp1 1.23 locus) of combined cellular and humoral immunity, thrombocytopenia, and a skin rash similar to eczema.¹¹ While the thymus is normal, there is T-cell depletion in the peripheral blood and lymphoid tissues. IgM levels are low, but IgA and IgE are elevated.⁷ Early mortality from pyogenic infection or bleeding secondary to the thrombocytopenia is high. Lymphoma has been reported in those who survive infancy. Bone marrow transplantation appears to be the only effective treatment to date.¹²

Ataxia-telangiectasia is an autosomal recessive disease (chromosome 1 1q22-23 locus) characterized by progressive cerebellar ataxia, ocular and cutaneous telangiectasia, and combined immunodeficiency including thymic hypoplasia and abnormal humoral immunity. ¹² Sinusitis, recurrent pneumonia, and bronchiectasis are common, but death usually results from the progressive neurologic defect or lymphoid malignancy.

Cartilage - hair hypoplasia is a rare form of short-limbed dwarfism associated with a partial combined immune defect. Severe varicella, vaccinia, and vaccine associated poliomyelitis have been reported as characteristic complications in this inherited bone dysplasia I immune deficiency syndrome.⁶

Disorders of phagocytosis

Chronic granulomatous disease of childhood is an inherited disorder in which bacteria may be ingested by neutrophils but are not killed because of the reduced capacity of intracellular oxidative enzymes (NADPH oxidase).⁶ X-linked and autosomal

recessive variants have been identified explaining an increased incidence in males. Recurrent infections due to catalase producing organisms such as *Staph. aureus*, *Staph. epidermidis*, and some gram-negative bacteria are common. Lymphadenitis, skin infection, osteomyelitis, liver abscess, and antral gastritis occur in addition to recurrent bacterial pneumonia and lung abscess. The nitroblue tetrazolium (NBT) test can measure the activity of neutrophil NADPH oxidase and thereby diagnose the disease. Multiple calcified granulomas in the liver, lung and other organs are radiologic clues.¹³

Chediak-Higashi syndrome is a rare, autosomal recessive, genetic disorder of neutrophil function manifest by recurrent bacterial infections.¹² While there is peripheral neutropenia, characteristic giant granules are found in those white cells which remain. A defect in the transfer of lysosomal enzymes is postulated leading not only to abnormal phagocytosis, but also to partial albinism, neurologic, and platelet disorders. An increased susceptibility to lymphoid malignancy also occurs.

Complement deficiency syndromes

A wide variety of rare inherited defects in the complement system have been described which can lead to rheumatologic syndromes as well as recurrent infection. The pattern of infection is similar to patients with gamma-globulin deficiency, i.e., increased susceptibility to bacterial disease.⁴

Acquired immune defects in children

The radiology of infection secondary to AIDS in children is similar their adult counterparts, but two thoracic manifestations are worthy of note: (1) lymphocytic interstitial pneumonitis (LIP) and (2) cystic enlargement of the thymus. LIP presents radiographically as a diffuse reticulonodular pattern throughout the lungs usually in relatively asymptomatic patients. In fact, these patients often have higher T-cell counts than those who develop more severe and overwhelming infection. Pathologically, lymphoid aggregates are found in the lung with very little evidence of acute inflammation. The presence of Epstein-Barr (EB) virus genome fragments in these lymphocytes has suggested the possibility that LIP represents an exaggerated response to EB virus infection. Intermittent steroid therapy usually causes both radiologic and clinical improvement but does not totally irradiate the abnormality.

Cystic enlargement of the thymus in pediatric and adolescent AIDS patients has been described but its cause is unknown. Mediastinal widening on chest radiography simulates lymphoma, while contrast enhanced CT reveals benign, cystic replacement of the gland.⁴ Long term follow-up remains to be determined.

Sickle cell disease is responsible for an acquired immunologic defect secondary to progressive splenic dysfunction in early childhood leading to an acquired deficiency of opsonin which is necessary for the ingestion of encapsulated bacteria. Infections with these organisms, especially the pneumococcus, can lead to sepsis, primary peritonitis, meningitis, and other serious life-threatening complications. So called "acute chest syndrome" often results in extensive lobar consolidations associated with fever and hypoxemia. Small pleural effusions are not uncommon. It may be impossible to differentiate in situ vascular thrombosis from consolidative pneumonia, therefore such patients are usually treated with antibiotics, transfusions, and oxygen. Repeat episodes are not uncommon and may lead to areas of scarring within the lungs.

Immune deficiency occurs frequently in pediatric patients with leukemia and lymphoma. Neutropenia before and especially after chemotherapy makes these patients especially vulnerable to infection. *Candida* and *Aspergillus* are among the most common pathogens, but common childhood viruses such as respiratory syncytial virus or varicella can be deadly as well. Chest CT is very sensitive in detecting early lesions of fungal and viral pneumonia and is often used to follow the progress and/or resolution following treatment.

Conclusions

Pulmonary infections are common in the pediatric age group and usually resolve uneventfully. An unusual pattern of infection or a high rate of infection should raise suspicion of an underlying defect in the complex, multi-factorial immune system. While inherited primary immune deficiency syndromes are relatively rare, immunologic compromise secondary to other disorders are very common. Specific immune defects generally predispose to different types of infection; i.e., absent or decreased gamma-globulin results in increased susceptibility to bacterial infection while diminished lymphocyte function can lead to viral, fungal and protozoal infection. Nevertheless, because of the complex interrelationships and redundancy of the immune system, there is a broad spectrum of pathologic distribution and patterns of clinical infection in these patients. Thus, while the genes may be specific, the clinical manifestations are not. As we learn more about immunology, genetics, and microbiology, our understanding of these disorders will grow, and hopefully, our ability to recognize, diagnose, and treat these seriously ill children will also improve.

REFERENCES :

- Infante AJ: Host defenses against infection, in Jenson HB, Baltimore RS (eds): *Pediatric infectious diseases: principles and practice*. Norwalk, CT, Appleton & Lange, 1995, pp3 1-58
- Schauer U: Respiratory problems in the immune-compromised host. *Pediatr Allergy Immunol* 7: 82-85, 1996
- Chandra RK: Nutrition and the immune system: an introduction. *Am J Clin Nutr* 66: 460S-463S, 1997
- Infante AJ: Primary immune deficiency disorders, in Jenson HB, Baltimore RS (eds): *Pediatric infectious diseases: principles and practice*. Norwalk, CT, Appleton & Lange, 1995, pp 1427-1436
- Kirkpatrick JA, Jr., DiGeorge AM: Congenital absence of the thymus. *AJR* 103: 32-37, 1968
- Cotran RS, Kumar V, Collins T: Diseases of immunity, in Cotran RS, Kumar V, Collins T (eds): *Robbins pathologic basis of disease*. Philadelphia, PA, W.B. Saunders, 1999, pp 231-236
- Waldman TA, Nelson DL: Inherited immunodeficiencies, in Frank MM, Austen KF, Claman HN, et al. (eds): *Samter's immunologic diseases*. Boston, MA, Little Brown and Company, 1995, pp 387-429
- Buckley RH, Wray BB, Belmaker EZ: Extreme hyperimmunoglobulinemia E and undue susceptibility to infection. *Pediatrics* 49: 59-70, 1972
- Fitch Si, Magill HL, Herrod HG, et al: Hyperimmunoglobulinemia E syndrome: pulmonary imaging considerations. *Pediatr Radiol* 16: 285-288, 1986
- Grimbacher B, Holland SM, Gallin II, et al: Hyper-IgE syndrome with recurrent infections - an autosomal dominant multisystem disorder. *N Eng J Med* 340: 692-702, 1999
- Shyur SD, Hill HR: Recent advances in the genetics of primary immunodeficiency syndromes. *J Pediatr* 129: 8-24, 1996
- Puck JM: Primary immunodeficiency diseases. *JAMA* 278: 1835-1841, 1997
- Kuhn JP, Slovis TL, Silverman FN, et al: Immune disorders and the lung, in Silverman FN, Kuhn JP (eds): *Caffey's pediatric x-ray diagnosis: an integrated imaging approach*. St. Louis, MO, Mosby, 1993, pp 561-577
- Leonidas JC, Berdon WE, Valderrama E, et al: Human immunodeficiency virus infection and multilocular thymic cysts. *Radiology* 198: 377-379, 1996
- Markowitz RI, Kramer SS: The spectrum of pulmonary infection in the immunodeficient child. *Seminars in Roentgenology* 35:171-180, 2000

Voice Recognition

Theresa C. McLoud, M.D.

Associate Radiologist-in-Chief, Director of Education; Thoracic Radiologist, Massachusetts General Hospital
Professor of Radiology, Harvard Medical School, Boston, Massachusetts

Voice recognition technology allows radiologists to achieve efficiency goals and become more competitive in the digital environment. It provides a link that can improve the speed of communication between radiologists and their referring physicians. Speech recognition systems were introduced into main stream large radiology departments in the United States in the mid 1990's. Most systems require limited amounts of learning and adaptation compared to other transcription systems and methods. Most software packages allow easy integration into existing radiology and hospital information systems. The major disadvantage of voice recognition comes from radiologists' resistance to change and fear of technology. In addition, voice recognition does require more radiologist time and secretarial skills. However, the benefits to the hospital, referring clinicians and patients, are impressive because radiology reports are immediately available on the radiology and hospital information systems.

Voice recognition software at the human interface level comprises four core technologies; 1) the recognition of spoken human speech, 2) the synthesis of the spoken speech into readable characters, 3) the identification of the speaker and author verification, and 3) the understanding of the recognized word. These technologies are often referred to as speech recognition or speech-to-text; speech synthesis or text-to-speech; speaker identification and verification; and natural language understanding.

Most voice recognition systems have certain hardware requirements. These include specific processor and speeds, usually a Pentium 200 MHz chip as well as an operating system usually a Windows NT platform. In addition to individual workstations, the system requires integration into a network. The network allows integration into the radiology information system and ultimately into PACS and the hospital information system. Most systems also require the use of high quality microphones and sound cards to achieve high accuracy rates.

Integration of a voice recognition system into a radiology department is not a trivial process. Most systems offer several

key features. These include an RIS interface, i.e. an interface with links to the radiology information system, the hospital information system, PACS and the billing system. The second component consists of standardized reports. These allow radiologists to create pre-defined reports for individual radiologists or the institution. The third components are templates/macros. Most systems allow the creation of not only standard reports but customizable templates and fields. The template capability gives the radiologist the flexibility to create a form with blank areas that vary with each dictation. Feature filled macros allow standard phrases or components of report to be easily inserted in the text. These functions allow greater efficiency. The fourth component is customizable fields. Most packages permit customized definitions by the institution and multiple fields associated with the report. These fields may include ICD-9, CPT, BI-RADS, ACR /NEMA codes or ACR pathology identifiers. The fifth component includes bar code interfaces. Most voice recognition software packages support the use of a bar code laser reader or integrated microphone laser reader into the system. The final component is a system for security.

The most important feature of speech recognition is report turnaround. In our own institution, the previously utilized dictation system required an average of over three days to complete. This included transcription, review by the radiologist and the resident. The introduction of voice recognition eliminates the transcription and correction steps and a report by a staff radiologist becomes immediately finalized after being dictated and edited. The turnaround time in our own department has now dropped to 0.4 days.

REFERENCES:

- Mehta A. Voice Recognition. In: PACS. A Guide to the Digital Revolution.
Eds: Dreyer KJ, Mehta A, Thrall JH. Springer-Verlag New York, Inc., 2002.
Chapter 11, pages 281-302.

The Internet and the Practice of Radiology: A New Educational Paradigm

Jud W Gurney, M.D., FACR

Objectives

Consider the Internet as an educational resource

Learn what online tools are currently available for education and practice

The education of a radiologist begins during residency and lasts during the professional's lifetime. How much information does a radiologist need to acquire to practice radiology? No one knows but there are estimates that it requires more than 2 million pieces of information to practice medicine.

Traditional sources of information include books, journals, and lectures. These traditional sources of information have been the mainstay of education since the development of the field of radiology. However, Internet technologies have the potential to markedly change how radiologists educate themselves.

The traditional sources of information have deficiencies. Books are expensive and the publishing cycle limits the timeliness of the information. Journals are unstructured making the information accessible only through secondary indices. Finally, lectures are extremely costly with travel and lodging. At the point of care, where questions arise, none of these sources may be either readily available or quickly accessed. In the current health care environment, radiologists have less time to search for information. Thus questions that arise when interpreting films often go unanswered.

Nearly all physicians have used the Internet as a source of information. In a 2001 survey, 90% have researched clinical problems, 80% read journal articles, 60% communicated with colleagues, 45% completed CME and 35% attended online conferences. With this background, let's examine what is currently available online and what the future possibilities are.

The Internet is a new publishing medium, similar but different than print publishing. Print publishing has had 500 years to craft the current style of books and journals. Thus the current Internet offerings are in an early stage of evolution as content providers find out what works and what doesn't (for example, it took 200 years before publishers added page numbers to books). Online reference tools can be roughly divided into 3 categories: search tools, online libraries, and expert knowledge systems.

Search Tools

Search tools such as MEDLINE and Google[®] are one of the first tools physician's turn to for information. The National Library of Medicine's MEDLINE is a database of more than 14 million citations dating from the 1960's. MEDLINE is simple to search but thorough access requires using the MeSH vocabulary by which all articles are indexed. MEDLINE rarely answers the clinical question, as the only accessible information beyond the citations are abstracts. Thus MEDLINE serves as an intermediary step to journal articles, which may or may not contain the information needed to answer the question.

Generalized search tools like Google are also used to access information. Search engines attempt to index all published web pages on the Internet. Currently there are over 40 billion web pages with a half-life of 44 days so that indexing is not a trivial task. In addition, much information exists in databases that are

not accessible to the search engines. Information in the web is unstructured and the results returned from a search query vary considerably. The quality of the information provided by individual web sites may also be of dubious quality. In contrast to book publishing, the barrier to web publishing is minimal, allowing anyone with a computer to become a publisher. Some may downplay the web as a source of information because of the lack of peer review and the content providers lack of credentials. However, surveys of physicians consistently show that availability is more important than credibility.

Online Libraries

The second category of online reference tool is the online library. The online library attempts to recreate textbooks, articles, and lectures online. Content is expensive to produce and most sites have little content. Because it is easier for societies to videotape lectures than write textbooks, lectures are more common online than textbooks. For example, RSNA has captured more than 250 lectures from their annual meeting online.

To be useful, online libraries need to be comprehensive, well organized and easy to search. Besides lacking content, the information architecture of existing sites is poor as is the technical quality of the lectures (small images of poor quality). When the dot com bubble burst, the activity of commercial sites which were one of the primary driving forces for online libraries fizzled. Sites such as AuntMinne and eMedicine have very little content. For example, eMedicine currently has only 32 topics in thoracic imaging.

Journals have effectively placed their print publications online, however, the current subscription business model severely hampers what will eventually become a powerful method of dissemination and organizing information. To be more useful, journals will have to abandon subscriptions. Then reference citations will be hypertext links to the reference article allowing professionals to rapidly find information of interest. Allowing physicians to evaluate the author's primary sources of information will also enhance scholarship.

Online content will eventually displace reference texts. The economics and ease of use favor the online text. For example, one text that would make an excellent online textbook is Keats and Anderson's Atlas of Normal Roentgen Variants that may Simulate Disease. Containing 5650 illustrations (and costing \$250) the book is primarily visual and is used exclusively at the point of care where questions of normal and abnormal arise. Having this resource online available at the workstation and next to the teleradiology monitor would be a "killer" application for radiologists.

Expert Systems

The last category of online reference tool is the expert knowledge system. One of the unique aspects of the Internet is that the user can interact with the information. Print publishing is passive; there is no interaction with the printed page. For example, the printed page can only publish formulas; the web page can solve formulas. The most exciting and most difficult

challenge is to develop services for radiologists that act as a curbside consult, allowing the radiologist to make better decisions. This is an area that is relatively unexplored. As a modest example, consider the evaluation of an incidental adrenal mass. The value of calculating the washout of intravenous contrast has been shown to be useful in separating benign masses from metastases. However, it's my observation that the calculation (which is simple algebra) is rarely performed. Programming the equation into the web page allows one to quickly calculate the washout values and by providing results in the context of published values allows the user to judge the strength of the evidence.

The personal curbside consult is commonly used in daily practice as a source of information. Unfortunately, with a shortage of radiologists and the dispersion of colleagues to separate sites makes this contact less common. Online contact with instant messaging will not only bring colleagues back together but also expand contact outside of our normal groups putting at our fingertips colleagues with expertise that are currently unavailable.

Predictions

Online education will continue to evolve. These are my predictions as to what we will see over the next decade.

Textbooks will be written specifically for online use. The role of print publications will not vanish but will be of much less importance than today.

Journals will eventually be taken back by the scientific societies and will be freely accessible online. Print journals will disappear. The interconnections between journals and articles will be a major source of information.

One of the major thrusts of current CME is to provide CME at the point of care where questions arise. Only Internet technologies are poised to provide and document that activity. Traveling to lectures in remote locations will become less common. Societies, like the STR will incorporate their meetings into the major meetings of the RSNA or ARRS where personal time with colleagues can be maximized.

Peer-to-peer technologies (like instant messaging) will produce a new type of practice where radiologists only exist online to serve as consultants to their colleagues all over the world.

URL's discussed:

PubMed:

<http://www.ncbi.nih.gov/entrez/query.fcgi>

Google:

<http://www.google.com>

Over 480 million searches are performed daily, Google accounts for 4 of every 5 searches.

AuntMinnie:

<http://www.auntminnie.com>
registration required

eMedicine:

<http://www.emedicine.com>
paid subscription required

[chestx-ray.com](http://www.chestx-ray.com)

<http://www.chestx-ray.com>

Workshop A1: Lymphoma: Spectrum of Disease

Kitt Shaffer, M.D., Ph.D.

Assistant Chief of Radiology, Dana-Farber Cancer Institute

Introduction and Objectives

Lymphoma is actually a very heterogeneous collection of disorders that can have a wide variety of clinical appearance and imaging features. In general, lymphomas are classified into either Hodgkin's disease (HD) or non-Hodgkin's lymphoma (NHL). In both HD and NHL, the chest is a very frequent site of involvement but the pattern of disease differs slightly between the two disorders. In terms of incidence, HD and NHL together make up about 5 percent of all newly diagnosed cancers and about 5 percent of all cancer deaths. The incidence of HD is similar to that of primary sarcomas while the incidence of NHL is similar to that of pancreatic cancer. Both are much less common than lung cancer. This workshop will review some general principles of imaging of HD and NHL and will introduce the complex topic of NHL classification, which is constantly evolving as our understanding of the mechanisms of disease expand. A brief review of some of the expected imaging findings after treatment of lymphoma will also be presented. After completing this workshop, participants should be more familiar with typical and atypical imaging features of HD, should be more aware of the various subtypes of NHL and some of the newer categories based on immunophenotyping and genetic analysis, and should be able to recognize common treatment effects and complications of treatment of both HD and NHL.

Hodgkin's disease

The typical appearance of thoracic disease in HD is an anterior mediastinal mass without calcification or necrosis. Unlike NHL, HD tends to spread contiguously, involving adjacent nodal groups in an orderly manner. Lung involvement at diagnosis is not uncommon in HD, but is always present in lung adjacent to a hilar mass, indicating contiguous spread. Lung involvement may be difficult to distinguish from atelectasis on imaging studies. The commonest nodal groups involved by NHL are first the anterior mediastinum followed by the right paratracheal nodes and hilar nodes. Atypical appearances are also possible in HD, and may include SVC syndrome, necrosis, and calcification pre-treatment. Calcification in masses after treatment are common.

Non-Hodgkins lymphoma

The imaging appearance of NHL is much more varied than HD. Nodal involvement may often be discontinuous and overall lung involvement is more common. Prognosis for NHL is also worse than HD although there is a wide range from indolent forms to more aggressive forms. In general, the indolent subtypes are harder to cure but survival times are longer. The more aggressive forms may kill the patient quickly but actually have the best chance of long-term cure as most treatment modalities (radiation and chemotherapy) depend on rapidly dividing cells, which are seen in the more aggressive cell types.

Classification of NHL is a particularly complex topic and is in constant flux. Many different systems have been used in the past, most depending on histologic appearance of cells. More current methods, such as the REAL classification system which will be used in this presentation, attempt to integrate histology with immunophenotype to approach a more pathophysiological-based approach to classification. Some subtypes of NHL

(diffuse large cell, follicular, MALT) were well known from prior systems but other subtypes (mantle cell, anaplastic large cell, mediastinal large cell) are relatively new. Most of these newer subtypes depend for diagnosis on either immunophenotyping or genetic analysis, which were not included in older classification systems.

Categories of NHL

Certain subtypes of NHL are so characteristic in histologic appearance that they were well described and consistently diagnosed even before the introduction of complex classifications involving immunohistochemistry and cytogenetics. Among these subtypes are diffuse large cell NHL, follicular NHL and mucosal-associated lymphomas. Other subtypes are of more recent origin, depending on more elaborate evaluations including immunohistochemistry or analysis for genetic markers and specific translocations. This includes anaplastic large cell NHL, mediastinal large cell NHL, T-cell rich B-cell NHL and mantle NHL.

Diffuse large cell NHL is one of the more common subtypes of NHL, and in the past probably included a very heterogeneous group of disorders, some of which are now better discriminated and reclassified into other categories, such as anaplastic large cell or mantle cell NHL. Diffuse large cell NHL often involves the chest and may include both nodal and extranodal disease. It is typical of aggressive or high-grade NHL, which can have a precipitous course, but is therefore often more responsive to treatment and more amenable to cure. Most are of B-cell origin, with about 20% demonstrating T-cell phenotype.

Follicular NHL is the prototype of indolent, low-grade lymphoma. It is very difficult to cure, but patients may survive with their disease for many years. Follicular NHL generally is restricted to nodal disease and often has discontinuous involvement of many nodal groups. Nodes may be small or bulky. If a particular node or group of nodes suddenly enlarges, the possibility of transformation to a higher grade tumor must be considered.

Lymphomas of the mucosal-associated lymphoid tissues (MALT) have been well-known for some time and are generally of the indolent variety. Most are of B-cell origin and most often involve the lungs, stomach, salivary glands and lacrimal glands. Almost any organ has been reported to give rise to MALT-like lymphomas, including the bladder, the kidney, the uterus, breast, and the thymus. Marginal zone lymphomas are neoplasms of similar cell type occurring in nodes, involving the marginal regions which surround germinal centers.

Anaplastic large cell NHL is a relatively recently described category of NHL in which the neoplastic cells express the Ki-1 antigen, CD30. This same antigen is found on Reed-Sternberg cells of HD as well as in activated T and B-cells. A characteristic translocation is also usually present except in the cutaneous form. Skin, lung and nodal involvement are common and the course is often aggressive.

Mediastinal large cell NHL is a subtype of large cell NHL that occurs specifically in the mediastinum and has a more aggressive course. Tumor masses often contain considerable sclerosis and the appearance can easily be mistaken for HD on imaging, although signs of aggressive behavior, such as necrosis, superior vena cava compression, and chest wall invasion, are more commonly seen than in HD.

T-cell rich B-cell NHL is a variety in which rare neoplastic B-cells are present in a background of much larger numbers of reactive, non-neoplastic T-cells. In the past, it was probably classified as either a variant form of HD, or as T-cell variety of NHL. With modern methods for detection of immunoglobulin gene rearrangements, the rare neoplastic clone of B-cells can now be more accurately identified.

Mantle cell NHL is an uncommon form of NHL with a relatively aggressive course. It demonstrates a typical and relatively specific translocation and may be nodular or diffuse in histologic growth pattern. It may involve the GI tract in the form of multiple lymphomatous polyposis, with a tendency to disseminate widely. This is in contrast to MALT lymphomas of the GI tract, which are typically indolent and often limited in extent.

Intravascular lymphomatosis is an extremely rare disorder in which neoplastic cells are found only within vascular structures. Most often patients present with central nervous system findings, but occasionally the diagnosis is made in other organs, such as the kidneys or the lungs. When lung involvement is present, patients may present with dyspnea or cough and imaging may show air-trapping or mosaic perfusion.

Treatment effects

In general, lymphomas are rarely treated surgically except in order to obtain tissue for initial diagnosis. Most treatment regimens use either chemotherapy, radiation therapy or a combination of the two. Therefore, it is important to recognize some of the expected imaging findings of toxicity associated with both of these treatments. Another important consideration is the incidence of second primary tumors, particularly after radiation therapy. Since HD is often seen in young patients, the long latency period of radiation-induced neoplasia must be kept in mind. Because chemotherapy is often administered using indwelling catheters, complications of long-term venous access must also be considered.

Typical findings of radiation are most often seen in the lungs on CT imaging. This can range from very subtle signs of volume loss in the irradiated region to extensive fibrosis and distortion of lung architecture. The typical imaging features of radiation fibrosis include bands of linear density, traction bronchiectasis, retraction and volume loss. Such marked findings are more common with higher doses of radiation and are also increased in patients receiving concomitant radiation and chemotherapy. Local lung function, as measured with ventilation and perfusion scanning, drops initially after radiation but then partially recovers at from 3-18 months.

Almost any chemotherapeutic drug can cause a toxic response, most often in the lungs. Such agents as bleomycin are well-known for this effect. The agents typically used to treat lymphoma have a much lower incidence of pulmonary toxicity than bleomycin, but occasionally can produce similar effects. The typical imaging features are patchy or ground-glass opacities, sometime evolving to reticular and fibrotic appearance, located in the lung periphery often with a basilar predominance. The most characteristic location on chest film is in the lateral costophrenic regions. In a patient with new interstitial abnormality after chemotherapy, a differential diagnostic consideration must also include edema from cardiac toxicity. Again, cardiac toxicity is most well-known in response to adriamycin but can occur with other agents.

Followup regimens

Most oncologists use a standard regimen of imaging in following patients treated for HD and NHL, but evidence-based investigations of these regimens are limited. Overall, imaging is

probably overused, since a combination of frequent clinic visits, thorough physical examinations and lab exams will probably detect most recurrent disease. Imaging could then be reserved for solving specific problems. In an investigational setting, obviously more thorough imaging is usually needed. In the future, positron emission imaging may simplify followup protocols and may replace routine followup CT scans in some cases.

Conclusions

Lymphoma is really a group of related diseases that can have a wide variety of appearances on imaging and can range from indolent, slow-growing disease to highly aggressive, rapidly fatal disease. Classification of lymphoma has undergone considerable change in recent years due to our evolving understanding of the genetic and cellular mechanisms of the various subtypes. It is important for radiologists to have an understanding of current classifications and how they may relate to the expected appearance of disease on imaging. It is also important for radiologists to have an appreciation of the expected findings related to the various treatments of lymphoma.

REFERENCES:

1. Skarin, Shaffer and Wiczork, editors, Atlas of Diagnostic Oncology, 3rd edition, Mosby (London), 2003.
2. L Kostakoglu and Sj Goldsmith, Positron emission tomography in lymphoma: comparison with computed tomography and Gallium-67 single photon emission tomography, *Clinical Lymphoma* 1:67-74, 2000.
3. A Elis, D Blickstein, O Klein, et al, Detection of relapse in non-Hodgkin's lymphoma: role of routine followup studies. *Am J Hematology* 69:41-44, 2002.
4. LJ King, SP Padley, AC Wotherspoon, AG Nicholson. Pulmonary MALT lymphoma: imaging findings in 24 cases. *European Radiol* 10:1932-1938, 2000.
5. JC Theuws, Y Seppenwoolde, SL Kwa, et al. Changes in local pulmonary injury up to 48 months after irradiation for lymphoma and breast cancer. *Int J Rad Onc, Biol, Physics* 15:1201-1208, 2000.
6. GC Ooi, CS Chim, AK Lie, KW Tsang, Computed tomography features of primary pulmonary non-Hodgkin's lymphoma. *Clin Radiol* 54:438-443, 1999.
7. O Honda, T Johkoh, K Ichikado, et al. Differential diagnosis of lymphocytic interstitial pneumonia and malignant lymphoma on high-resolution CT. *AJR* 173:71-74, 1999.
8. JG Wall, YG Hong, JE Cox, et al. Pulmonary intravascular lymphomatosis: presentation with dyspnea and air trapping. *Chest* 115:1207-1210, 1999.
9. P Porcu, CR Nichols. Evaluation and management of the "new" lymphoma entities: mantle cell lymphoma, lymphoma of mucosa-associated lymphoid tissue, anaplastic large cell lymphoma and primary mediastinal B-cell lymphoma. *Curr Prob Cancer* 22:283-368, 1998.
10. American Cancer Society. Cancer Facts and Figures 2001, ACR(Atlanta), 2001.
11. R Bar-Shalom, M Mor, N Yefrmov, SJ Goldsmith. The value of Ga-67 scintigraphy and F-18 fluorodeoxyglucose positron emission tomography in staging and monitoring the response of lymphoma to treatment. *Sem Nuc Med* 31:177-190, 2001.
12. L Bordeleau, NL Berinstein. Molecular diagnostics in follicular non-Hodgkin's lymphoma: a review. *Sem Oncol* 27:42-52, 2000.
13. M Hummel, H Stein, Clinical relevance of immunoglobulin mutation analysis. *Curr Opinion Oncol* 12:395-401, 2000.
14. RC Hankin, SV Hunter. Mantle cell lymphoma. *Arch Pathol Lab Med* 123:1182-1188, 1999.
15. E Morra. The biological markers of non-Hodgkin's lymphomas: their role in diagnosis, prognostic assessment and therapeutic strategy. *Int J Biol Markers* 14:149-153, 1999.

Digital Images: Camera to Powerpoint

Eric J. Stern, M.D.

University of Washington School of Medicine, Department of Radiology
Harborview Medical Center, Seattle, Washington

The use of digital images has become more commonplace, especially with the ability to obtain images directly from a picture archival and communication system (PACS) or low cost digital cameras. For many academic radiologists, using these digital images for slides is a relatively new and potentially intimidating process. It is important to be able to use digital images effectively and efficiently, creating a visually optimized image while keeping the file size appropriate to its application. For such optimal use, not all digital images are created equally. I will focus on how to optimize your use of digital images for electronic presentation.

Definitions

Pixel dimensions

A digital image is composed of a two dimensional array of pixels (picture elements), similar to dots on a newspaper photograph or grains on a photographic print, arranged according to a predefined ratio of columns and rows. Each pixel represents a portion of the image in a particular color, or shade of gray. The pixel dimensions of an image (e.g. 600 x 800, 1024 x 768, 1200 x 1600, etc) define the information content of the image. The more pixels there are in an image, the more information is contained within it.

Image "size"

Image size is a slippery and often misused term. When one speaks of a "large" image, one could be referring to an image with a large pixel dimension (e.g., 2000 x 3000), one with a large file size (requires a lot of storage space on a hard disk), or a large physical size (e.g., 3 x 4 feet). Because of this large potential for confusion, I greatly prefer the terms "pixel dimensions," "file size," or "physical size" over the easily misused term "image size." The image file is determined by pixel dimensions, bit depth and the level of file compression. To determine the file size of an uncompressed digital image, use this formula:

$$\text{File size} = (\text{pixel width} \times \text{pixel height}) \times (\text{bit depth} \div 8)$$

The result will be the file size in bytes. Divide this by 1024 to determine the size in kilobytes (Kb) (and by 1024 again if you want the size in megabytes). For example, a 24-bit RGB image that is 459 pixels wide and 612 pixels tall would have a file size of 823Kb:

$$(459 \times 612) \times (24 \div 8) = 842,724 \text{ bytes} \div 1024 = 823\text{Kb}$$

An 8 bit grey scale image that is 459 pixels wide and 612 pixels tall would have a file size of 274Kb:

$$(459 \times 612) \times (8 \div 8) = 280,908 \text{ bytes} \div 1024 = 274 \text{ K}$$

Output resolution

Output resolution is a measurement of clarity or detail of the displayed image, and is expressed as the number of pixels displayed per unit length. This ratio varies widely, depending on

which output device one is using. On a computer monitor, it is usually expressed in terms of dots per inch (dpi) or pixels per inch (ppi). The output resolutions of typical computer monitors range between 72 and 100 dpi.

For example, consider an image with pixel dimensions of 1200 x 1800 pixels which is to be output to both a computer screen with an output resolution of 100 dpi and a laser printer with an output resolution of 600 dpi. On the computer screen, the physical size of the image will be 12 X 18 inches. On the laser print, the physical size of the image will be 2 x 3 inches. Both images have the same pixel dimension, and hence the same information content.

For another example, imagine that you need a new computer monitor with a 20 inch wide screen. After shopping around, you narrow down your decision to two monitors, differing only in output resolution: one will display 1200 x 800 pixels and the other will display 1800 x 1200. The first monitor will have an image resolution of 1200/20 or 60 dpi, while the second monitor will have a resolution of 1800/20 or 90 dpi.

Software and hardware requirements

One can choose from a number of programs for optimizing digital images. However, I use and highly recommend newer versions of ADOBE PHOTOSHOP® (Adobe Systems Incorporated, San Jose CA) which is one of the most powerful and widely-available programs for general image manipulation. Many of the principles discussed will also apply to other software packages.

One can use either a Macintosh (Apple, Inc. Cupertino, CA), Windows (Microsoft Corp, Redmond, WA), or Unix-based computer to do image manipulation. The interfaces might differ slightly between platforms, but the concepts are the same.

Steps in image Processing

Once you have obtained a digital image, there are several steps you can go through to optimize the image for an electronic presentation.

Step 1: Convert to grayscale. Unless you are dealing with true color images, most of your radiologic images should be converted to grayscale, if they are not already. This immediately cuts the file size by two thirds without any loss of image quality. This is simply preformed by opening the image pop-down menu, selecting mode, then selecting grayscale.

Step 2: Crop your image as necessary, removing unwanted or distracting data such as patient identifiers, non-pertinent body parts, white borders, or artifacts. This will also help reduce file size. Patient identifiers can be covered up with a box filled with black or by cutting out the text when a black background has been selected.

Step 3: Adjust the levels to take advantage of the entire grey scale available. This is one of the most important steps. You can use the auto levels function from the image pop-down menu, but recommend fine tuning your image with the manual level adjustment.

Step 4: Rescale your image to the appropriate physical size for the output device you have chosen. Using the image pop-down menu, select image size. The new dialog box will allow you to adjust the pixel dimensions and print size as needed. For example, consider a 512 x 512 pixel CT image destined for both a website and for a journal article. Without rescaling the image, it would appear to be $512/75 = 6.83$ inches wide on a 75 dpi monitor screen but only $512/300 = 1.70$ inches wide when printed at 300 dpi in a journal. Rescaling works by throwing away pixels or adding new pixels to the image file.

Step 5: Save the image in an appropriate file format. Images can be saved in a variety of file types, including TIFF, JPEG, GIF or PNG. File compression can be used to reduce the file size for storage purposes or for transmission across the web. This is done using compression software that removes redundant information from the file.

GIF images (Graphic Interchange Format) and JPEG (Joint Photographic Experts Group) are generally used specifically for display on a computer monitors. JPEG is a lossy compression format, in that it deletes redundant information from an image. JPEG compression can range from small to large amounts of lossy compression, and is commonly used on the WWW and for computer presentations. Lossless compression of images typically reduces the file size by about 50 to 70 percent. Significantly greater storage savings can be achieved if one is willing to compromise some quality by using lossy compression. In practice, though, 1:7 JPEG compression can be used with little or no perceptible loss in image quality, even for a difficult to reproduce chest radiograph. The amount of JPEG compression is selected when performing a "save as" from the file pop-down menu, selecting JPEG format, then by selecting the relative amount of compression desired in the resulting dialog box.

Step 6: Unsharp masking: During many image manipulations, such as the initial digitization process itself and rescaling, tiny amounts of image detail are lost. Some of this image sharpness can be restored by means of various image sharpening filters. The filter used by most graphics professionals has the unlikely name of unsharp masking. The downside of image sharpening is that it adds a tiny bit of noise to the image. By choosing appropriate settings of the unsharp masking filter, one can usually significantly improve the image sharpness with only minimal increase in perceptible noise. Use a radius setting approximately equal to the output resolution / 200. This usually equates to a radius of 1-2. Use a threshold between 2-6 (usually 3).

If you choose to use unsharp masking, it should be the last thing you do before the final save. You should always apply unsharp masking to a copy of your image and never to the original image.

Automation

It can be time consuming to repetitively apply the same image manipulations over and over to numerous images. However, this need not be the case. Automation is one of the best features of the newer versions (5.0 or later) of Photoshop. It is easy to set up a macro, called an "action," to perform many repetitive different tasks with the touch of one key stroke. What used to take an entire lunch hour to perform now takes seconds to minutes. The ACTION palettes can be found in the window pop-down menu. There are many default actions, but it is easy to record and save your own personalized action.

Once the action is recorded, you can then choose the automate "batch" command from the file pull-down menu to perform the macro on an entire folder full of images in just seconds.

Finally

If you are going to use Adobe Photoshop to generate or adjust images, it may be helpful to receive some formal training in its use. Unfortunately, many of the books and courses for PhotoShop are geared to graphic artists, and devote a great deal of time to color, logo-making, and other topics irrelevant to more radiologists. However, at least one book contains considerable information relevant not only for a professional photographer but also for a radiologist [2]. Consider taking advantage of the many free resources available on the world wide web such as: <http://cpc.cadmus.com/da/>, www.photoshopcentral.com, www.adobe.com, desktoppublishing.com, www.user-groups.net, www.graphic-design.com, <http://www.bh.com/focalpress/evening6>.

REFERENCES:

Journal of Vascular and Interventional Radiology web site.

Available at: <http://www.jvir.org/misc/fora.shtml#sub>.

Accessed November 4, 2002.

Evening M. Adobe PhotoShop 6.0 for photographers – a professional image editor's guide to the creative use of PhotoShop for the Macintosh and PC. Oxford England, Focal Press, 2001

Analysis of Mediastinal Contours

James C. Reed, M.D., F.A.C.R.

University of Louisville
Louisville, KY

Objectives:

1. Review normal mediastinal contours to improve perception of mediastinal abnormalities.
2. Distinguish true mediastinal from paramediastinal abnormalities.
3. Review differential diagnosis of mediastinal widening and masses based on alterations of mediastinal contours, location and variations in opacity.

Perception of mediastinal abnormalities requires a thorough knowledge of the many variations in the normal mediastinal contours. There are numerous mediastinal abnormalities that may be readily detected and diagnosed by plain film analysis; however, many abnormalities are suspected from the radiograph and require multi-planar imaging with CT or MR for confirmation. Mediastinal contours are visualized as a result of the interface of the mediastinal pleura with the lung. Abnormalities are perceived when there are alterations in the normal mediastinal structures. Additional structures such as an aneurysm, masses, or cysts may displace the pleura while invasive processes such as invasive cancers, or lymphoma and some infections may cross the mediastinal pleura eradicating the normal lung-pleura interface.

Analysis of mediastinal contours may be facilitated by dividing the mediastinum into four quadrants and reviewing anatomy on plain radiographs, CT and MR. The right superior mediastinal contours are determined by the following: brachiocephalic veins, superior vena cava, azygous vein, paratracheal line, and the right main bronchus. The left superior mediastinal contours include the bronchocephalic vein, subclavian vein and artery, aortic arch, aorticopulmonary window, main pulmonary artery and left pulmonary artery. The heart is the largest contour in the inferior mediastinum, but the inferior vena cava and vertebrae are identifiable on the right while the vertebrae, descending aorta and paraspinal stripe should be visualized on the left.

Sagittal MR, the lateral plain film and axial images permit examination with emphasis on anterior to posterior anatomy. Anteriorly, we may identify abnormalities of the thymus, lymph nodes, fat, and right heart. The middle structures include the trachea, esophagus, superior vena cava, aorta, great vessels, and lymph nodes. Posteriorly, we observe the descending aorta and the spine.

Mediastinal lipomatosis is a common variant of normal seen in obese patients. It is also seen in patients with endocrine disturbances such as Cushing's disease or those on high dose steroid therapy. The opacity of fat is between that of the mediastinal soft tissues and the aerated lung. This is sometimes recognized on plain film, but usually requires CT for confirmation.

Since a number of mediastinal contours are the result of the interface of vascular structures with the lung, there are important differences in mediastinal contours based on the patient's age. This is especially true of the contours of the heart and great vessels, especially the aorta and superior vena cava. Enlarged vessels and vascular abnormalities must always be distinguished from mediastinal masses especially before consideration of biopsy.

Pulmonary consolidations should be distinguishable from mediastinal abnormalities by the presence of ill-defined or irregular borders and the presence of air-bronchograms or even lucent spaces. Lung masses are often irregular and sometimes heterogeneous, but may be smooth and when closely applied to the mediastinal pleura could be difficult to distinguish from a mediastinal mass. Lung masses which are firm and round may form a characteristic sulcus with the mediastinal pleura. This appearance is often distinctive from the expected tapered interface that is seen when a mediastinal mass displaces the pleura into the lung. Primary lung cancers may be even more difficult to evaluate because they are locally invasive and may extend directly into the mediastinum or they may metastasize to the mediastinal nodes. In contrast with invasive primary lung tumors, mediastinal lymphomas arise in the mediastinal nodes or thymus and may also be locally invasive and spread into the lung. Serial films may document the progression of the tumor and provide reliable signs for distinguishing lung tumors from lymphoma, but this often requires biopsy when patients present with advanced disease. Infrequently, other mediastinal tumors in particular malignant thymoma may be locally invasive and mimic the appearance of lymphoma or extensive metastatic disease.

Chest wall abnormalities may arise anteriorly from the sternum or from posterior ribs and may suggest a mediastinal abnormality on the plain film. They may be accurately identified by the presence of bone destruction or by multiplanar images that show extension of the abnormality into the chest wall. Pleural abnormalities that arise from the medial pleura may be more difficult to correctly localize and are often indistinguishable from primary mediastinal abnormalities by plain film and often require CT for correct diagnosis.

Masses are challenging to evaluate, but processes that spread diffusely through the mediastinum produce an even less distinctive radiographic appearance of diffuse mediastinal widening. Mediastinal widening may result from hematoma, vascular abnormalities, invasive masses, infection, fibrosis, accumulations of fat and abnormalities of the esophagus.

While the expected appearance of adenopathy may be that of circumscribed masses, very extensive adenopathy from both infectious and neoplastic causes may diffusely widen the mediastinum. Clinical correlation is essential, for example, patients with AIDS who develop mediastinal adenopathy often have very extensive adenopathy involving multiple node groups. This requires consideration of infections by mycobacteria, or fungi, and may also result from Kaposi's sarcoma or lymphoma. While reactive lymph node hyperplasia may cause progressive generalized adenopathy this is not a frequent cause of nodes that are detectable by plain film and rarely causes adenopathy with nodes greater than 1cm on CT.

Careful analysis of mediastinal contours is required to distinguish primary mediastinal from pleural, pulmonary and chest wall abnormalities. Most mediastinal abnormalities are detected with plain films, and in some cases the correct diagnosis may be suspected, but most require CT, MR or biopsy.

SUGGESTED READING:

Creasy JD, Chiles C, Routh WD, Dyer RB: Overview of traumatic injury of the thoracic aorta. *Radiographics* 1997; 17:27-45.
Gaerte SC, Meyer CA, Winer-Muram HT, et al: Fat-containing lesions of the chest. *Radiographics* 2002;22: S61-S78.
Jeung MY, Gasser B, Gangi A, et al: Imaging of cystic masses of the mediastinum. *Radiographics* 2002; 22: S79-S93.

Proto AV: Conventional chest radiographs: Anatomic understanding of newer observations. *Radiology* 1992; 183: 593-603.
Proto AV, Corcoran HL, Ball JB Jr; The left paratracheal reflection. *Radiology* 1989;171:625-628.
Rossi SE, McAdams HP, Rosado-de-Christenson, et al; From the Archives of the AFIP: Fibrosing Mediastinitis. *Radiographics* 2001; 21: 737-757.

Unusual Manifestations of Lung Cancer

Michelle S. Ginsberg, M.D.

Objective

The common cell types of lung cancer have certain typical radiographic appearances which will be briefly discussed. However it is important to be familiar with the more unusual presentations as well. The purpose of this review is to suggest the correct diagnosis of bronchogenic carcinoma when the radiographic manifestations of a particular tumor are rare, mimic benign disease, or suggest disease of organs other than the lung. The appearance of missed lung cancer, and means of improving detection of these lesion will also be discussed.

Adenocarcinoma

Adenocarcinoma is the most common cell type of bronchogenic carcinoma and accounts for approximately 50% of cases. CT usually demonstrates a solitary peripheral pulmonary nodule. The nodule may be smooth or spiculated. Hilar and mediastinal lymph node involvement and distant metastases are frequently present at the time of diagnosis. Peripheral tumors may directly invade the pleura and grow circumferentially around the lung and mimic diffuse malignant mesothelioma.¹ Central tumors may directly invade mediastinal structures or via the pulmonary veins invade the left atrium.

Bronchioloalveolar carcinoma

Bronchioloalveolar carcinoma is considered a subtype of adenocarcinoma and commonly presents as a solitary nodule.² There may also be surrounding ground glass opacity. Cavitation an infrequent finding in adenocarcinoma may be seen in bronchioloalveolar carcinoma.³ Although less common, consolidation and multiple small pulmonary nodules are other forms of presentations.³ High-resolution CT may demonstrate air attenuation and pseudocavitation within the nodules corresponding to small bronchi and cystic spaces.⁴ Unusual radiographic appearances include lobar atelectasis, expansile consolidation without air bronchograms, or elongated lobulated opacity resembling mucoid impaction.^{5,6}

Squamous cell carcinoma

Squamous cell carcinoma most often presents as a central endobronchial obstructing lesion with associated atelectasis or post obstructive pneumonia. Less commonly approximately a third of these tumors may present as a solitary peripheral nodule with or without cavitation.⁷ When the tumor cavitates, the inner wall is typically thick and irregular, and if secondarily infected may develop an air fluid level.

Undifferentiated large cell carcinoma

Undifferentiated large cell carcinoma usually presents as a large peripheral lesion, although a smaller proportion may also be centrally located. These tumors grow rapidly and metastasize early often presenting with hilar or mediastinal adnopathy. Giant-cell carcinoma is a subtype with multiple giant cells and a more aggressive behavior and poorer prognosis.

Multiple primary carcinomas

Synchronous lesions are defined as the presence of two tumors at the time of or closely following initial diagnosis. The incidence of synchronous multiple primary tumors is less than 3.5% of all lung cancer patients.⁹ This number may even be higher depending on the cell type and how carefully further primary tumors are sought as well as the rigidity of the criteria used to define the tumors as primary lesions. Difference in cell type is an accepted criteria, however tumors of the same histologic type must be physically quite separate as well as separated by noncancerous lung tissue.^{9,10}

Metachronous lesions are defined as the second cancer appearing after a time interval, usually 12 months or more. These lesions compromise at least two thirds of multiple pulmonary neoplasms, and on average are recognized 4 to 5 years after the first primary. 10%-32% of patients surviving resection for lung cancer may develop a second primary tumor.⁹ These lesions are regarded as multiple primary lesions only if they show unique histologic features. Squamous cell cancer is the most common histologic type of multiple carcinomas.

Metastases

The adrenal glands are one of the most common sites of metastases from lung cancer ranging from 5-10% of the time at presentation. In our experience we have also seen two cases of a mass within the adrenal gland that represented a collision tumor consistent of contiguous adrenal adenoma and metastasis.

Lung cancer may present with unusual sites of metastases. For example the gallbladder an unusual site of metastatic disease in general can be the site of a lung metastasis.

The kidneys, pancreas and small bowel may also be sites of metastases and may be radiographically indistinguishable from a primary tumor of that organ. Serosal and mesenteric implants may become quite large. Invasion with perforation of the adjacent bowl may result in a large mass with air within it having an appearance indistinguishable from an abscess.

Muscle and subcutaneous tissues are other infrequent sites of metastases from bronchogenic cancer.

Missed lung cancer

A missed lung cancer is unusual by virtue of the fact that it was not detected. In contrast, most usual ones are detected when in "easy" areas of lungs on a chest radiograph or CT. Potentially resectable NSCLC lesions missed at chest radiography were characterized by predominantly peripheral (85%) and upper lobe (72%) locations and by apical and posterior segmental/subsegmental locations in an upper lobe (60%). The missed cancers had a median diameter of 1.9 cm. Most of these missed lesions (98%) were obscured by anatomic structures on the chest radiograph, most often by bones (ribs and clavicle). Only the lateral radiograph revealed the cancer retrospectively in 5% of patients.¹¹

Although chest CT is more sensitive for the detection of lung nodules than chest radiographs, the potential for missing small lung cancers at CT exists. A recent study by Li et al. evaluated

missed lung cancers on low-dose CT in a general population which identified 83 lung cancers in 17,892 examinations. Thirty-two (39%) of these lung cancers were missed on 39 CT scans. The mean size of cancers missed owing to detection error was 9.8 mm, smaller than that of cancers missed due to interpretation error, 1.59 cm.¹²

Conclusion

An understanding of the usual and more unusual appearances of lung cancer and its metastatic sites is important in the accurate detection and staging of lung cancer. Information on characteristics of missed lung cancer may have the potential to reduce the number of lung cancers missed by radiologists.

REFERENCES:

Rosado-de-Christenson ML, Templeton PA, Moran CA.

Bronchogenic carcinoma: radiologic-pathologic correlation. *Radiographics* 1994; 14:429-446

Epstein DM. Bronchioalveolar carcinoma. *Semin Roentgenol* 1990; 25:105-111

Berkman YM. The many faces of bronchiolo-alveolar carcinoma. *Semin Roentgenol* 1977; 12:207-214

Adler b, Padley S, Miller RR, Muller NL. High-resolution CT of bronchoalveolar carcinoma. *AJR* 1992; 159:275-277

Wiesbrod GL, Towers MJ, Chamberlin DW, Herman SJ, Matzinger FRK. Thin-walled cystic lesions in bronchioalveolar carcinoma. *Radiology* 1992; 185:401-405

Huang D, Wiesbrod GL, Chamberlin DW. Unusual radiologic presentations of bronchioalveolar carcinoma. *J Can Assoc Radiology* 1986; 37:94-99

Haque AK. Pathology of carcinoma of lung: an update on current concepts. *J Thorac Imaging* 1991; 7:9-20

Hartman TE, Tazelaar HD, Swensen SJ, Muller NL. Cigarette Smoking: CT and pathologic findings of associated pulmonary diseases. *Radiographics* 1997; 17:377-390

Bower SL, Choplin RH, Muss HB. Multiple primary bronchogenic carcinomas of the lung. *AJR* 140:253-258

Armstrong P, Wilson AG, Dee P, Hansell DM: *Imaging of Diseases of the Chest*. 2nd Ed. Mosby-Year Book, Inc., St. Louis, 1995; 272-369

Shah PK, Austin JHM, White CS, Patel P, Haramati LB, Pearson GDN, Shiao MC, Berkman YM. Missed Non-Small Cell Lung Cancer: Radiographic Findings of Potentially Resectable Lesions Evident Only in Retrospect. *Radiology* 2003; 226:235-241

Li F, Sone S, Abe H, MacMahon H, Armato SG, and Doi K. Lung Cancers Missed at Low-Dose Helical CT Screening in a General Population: Comparison of Clinical, Histopathologic, and Imaging Findings. *Radiology* 2002; 225:673-683

Wednesday

March 5, 2003 General Session

7:00 – 8:00 am Continental Breakfast Americana Foyer

8:00 - 11:00 am Guest Hospitality Suite Moon Room

Scanlon Symposium Part I: Lung Cancer Screening & Detection

Moderator: Reginald Munden, DMD, MD Americana 3

7:50 - 8:10 Screening: Ethics & Principles
Caroline Chiles, MD

8:10 - 8:30 Lung Cancer Screening Trials: An Update
Thomas Hartman, MD

8:30 - 8:50 Lung Cancer Detection Failures (CXR & CT)
Phillip Boiselle, MD

8:50 - 9:10 Role of Computer Aided Diagnosis in Lung Cancer Screening
Jane Ko, MD

9:10 - 9:30 Small T1 Lung Cancer: Imaging & Prognostic Implications
Kyung Soo Lee, MD

9:30 - 9:50 Session Discussion

9:50 - 10:10 am Coffee Break Americana Foyer

Scanlon Symposium Part II: Lung Cancer Diagnosis

Moderator: Robert Pugatch, MD Americana 3

10:10 - 10:30 Reporting Tumor Measurements in Oncology
Todd Hazelton, MD

10:30 - 10:50 Assessing Growth of Indeterminate Nodules
Helen Winer-Muram, MD

10:50 - 11:10 Lung Cancer Staging
Ann Leung, MD

11:10 - 11:30 Role of Endoscopic US in Staging
James Ravenel, MD

11:50 - 12:00 Session Discussion

12:00 - 1:00 pm Lunch (on your own)

Wednesday

March 5, 2003

General Session

Wednesday

Workshops (choose 1)

1:00 - 1:45	D1: Metastatic Disease to the Thorax <i>Gordon Weisbrod, MD</i>	Americana 3
1:00 - 1:45	D2: Use of MDCT 3D Reconstructions of Cardiovascular Structures: Clinical & Classroom <i>Anna Rozenshtein, MD and Lawrence Boxt, MD</i>	Americana 4
1:45 - 2:30	E1: Thoracic ICU Radiology <i>Joel Fishman, MD, PhD</i>	Americana 3
2:30 - 3:15	F1: Pulmonary Hypertension: Less Common Causes and New Therapies <i>Marc Gosselin, MD and Jeffrey Edelman, MD</i>	Americana 3
3:15 - 3:30 pm	Coffee Break	Americana Foyer
3:30 - 5:30 pm	Scientific Session II (non-CME Session) Moderators: Smita Patel, MBBS and Eric Stern, MD	Americana 3

Principles and ethics of lung cancer screening

Caroline Chiles, M.D.

Objectives

The participant will understand the biases of cancer screening (length-time bias, lead time bias, and overdiagnosis), and the necessary elements of informed consent for cancer screening programs.

Introduction

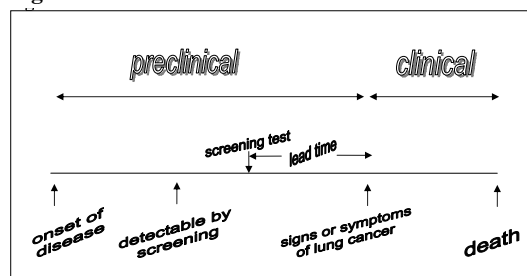
Screening is the application of a test to detect a disease or condition in an individual who has no known signs or symptoms of that disease or condition. The goal of imaging studies for cancer screening is the early detection of disease at a point when treatment is more effective. The assumption is that early detection (the preclinical phase of disease, prior to the onset of clinical manifestations of the disease) will lead to a more favorable outcome. In lung cancer, the improved survival in Stage I disease as a result of surgical resection fuels the effort towards finding an effective screening test.

Lung cancer meets many of the criteria required for screening programs to be effective. It is a disease that affects a large number of people, and which has serious consequences (150,000 lung cancer deaths in the US in 2002). It is possible to choose a population at increased risk (smokers, former smokers) in whom a preclinical phase of the disease is detectable (the asymptomatic patient with a solitary pulmonary nodule). Screening tests can detect lung cancer not only prior to its clinical presentation, but prior to a critical point – metastatic disease. Both CXRs and CTs are widely available, “affordable” examinations with little morbidity. Most importantly, an individual with an early stage lung cancer may have surgically respectable disease, and the potential for cure.

Principles of cancer screening

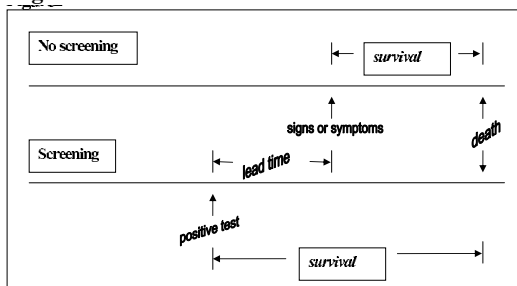
The preclinical phase of lung cancer can be divided into two parts: (1) the interval from the onset of disease, before the disease is detectable to the time at which the disease becomes detectable by the screening test, and the interval from the time at which the disease is detectable by the screening test to the onset of signs and symptoms. This is most clearly shown by use of time lines, which are adapted from Black and Welch, AJR 1997; 168: 3-11. The lead time is defined as the interval between the diagnosis of a disease at screening and the time it would have otherwise been detected due to the appearance of clinical signs and symptoms. The amount of lead time that can be gained by a screening test is a function of the time from disease detectability to the onset of symptoms and the frequency of testing.

Figure1



The lead time bias describes the comparison between the survival time in patients who are not screened and those who are. Even if intervention in the course of disease has no effect, the individual who has screening-detected cancer can appear to have a longer survival than the individual who has a diagnosis made on the basis of clinical presentation, as survival is measured from the date of diagnosis, rather than from the true onset of disease. The rate of progression of screening-detected lung cancers cannot be known at this time and therefore it is impossible to accurately adjust survival times to account for lead time.

Figure2



Length bias describes the tendency of screening to detect slowly growing cancers, rather than rapidly progressing ones. As can be seen by looking at the timeline in Figure 1, if the detectable phase of disease is long, there is a greater likelihood that a screening test will be performed and the disease will be detected. More rapidly growing tumors have a shorter detectable preclinical phase and are less likely to be detected by a screening examination prior to the onset of symptoms. Therefore, lung cancer screening programs are more likely to detect slowly growing lung cancers.

Overdiagnosis bias has become a widely appreciated phenomenon as a result of prostate cancer screening using PSA. Overdiagnosis relates to the number of cases that would not have caused the death of the patient even without screening. The survival in these patients may be erroneously attributed to early detection and treatment.

The biases inherent in screening can be reduced with a randomized controlled trial in which effectiveness is measured by disease-specific mortality --- comparing the number of deaths from lung cancer in a screened population to the number of deaths from lung cancer in an unscreened population.

Ethics of lung cancer screening

The ethics of lung cancer screening can be considered from two perspectives: screening as part of a research study evaluating lung cancer screening and screening within a clinical environment.

Research involving human subjects is governed by the Declaration of Helsinki, first adopted by the World Medical Association in 1964, and most recently revised in 2002. (http://www.wma.net/e/policy/17-c_e.html) The Declaration contains 32 ethical principles for medical research. A basic

principle is that “conditions related to the well-being of the human subject should take precedence over the interests of science and society”. The Declaration of Helsinki also states that “The benefits, risks, burdens and effectiveness of a new method should be tested against those of the best current prophylactic, diagnostic, and therapeutic methods. This does not exclude the use of placebo, or no treatment, in studies where no proven prophylactic, diagnostic or therapeutic method exists.” This introduces the concept of equipoise. The principle of clinical equipoise was re-defined by Dr. Barry Freedman as “a genuine uncertainty within the expert medical community regarding the comparative therapeutic methods of each arm in a trial.” At the start of a trial, there must be a state of clinical equipoise regarding the merits of the two arms. The trial must be designed in such a way as to expect that clinical equipoise will be disturbed. In this case, the expert medical community must agree that the relative value of screening for lung cancer with one technique (CT) versus another (CXR) is uncertain. Herein lies some of the controversy over lung cancer screening.

Screening for lung cancer with either CXR or CT has not been proven to change the outcome – to reduce the likelihood of death from lung cancer – and this must be explained clearly to participants in either a research study or within a clinical environment. In addition, individuals in both research screening programs and clinical screening programs must be informed of the risks and benefits of lung cancer screening. The risks of false positive examinations, particularly with respect to the risks inherent in the work-up of both incidental and false-positive findings must be thoroughly explained. The risk that a screening examination is incorrectly interpreted – and is a false negative should be included. Even a true negative examination must be

described as a risk, in that it may prejudice the patient from recognizing and acting on symptoms of disease that develop at a later date. The informed consent should also include information about the risks of radiation exposure, and about intravenous administration of contrast material, if applicable.

In programs that are screening patients who are self-referred, the radiologist assumes the role of personal physician. In this regard, the radiologist must not only communicate the results of the examination to the patient, but must be available to assist the patient in the evaluation of any abnormality revealed by the screening examination.

An unresolved issue remains, and will only add to this controversy over time. The ethical dilemma for society is – who should bear the financial burden of the evaluation of findings on screening examinations?

REFERENCES

- Black WC, Welch HG. Screening for disease. *AJR* 1997; 168: 3-11
- Freedman B. Equipoise and the ethics of clinical research. *New Engl J Med* 1987; 317:141-145
- Herman CR, Gill HK, Eng J, Fajardo LL. Screening for preclinical disease: Test and disease characteristics. *AJR* 2002; 179:825-831
- Kramer BS, Brawley OW. Cancer screening. *Hematology/Oncol Clin N Amer* 2000; 14(4): 831-848
- Obuchowski NA, Graham RJ, Baker ME, Powell KA. Ten criteria for effective screening: Their application to multislice CT screening for pulmonary and colorectal cancers. *AJR* 2001; 176: 1357-1362
- Soda H, Oka M, Tomita H, Nagashima S, Soda M, Kohno S. Length and lead time biases in radiologic screening for lung cancer. *Respiration* 1999; 66:511-517

Lung Cancer Screening Trials: An Update

Thomas E. Hartman, M.D.

Objective:

1. Identify the strengths and limitations of previous trials of imaging in lung cancer screening.
2. Identify the strengths and limitations of currently ongoing lung cancer screening trials.
3. Identify strengths and weaknesses of randomized control trials.

In order to make informed decisions regarding a screening CT practice, individuals need to be familiar with the history of lung cancer screening as well as the risks and benefits of the current lung cancer screening trials.

Background

Lung cancer is now the most common cause of cancer death in the United States. More individuals will die from a lung cancer than colon, breast, and prostate cancers combined. Overall 5 year survivor from lung cancer is less than 15%. However, patients with Stage I non-small cell lung cancer who undergo curative resection have a 5 year survival rate of up to 70%⁽¹⁾. The improved survival seen with early stage non-small cell lung cancer has formed the rationale for lung cancer screening.

Historical Lung Cancer Screening Trials.

In the 1970s there were four major prospective randomized controlled trials⁽²⁻⁵⁾ which concluded that screening did not reduce lung cancer specific mortality. Although the trials showed advantages to the screened group with respect to earlier stage at diagnosis, resectability and survival, they also demonstrated increases in cumulative lung cancer incidence above that of the control groups. Therefore significant improvements in case fatality (number of cancer deaths/number of individuals with cancer) did not translate into significant reductions in lung cancer mortality (number of cancer deaths/number of individuals screened).

Biases in Screening

There are three biases which need to be addressed in regard to screening trials. These biases are lead time, length, and over diagnosis biases.

Lead Time Bias

Early detection of disease with screening may result in increased survival time even if there is no change in the time to death from the disease process. Therefore survival is an inadequate measure of the effectiveness of screening and has no predictable relationship to mortality.

Length Bias

The likelihood of detection by screening is directly related to how quickly a cancer grows. The more slowly growing the neoplasm, the longer it is present without symptoms and the

greater likelihood of detection. Overall, screening will tend to detect more indolent tumors. This increased detection of indolent tumors will skew the survival results in favor of the screening group.

Over Diagnosis Bias

This is basically the detection of pseudo disease (a lung cancer that would have remained subclinical before the individual's death from other causes). The idea of over diagnosis is controversial, but if over diagnosis bias exists it would manifest as a study which showed increased number of cancers detected, down staging of the detected cancers, increased resectability and increased survival, but no change in the number of advanced cancers and no change in mortality. This is exactly what was seen in the Mayo Lung Project⁽⁶⁾.

Lung Cancer Screening with Helical CT

Screening trials using low dose CT are in progress in many countries throughout the world⁽⁷⁻⁹⁾. Many of these single arm (no control) trials have demonstrated increases in the detection of early stage lung cancer. These findings confirm the sensitivity of CT over chest radiography in detecting smaller, earlier stage lung cancers. Unfortunately because these trials are single arm trials, it will be very difficult to determine whether CT screening can achieve a true decrease in lung cancer specific mortality or whether the "improved survival" seen with these trials was simply due to the screening biases of lead time, length, and over diagnosis.

PLCO

The Prostate, Lung, Colorectal, Ovarian (PLCO) trial is a randomized control screening trial sponsored by the National Cancer Institute⁽¹⁰⁾. One objective of the trial is to see if using chest radiographs for lung cancer screening can reduce lung cancer specific mortality by at least 10% relative to the unscreened group. The reason for this objective was that the previous trials of lung cancer screening, particularly the Mayo Lung Project, did not prove that chest radiographs are ineffective for lung cancer screening, but merely that chest x-ray screening could not be endorsed without a better demonstration of a screening benefit. Therefore it is hoped that this PLCO trial will resolve lingering questions about the utility of chest radiographic screening.

National Lung Cancer Screening Trial

The National Lung Cancer Screening Trial (NLST) sponsored by ACRIN recently began enrolling participants. A total of 50,000 participants will be enrolled and randomized in a one to one ratio to the experimental and control arms of the study. The experimental arm will receive a baseline low dose helical CT and two annual incidence screening CTs. The control arm will receive a baseline PA chest radiograph and two annual incidence screening PA chest radiographs. Samples of blood, sputum, and urine will be obtained from both arms of the study. The prime eligibility criteria will include an age between 55-74

years and a current or previous cumulative cigarette smoking history of greater than or equal to 30 pack years. Former smokers must have quit smoking within the previous 15 years. By undertaking a randomized control study it is hoped that the screening biases seen with the single arm studies can be eliminated and the effect of CT screening on lung cancer specific mortality can be addressed. However, there are limitations of randomized control trials in general.

First, the validity of the measurement of lung cancer specific mortality depends on the integrity of the different cohorts with respect to the assigned interventions. If a large number of participants in the experimental arm drop out of the study, and/or a large portion of the control participants undergo the experimental intervention this will result in contamination of the control group. This noncompliance by either arm may diminish the observed effect of the intervention. For lung cancer screening this could reduce the potential mortality benefit of screening.

The sample size requirements of a randomized control trial for screening are important. This is due to the fact that despite targeting individuals at the highest risk of developing lung cancer, few participants will actually develop lung cancer during the screening period. Estimates of the sample size that would be required to detect a 30% difference in mortality between cohorts screening for lung cancer with helical CT exceed 20,000 participants. Therefore, there will be ongoing concern about the sample size for the current NLST study.

The required duration of surveillance of the separate cohorts is another important factor. The effects of lead time and length bias may be such that the adequacy of a prevalence scan and only two annual screening exams may be called into question.

A final challenge for randomized control studies is misclassification. While over diagnosis bias may exist in the screened group, under diagnosis of lung cancer may exist in the control group. Under diagnosis in the control group would be caused by misclassification of the cause of death in the control group. This misclassification could underestimate lung cancer incidence and mortality in the control group and would lower the observed benefit of screening. Determining the outcomes of all the participants in the NLST will require long term surveillance of the cohorts with long term medical followup and review of the National Death Index.

Conclusion

Previous and ongoing studies of imaging for lung cancer screening have failed to demonstrate reductions in lung cancer

mortality. However, none of these studies have demonstrated that screening is futile and the results from several single arm CT screening studies are encouraging. However, without demonstrating a significant reduction in lung cancer mortality, it is unlikely that the government or third party payers will recommend or reimburse for lung cancer screening.

Randomized control trials such as the PLCO and NLST are currently underway which may provide better information with regard to any reductions in lung cancer mortality with chest radiographic or CT screening. However, it should also be remembered that randomized control trials have their own limitations and thorough review of the data from these trials will be necessary to determine the effectiveness of the screening modalities.

REFERENCES

1. Fry W, Mench H, Winchester D. The national cancer database report on lung cancer. *Cancer* 1996;77:1947-1955.
2. Tockman M. Survival and mortality from lung cancer in a screened population: The Johns Hopkins Study. *Chest* 1986;57:44-53.
3. Flehinger BJ, Melamed MR, Zaman MB, et al. Early lung cancer detection: results of the initial (prevalence) radiologic and cytologic screening in the Memorial Sloan-Kettering study. *Am Rev Respir Disease* 1984;130:555-560.
4. Fontana R, Sanderson DR, Woolner LB, et al. Lung cancer screening: The Mayo Program. *J Occup Med* 1986;28:746-750.
5. Kubik A, Polak J. Lung cancer detection: results of a randomized prospective study in Czechoslovakia. *Cancer* 1991;67:1155-1164.
6. Marcus PM, Prorok PC. Reanalysis of the Mayo Lung Project data: the impact of confounding and effect modification. *J Med Screen* 1999;6:47-49.
7. Kaneko M, Eguchi K, Ohmatsu H, et al. Peripheral lung cancer: screening and detection with low-dose spiral CT versus radiography. *Radiology* 1996;201:798-802.
8. Henschke CI, McCauley DI, Yankelevitz DF, et al. Early lung cancer action project: overall design and findings from baseline screening. *Lancet* 1999;354:99-105.
9. Swensen SJ, Jett JR, Sloan JA, et al. Screening for lung cancer with low-dose spiral computed tomography. *Am J Respir Crit Care Med* 2002;165:508-513.
10. Kramer BS, Golagan J, Prorok PC, et al. National Cancer Institute sponsored screening for prostatic, lung, colorectal and ovarian cancers. *Cancer* 1993;71:589-593.

Lung Cancer Detection Failures (CXR & CT)

Phillip M. Boiselle, M.D.

Introduction and Objectives:

Approximately 1 decade ago, Lillington estimated that 150,000 new solitary pulmonary nodules were detected each year in the United States. Considering advances in CT technology and CT utilization in the past decade, it is likely that the number of nodules detected has increased substantially since that time.

Although it is difficult to arrive at an accurate estimate of the number of nodules detected each year, it is even more challenging to determine how many nodules are missed. For example, in routine clinical practice, the generally accepted error rate for missed early lung cancer on chest radiographs is 20 to 50%. However, error rates as high as 90% have been reported.

The learning objectives of this lecture are:

- To review the causes of lung cancer detection failures on chest radiographs & CT
- To describe methods that can help to reduce lung cancer detection failures.

Factors Contributing to Missed Lung Cancer:

Factors contributing to missed lung cancer include technical considerations of the study (e.g. exposure factors, motion, and suboptimal inspiration), lesion characteristics (e.g. lesion size and conspicuity), and observer error. The latter is considered the most important factor. There are three major types of observer error: 1) scanning error: occurs if a nodule is not fixated during the 350 msec that a lesion is focused on the fovea; 2) recognition error: occurs if a lesion is adequately scanned but not recognized; and 3) judgement error: occurs when a recognized abnormality is incorrectly interpreted as normal or not clinically significant. Another type of observer error is satisfaction of search, which describes the situation that occurs when a radiologist fails to detect a lung cancer due to distraction by an unrelated radiographic finding.

Missed Lung Cancer on Chest Radiographs:

In 1992, Austin et al. evaluated 27 cases of potentially resectable non small cell lung cancers that were missed on chest radiographs. The mean size of missed lesions was 1.6 cm, and nearly one-third of lesions were greater than 2 cm in size. These authors concluded that the single most frequently identified cause of missed lung cancer was failure to compare the current chest radiograph with multiple older chest radiographs. Austin and colleagues recently revisited this topic in order to determine whether there were changes in the last decade in the failure of detection of potentially resectable non small cell lung cancers. Interestingly, the mean size (2.1 cm) of missed lesions in the new study was slightly but significantly increased compared to the prior study. Both studies showed a striking predilection for missed lung cancer in the upper lobes, especially the apical and posterior segments of the right upper lobe.

In order to reduce the risk of missing lung cancer on chest radiographs, one should always try to interpret chest radiographs in the context of comparison to older chest radiographs. Additionally, search satisfaction should be avoided by resisting

the temptation to end a search once a radiographic finding has been made. Additional important factors for reducing detection failures include optimizing the technical aspects of the study and using appropriate viewing conditions.

Recent technological advances in chest radiography, including dual energy subtraction and temporal subtraction techniques, should lead to further improvements in nodule detection. It is likely that these techniques will play an increasing role in the future, along with methods of computer-aided diagnosis.

Missed Lung Cancer on CT

In 1996, studies by White et al. and Gurney described the features of missed lung cancer on CT in 23 patients. Gurney reported that failure of detection was predominantly due to observer error. Small lesion size was considered a major factor in this study as all peripherally located missed lesions measured less than 3 mm in diameter. White et al. reported that endobronchial lesions were most often overlooked, accounting for two-thirds of missed cases. Mean lesion size was greater than 1 cm. Search satisfaction and observer fatigue were also cited as factors for detection failure in this study.

In recent years, low-dose spiral CT (LDCT) has been used as a screening tool for lung cancer detection, primarily in research settings. Kakinuma et al. recently reported 7 cases of lung cancer that were initially missed at screening LDCT and subsequently detected on repeat LDCT screening studies performed 6 to 18 months later. Missed nodules were retrospectively categorized as either conspicuous (mean diameter=11 mm; n=3) or inconspicuous (mean diameter=6 mm; n=4). In order to reduce the number of false-negative cases, these authors emphasize the importance of examining noncalcified nodules with thin-section CT, even when adjacent lesions of prior tuberculosis exist. They also caution that one should carefully inspect pulmonary vessels in order to distinguish them from small pulmonary nodules. Despite an initial "missed" diagnosis, 6 of 7 lesions were Stage I neoplasms at the time of diagnosis.

The ELCAP investigators have reported an analysis of missed lung nodules on screening LDCT that were subsequently identified on follow-up diagnostic CT scans. Among the 163 patients who underwent diagnostic CT imaging, 36 (22%) had additional nodules which were not detected on LDCT. The majority (85%) of missed nodules measured 5 mm in diameter or less and none were greater than 10 mm in diameter. Thus, small size appears to be an important factor related to missed nodules on LDCT. Interestingly, a majority of missed nodules were located peripherally.

Li et al. recently described the characteristics of missed lung cancer in a large low-dose screening trial. In this study, 32 (39%) of 83 primary lung cancers detected in an annual screening program were missed on 39 CT scans. Detection errors were responsible in approximately 60% of cases and interpretation errors were responsible in the remaining 40% of cases. Lesions missed due to detection error were significantly smaller (9.8 mm versus 15.9 mm) than those missed due to interpretative error. Lesions missed due to detection error were also more likely to be ground-glass in attenuation. With regard to interpretation error cases, the

lesions generally mimicked benign diseases and typically occurred in patients with underlying lung disease such as emphysema or fibrosis. Interestingly, despite being missed on one or more prior studies, 28 (88%) of 32 missed lesions were still Stage IA lung cancers at the time of diagnosis. In a separate study, these authors determined that an automated lung nodule detection method correctly identified 84% of missed cancers.

In order to reduce the risk of missing lung cancer on CT, one should pay careful attention to both the peripheral and central portions of the lungs. Cine methods of viewing, which enhance the ability to distinguish small nodules from vascular structures, should be used in settings where they are available. Additionally, one should consider the use of sliding-thin-slab MIP images as a complement to routine axial images. Gruden et al. have recently shown that MIP slabs enhance the detection rate of nodules, especially in the central portion of the lungs. In addition to carefully inspecting the lung parenchyma, one should thoroughly evaluate the airways in order to avoid missing a nonobstructing endobronchial lesion. In the near future, it is likely that computer-aided diagnosis will play an important role in reducing lung cancer detection failures. This topic is addressed in the following lecture.

REFERENCES:

- Armato SG, Li F, Giger ML, et al. Lung cancer: performance of automated lung nodule detection applied to cancers missed in a CT screening program. *Radiology* 2002;225:685-692.
- Austin JHM, Romney BM, Goldsmith LS. Missed bronchogenic carcinoma: radiographic findings in 27 patients with a potentially respectable lesion evident in retrospect. *Radiology* 1992;182:115-122.
- Gruden JF, Ouanounou S, Tigges S, et al. Incremental benefit of maximum-intensity-projection images on observer detection of small pulmonary nodules revealed by multidetector CT. *AJR* 2002; 179:149-157.
- Gurney JW. Missed lung cancer at CT: imaging findings in 9 patients. *Radiology* 1996;199:117-122.
- Kakinuma R, Ohmatsu H, Kaneko M, et al. Detection failures in spiral CT screening for lung cancer: analysis of CT findings. *Radiology* 1999;212:61-66.
- Kundel HL, Nodine CF, Carmody D. Visual scanning, pattern recognition and decision-making in pulmonary nodule detection. *Investigative Radiology* 1978;13:175-181.
- Li F, Sone S, Abe H, et al. Lung cancer missed at low-dose helical CT screening in a general population: comparison of clinical, histopathologic, and imaging findings. *Radiology* 2002;225:673-683.
- Naidich DP, Yankelivitz DF, McGuinness G, et al. Noncalcified nodules missed on low-dose helical CT (abstr.). *Radiology* 1999;213(p):303.
- White CS, Romney BM, Mason AC, et al. Primary carcinoma of the lung overlooked at CT: analysis of findings in 14 patients. *Radiology* 1996;199:109-115.
- White CS, Salis AI, Meyer CA. Missed lung cancer on chest radiography and CT: imaging and medicolegal issues. *Journal of Thoracic Imaging* 1999;14:63-68.

The Role of CAD in Lung Cancer Screening

Jane P. Ko, M.D.

Computer aided diagnosis (CAD) refers to computer methods that aid in interpretation. CAD has been applied to medical applications, primarily within the fields of radiology and dermatology. CAD functions range from detection and diagnosis, characterization, and follow-up of pathology.

Background

Investigations into the analysis of radiographs by computers were first published in the 1960s. The specific analysis of chest radiographs began with reports in the 1970s. The further development of CAD has been aided by the concurrent invention of digital imaging in the 1970s. In the past decade, the advancement in the field of CAD has particularly accelerated, with application of this technology to mammography, chest computed tomography (CT), in particular screening chest CT, and CT colonography. These fields require high diagnostic sensitivity despite a large proportion of normal studies. With the current interest in evaluating CT for lung cancer screening, the development of CAD for thoracic CT has concentrated on the diagnosis of the pulmonary nodule.

Pulmonary Nodule Detection

In comparison to chest radiography, CT provides better contrast between the nodule and lung and eliminates overlying structures such as the chest wall, mediastinum, diaphragm, and vessels. However, limitations in nodule identification on CT have been noted that may translate to missed cancers. Nodules on CT have been missed in an endobronchial or lower lobe location. On screening CT, overlooked nodules were small, on the order of 4-6 mm, faint in attenuation, adjacent to vessels, and adjacent to findings of prior tuberculosis.

A number of factors affecting nodule recognition include reader experience and variability, CT technique and viewing conditions, and nodule characteristics. It has been demonstrated that inter- and intra-observer variability in nodule detection plays a factor in the number of nodules identified. Wormanns et al showed that, from a total of 230 nodules found by either of 2 readers, only 45% (103/230) of nodules were found by both readers on 5 mm sections at 3 mm overlapping intervals. 29% (66/230) of the nodules were graded as definite by one reader and missed by the other. The number of overlooked nodules and of false-positive diagnoses differs between readers with greater and less experience. Fatigue plays a major role in screening examinations, where there are a large number of normal studies, but the consequence of not diagnosing a cancer would be major.

Viewing methods have also been shown to affect interpretation. Larger image sizes when viewing at a fixed distance and cine viewing have been shown to improve nodule detection. Similarly, cine viewing of post-processed data in maximum-intensity-projection images (MIP) may improve nodule perception. The MIP technique takes advantage of the spatial resolution benefits provided by high-resolution volumetric data that can now be obtained with multi-slice CT (MSCT). Viewing of MIPs may minimize the need for the radiologist to review large

data sets, which can approach 300 images if the thorax is reconstructed into 1 mm sections, subsequently adversely affecting interpretation time. The MIP technique enables visualization of small vessels and other structures with the speed and convenience of thick slabs. The MIP technique, however, is not optimal for visualization of the airways and needs to be viewed in conjunction with conventional axial sections.

CAD

Given the number of factors that may affect nodule detection, CAD may provide tools that overcome these factors and play a crucial role in ensuring that abnormalities are not overlooked. This is of particular interest when considering the immense size of data sets generated by MSCT scanners. The concept of using CAD as a "second reader" began with screening mammography. For thoracic applications, use of CAD as a second reader may not only decrease the number of missed pulmonary nodules, but also improve clinical efficiency. Volume and morphologic analysis of nodules will also be facilitated by computerized techniques.

CAD for nodule diagnosis was initially applied to chest radiography and has been supported by the development of digital chest radiography. In comparison with CT, lung nodule perception on radiographs is more difficult because of the lower contrast of a nodule with the lung as well as superimposition of densities. MacMahon et al reported improved accuracy for nodule identification on chest radiographs with a group of 104 chest radiologists, other radiologists, radiology residents, and non-radiologists. Therefore the Food and Drug Administration has recently approved of CAD for chest radiography.

For chest CT, CAD can analyze high-resolution data while the radiologist analyzes more clinically practical thicker sections. CAD programs need to accomplish a number of processes to succeed. Typically, the thorax is identified within the FOV of an image, and then the lungs are segmented from the thorax. Regions that may represent normal structures or nodules in the lung are then identified and differentiated. One major obstacle pertains to the identification of lung from the remaining thorax, particularly when parenchymal abnormalities abut the pleura. Methods to overcome this challenge have been proposed, including a "rolling-ball filter" and comparing slopes at different points along the lung border. The challenge for CAD systems is to minimize the number of false positive nodules detected that translates to decreasing radiologists' interpretation time and false positive diagnoses. Additionally, CAD methods still need to address ground-glass or subsolid nodules, which have obtained greater clinical significance given their recent association with the spectrum of adenocarcinoma including preneoplastic atypical adenomatous hyperplasia and bronchoalveolar carcinoma. CAD systems may need different criteria to detect these lower attenuation nodules as compared to their solid counterparts. Other obstacles presented to CAD developers is the segmentation of nodules from vessels, which play a role in the identification of nodules in addition to quantification of size.

With computer-aided analytical techniques, we are more

capable of studying the internal architecture of nodules through texture analysis. McNitt-Gray et al used texture measures to identify nodules with uniform attenuation from those with inhomogeneous attenuation. This could be applied to non-contrast and contrast CT studies of nodules. Integration of the results of computer analysis with a database management system may not only assist in daily clinical activities but also provide indispensable data for research.

Volume Measurement

Precise measurement of nodule size and assessment for growth is very important, particularly for the interpretation of screening chest CT. Nodule size on CT has been traditionally expressed as bi-dimensional perpendicular measurements (the largest dimension and its perpendicular dimension) that are then multiplied to obtain a bidimensional cross product, as recommended by the World Health Organization criteria. Size has also been recorded in terms of the largest dimension, as suggested by the Response Evaluation Criteria in Solid Tumors Guidelines. However, inter-observer error occurs when small nodules are measured using manual calipers, in combination with film scales, or electronic calipers.

Volume measurement can be quantified using two (2D) or three-dimensional (3D) methods that can be manual, semi-automated- or automated. 2D methods require an assumption of a nodule's shape. The largest nodule dimension is converted into nodule volume by assuming a spherical shape, or the bi-dimensional perpendicular measurements are used with the presumption that a nodule is an ellipse. 3D measurement entails using the entire CT data set in which the nodule is encoded to calculate nodule volume. The superiority of 3D methods was demonstrated by Yankelevitz et al, particularly for deformed non-spherical nodules. 3D methods sum the volumes of the nodule on each axial section to obtain total nodule volume and therefore may more accurately measure irregularly shaped nodules.

Nodule volume quantification with automated methods can potentially detect smaller differences in nodule size at earlier intervals than simply relying on cross-sectional dimensions. However, there are a number of impediments to performing automated/ semi-automated volume quantification. The major problem is the reproducibility of volume measurements. Partial volume effects play a major role in generating errors in measurement. Threshold-based methods are frequently used to separate or segment nodules from the surrounding lung parenchyma. If a nodule does not fill an entire voxel, the nodule's attenuation will be averaged with the surrounding lung parenchyma. Hence, depending on the threshold, the voxel may or may not be considered as part of the nodule. Validation of these methods is therefore important. Using synthetic nodules imaged in air and 2D and 3D quantitative methods for volume measurement, Yankelevitz et al demonstrated that 0.5 mm axial sections were associated with smaller errors as compared to nodule volume measurements performed on 1.0 mm sections. It is important to understand the error in measurement methods so that identification of change in nodule volume can be interpreted with knowledge of the limitations of a measurement system, whether automated or semi-automated.

In patients, the volume measurement error is likely to be higher secondary to a number of factors. These include lung pathology such as emphysema, consolidation, and/ or infiltrative lung disease in addition to adjacent normal parenchymal struc-

tures, such as bronchi and vessels. Automated segmentation of nodules from vasculature has been addressed recently by Zhao et al. 3D volume measurement methods may use 2D and 3D criteria for segmentation. Automated segmentation techniques are difficult to validate, as there is no gold standard for segmentation accuracy.

Image Registration

The follow up of pulmonary nodules emphasizes the need for image registration. Image registration entails "superimposing" image data or determining the spatial alignment between different images from the same modality at different points in time (intramodality registration) or between different imaging modalities such as CT, MR and positron emission tomography (intermodality registration). To accurately correlate a nodule on a given CT study with its matching counterpart on a subsequent CT, global registration of the thorax and local registration of nodules and smaller structures need to be performed.

A large number of reports concerning image registration have been published, primarily in the brain and to a lesser degree in other organ systems. Within the chest, primary interest has focused on registering the metabolic information provided by nuclear medicine studies and CT. Due to the recent attention focusing on screening CT and the need to better measure and compare nodule size, significant interest in comparing CT studies has emerged.

Image registration techniques include rigid body, affine, and elastic image methods.¹¹² On a CT scan, *translational* differences may occur in the x, y, or z position without rotation or distortion. *Rotational* differences occur when the torso is rotated in the axial plane (x, y rotation) and rotated out of the axial plane (z rotation). Rigid body transformation methods account for these rotational and translational differences. Image distortion, termed *skewing*, from non-uniform image reconstruction or changes in perspective, affects 2D radiographic images more than CT. However, global skewing can be introduced when different gantry tilts are used and would be particularly relevant for head CTs. Skewing is introduced as the patient exhales and the thorax deforms. Global *scaling* factors are related to the FOV and slice thickness on CT. Affine transformations address differences in scaling and skewing in addition to rigid body parameters and globally represent the differences between two data sets.

The lung is a deformable structure that differs in shape and volume related to the degree of patient inspiration. Each lobe may have a distinct deformation or strain pattern in response to varying inspiratory volumes that may translate to different shapes and attenuation on CT. Deformable models may ultimately compensate for global and local differences in thorax shape; however, deformable models have been primarily studied in the heart. In addition to problems created by different levels of inspiration, pathology such as atelectasis, which can change the shape of the thorax and shift anatomical structures and any disease distorting the normal contours of structures within the bony thorax could pose difficulties.

CAD in Clinical Workflow

The ultimate goal is an interactive system that enables easy identification of corresponding structures on initial and subsequent CT studies, documentation of nodules and their characteristics, and storage of image results for future analysis and documentation. This would prove vital to the follow up of a large

number of nodules in patients with known malignancies involving the lung as well as those patients with incidentally detected nodules. Additionally, a wealth of data will be available for research to understand the specific nodule characteristics that are associated with malignancy. CAD's value will lie in its ability to not only preprocess high-resolution CT data but also to interact "real-time" with the radiologist and provide automated characterization of nodules. Nodules may be missed secondary to the reader's attention being drawn to specific marked areas by the CAD, and therefore it may be optimal to withhold the CAD results until the radiologist has reviewed the study to minimize this effect. Once the radiologist approves of or ignores the results of the CAD, the information can be automatically archived in a database.

There is concern that computer programs would replace radiologists by assisting non-radiologists in interpretation of studies. While CAD is very promising, a large amount of work to develop CAD is still needed so that a system will achieve high sensitivity and specificity of that of a radiologist. Moreover, if CAD achieves the expertise of a thoracic radiologist, this would provide a valuable tool for general radiologists. Moreover, the expertise of a radiologist will be irreplaceable in the detection and interpretation of unexpected findings. Finally, it is difficult to justify not developing and using CAD. Similar issues occurred with the implementation of PACS, which was initially met by the concern by some that such systems would minimize the role of the radiologist by decreasing interaction with clinical referrers. These concerns have been outweighed by its invaluable assistance reflected in increased productivity of radiologists in addition to rapid access to patient's studies.

REFERENCES;

- Armato SG, 3rd, Giger ML, Moran CJ, et al: Computerized detection of pulmonary nodules on CT scans. *Radiographics* 19:1303-1311, 1999
- Erikson BJ, Bartholmai B. Computer-aided detection and diagnosis at the start of the third millennium. *J Dig Imaging* 15:59-68, 2002.
- Gruden JF, Ouanounou S, Tigges S, et al: Incremental benefit of maximum-intensity-projection images on observer detection of small pulmonary nodules revealed by multidetector CT. *AJR Am J Roentgenol* 179:149-157, 2002
- Kakinuma R, Ohmatsu H, Kaneko M, et al: Detection failures in spiral CT screening for lung cancer: analysis of CT findings. *Radiology* 212:61-66, 1999
- Ko JP, Betke M: Chest CT: automated nodule detection and assessment of change over time-preliminary experience. *Radiology* 218:267-273, 2001
- MacMahon H: Improvement in detection of pulmonary nodules: digital image processing and computer-aided diagnosis. *Radiographics* 20:1169-1177, 2000
- McNitt-Gray MF, Hart EM, Wyckoff N, et al: A pattern classification approach to characterizing solitary pulmonary nodules imaged on high resolution CT: preliminary results. *Med Phys* 26:880-888, 1999
- Wormanns D, Diederich S, Lentschig MG, et al: Spiral CT of pulmonary nodules: interobserver variation in assessment of lesion size. *Eur Radiol* 10:710-713, 2000
- Yankelevitz DF, Reeves AP, Kostis WJ, et al: Small pulmonary nodules: volumetrically determined growth rates based on CT evaluation. *Radiology* 217:251-256, 2000
- Zhao B, P. RA, Yankelevitz DF, et al: Three-dimensional multicriterion automatic segmentation of pulmonary nodules of helical computed tomography images. *Opt Eng* 38:1340-1347, 1999

Small T1 Lung Cancer: Imaging and Its Prognostic Implication

Kyung Soo Lee, M.D.

Department of Radiology, Samsung Medical Center, Sungkyunkwan University School of Medicine, Seoul, Korea

Introduction

Patients with peripheral lung cancer less than 3 cm in diameter (T1 lung cancer) without nodal or distant metastasis, designated as stage IA (T1N0M0) in the TNM staging system, have a greater than 50% 5-year postoperative survival rate. Although initial studies suggested a low prevalence of nodal metastases in T1 lung cancer, several recent studies have reported relatively high frequency of mediastinal lymph node metastases. Seely et al (1) reviewed the CT scans and surgical findings in 104 patients with T1 lesions, and found that 21% of patients had nodal metastases as proved by complete nodal sampling using either mediastinoscopy or thoracotomy. The reported frequency of extrathoracic metastases in T1 lung cancer differs widely (0-24%), because of lack of uniformity in patient selection as well as methods of assessing the presence of metastases. Recently Jung et al (2) saw 13% of patients with T1 lung cancer had extrathoracic metastases at the time of diagnosis and additional 11% of patients (total 24% of patients) had metastases at one-year follow-up study.

Because small T1 peripheral lung cancers show sizable frequency of mediastinal nodal or extrathoracic metastasis, it is important to know on imaging studies which tumor will have mediastinal nodal or extrathoracic metastasis. In this lecture, the author will focus on imaging (CT and ^{18}F -fluorodeoxyglucose positron emission tomography: FDG-PET) findings of small peripheral lung cancer correlated with prognostic implications.

CT Findings of Small Peripheral Adenocarcinoma of the Lung and Prognostic Implication

Adenocarcinoma of the lung is the commonest histopathologic type of lung cancer and its incidence is reported to increase. In addition, it is reported that screening with low-dose CT can improve the detection of lung cancer, especially adenocarcinoma, at an earlier and potentially more curable stage. Because adenocarcinoma of the lung comprises histopathologically of heterogeneous group of tumors, it is difficult to predict a prognosis in patients with surgically resectable peripheral adenocarcinoma of the lung (3). However, in recent several studies, it was suggested that the extent of bronchioloalveolar carcinoma component in a small peripheral adenocarcinoma reflects clinicopathologic and prognostic characteristics of the tumor. As the component of bronchioloalveolar carcinoma within a tumor increases in extent, the adenocarcinoma shows better prognosis. Furthermore, pure bronchioloalveolar carcinoma without central fibrosis shows better prognosis than that with fibrosis (4).

Localized bronchioloalveolar carcinoma may appear as an area of GGO, as a mixed area of GGO and more dense consolidation, or as a nodule (5,6). Kuriyama et al (7) suggested that the percentage of GGO in a localized bronchioloalveolar carcinoma is larger than that in other adenocarcinomas. Aoki et al (8) asserted that adenocarcinoma appearing as localized GGO shows slow growth. In addition, Jung et al (2) suggested that the prevalence of extrathoracic metastasis is significantly lower in a small peripheral lung cancer with GGO than without it.

Kim et al (9) correlated the high-resolution CT findings of

peripheral small adenocarcinoma of the lung in 224 patients with histopathologic subtypes and evaluated whether there are any CT findings that help to predict a prognosis of the tumor. One hundred and thirty-two patients had bronchioloalveolar carcinoma and 92 had adenocarcinoma. The extent of GGO was greater in bronchioloalveolar carcinomas ($29\% \pm 31.6$, mean \pm standard deviation) than in other adenocarcinomas ($8\% \pm 13.3$) ($p < .001$). The extent of GGO was significantly greater in patients without recurrence ($p = .020$), nodal ($p = .017$), and distant ($p = .007$) metastases than in patients with them. They concluded that the extent of GGO within a nodule is greater in bronchioloalveolar carcinomas than in other adenocarcinomas. Greater extent of GGO also correlates with improved prognosis.

Similarly Aoki et al (10) evaluated the prognostic importance of high-resolution CT findings of peripheral lung adenocarcinoma. The marginal characteristics of nodules and extent of GGO within the nodules at preoperative high-resolution CT were analyzed retrospectively. Regional lymph node metastasis and vessel invasion were histologically examined in surgical specimens. Survival curves were calculated according to the Kaplan-Meier method. The frequency of lymph node metastasis (4% [1 of 24]) and vessel invasion (13% [three of 24]) in adenocarcinomas with GGO components of more than 50% were significantly lower than those with GGO components of less than 10% (lymph node metastasis, $p < .05$; vessel invasion, $p < .01$). The patients with GGO components of more than 50% showed a significantly better prognosis than those with GGO components less than 50% ($p < .05$). All 17 adenocarcinomas smaller than 2 cm with GGO components of more than 50% were free of lymph node metastasis and vessel invasion, and all these patients are alive without recurrence. Coarse spiculation and thickening of bronchovascular bundles around the tumors were observed more frequently in tumors with lymph node metastasis or vessel invasion than in those without lymph node metastasis or vessel invasion ($p < .01$). They concluded that high-resolution CT findings of peripheral lung adenocarcinomas correlate well with histologic prognostic factors.

Focal GGO has been detected increasingly by low-dose helical CT in lung cancer screening. Although focal GGO suggests *in situ* neoplastic lesion in the peripheral lung, it remains controversial how to manage these lesions. Nakata et al (11) evaluated the pathologic and radiologic characteristics of focal GGO. Forty-three patients with persistent (mean of 3.7 months) focal GGO ≤ 2 cm in diameter were studied. The histologic diagnoses were bronchioloalveolar carcinoma in 23 patients, adenocarcinoma with mixed subtypes in 11 patients, and atypical adenomatous hyperplasia (AAH) in nine patients. None of 34 patients with carcinoma had lymph node metastasis. GGO with solid components on CT were highly associated with adenocarcinoma (malignant rate, 93%). They concluded that focal GGO after observation for several months is a finding of early adenocarcinoma or its precursors. Especially lesions > 1 cm in diameter or GGO with solid components are significant signs of malignancy.

In a study to determine the relationship between tumor size and survival in patients with stage IA non-small cell carcinoma,

Patz et al (12) identified that there is no significant relationship between tumor size and survival. In a similar study to investigate the relationship between tumor size and stage distribution, Heyneman et al (13) could not find a statistically significant relation between the size of small primary lung cancers and the distribution of disease stage at the time of presentation.

Small T1 Lung Cancer: Evaluation with FDG-PET and Dynamic CT

¹⁸F-luorodeoxyglucose (FDG) positron emission tomography (FDG-PET) is a noninvasive diagnostic technique using metabolic (biochemical) differences between benign and malignant tissues. Increased glucose metabolism in malignant tissue may be related to multiple factors such as proliferation rate and number of viable cancer cells. FDG PET, however, is neither uniformly specific nor sensitive, especially when the abnormality is small. The localized form of bronchioloalveolar carcinomas and carcinoid tumors demonstrate less FDG uptake than other non-small cell lung cancers (14,15). False negative FDG PET scans are seen in about 5% of T1 lung cancers and in only 3% of such lesions with their diameters greater than 5 mm. The long-term survival for patients with a negative PET scan with lung cancers suggests that these tumors of low FDG uptake behave indolently. Therefore, management decision to follow up such lesions with conventional imaging to determine interval growth may be justified (15).

Angiogenesis is a complex process and may be determinants to the growth and metastasis of a malignant tumor. Vascular endothelial growth factor (VEGF) has been known as a vascular permeability factor and plays a crucial role in tumor angiogenesis. Microvessel density (MVD) measurements with immunohistochemical staining technique have been used to measure angiogenic activity. VEGF expression is significantly associated with MVD of non-small cell lung cancer, especially in adenocarcinomas of the lung. Dynamic CT of pulmonary nodules provides quantitative information on blood flow pattern and is a useful diagnostic method in distinguishing between benign and malignant nodules. The peak attenuation of tumor on dynamic CT mirrors intra-lesional micro-vessel densities (MVDs), especially in adenocarcinoma of the lung. The peak attenuation value of dynamic CT may be an index for VEGF-related tumor angiogenesis (16). In addition, the peak attenuation and relative flow on dynamic CT correlate with the standardized uptake value of FDG-PET scans in lung cancer. The peak attenuation and relative flow on dynamic CT as an index of blood pooling may be related to increased glucose metabolism in lung cancer (17).

Extrathoracic Metastasis of Small T1 Lung Cancer

It has been suggested that because the prevalence of extrathoracic metastases is low, routine metastatic work up using bone scans, liver scans, or brain imaging is not justified in patients with T1 lung cancer, especially in stage-I T1 cancer (T1 cancer without nodal metastasis). In addition, positive bone or liver scans frequently represent areas of nonmalignant change (e.g., inflammation or old fracture) and may unnecessarily delay surgery while leading to an invasive and costly work up. Furthermore, the adrenals are prominent site of nonmalignant lesions even in patients with lung cancer.

Salbeck et al (18) reported that none of 26 patients with stage-1 lung cancer had extrathoracic metastasis. Salvatierra et al (19) reported the frequency of metastases in stage 1 (without hilar or mediastinal nodal metastasis) and 2 (with hilar nodal metastasis) T1 lung cancer as being 8% (2/12 patients had metastases). In the study of Kormas et al (20), four (3%) of 158 patients with non-small cell lung cancer had brain metastases at the time of diagnosis and additional five patients (total of nine patients, 6%) had brain metastases within one year. Ferrigno et al (21) reported that 3/20 patients (15%) with stage 1 lung cancer had brain metastases. It is generally accepted that adrenal metastases occur in about 3% of patients with lung cancer (22).

Jung et al (2) performed a study to determine the frequency of extrathoracic metastases in T1 non-small cell lung cancer at the time of diagnosis and at one-year follow-up study and to compare the frequency of metastases in terms of cell type of lung cancer, the size and CT findings of the tumor at the time of diagnosis. Ninety patients with T1 lung cancer at CT were included. Evaluation of extrathoracic metastases was made at the time of initial diagnosis and at one-year follow-up study. The frequency of metastases was compared in terms of cell type (squamous vs. nonsquamous), size (≤ 2 cm vs. > 2 cm) and the initial CT findings of the tumor. Twelve (13%) of 90 patients had extrathoracic metastases demonstrated at the time of diagnosis and ten at one-year follow-up study [total, 22/90 (24%)]. The most frequent sites of extrathoracic metastases at one year follow-up study were brain (12/90, 13%), bone (6/90, 7%) and liver (5/90, 4%) in order of frequency similar to those of the previous reports (11,39). Tumors with GGO at CT showed significantly lower prevalence of metastases ($p = .042$). Area of GGO ($n = 23$) was seen in 11/13 (85%) patients with bronchioloalveolar carcinoma and 12/53 (23%) patients with adenocarcinoma other than bronchioloalveolar carcinoma ($p < .001$). There was no significant difference in the prevalence of metastases between squamous and nonsquamous cell carcinoma, between tumors of ≤ 2 cm ($n = 17$) and of > 2 cm in diameter ($n = 73$) and between tumors with or without mediastinal nodal metastases ($p > .05$). They concluded that extrathoracic metastases are evident at presentation in 13% of patients and at one-year follow-up in an additional 11% of patients. The prevalence is significantly lower in tumors with GGO.

Conclusion

Small T1 lung cancer with large area of GGO ($> 50\%$ of tumor volume) within it on thin-section CT shows good prognosis and less likelihood of mediastinal nodal or extrathoracic metastasis, whereas the cancer with coarse spiculation and thickening of bronchovascular bundles around the lesion shows more frequent lymph node metastasis or local vessel invasion than cancer without such findings. About 5% of T1 lung cancers, mostly focal nodular bronchioloalveolar carcinoma and carcinoids, show negative uptake on FDG PET scans and appear to be indolent in their growth therefore lead to long-term survival of patients with such tumors. About 21% of T1 lung cancers show mediastinal nodal metastasis at the time of diagnosis and about 24% of T1 lung cancers show extrathoracic metastasis, mostly brain metastasis at the time of diagnosis or at one year follow-up studies.

REFERENCES

- Seely JM, Mayo JR, Miller RR, Müller NL. T1 lung cancer: prevalence of mediastinal nodal metastases and diagnostic accuracy of CT. *Radiology* 1993;186:129-132.
- Jung K-J, Lee KS, Kim H, et al. T1 Lung Cancer at CT: Frequency of Extrathoracic Metastases. *J Comput Assist Tomogr* 2000;24:711-718.
- Nomori H, Hirohashi S, Noguchi M, Matsuno Y, Shimosato Y. Tumor cell heterogeneity and subpopulations with metastatic ability in differentiated adenocarcinoma of the lung. Histologic and cytofluorometric DNA analysis. *Chest* 1991;99:934-940.
- Noguchi M, Morikawa A, Kawasaki M, et al. Small adenocarcinoma of the lung. Histologic characteristics and prognosis. *Cancer* 1995;75:2844-2852.
- Jang HJ, Lee KS, Kwon OJ, Rhee CH, Shim YM, Han J. Bronchioloalveolar carcinoma: focal area of ground-glass attenuation at thin-section CT as an early sign. *Radiology* 1996;199:485-488.
- Lee KS, Kim Y, Han J, Ko EJ, Park C-K, Primack SL. Bronchioloalveolar carcinoma: clinical, histopathologic, and radiologic findings. *RadioGraphics* 1997;17:1345-1357.
- Kuriyama K, Seto M, Kasugai T, et al. Ground-glass opacity on thin-section CT: value in differentiating subtypes of adenocarcinoma of the lung. *AJR* 1999;173:465-469.
- Aoki T, Nakata H, Watanabe H, et al. Evolution of peripheral lung adenocarcinomas: CT findings correlated with histology and tumor doubling time. *AJR* 2000;174:763-768.
- Kim EA, Johkoh T, Lee KS, et al. Quantification of ground-glass opacity on high-resolution CT of small peripheral adenocarcinoma of the lung: pathologic and prognostic implication. *AJR* 2001;177:1417-1422.
- Aoki T, Tomoda Y, Watanabe H, et al. Peripheral lung adenocarcinoma: correlation of thin-section CT findings with histologic prognostic factors and survival. *Radiology* 2001;220:803-809.
- Nakata M, Saeki H, Takata I, et al. Focal ground-glass opacity detected by low-dose helical CT. *Chest* 2002;121:1464-1467.
- Patz EF, Rossi S, Harpole DH, Herndon JE, Goodman PC. Correlation of tumor size and survival in patients with stage IA non-small cell lung cancer. *Chest* 2000;117:1568-1571.
- Heyneman LE, Herndon JE, Goodman PC, Patz EF. Stage distribution in patients with a small (< 3 cm) primary nonsmall cell lung carcinoma. Implication for lung carcinoma screening. *Cancer* 2001;92:3051-3055.
- Kim B-T, Kim Y, Lee KS, et al. Localized form of bronchioloalveolar carcinoma: FDG PET findings. *AJR* 1998;170:935-939.
- Marom EM, Sarvis S, Herndon JE, Patz EF. T1 lung cancers: sensitivity of diagnosis with fluorodeoxyglucose PET. *Radiology* 2002;223:453-459.
- Tateishi U, Nishihara H, Watanabe S, Morikawa T, Abe K, Miyasaka K. Tumor angiogenesis and dynamic CT in lung adenocarcinoma: radiologic-pathologic correlation. *J Comput Assist Tomogr* 2001;25:23-27.
- Tateishi U, Nishihara H, Tsukamoto E, Morikawa T, Tamaki N, Miyasaka K. Lung tumors evaluated with FDG-PET and dynamic CT: the relationship between vascular density and glucose metabolism. *J Comput Assist Tomogr* 2002;26:185-190.
- Salbeck R, Grau HC, Artmann H. Cerebral tumor staging in patients with bronchial carcinoma by computed tomography. *Cancer* 1990;66:2007-2011.
- Salvatierra A, Baamonde C, Llamas JM, Cruz F, Lopez-Pujol J. Extrathoracic staging of bronchogenic carcinoma. *Chest* 1990;97:1052-1058.
- Kormas P, Bradshaw JR, Jeyasingham K. Preoperative computed tomography of the brain in non-small cell bronchogenic carcinoma. *Thorax* 1992;47:106-108.
- Ferrigno D, Buccheri G. Cranial computed tomography as a part of the initial staging procedures for patients with non-small-cell lung cancer. *Chest* 1994;106:1025-1029.
- Oliver TW, Bernardino ME, Miller JI, Mansour K, Greene D, Davis WA. Isolated adrenal masses in nonsmall-cell bronchogenic carcinoma. *Radiology* 1984;153:217-218.

Reporting Tumor Measurements in Oncologic Imaging

Todd R. Hazelton, M.D.

Assistant Professor of Radiology and Oncology
H. Lee Moffitt Cancer Center and Research Institute
At the University of South Florida

Objective: To review the role of the radiologist in reporting tumor measurements in thoracic oncology with emphasis on newer RECIST criteria and older WHO criteria.

In addition to clinical, biochemical, surgical, and pathologic data, evaluation of tumor response by quantitative measurements on cross-sectional imaging provides objective information regarding chemotherapy efficacy that is used both clinically and in the development of new anticancer drugs. For these reasons, radiologists should be familiar with the standards for reporting tumor measurements that have been established and are widely used in oncology for clinical trials.

WHO Criteria for Reporting Tumor Response:

The older World Health Organization (WHO) tumor response assessment criteria were established to standardize the recording and reporting of tumor response outcomes.¹ This system utilizes *bidimensional measurements* as a quantitative component in the assessment of tumor response to chemotherapy drugs. Measurements are reported in centimeters (cm) as the maximum diameter and the greatest perpendicular diameter (at a right angle) in the same plane for primary and metastatic lesions whose margins are clearly defined on CT, MRI, or other imaging study. With this technique, typically up to three lesions per organ, whose diameters are greater than the image thickness, are selected as “measurable” and bidimensional measurement values are then reported. The same acquisition technique must be utilized for follow-up studies to ensure comparability of subsequent measurements. Nonmeasurable disease sites are primary or metastatic lesions which cannot be accurately measured in two dimensions as they are either measurable in only one dimension (unidimensional) or are unmeasurable.

In the WHO criteria, the percentage of the decreased or increased tumor measurements is used to determine whether there is response or progression of disease, respectively.

Progression of disease (PD) occurs if the surface area approximation (product of the longest diameter by greatest perpendicular diameter) for one or more measurable lesions increases by 25% or if one or more new lesions appear. A **complete response (CR)** is when all lesions disappear and are absent on two different observations that are no less than four weeks apart. A **partial response (PR)** is noted when the measurable lesions persist, but have decreased in size by 50% or more as measured on two different observations not less than four weeks apart. When measurable disease has not increased more than 25% in size nor decreased greater than 50% in size, the classification of “no change (NC)” is given. Both measurable disease and unmeasurable disease are used in the evaluation of the patient, with assessment of response involving all parameters. In measurable disease, the poorest response designation prevails in the final response classification.^{1, 2}

RECIST Criteria for Reporting Tumor Response:

In contrast to the standard bidimensional WHO criteria for the radiologic assessment of response of solid tumors, which were developed prior to helical CT and other digital imaging

techniques, new guidelines which utilize *unidimensional measurements* and modern imaging techniques have been widely adopted for clinical research protocols. A special report published in 2000 outlined the new “Response Evaluation Criteria in Solid Tumors (RECIST).³ The primary changes with the newer criteria relate to the adoption of unidimensional tumor size measurement, better defining the cut-off point for progressive disease, and specifying clear-cut guidelines about minimum lesion size and the number of lesions to evaluate when multiple ones are present.

With the RECIST criteria, only patients with measurable disease at baseline are included in protocols where objective tumor response is the primary end point. Measurable disease means the presence of at least one measurable, histologically confirmed lesion that can be accurately measured in at least one dimension of 2 cm or greater for conventional radiographic, CT, and MRI techniques and 1 cm or greater with helical CT techniques. Lesions smaller than these values, as well as bone lesions, leptomeningeal disease, ascites, pleural effusion, pericardial effusion, lymphangitic carcinomatosis, cystic lesions, and abdominal masses that are not confirmed and followed by imaging techniques are considered non-measurable lesions. The recommendations favor the use of MRI and helical CT given their reproducibility and ability to consistently display measurable target lesions. Lesions on chest radiography may be used as measurable disease if they are clearly defined and surrounded by aerated lung. Ultrasound (US) should not be used to measure target lesions for objective tumor response.

With the RECIST criteria, it is important for the radiologist to properly select and document “target” and “non-target” lesions. For **target lesions**, representative measurable lesions up to a maximum of five per organ and ten in total should be identified and recorded at baseline. These lesions should be selected with regard to their size, with longer diameter lesions favored, as well as lesions which are suitable for accurate, repeated measurements on imaging follow-up. All other lesions or sites of disease should be identified as **non-target lesions** and should also be recorded at baseline. These lesions are not measured, but the presence or absence of each should be reported on all follow-up examinations.

Response criteria with RECIST for target lesions includes **complete response (CR)** with the disappearance of all lesions, **partial response (PR)** with at least a 30% decrease in the sum total of the longest diameters of the target lesions compared to baseline, **progressive disease (PD)** with the appearance of new lesions or at least a 20% increase in the sum total of the longest diameters of the target lesions compared to the smallest sum total of longest diameters since treatment started, and **stable disease (SD)** where there is neither significant tumor shrinkage nor growth to qualify as PR or PD, respectively.³

Applications in Thoracic Oncology:

While new protocols will typically utilize the RECIST criteria to assess solid tumor response to drug therapy, some older protocols may still be active which used the older WHO criteria.

Therefore, radiologists should be familiar with both criteria and their role in oncologic imaging. A meta-analysis of the data in eight studies of different solid tumors where the two different criteria were separately applied and reanalyzed demonstrated generally good correlation in that unidimensional measurement of maximal tumor diameter was felt to be sufficient to assess significant change in tumor size.⁴ Similar results have been obtained in studies of lung cancer response where the unidimensional and bidimensional criteria were compared.^{5,6} In these studies, there was generally good correlation between the final assessments, with a small number of differences noted in the some response categories. Interestingly, in the study by Werner-Wasik *et al.*, which also included comparison with tumor volume, the validity of the RECIST criteria were confirmed and volume did not appear to represent a significantly superior method for evaluating tumor response.

REFERENCES :

1. Who handbook for reporting results of cancer treatment. Geneva (Switzerland): World Health Organization Offset Publication No. 48.; 1979.
2. General forms and guidelines. In: Southwest Oncology Group Clinical Research Associate Manual. Vol. II; 2002.
3. Therasse P, et al. New guidelines to evaluate the response to treatment in solid tumors. *J Natl Cancer Inst*; 92(3): 205-216.
4. Eisenhauer JK, et al. Measuring response in solid tumors: unidimensional versus bidimensional measurement. *J Natl Cancer Inst* 1999;91(6):523-528.
5. Cortes J, et al. Comparison of unidimensional and bidimensional measurements in metastatic non-small cell lung cancer. *Br J Cancer* 2002;87:158-160.
6. Werner-Wasik M, et al. Assessment of lung cancer response after nonoperative therapy: tumor diameter, bidimensional product, and volume. A serial CT scan-based study. *Int J Radiat Oncol Biol Phys* 2001;51:56-61.

Assessing Growth of Indeterminate Nodules

Helen T. Winer-Muram, M.D.

Indiana University

Why measure growth?

Indeterminate lung nodules have been considered to be benign if they 1) have a “benign” pattern of calcification or 2) do not grow over a period of two years. Controversy has arisen, however, about these indicators. Gurney had four radiologists review radiographic features of 44 malignant nodules and showed that 5% had a “benign” pattern of growth. Yankelevitz et al. have used data from early studies of radiographic nodule growth to calculate that the predictive value of no growth is only 65%.

Measurement of nodule growth rates offer a way to separate benign from malignant nodules. Chest radiographic data have shown that most malignant nodules double in volume in between 20 and 400 days. Nodules that grow more quickly are more likely to be infectious, while those that grow more slowly are likely to be benign nodules (e.g., hamartomas, granulomas) (Nathan).

Moreover, the advent of lung cancer screening makes the determination of nodule growth rates even more important. Screening may preferentially detect slow-growing nodules that may not be lethal. Patients with fast-growing nodules may not be curable even if the nodules are detected when they are small. In addition, the rate of growth of the lung cancer might be correlated with disease-specific mortality.

How do tumors grow?

For growth rates to be used for clinical decision making, it is best that the tumor growth is linear. This fact has been suggested by past radiological studies. From chest radiography (41 cases) it has been shown that tumors have a linear increase in volume over time (Garland, 1963). Once the growth levels off, (upper horizontal asymptote) there is a lethal burden of tumor and the patient is near death. That is generally at about 40 doubling times.

As radiologists view nodules, we get the misconception that tumors grow faster as they enlarge. The same percent growth of a large diameter is more noticeable than that of a smaller diameter.

Why “watch” a nodule and not immediately get tissue?

Many CT-detected indeterminate nodules are too small (< 1 cm diameter) for fine needle aspiration biopsy, and some larger nodules are in anatomic locations that make biopsy difficult. In areas endemic for fungal disease, we cannot biopsy all of the indeterminate nodules that are discovered with CT. Lung cancer screening programs in the Midwest have shown that 50% of patients have indeterminate nodules, most of which are benign at biopsy. Currently 20% to 40% of all resected nodules are benign. Swenson et al. have proposed including an enhanced CT study to aid in discriminating benign from malignant nodules; nodule enhancement of < 20 HU with CT (4 scans at 1 minute intervals after contrast injection) has a negative predictive value of 98%.

To use nodule growth rate as a way to distinguish between benign and malignant lesions, it must be demonstrated that a clinically acceptable delay between initial and followup CT scans is

usually sufficient to show growth. “Watchful waiting” even for one month is controversial, even though no one has shown that such a delay would have deleterious effects. In addition, measurements to assess for growth must be reproducible. Several studies using different methods have been reported.

Radiography studies – diameter method

(For spherical tumors a 25% increase in diameter ~ a 100% increase in volume.)

Usada et al measured the doubling times (DTs) of lung cancer nodules in 174 patients. The DTs ranged from 30 to 1077 days; 7% of patients had DTs > 500 days. In that study the DT was an independent predictor of mortality. In a retrospective review of 300 cases, the DTs for adenocarcinomas were 185 days, squamous cell carcinomas were 90 days, and small cell carcinomas were 65 days (Friberg). Aoki et al. described DTs vary that ranged from 42 to 1486 days in 27 cases of bronchioloalveolar cell carcinomas.

Hopper found the interobserver variability to be < 15%, with a minimal detectable change of 3 to 5 mm (Hopper).

CT studies – diameter method

Yankelevitz et al. (1999) have calculated that the minimal measurable change in diameter is 0.3 mm or one pixel. Even a nodule of 1 cm diameter with a 180 day DT will have measurable change in diameter if the interval between CT scans is at least 28 days.

In a screening study, Hasegawa et al. measured 82 cancers (most adenocarcinoma) and found 27 had DTs > 450 days (33%) and 12 had DTs > 730 days (15%). They pointed out that use of a screening population may lead to a bias toward slow-growing tumors.

Harris measured phantoms using different window/level settings. Measurements were highly accurate with lung window settings and inaccurate with soft tissue settings. This is evidence that serial measurements should be done with the same window/level settings.

CT studies – maximum cross sectional area method

Yankelevitz measured the maximal cross-sectional areas of 9 malignant nodules. All had diameters < 10 mm and all had projected change in area of $\geq 18\%$ in 30 days. The DTs were all < 124 days. (range 53-124 days, median 75 days)

For repeated area measurements of small tumors, Staron found the intraobserver coefficient of variation to be only 4-7% for an object of cross-sectional area of 705 mm^2 , a typical size for a stage I lung tumor.

CT studies – volume method

An exciting new development is that of volumetric measurement of nodules. Because volume varies with the cube of the diameter, for a given time period the percent change in volume is greater than the percent change in the diameter. If volume and diameter measurements are equally precise, volume changes should be detectable earlier than diameter changes. As cross-

sectional area varies with the square of the diameter, volume change should be detectable more quickly than area change as well.

Tiitola showed excellent interobserver agreement ($k = 0.78$) for manual volume measurements of irregular phantoms (8.7 cm^3 to 31.6 cm^3). Intraobserver agreement was even better. Yankelevitz et al. measured volumes of spherical phantoms (3-11 mm diameter) and showed $<3\%$ variation in measurements. They also used automated 3-D reconstruction to measure the volumes of 5 malignant and 8 benign nodules on initial and followup CT scans, and showed no overlap in DTs (cross-sectional area derived DTs did show overlap).

Our group has published the results of manual volume measurements in 50 patients with early lung cancer. The median DT was 181 days; 11 had DTs > 465 days (22%). There was considerable overlap between histologic subtypes. We continue to accrue patients and refine our methodology, and continue to find a wide range in DTs and a large number of patients with very long DTs.

Advantages of volume measurement

As previously mentioned, volume change should be detectable more quickly than area or diameter change. In addition, volume measurement accounts for growth in the z -axis, which may be asymmetric compared with that in the x - y plane. One also does not need to match images as one does for diameters and cross sectional areas.

Problems of volume measurement

The major source of error in volume measurement is the partial volume effect. The magnitude of this source of error varies inversely with the size of nodule (larger is better), directly with section width (smaller is better), and directly with the orientation of the nodule (long axis along z -axis is better). We have been developing methods to reduce this error with some success. Patient motion (breathing and cardiac) decreases measurement precision and is noticeable in up to 25% of studies. Misregistration may also lead to errors.

In addition, errors common to all measurement methods include the inclusion of adjacent structures, or adjacent areas of atelectasis or pneumonitis, in the dimensions of the tumor.

For precise manual measurement of volumes on serial CT scans -

KEEP EVERYTHING THE SAME!

Same CT scanner

Same scan parameters (kVp and mA)

Same pitch and section width

Same viewing station and window/level settings

Same field-of-view (FOV) – this may be less important

Same radiologist if possible

The introduction of multislice scanners and automated measurement techniques will reduce some of the sources of error in volume measurement because reproducibility will increase, and patient motion will become less noticeable. In addition, narrower section widths will reduce the partial volume effect. However, separating tumor from other structures (segmentation) will still be an issue, and appropriate window/level setting must be chosen (threshold selection).

Final thought

If a 1 cm^3 nodule = 32 generations = 10^9 cells, and we assume that the rate of growth is linear, an adenocarcinoma will grow for 22.5 years to become 1 cm^3 and a squamous cell carcinoma will grow for 7.8 years to become 1 cm^3 . It will be interesting to see if lung cancer screening can actually reduce disease specific mortality.

REFERENCES:

- Yankelevitz DF, Henschke CI. Does 2-year stability imply that pulmonary nodules are benign? *AJR* 1997;168:325-328
- Good CA, Wilson TW. The solitary circumscribed pulmonary nodule: study of seven hundred fifty cases encountered roentgenologically in a period of three and one half years. *JAMA* 1958;166:210-215
- Lillington GA. Benign tumors. In Murray JF, Nadel JA. eds *Textbook of respiratory medicine* 2nd ed. Philadelphia Saunders 1995;1622-1630
- Midthun DE, Swenson SJ, Jett JR. Clinical strategies for solitary pulmonary nodule. *Annu Rev Med* 1992;43:195-208
- Lillington GA, Caskey CI. Evaluation and management of solitary and multiple pulmonary nodules. *Clin Chest Med* 1993;14:111-119
- Gurney JW, Lyddon DM, McKaay JA. Determining the likelihood of malignancy in solitary pulmonary nodules with Bayesian analysis Part II. *Application Radiology* 1993;186:415-422
- Friberg S, Mattson S. On the growth rates of human malignant tumors: Implications for medical decision making. *J of Surgical Oncology* 1997;65:284-297.
- Garland LH, Coulson W, Wollin E. The rate of growth and apparent duration of untreated primary bronchial carcinoma. *Cancer* 1963;16:694-707
- Nathan MH, Collins VP, Adams RA. Differentiation of benign and malignant pulmonary nodules by growth rate. *Radiology* 1962;79:221-231
- Cummings SR, Lillington GA, Richard RJ. Managing solitary pulmonary nodules: the choice of strategy is a "close call." *Am Rev Resp Dis* 1986;134:453-460
- Swenson SJ, Brown LR, Colby TV, Weaver AL, Midthun DE. Lung nodule enhancement at CT: Prospective findings. *Radiology* 1996;201:447-455
- Aoki T, Nakata H, Watanabe H, et al. Evolution of peripheral lung adenocarcinomas: CT findings correlated with histology and tumor doubling time. *AJR* 2000;174:763-768
- Staron RB, Ford E. Computed tomographic volumetric calculation reproducibility. *Invest Radiol* 1986;21:272-274
- Harris KM, Adams DC, Lloyd DCF, Harvey DJ. The effect on apparent size of simulated pulmonary nodules of using three standard CT window settings. *Clin Radiology* 1993;47: 241-244
- Usada K, Saito Y, Sagawa M, et al. Tumor doubling time and prognostic assessment of patients with primary lung cancer. *Cancer* 1994;74:2239-44
- Yankelevitz DF, Gupta R, Zhao B, Henschke CI. Small pulmonary nodules: Evaluation with repeat CT – preliminary experience. *Radiology* 1999;212:561-566
- Hasegawa M, Sone S, Takashima S, et al. Growth rate of small lung cancers detected on mass CT screening *Br J Radiol* 2000;73:1252-1259
- Yankelevitz DF, Reeves AP, Kostis WJ, Zhao B, Henschke CL. Small pulmonary nodules volumetrically determined growth rates based on CT evaluation. *Radiology* 2000;217:251-256
- Tiitola M, Krivisaari L, Tervaahaartiala P, Palomaaki M, Kivisaari RP, Mankinen P, Vehmas T. Estimation or quantification of tumor volume? CT study on irregular phantoms. *Acta Radiologica* 2001;42:101-105

Van Hoe L, Haven F, Bellon E, Baaert AL, Bosmans H, Feron M, Suetens P, Marchal G. Factors influencing the accuracy of volume measurements in spiral CT: A phantom study. *JCAT* 1997;21:(2)3322-338.

Winer-Muram HT, Jennings, SG, Tarver R, Aisen AM, Tann M, Conces DJ, Meyer CA. Volumetric growth rate of stage I lung cancer prior to treatment: Serial CT scanning. *Radiology* 2002;223:798-805

Winer-Muram HT, Jennings, SG, Meyer CA, Liang Y, Aisen AM, Tarver R, McGarry R. Effect of varying CT section width on volumetric measurement of lung tumors and application of compensatory equations. *Radiology* (in press)

Swensen SJ, Brown LR, Colby TV, Weaver AL, Midthun DE. Lung nodule enhancement at CT: prospective findings. *Radiology* 1996;201:447-455

Lung Cancer Staging

Ann N. Leung, M.D.

Objective: To review the international (TNM) system for staging lung cancer with emphasis on identification of non-resectable disease.

INTERNATIONAL SYSTEM FOR STAGING LUNG CANCER

In patients with non-small cell lung cancer, staging is performed for both prognostic and therapeutic purposes. The international system enables a consistent and reproducible description of the extent of tumor by use of three anatomic descriptors: T, N, and M (1). T refers to the status of the primary tumor with numerical suffixes ranging from 1 – 4 which describe increasing size or extent. N refers to the status of the regional lymph nodes with suffixes ranging from 0 – 3 which describe increasing extent; M refers to the status of metastatic involvement with suffixes 0 and 1 which describe its absence or presence, respectively. Overall stage of disease is then derived from grouping of TNM subsets, which share similar prognosis and treatment options.

CT AND MR ASSESSMENT OF TNM DESCRIPTORS

Assessment of the T descriptor requires determination of the size and anatomic extent of tumor and its relation to a number of intrathoracic structures. In the TNM system, T4 or unresectable primary tumors invade the mediastinum, heart, great vessels, trachea, esophagus, vertebral body, or carina; or are associated with a malignant pleural or pericardial effusion; or are associated with a satellite tumor nodule or nodules within the ipsilateral primary tumor lobe. CT and MR are roughly equivalent in their accuracy of T staging in patients with lung cancer (2); MR has been shown to be slightly superior in the assessment of chest wall invasion and mediastinal invasion and in determining the superior extent of Pancoast tumors (2-4).

Assessment of the N descriptor requires determination of the extent of regional lymph node involvement. In the regional lymph node classification system (5) adopted by the American Joint Committee on Cancer in 1997, 14 numbered stations are used to designate the status of mediastinal, hilar, and intrapulmonary nodes. In the TNM system, N3 or unresectable nodal disease consists of metastasis to contralateral mediastinal, contralateral hilar, ipsilateral or contralateral scalene, or supraclavicular nodes. CT and MR have been shown to be roughly equivalent in their accuracy of N staging in patients with lung cancer (2, 6). Using 1 cm short axis diameter as the size criterion for a pathologically enlarged node, sensitivity and specificity of CT for nodal metastases have been reported to range from 61-64% and 62-93%, respectively (7,8).

Distant metastases in a patient with non-small cell lung is classified as M1, unresectable disease. Traditionally, the standard evaluation for detection of metastatic disease has consisted of a history and physical, hematologic survey, liver enzyme analysis, and CT of the chest and upper abdomen. In the absence of clinical signs and symptoms or laboratory and radiologic abnormalities, the patients have been presumed to be free of distant disease.

PET STAGING OF LUNG CANCER

Staging of lung cancer with whole-body PET imaging is an accurate method to distinguish between patients with resectable versus nonresectable disease (9). In comparison to cross-sectional modalities, PET has both significantly higher sensitivity (range, 83 – 93%) and specificity (range, 82 – 99%) in identifying nodal involvement (N status). Whole-body PET imaging also permits detection of distant metastases without any further increase in radiation exposure to patients. This ability to detect both local and distant metastatic disease has been shown to significantly alter management in up to 37% of evaluated patients presenting with non-small cell lung cancer (10).

Marom et al (9) compared the accuracy of whole-body PET to conventional imaging (thoracic CT, bone scintigraphy, and brain CT or MR) for detection of extrathoracic metastases, PET was shown to be superior for identification of metastases involving the bone, adrenals, and liver. However, because of normally high levels of glucose uptake in the brain, PET had lower sensitivity than CT or MR for detection of metastases to the brain.

REFERENCES:

1. Mountain CF. Revisions in the International System for Staging Cancer. *Chest* 1997; 111: 1710-1717.
2. Webb WR, Gatsonis C, Zerhouni EA, et al. CT and MR imaging in staging non-small cell bronchogenic carcinoma: report of the Radiologic Diagnostic Oncology Group. *Radiology* 1991; 178:705-713.
3. Musset D, Grenier P, Carrette MR, et al. Primary lung cancer staging: prospective comparative study of MR imaging with CT. *Radiology* 1986; 160:607-611.
4. Heelan RT, Demas BE, Caravelli JF, et al. Superior sulcus tumors: CT and MR imaging. *Radiology* 1989; 170: 637-641.
5. Mountain CF, Dresler CM. Regional lymph node classification for lung cancer staging. *Chest* 1997; 111:1718-1723.
6. Martini N, Hellan R, Westcott J, et al. Comparative merits of conventional, computed tomographic, and magnetic resonance imaging in assessing mediastinal involvement in surgically confirmed lung cancer. *J Thorac Cardiovasc Surg* 1985; 90:639-648.
7. Staples CA, Muller NL, Miller RR, Evans KG, Nelems B. Mediastinal nodes in bronchogenic carcinoma: comparison between CT and mediastinoscopy. *Radiology* 1988; 167:367-372.
8. McLoud TC, Bourguoin PM, Greenberg RW, et al. Bronchogenic carcinoma: analysis of staging in the mediastinum with CT by correlative lymph node mapping and sampling. *Radiology* 1992; 182:319-323.
9. Marom EM, McAdams HP, Erasmus JJ, et al. Staging non-small cell lung cancer with whole-body PET. *Radiology* 1999;212:803-809.
10. Saunders CAB, Dussek JE, O'Doherty MJ, Maisey MN. Evaluation of fluorine-18-fluorodeoxyglucose whole body positron emission tomography imaging in the staging of lung cancer. *Ann Thorac Surg* 1999;67:790-797.

Endoscopic Ultrasound Staging of Lung Cancer

James Ravenel, M.D.

Medical University of South Carolina

Learning Objectives:

- 1) Discuss the role in EUS in the staging of lung cancer
- 2) Identify appropriate indications for EUS
- 3) Identify typical locations for performing EUS/FNA

Endoscopic ultrasound (EUS) is a relatively recent technique that was initially utilized to evaluate gastrointestinal tumors. As the ultrasound probes and skills of endoscopists improved a wider array of applications have become available including evaluation of the liver, and mediastinum. At our institution EUS with fine needle aspiration (FNA) has become a vital tool in the staging of lung cancer, complementing CT, PET bronchoscopy and surgical staging.

Technique

Although a trained endoscopist is required, one of the great advantages of EUS/FNA is that it can be performed in an outpatient setting with conscious sedation. Using an echoendoscope, the procedure is similar to traditional endoscopy. Sonography is performed most frequently with a 5-10 MHz linear-array probe. Radial scanning may be used as well. Our endoscopists sample any lymph node greater than 1 cm seen, followed by non-enlarged lymph nodes (usually levels 5,7 and 8) as appropriate. Typically, three to four passes are made into each node evaluated with a 22-gauge needle. The entire procedure takes approximately 20-30 minutes. The complication rate is extremely low (0.03% for perforation of the cervical esophagus). The instances of perforation at the biopsy site and procedure induced bacteremia are likewise extremely rare.

Results

EUS Alone

Initial reports utilizing EUS staging focused on morphologic and sonographic features of lymph nodes. Sonographic features suggestive of malignancy include size > 1cm, distinct margin, round shape and decreased echogenicity. Combining the first three criteria results in a specificity of 80%. Features favoring benignity include oval or triangular shape and a central echogenic region. The majority of lymph nodes, however, are uniformly hypoechoic. Overall, sonographic criteria alone have a sensitivity ranging from 45-75% for malignancy. EUS may also be useful by confirming T4 disease. EUS can demonstrate direct invasion of the trachea, esophagus and vascular structures. EUS tends to overstage tumors when mediastinal invasion without organ or vascular involvement is suspected.

EUS with FNA

When coupled with FNA, morphologic and sonographic criteria need not be applied. While suspicious nodes by these criteria may be sampled first, any N2 lymph node visualized can usually be aspirated. Because a positive result is generally accepted as proof of mediastinal disease, specificity is usually quoted at 100% and based on this result no more invasive staging needs to be performed. False negative results in mediastinal staging may occur for two reasons. The first is due to sampling error; that is FNA fails to obtain malignant cells from a metastatic node. The second relates to regions not evaluated by EUS. Pre- and paratracheal lymph nodes are infrequently seen by EUS due to the inability of ultrasound to penetrate the air-filled

trachea. Prevascular lymph nodes (level 6) can be seen by EUS but are usually not sampled due to major blood vessels (aorta, pulmonary artery) in the path of the needle. Even so, most reports show a sensitivity for EUS-FNA to range from 87-95%. The use of this technique is particularly helpful in limiting the number of mediastinoscopies by documenting N2 disease (up to 80% in some reports). Because level 2, 3, and 4 lymph nodes are generally not visualized, a negative EUS-FNA does not preclude mediastinoscopy prior to planned curative resection especially if enlarged, or PET positive lymph nodes are seen on cross sectional imaging.

In most cases, the positive yield of EUS can be increased by selecting individuals with enlarged lymph nodes at levels 5, 7, and 8 at CT. In patients with no enlarged lymph nodes at CT, EUS still may find N2 disease in up to 1/3 of patients. Because level 5 requires either extended cervical medianstinoscopy or anterior mediastinotomy, EUS is particularly well suited for the evaluation of the mediastinum in left upper lobe neoplasms. Similarly, EUS offers a more complete evaluation of the sub-carinal lymph nodes compared to mediastinoscopy.

Distant disease is also occasionally accessible by EUS-FNA. Pleural effusions, the left adrenal gland and selected liver lesions are sites outside the mediastinum that have been successfully biopsied during EUS.

Conclusion

EUS-FNA is a valuable adjunct for staging lung cancer. It is particularly useful for confirming mediastinal disease and therefore obviating the need for surgery.

REFERENCES:

- Bhutani MS, Hawes RH, Hoffman BJ. A comparison of the accuracy of echo features during endoscopic ultrasound (EUS) and EUS-guided fine-needle aspiration for diagnosis of malignant lymph node invasion. *Gastrointest Endosc.* 1997; 45:474-479.
- Gress FG, Savides TJ, Sandler A., et. al. Endoscopic ultrasonography, fine-needle aspiration biopsy guided by endoscopic ultrasonography, and computed tomography in the preoperative staging of non-small-cell lung cancer: A comparison study. *Ann Intern Med.* 1997; 127:604-612.
- Fritscher-Ravens A, Soehendra N, Schirrow L, et. al. Role of transesophageal endosonography-guided fine-needle aspiration in the diagnosis of lung cancer. *Chest.* 2000; 117:339-345.
- Larsen SS, Krasnik M, Vilmann P, et. al. Endoscopic ultrasound guided biopsy of mediastinal lesion has a major impact on patient management. *Thorax.* 2002; 57:98-103.
- Silvestri GA, Hoffman BJ, Bhutani MS, et. al. Endoscopic ultrasound with fine-needle aspiration in the diagnosis and staging of lung cancer. *Ann Thorac Surg.* 1996; 61:1441-1446.
- Wallace MB, Silvestri GA, Sahai AV, et. al. Endoscopic ultrasound-guided fine needle aspiration for staging patients with carcinoma of the lung. *Ann Thorac Surg.* 2001; 72:1861-1867.
- Wiersema MJ, Vazquez-Sequeiros E, Wiersema LM. Evaluation of mediastinal lymphadenopathy with endoscopic US-guided fine-needle aspiration biopsy. *Radiology.* 2001; 219:252-257.
- Wiersema MJ, Vilmann P, Giovanni M, et. al. Endosonography-guided fine-needle aspiration biopsy: Diagnostic accuracy and complication assessment. *Gastroenterology.* 1997; 112:1087-1095.

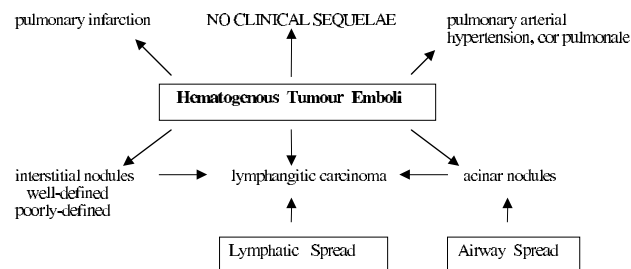
Metastatic Disease to Lung

Gordon L. Weisbrod, M.D.

Medical Imaging

University Health Network

Pulmonary Metastatic Disease



Spread of Tumour to Lungs

1. Via pulmonary (or bronchial) arteries
→ interstitial nodules or lymphangitic spread.
2. Via pulmonary and pleural lymphatics
→ lymphangitic spread from mediastinal and hilar nodes.
3. Via thoracic duct into right side of heart.
4. Via the airways (BAC).
5. Via communicating lymphatic channels from upper abdominal nodes and peritoneal cavity (i.e. Ca ovary).

Pulmonary Metastatic Disease: Radiological-Surgical Correlation

100 lungs – 84 patients – previously treated extrathoracic malignancies

237 nodules resected – 173 (73%) CT – 151 (82%) metastatic
 207 (87%) metastatic
 21 (9%) benign
 9 (4%) bronch Ca

nodules - +CT } 100%
 +CHX } Metastatic

nodules: + CT }
 - CXR } 84% Metastatic

65 solitary nodules on CXR - 35 (54%) solitary at surgery
 44 solitary nodules on CT - 35 (80%) solitary at surgery
 (Peuchot and Libshitz, Radiology 1987; 164:719-722.)

Frequency of Pulmonary Metastases

Autopsy 30-53%

High frequency - rich vascular supply Renal cell
 - systemic venous drainage Chorio
 Bone sarcoma

Incidence of Metastases Found at Initial Presentation versus Autopsy

Choriocarcinoma (female)	60	70-100
Lung (unresectable)	34	20-40
Kidney	5-30	50-75
Rhabdomyosarcoma	21	25
Wilms'	20	60
Ewing's	18	77
Osteosarcoma	15	75
Testis	2-12	70-80
Bladder	5-10	25-30
Thyroid	4-10	65
Melanoma	5	66-80
Prostate	5	13-53
Head and Neck	5	13-40
Colon/Rectum	<5	25-40
Cervix	<5	20-30
Ovary	<5	10
Lung (resectable)	5	---
Breast	4	60

Thoracic Metastases from Thyroid Carcinoma

- Direct invasion of trachea – usually poorly differentiated Ca.
- 10% follicular; 5% of papillary Ca.
- I¹³¹ uptake – 50% (CXR may be N).
- More favourable prognosis: micronodular mets; I¹³¹ uptake; papillary type; age <40.
- Micronodules may persist for many years unchanged.

Medullary Carcinoma of Thyroid

- 3.5-10% of thyroid malignancies.
- Mediastinal/hilar adenopathy – calcification; interstitial infiltrate (amyloid); calcified lung nodules.
- Sporadic or familial (MEA II); biochemical marker – calcitonin

Thoracic Metastases in Melanoma

- Uncommon clinically (12%) but common at autopsy.
- Solitary, *multiple, miliary nodules
- Lymphangitic spread
- Diffuse alveolar infiltrate
- Endobronchial

*hilar/mediastinal adenopathy (~50%); pleural effusion
 FNA usually diagnostic (melanin; protein S-100 IMH)

Thoracic Metastases from Breast Carcinoma

- Lymphatic spread is commoner than vascular
- Lymphangitic carcinomatosis
- Mediastinal /hilar adenopathy
 lung nodules (15-25%)
 endobronchial
- Pleural effusion – usually unilateral on same side as breast Ca
- May occur late

Thoracic Metastases from Bronchogenic Carcinoma

Autopsy incidence 7-50%

Clinical incidence low except for SCAC and BAC

- Routes via:
- systemic vv from systemic metastases (liver)
 - pulmonary lymphatics and R lymphatic duct to R subclavian v
 - bronchial vv to systemic vv
 - pulmonary vv to systemic aa (bronchial aa)
 - pulmonary a (primary invasion)
 - airways (BAC)

Thoracic Metastases from Colorectal Carcinoma

- Incidence 10-20%
- Single or multiple nodules – cavitation
- Endobronchial
- Single nodule an equal chance of being a primary or secondary neoplasm
- Most have liver mets
- Survival after resection 40% at 5 years, 30% at 10 years

Thoracic Metastases from Renal Cell Carcinoma

- 30-45% of patients with metastatic RCC to lung will have no kidney symptoms
- >60% involve thorax at some time (autopsy incidence 55-77%)
 - *single or multiple pulmonary nodules; embolic occlusion of pulmonary arteries; endobronchial (stimulate bronchogenic Ca)
 - hilar/mediastinal adenopathy (7.2-28.2%) – pseudosarcoid; isolated R lower hilar
 - pleural
- Late appearance of metastases (up to 50 years)
- Spontaneous disappearance of metastases (postnephrectomy)

Thoracic Metastasis from Testicular Neoplasms

- Incidence of pulmonary metastases – chorio Ca 81%, seminoma 19%, nonseminoma 18%.
- (Seminoma) – mediastinal lymphadenopathy – subcarinal, post med
- (Teratoma) – single or multiple pulmonary nodules; endobronchial; low attenuation masses (CT)
- Chemotherapy – metastatic teratoma – cure rate > 70%
- Persistent nodules after chemotherapy
 - Resistant metastases
 - Necrotic/fibrotic sterile metastases } Tumour Markers
 - Benign well-differentiated teratomas (25%) } Normal
 - (selective destruction of malignant elements)

Nodules – Not Too Concerning

- Ill-defined
- Small
- Subpleural
- Calcified
- Clusters or groups in one area
- Associated with bronchial abnormalities (wall thickening, mucoid impaction, dilatation)
- Tree-in-bud
- Centrilobular
- No history of malignancy

Nodules – More Concerning

- Well-defined
- Small or larger
- Random
- Growing
- History of malignancy

Accuracy of Imaging

- 37%
- Underestimated in 39%
- Overestimated in 24%

Thoracic Metastases from Prostate Carcinoma

Clinical incidence 4.9-6.7%

Autopsy incidence 13-53%

- Lymphangitic carcinomatosis
- Nodules
 - Pleural effusion } Unusual
 - Adenopathy }
- Endobronchial
- Most patients have associated bony metastases
- Immunoperoxidase stain specific for prostatic acid phosphatase

Multiple Pulmonary Leiomyosarcomas

(Benign Metastasizing Fibroids)

- Usually in females with a history of hysterectomy for fibroids
- Multiple well defined noncalcified pulmonary nodules
- Slow progression (regression during pregnancy) – good prognosis
- Probably metastatic low grade leiomyosarcoma rather than hamartoma

Thoracic Metastases from Cervical Carcinoma

Incidence 1.7-9.1%

Autopsy incidence 15-25%

- Single or multiple nodules – cavitation
- Adenopathy
- Pleural

Thoracic Metastases from Ovarian Carcinoma

Incidence 1-34%

- *Pleural effusion (via diaphragmatic lymphatics)
- Lung nodules (interstitial or alveolar)
- Lymphangitic

Thoracic Metastases from Gestational Trophoblastic Neoplasms

Hydatidiform mole, invasive mole, choriocarcinoma

Choriocarcinoma – mets common – incidence 45-87%

Remission rate after chemotherapy high (up to 88%)

- Multiple well-defined nodules
- Multiple poorly-defined alveolar nodules (hemorrhage) – halo sign on CT
- Embolic occlusion of pulmonary arteries
 - pulmonary infarction
 - pulmonary arterial hypertension
- Arteriovenous shunting
- Sterile metastasis – HCG normal
- Spontaneous remission after removal of primary

Thoracic Metastases from Osteosarcoma

- Frequent
- Lungs are initially the sole site of metastasis in most patients
- Aggressive resection of pulmonary metastases
- Single or multiple nodules - calcification
 - cavitation
- Spontaneous pneumothorax

Thoracic Metastases from CNS

- Rare
- Meningioma – usually prior surgery or shunting

Nodular Metastases

- Multiple, lower lung, variable size, peripheral
- May occur in relation to peripheral pulmonary arteries (CT) but more commonly eccentric or peripheral in 2° lobule
- Rarely miliary
- Acinar nodules (stomach, pancreas)
- Lepidic grown similar to BAC
- CT (especially “cine” spinal CT on workstation) highly sensitive
- Specificity is lower – granulomas and nodes
- DDX sarcoidosis, silicosis, amyloidosis, granulomas

Nodular Metastases

- Halo of GGO – highly vascular or hemorrhagic tumours (angiosarcoma, chorio)

Nodular Metastases

- Nodular or beaded thickening of the peripheral pulmonary aa
- Intravascular tumour emboli

Solitary Lung Metastases

Relatively uncommon (2-10% of SPN)

Colon (esp. rectosigmoid) 30-40%

Sarcomas (bone), kidney, breast, testis, melanoma

- Usually smooth and well-defined but may be irregular or spiculated
- Squamous Ca elsewhere – new primary lung (us squamous)
- Adeno Ca elsewhere – equal chance of new 1 vs 2
- Soft tissue tumour, bone sarcoma, melanoma elsewhere - metastatic
- 5 year survival postresection – 25-30%

Sterilized Metastases

- Testicular Ca
- Chorio Ca

Lymphangitic Carcinomatosis – Chest Radiology

Reticular/nodular infiltrate

Kerley B lines unilateral findings – lung

Pleural/subpleural edema – breast

Hilar/mediastinal adenopathy – (20-40%)

Pleural effusion (30-50%)

- ?specificity of findings - low
- sensitivity ~50%

Lymphangitic Carcinomatosis – HRCT

Irregular or nodular thickening of bronchovascular bundles

Polygonal lines; interlobular septal thickening

Increased number/thickness of interstitial lines

Nodules

Thickening/irregularity or nodularity of fissures

Adenopathy <50%

Effusion (30%)

Preservation of normal lung architecture

Much more sensitive and specific than CHX

Lymphangitic Carcinomatosis

23 autopsy cases of L.C. (Janower, Blennerhassett)

- 11 metastasis in hilar nodes (5 radiol)
- 20 tumour emboli in small vessels

Common – seen in over 50% of lung mets

Sites: stomach, lung, breast, prostate, pancreas

Cavitation in Pulmonary Metastases

- Main cause is vascular invasion and ischemic necrosis; specific tissue characteristics
- 4% of metastases cavitate (9% of primary)
- 69% squamous cell – head and neck in males – small, thin-walled – cervix in females
- 31% adenocarcinoma (colon, breast)
- Sarcomas (especially bone)

Spontaneous Pneumothorax in Pulmonary Metastases

- Most commonly osteosarcoma (5% with mets)
- May antedate metastases radiologically
- Mechanism
 - Rupture of metastasis into bronchus and pleura
 - bronchopleural fistula
 - May occur during or after a good response to cytotoxic chemotherapy
 - Partial bronchiolar obstruction with check - valve mechanism

Calcification in Pulmonary Metastases

- Rare
- Osteogenic, chondro, synovial carcinoma
- Papillary and mucinous adenocarcinomas of thyroid, ovary, GIT
- Dystrophic calcification in necrotic tumour post-treatment

Endotracheobronchial Metastases

- Clinically important incidence of 2-5% in patients dying from metastatic disease
- May simulate bronchogenic carcinoma clinically and radiologically
- Renal cell, colorectal, breast carcinoma, and melanoma most frequent
- Mechanism – via bronchial artery
 - via peribronchial lymphatics

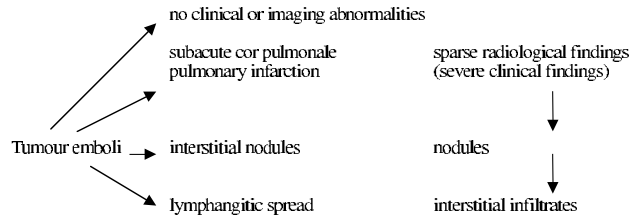
Tumour – Embolic Pulmonary Arterial Hypertension

Tumour emboli occur in 26% of cancer patients at autopsy

Clinically significant in <1%

- Bronchogenic Ca (especially adeno)
- Renal cell
- Chorio
- Hepatocellular
- Breast } especially with hepatic metastases
- Stomach }

Tumour – Embolic Pulmonary Arterial Hypertension



Selection of Patients for Pulmonary Resection

- Primary tumour is controlled or controllable
- No extrapulmonary tumour (except primary colon cancer with liver mets)
- No better method of proven treatment value is available (ie, chemosensitive tumours)
- Adequate medical status for planned resection
- Complete resection is possible based on CT
- Stable disease (no new lung mets during staging)

Probability of New Primary Cancer vs. Metastasis in patients presenting with a Solitary Lung Nodule after Prior Treatment for Malignant Tumour

Prior Tumour	New Primary (%)	Metastasis	Total
Wilms	0	8	8
Sarcoma	5 (8)	55	60
Melanoma	7 (19)	29	36
Testis	6 (33)	12	18
Kidney	11 (55)	9	20
Colon – rectum	30 (58)	22	52
Breast	40 (63)	23	63
Ovary	6 (66)	3	9
Bladder	25 (89)	3	28
Lung	47 (92)	4	51
Head & Neck	158 (94)	10	168
Other (oesophagus, prostate, pancreas, skin, lymphoma, leukemia)	140 (100)	0	140

Rationale of Metastasectomy in Various Primary Tumours

Primary Site	Aim	Usual Application
Sarcoma	Permanent cure	Whenever possible
Germ Cell	Confirm complete remission Residual teratoma	Systematic
Colon-rectum	Permanent cure ± Liver resection	Selective
Kidney	Occasional cure	Highly selective
Melanoma	Occasional cure New primary	Only single lesion Controversial
Breast	Hormone receptors New primary	Only single lesion
Head & Neck	New primary	Single lesion Highly selective with multiple nodules

Results of Surgery (International Registry of Lung Metastases)

- Aim is cure, not debulking
- Actuarial survival rate after Complete resection 5 yr 36% 10 yr 26% 15 yr 22%
Incomplete resection 13% 7% --

Prognostic Factors

- Tumour doubling time – inconclusive results
- Disease-free interval – conflicting results
- Number of metastases – survival decreased as number increases
- Hilar-mediastinal nodes – unknown
- Macroscopically complete resection – most important factor

STR tutorial: Use of MD CT reconstruction of cardiovascular structures: Clinical and classroom

A. Rozenshtein, M.D. and L. Boxt, M.D.

The remarkable gains in scanning speed achieved with the advent of multidetector CT have allowed radiologists to image the heart with narrow (3mm or less) collimation, thus enhancing resolution, minimizing breathing motion, and vastly improving data sets for multiplanar reconstructions of intrathoracic structures. At the same time, reliable and user-friendly 3-D reconstruction software is now available on most PACS systems and many dedicated workstations. Consequently, 3-D reconstructions are becoming commonplace in clinical practice.

For several years we have used 3-D reconstruction of data obtained from multidetector CT examinations of the cardiovascular system to aid in diagnosis, communicate with the referring clinicians, and enhance education of fellows, residents and medical students. In the course of this tutorial we will demonstrate the use of the multiplanar reconstructions of the heart, great vessels, and the pulmonary arteries and veins in clinical practice and classroom.

Heart: understanding complex three-dimensional relationships of the cardiac chambers, valves, and coronary arteries.

Great vessels: their origins, spatial relationships, and common variants, such as aberrant subclavian arteries and persistent left superior vena cava; demonstration of dissections and aneurysms.

Pulmonary arteries: understanding normal anatomy and common congenital abnormalities (pulmonary artery agenesis; pulmonary stenosis); common pitfalls in pulmonary embolism.

Pulmonary veins: demonstrating partial anomalous pulmonary venous return; providing a roadmap for pulmonary venous ablation in patients with atrial fibrillation.

Critical Care Unit Imaging

Joel E. Fishman, M.D., Ph.D.

Assistant Professor of Radiology

University of Miami School of Medicine

Objectives

1. Review published data regarding efficacy of ICU chest radiology
2. Discuss specific pleural & parenchymal diseases affecting ICU patients, including atelectasis, pneumonia, aspiration, edema, ARDS, and effusion
3. Identify abnormal air collections and barotrauma
4. Evaluate life support devices and their complications
5. Discuss the role of chest CT in the ICU

Introduction

Physical examination is often difficult in the ICU setting, and for many years has been complemented by the portable chest radiograph (CXR). The most common specific indications for obtaining such a radiograph, whether film-screen or digital, have included

1. rapidly evolving changes in cardiopulmonary status
2. evaluation of the immediate postprocedure and subsequent position of life support devices, as well as their complications
3. ventilator-associated complications including barotrauma
4. specific pleuroparenchymal diseases such as pleural effusion, atelectasis, aspiration, pneumonia, edema, ARDS, and pulmonary embolism (1).

The interpretation of portable ICU radiographs is often difficult, due to the limitations of applying optimal radiographic technique in the ICU setting, as well as patient condition and the presence of monitoring and other devices (either in or on the patient) obscuring portions of the chest. As might be expected, studies have shown a wide range of measures of effectiveness of these radiographs, and there has been to date only limited study claiming to demonstrate cost-effectiveness, but this is not universally accepted. According to some studies, 43-65% of all ICU CXR had “unexpected or abnormal findings”, many affecting management. However, considering routine, daily chest radiographs lowers the efficacy to 15-18% in an MICU/respiratory ICU setting and even lower (5%) in the cardiothoracic ICU. The American College of Radiology has weighed in to the discussion with its Appropriateness Criteria (2), stating that a daily CXR is indicated for patients with acute cardiopulmonary problems and for patients on mechanical ventilation. In cases of CVP, feeding tube, and chest tube placement, only post-procedure radiographs are indicated. Postprocedure radiography is possibly indicated for nasogastric (nonfeeding) tubes. According to the ACR, Swan-Ganz catheters only require post-procedure films, but this is more controversial.

Atelectasis

Atelectasis may occur in any patient, especially those having undergone general anesthesia, or whom have preexisting lung disease, smoking history, obesity, or elderly age. Approximately 50% of patients with atelectasis but without pneumonia have fever. Lobar atelectasis is usually secondary to poor inspiratory effort and is often seen postoperatively and after extubation. It has a propensity to affect the left lower lobe more than others;

one evaluation revealed left lower lobe atelectasis in 66%, right lower lobe in 22%, and right upper lobe in 11%. Lobar atelectasis is generally a result of small airway collapse, not mucus plugs, so it may not respond to bronchoscopy. Pneumonia is more likely to occur if atelectasis persists past 3 or 4 postoperative days. Radiographically, lobar atelectasis is indistinguishable from lobar pneumonia. Atelectasis without air bronchograms suggests mucus plugging as the etiology. The CXR has approximately 74% sensitivity and 100% specificity for detecting atelectasis (or consolidation) vs. CT scanning (3). The mildest and most common radiographically visible form is subsegmental atelectasis, which often appears platelike or discoid, and can cross fissures.

Pneumonia

ICU patients are at high risk for nosocomial pneumonia, a disease that has an incidence of 6/1000 discharges and accounts for 18% of all infections. It occurs in 8-12% of MICU/SICU patients, and in up to 60% of patients with ARDS. The presence of an ET tube and feeding tube promotes aspiration with possible subsequent infection, and immunocompromised patients are naturally predisposed to infection. The mortality rate is 13-55% (4). Organisms include aerobic gram-negative rods, especially pseudomonas, enterobacter, and klebsiella. Of gram-positive organisms, staph aureus is most common (15%), and is increasingly methicillin-resistant (MRSA). The most common non-bacterial agent is candida (4%). Nosocomial pneumonia can be difficult to diagnose. Bronchoalveolar lavage has become an important tool in helping to diagnose pneumonia in the ICU.

A study of ventilated patients showed a CXR accuracy of 50% for diagnosing pneumonia (5); interestingly, clinical input and the use of prior films did not improve accuracy. Other studies have shown a CXR specificity for nosocomial pneumonia of only approximately 30% (4). The CXR is especially difficult in patients with ARDS. Radiographic opacities may be due to atelectasis (see above), edema, ARDS, aspiration, hemorrhage, or infarct (see below). Bronchopneumonia typically displays alveolar opacities. Helpful signs include airspace opacity abutting a fissure, air bronchogram (especially if solitary), and cavitation. The “silhouette sign” and bilateral airspace disease is more nonspecific. Rapid change in minutes or hours suggests atelectasis, aspiration, or even patchy edema rather than pneumonia. CT shows that the CXR underestimates basal consolidations in post-op patients by 26% (3). Nondependent opacities are more suspicious for pneumonia than dependent ones. Antibiotics do not alter the CXR appearance for the first two days, but lack of radiographic improvement after 14 days strongly suggests treatment failure.

Edema

Pulmonary edema is broadly grouped into two categories: (1) Hydrostatic edema: heart failure, overhydration, and renal failure; (2) Permeability edema: aspiration, sepsis, drug reaction or allergy, near drowning, smoke or toxic fume inhalation, neu-

rogenic edema, fat embolism, heroin toxicity, and ARDS.

Edema is one of the most common abnormalities affecting ICU patients, and furthermore the distinction between hydrostatic and permeability edema can be quite difficult. The first radiographic clue to oncoming hydrostatic edema is engorgement of the pulmonary vasculature, both venous and arterial. However, cephalization of the vasculature is not very helpful in the ICU setting because many films are obtained in the supine position, which artificially redistributes the vessels. The true edema phase is first characterized by interstitial fluid, manifested by indistinct vessel margins, thickening of bronchi, Kerley lines (A/B/C), hazy or “ground-glass” opacities, and a gravity-dependent increase in density (particularly on CT scans). Pleural effusions begin to accumulate as interstitial fluid overloads the venules and lymphatics of the interstitium. Effusions may be bilateral or only right-sided; solely left-sided effusion suggests a superimposed process (or gravity). Edema with the highest LVEDP manifests as alveolar opacification, typically bilateral and reasonably symmetric. However, there are many reasons for asymmetric edema, including gravity (bedridden, immobile patients), underlying lung disease altering blood flow (COPD, fibrosis), and underlying pulmonary vascular disease (shunts, pulmonary embolism, hypoplastic vessels). Alveolar edema may be indistinguishable from hemorrhage or diffuse pneumonia. Radiographs might not correlate with LVEDP measurements.

Permeability edema (often called noncardiogenic) lacks the pulmonary venous engorgement noted above. An advanced form of permeability edema is ARDS (defined by decreased lung compliance, normal LVEDP, and hypoxia refractory to O_2), which may initially have no abnormalities on the CXR (up to 12 hr post-insult). Subsequently the radiograph shows a pattern of edema (at 12-24 hr), which is usually patchy although it can progress to diffuse disease (36-72h). Air bronchograms are characteristic (89%), and help distinguish ARDS from hydrostatic edema. Decreased lung volumes are frequently observed. Conversely, while effusions may occur they are often small. Radiographic signs of barotrauma are common (see below).

Studies have been performed to assess how well the radiograph can distinguish these two types of edema. A study of 135 supine ICU patients found that pulmonary wedge pressures above 18mm Hg can be detected by a vascular pedicle (mediastinal width at the SVC) of 70mm or more and a cardiothoracic ratio (width of heart to width of lungs at the bases) of 55% or more, yielding a 70% accuracy. These results were better than subjective interpretation of the films without (56%) or with (65%) clinical data. Aberle et al (6) found that 87% of hydrostatic and 60% of permeability edema could be correctly identified, with a patchy peripheral distribution seen in 58% with permeability edema but only 13% with hydrostatic.

Barotrauma

An estimated 4-15% of patients on ventilators develop barotrauma, manifesting as abnormal air collections in the chest. Underlying lung disease, such as pneumonia and especially ARDS, raise the risk significantly. The effects of barotrauma are generally more severe in children and adults up to the age of 40. The major factors associated with development of barotrauma include a peak inspiratory pressure of greater than 40cm H_2O , the use of positive end-expiratory pressure (PEEP), and an inappropriately large tidal volume. The CXR visually improves with PEEP and “sighs,” especially in edema. The heart size decreases, as does the cardiac output. Pulmonary vessels may

decrease or increase in size. Interstitial pulmonary edema has a protective effect against barotrauma, due to the elevated interstitial pressures. Despite the improved CXR appearance, however, positive pressure ventilation can cause edema and lung damage similar to ARDS.

The initial abnormal air collection in barotrauma is pulmonary interstitial emphysema (PIE). It occurs when pressure in the air spaces becomes greater than the tension in perivascular connective tissues and septae. It is most often identified in children. PIE carries a significant risk of pneumothorax (77%) from rupture of a cyst. Pneumothorax (PTX) is the most feared sequel of barotrauma. It occurs in up to 25% of ventilated patients, and the risk increases with increased time on the ventilator. PTX is often associated with, but not caused by, pneumomediastinum. In the supine patient, PTX is usually anteromedial or subpulmonic. Less often the PTX is apical, lateral (displaces the minor fissure from the chest wall) or posteromedial. If PTX is suspected but not definite on supine CXR, then upright, expiratory, or bilateral decubitus radiographs should be obtained. False-positive appearances of PTX may be due to skin folds, overlying tubing/dressing/lines, and prior chest tube tracks. The size of the PTX is unrelated to its significance, since even a tiny PTX can acutely enlarge in ventilated patients. Tension is present in 60-96% of ventilated PTX cases (7) and signifies that pleural pressure exceeds atmospheric pressure. Mediastinal shift is not always present in tension PTX, possibly masked by PEEP. Signs of tension include displacement of the anterior junction line, azygosophageal recess, and flattening of heart and vascular shadows.

Pneumomediastinum is important as a general sign of barotrauma and must be distinguished from a PTX, but except in rare cases of tension, pneumomediastinum is not a life-threatening condition. PTX, pneumopericardium, and the Mach effect all mimic pneumomediastinum. Pneumomediastinum may show air streaking into the neck, a “continuous diaphragm,” and retroperitoneal air. Other manifestations of barotrauma include subcutaneous air and pneumopericardium.

Pleural Effusion

Pleural effusions are common in the ICU. The supine CXR demonstrates a 67-95% accuracy for detecting effusion (8), which is improved on lateral and decubitus films. Upright films may be problematic for differentiating atelectasis vs. a small effusion. Approximately 300 ml of effusion must accumulate before manifesting on the adult CXR. The effusion is difficult to characterize on plain films, with a few exceptions. Sudden large effusions suggest hemothorax in a post-procedure patient. Empyema is may appear as a loculated effusion in a patient with fever. Loculated effusions do not move with changes in patient position. Post-cardiac surgery, effusions are common particularly as pulmonary edema moves into the pleural space. However, increasing effusion past the 3rd post-op day may signal a post-pericardiotomy syndrome, especially if pericardial effusion and pulmonary opacity is present.

Aspiration

Aspiration is common in patients who are post-anesthesia, obtunded, intubated or have a nasogastric tube, suffer neuromuscular discoordination, or have a variety of GI problems. In aspiration, the CXR often changes over a few hours' time. New airspace disease is more common on the right than left; in upright patients the bases predominate, but in supine ICU

patients the upper lobes and superior segments of the lower lobes are affected. Disease may rapidly clear (1-2 d) or progress over 24-48 hr. If clearing does not occur by 72 hrs then consider a complication. The three patterns of disease caused by aspiration are gastric aspiration and chemical tracheo-bronchitis/pneumonitis, infection (pleuroparenchymal), and airway obstruction (9).

Life Support Devices

Much of ICU radiology pertains to life support lines and devices, to evaluate both the position of the device and for complications related to the insertion procedure or to the presence of the device itself. Following are the most important radiologic features of common life support devices.

Endotracheal (ET) tube: optimal position is 5cm above the carina in an adult. The tube moves ± 2 cm with flexion/extension of the neck. Malposition is present in 12-15% of patients. ET width should be $\frac{1}{2}$ to $\frac{2}{3}$ the width of the trachea, and the cuff should fill but not expand the trachea. Misplaced tubes invariably enter the right mainstem bronchus. A study of 101 intubations found that there were 10 malpositions (1 urgent). Rupture of the larynx or trachea is suggested by projection of the ET tip outside and to the right of trachea with cuff overdistention.

Tracheostomy: will not move with flexion/extension of the neck. The tip should project approximately at T3. The cuff should hug but not distend the tracheal wall. High-pressure cuffs may cause pressure erosion of the trachea and eventual TE fistula.

Central venous pressure monitor: tip location should be between the venous valves (proximal subclavian and IJ veins) and the right atrium. Subclavian catheters should project medial to the anterior portion of the 1st rib. Central venous catheter placement incurs a PTX rate of 5.6%. A catheter inadvertently placed into the subclavian artery will project superiorly and medial to the expected subclavian venous course. Local bleeding may ensue but is usually easily controlled. Catheter placement (left subclavian) against the wall of the SVC may lead to erosion.

Swan-Ganz catheter: The tip should not be distal to the proximal interlobar pulmonary arteries. There is a 24% malposition rate on the 1st CXR (1). Infarct, arterial perforation, knotting, and endocarditis/sepsis are unusual complications.

Intra-aortic balloon pump: The tip should project just inferior to the aortic arch. The balloon is inflated during diastole and may sometimes appear as a long ovoid lucency on the CXR.

Pacer: a lateral film is needed to show the RV tip projecting anteriorly (cf. posterior deviation if the lead enters the coronary sinus). Perforation has occurred if the tip is outside the heart shadow.

Chest tube: should be positioned antero-superiorly for PTX drainage, and postero-inferiorly for effusions. Malpositioning may show the tube in a fissure, through the lung parenchyma, or in the extrapleural tissues (malposition is best seen on CT).

Nasogastric (NG) tube: the side hole should project in the stomach. If a feeding tube is inadvertently placed into the lung, a post-removal CXR should be carefully evaluated for PTX.

Use of Chest CT in the ICU

CT scanning is increasingly being used in critically ill patients who may have multiple medical problems, not easily discriminated by the CXR. It has been estimated that 24-75% of ICU chest CTs show "clinically useful" information (10), translating to a change in management in 22-39% of scanned cases. A portable CT scanner has been described which could help circumvent problems with transportation of critically ill patients. Major categories in which chest CT has proven useful are pleural disease (especially empyema), lung abscess, life line malpositioning, complications of mechanical ventilation (unsuspected PTX was found in 7% of ventilated patients by CT), and pulmonary embolism.

REFERENCES:

1. Henschke CI, Yankelevitz DF, Wand A, et al. Accuracy and efficacy of chest radiography in the intensive care unit. *Rad Clin North Am* 34(1):21-31, 1996.
2. Tocino I, Westcott J, Davis SD, et al. Routine daily portable x-ray. American College of Radiology. ACR Appropriateness Criteria. *Radiology* 215(Suppl):621-6, 2000.
3. Beydon L, Saada M, Liu N, et al: Can portable chest x-ray examination accurately diagnose lung consolidation after major abdominal surgery? A comparison with computed tomography scan. *Chest* 102:1697-1703, 1992
4. Lipchik RJ, Kuzo RS. Nosocomial pneumonia. *Rad Clin North Am* 34(1):47-58, 1996.
5. Winer-Muram HT, Rubin SA, Ellis JV, et al: Pneumonia and ARDS in patients receiving mechanical ventilation: Diagnostic accuracy of chest radiography. *Radiology* 188:479-485, 1993
6. Aberle DR, Wiener-Kronish JP, Webb WR, et al: Hydrostatic versus increased permeability pulmonary edema: Diagnosis based on radiographic criteria in critically ill patients. *Radiology* 168:73-79, 1988
7. Zimmerman JE, Goodman LR, Shahvari MGB: Effect of mechanical ventilation and positive end-expiratory pressure (PEEP) on chest radiograph. *AJR Am J Roentgenol* 133:811, 1979
8. Ruskin JA, Gurney JW, Thorsen MK, et al: Detection of pleural effusions on supine chest radiographs. *AJR Am J Roentgenol* 148:681-683, 1987
9. Shifrin. Aspiration and complications. *Rad Clin North Am* 34(1):21-31, 1996.
10. Miller WT Jr. Thoracic computed tomography in the intensive care unit. *Sem Roentgenol* 32(2):117-121, 1997.

Pulmonary Arterial Hypertension: Concepts, Emerging Therapies and Uncommon Causes.

Marc V. Gosselin, M.D.

Jeffrey D. Edelman, M.D.

Objectives:

- Review clinical classification of pulmonary hypertension and the approach to patient evaluation
- Discuss the current treatment options and emerging therapies available to clinicians.
- Discuss the emerging role of multidetector CT in the evaluation of pulmonary arterial hypertension.
- Discuss radiological findings associated with uncommon causes of PH

Table 1: Clinical Classification of Pulmonary Hypertension (1998 World Symposium on Primary Pulmonary Hypertension)

- 1. Precapillary/Pulmonary Arterial Hypertension**
 - a) Primary Pulmonary Hypertension
 - Sporadic
 - Familial
 - b) Related to
 - Collagen vascular disease
 - Congenital systemic to pulmonary shunts
 - Portal hypertension
 - HIV infection
 - Drugs/toxigens (anorexigens and others)
 - Persistent pulmonary hypertension of the newborn
- 2. Pulmonary Venous Hypertension**
 - a) Left-sided atrial or ventricular heart disease
 - b) Left sided valvular disease
 - c) Pulmonary veno-occlusive disease
 - d) Extrinsic compression of central pulmonary veins
 - Fibrosing mediastinitis
 - Adenopathy/tumor
- 3. Disorders of the Respiratory System and/or Hypoxemia**
 - a) Chronic obstructive pulmonary disease
 - b) Interstitial lung disease
 - c) Sleep disordered breathing
 - d) Alveolar hypoventilation disorders
 - e) Chronic high altitude exposure
 - f) Neonatal lung disease
 - g) Alveolar-capillary dysplasia
- 4. Pulmonary Hypertension due to Chronic Thrombotic and/or Embolic Disease**
 - a) Thromboembolic obstruction of proximal pulmonary arteries
 - b) Obstruction of distal pulmonary arteries
 - Pulmonary embolism (thrombus, tumor, ova and/or parasites, foreign material
 - In-Situ Thrombosis
 - Sickle Cell Disease
- 5. Pulmonary Hypertension due to Disorders Directly Affecting the Pulmonary Vasculature**
 - a) Inflammatory
 - Schistosomiasis
 - Sarcoidosis
 - b) Pulmonary capillary hemangiomatosis

General Concepts

Pulmonary hypertension (PH) is defined as mean pressures greater than 25mmHg at rest or greater than 30mmHg with exercise. PH generally results from chronically elevated venous pressure, vascular obliteration, parenchymal destruction or increased blood flow.

Clinical Classification of Pulmonary Hypertension (Table 1):

The 1998 World Symposium classification categorizes pulmonary hypertension according to clinical similarities (1)

Evaluation of Patients with PH or Suspected PH (Table 2):

1. Detect presence of PH
2. Assess severity of PH
3. Assess for underlying causes and associated conditions

Table 2: Studies Obtained in Evaluation of Patients with PH or Suspected PH:

Echocardiogram:
Detection of PH; evaluate for structural heart disease

Pulmonary Function Testing:
Airflow obstruction, restriction, or gas exchange impairment

Cardiopulmonary Exercise testing (or six minute walk):
Cause and severity of functional limitations

Collagen vascular serologies (LETS, HIV test)

Polysomnography:
Sleep disordered breathing

Right Heart Catheterization:
Severity of hemodynamic impairment
Presence/absence of vasoreactivity

Thoracic Imaging (Chest X-Ray, Ventilation-Perfusion Lung Scan, Computerized Tomography):
Parenchymal lung disease
Thromboembolic disease

Suggested Therapeutic Approach to Pulmonary Arterial Hypertension

Current Treatments:

1. Supplemental oxygen
2. Diuretics
3. Anticoagulation
4. Calcium channel blockers
5. Inotropic agents (Digoxin)
6. Continuous Intravenous Epoprostenol (Prostacyclin/Flolan)
7. Subcutaneous Treprostinil (Remodulin)
8. Endothelin-1 receptor blockers - Bosentan (Tracleer)
9. Atrial septostomy
10. Lung or heart-lung transplantation

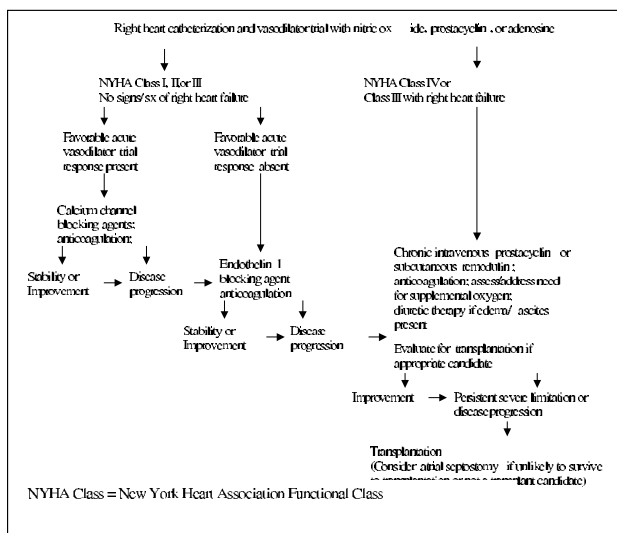
Investigational Treatments:

1. Inhaled iloprost
2. PDE5 inhibitors (Sildenafil)
3. Endothelin-1a receptor blockade (Sitaxsentan)
4. Combination therapy

The traditional radiological classification is anatomically based divided into pre-capillary, capillary and post-capillary eti-

ologies. Another approach involves a physiological division into four categories: increased pulmonary flow, chronic hypoxia, vessel obliteration and chronic pulmonary venous hypertension.

1. **Increased (Hyperdynamic) flow:** ASD, VSD, PDA, Transposition of the Great Vessels, Common AV canal and partial anomalous pulmonary venous drainage.
2. **Chronic Hypoxia:** Chronic bronchitis, Bronchiolitis obliterans, advanced pulmonary fibrosis, Sleep apnea, Cystic fibrosis and chronic high altitude exposure.
3. **Vessel obliteration:** Emphysema, Primary pulmonary hypertension, chronic thromboembolic disease, Vasculitis, sickle cell disease, schistosomiasis and tumor emboli.
4. **Chronic Venous hypertension:** Left ventricular or atrial disease, left sided valvular disease, and pulmonary venoocclusive disease.



Chest Radiographic Evaluation

Enlargement of the main pulmonary artery is often the first radiographic manifestation, likely based on the principals from Laplace's law. Increased lobar and segmental vessel size, along with right ventricular chamber and outflow tract enlargement eventually occur. Rapid tapering ("pruning") from the central to peripheral arteries and increased tortuosity of the arterial course are seen in advanced stages. (2) The increase in the relative diameter of the arterial and venous ratio is another radiographic manifestation of PH. (3)

Once the diagnosis of PH is suspected or known, the underlying etiology may be identified on the radiograph. Increased pulmonary flow with large arteries and veins along with a decreased aortic arch size support a left to right shunt (hyperdynamic flow) as the cause for PH. Hyperinflation, extensive bronchiectasis, or pulmonary fibrosis support a secondary development of PH from a primary lung disorder, often secondary to chronic hypoxia. Patients who are morbidly obese with enlargement of the pulmonary arteries PH may be secondary to sleep apnea or potentially weight loss medication. The presence of a TIPS stent in the right upper quadrant of the abdomen and increased flow and vessel conspicuity in the lower lobes often reflects hepatopulmonary syndrome/cirrhotic-associated PH. Normal lungs with radiographic patterns of PH suggest a primary vascular cause such as plexogenic arteriopathy, drug induced or chronic thromboembolic disease (obliteration of ves-

sels). Finally, when radiographic evidence of enlarged upper lobe vessels and constricted lower vessels are present ("cephalization"), this supports chronic pulmonary venous hypertension as the most likely cause. Enlargement of the left atrium and possibly the left ventricle should be present.

Multidetector CT Evaluation

Multidetector CT is being used increasingly at our institution for the evaluation of patients with known or suspected PH. It is useful in documenting the imaging presence or absence of PH, evaluating for chronic thromboembolic disease and deciding between a *primary* lung disease as the main factor versus *intrinsic* pulmonary vascular disease. Primary and secondary cardiac abnormalities are also better seen with the thinner collimation and increased speed of image acquisition.

The exams are performed as a CT pulmonary angiogram, beginning from adrenals and scanning cranially through the apices. Some thin section expiratory images are also performed to evaluate for air trapping. By beginning the image acquisition caudally, it is possible to see any initial reflux of hyperdense contrast into the dilated IVC and hepatic veins. This dynamic contrast flow is helpful as it often signifies elevated right atrial and ventricular end diastolic filling pressures. (4) The absence of this or the presence of unopacified mixing in the right heart chambers from a decompressed IVC argues against any significantly elevated right pressures and concurrently, the presence of PH. Further evaluation with direct right heart catheter pressures may be required in these patients since it is unlikely they have significant PH.

Supportive cardiac findings include right atrial and ventricular chamber and outflow tract hypertrophy. The presence of left heart chamber dilation and cephalization supports pulmonary venous hypertension as an important contributor to the PH. Septal thickening, patchy and/or centrilobular ground glass nodules are supportive evidence for pulmonary venous abnormalities. (5) As the collimation of the CT scanners narrows, our ability to detect septal defects and potentially valve thickening and calcification should also improve.

The main pulmonary artery size is considered enlarged when greater than 2.9cm and when lobar arteries are larger than the accompanying bronchus, the latter being a useful sign for conventional radiographs too. Chronic pulmonary thromboembolic disease is well seen with CT, especially in more proximal vessels. Eccentric mural thickening, asymmetric pulmonary enlargement, webs, mural calcification and abrupt narrowing of the lumen at the distal lobar or segmental levels are the most common imaging findings. (6)

The lungs often demonstrate mosaic lung attenuation, especially with chronic thromboembolic disease. However, the presence of severe air trapping on the expiratory images favors an airways disease such as bronchiolitis obliterans, long-standing asthma or tracheomalacia as the primary problem with PH a secondary consequence.

Uncommon Causes

Pulmonary Venocclusive Disease/Pulmonary Capillary Hemangiomatosis

Pulmonary venocclusive disease is an uncommon disorder, which is caused by the gradual obliteration of pulmonary veins. Intimal proliferation and fibrosis of the veins are found on pathology. The chronic elevation of the venous pressures eventually leads to PH. Multiple etiologies are associated with this

pathological process, such as viral infections, cytotoxic chemotherapeutic agents, radiation injury and inhaled toxins. The prognosis is poor, with progression of symptoms and death often over a few years. The most common findings include smooth interlobular septal thickening, patchy and/or centrilobular ground glass opacities, and pleural effusions with normal caliber pulmonary veins and left heart structures. (5,6) This latter finding helps distinguish it from the more common cardiac causes. These imaging findings have been reported to predict a poor response to Prostacyclin therapy. (7)

Pulmonary capillary hemangiomatosis is a rare cause of PH, representing the proliferation of thin walled capillary-like vessels, which invade the veins and arterioles. It is associated with intimal fibrosis, hemorrhage and venous stenosis. The etiology is unknown, but may represent a form of low-grade malignancy or metastatic dissemination of an angiosarcoma. Its imaging, clinical course and prognosis are similar to pulmonary venoocclusive disease. (6, 7)

Pulmonary Arterial Tumor Embolism

Pulmonary arterial tumor embolism often presents with progressive dyspnea due to PH. It is a difficult diagnosis to make clinically, requiring a high clinical suspicion. Intravascular embolic disease on CT is usually manifested with numerous branching "tree-in-bud" opacities; however, often have a beaded appearance. Peripheral areas of infarction have been described. (5) Of importance, despite its tree-in-bud manifestation, it is unlikely to demonstrate any air trapping on expiratory maneuvers, thus raising the suspicion for the diagnosis.

Hepatopulmonary syndrome/Cirrhosis associated PH

Hepatopulmonary syndrome is defined by the presence of liver cirrhosis, intrapulmonary vascular dilation and hypoxemia. Clinically patients often have platypnea and orthodeoxia. Two major manifestations exist; type 1 (85%) has a spidery appearance of the pulmonary vessels and type 2 (15%) associated with numerous small arteriovenous fistulas. The former responds well to 100% oxygen therapy while the latter does not. These vascular changes are most notable in the lower lobes bilaterally. The increased ratio of arterial diameter with the adjacent bronchus is useful in making the diagnosis in patients with severe hepatic disease. The exact etiology for some patients developing PH is unclear, but may relate to the increased pulmonary flow and vasoactive or vasotoxic substances normally degraded by the liver, which reach the pulmonary circulation. (5,6)

Sickle Cell Anemia

Sickle cell anemia is associated with multiple pulmonary abnormalities, including PH, though the latter is reported as a rare complication. The precise etiology may relate to the multiple episodes of acute chest syndrome classically described in this patient population. (8) Consolidation and/or ground glass opacities are most commonly seen, representing either hemorrhage/infarction or pneumonia. Multiple sickling events with occlusion of the microvasculature likely predisposes to eventual PH. Concurrent pulmonary fibrosis may be present.

Pulmonary Vasculitis

Pulmonary vasculitis is a disease spectrum of inflammation directed towards the small arteries and capillaries. There are numerous causes of this pathological reaction, including Wegener's Granulomatosis, Churg-Strauss syndrome, collagen-vascular diseases and granulomatosis reactions to talc injection. The greater proportion of vessels involved increases the likelihood of developing PH. Patchy ground glass opacities and/or centrilobular ill defined ground glass nodules are described imaging findings, especially in active disease. (5) These correlate with the widespread perivascular inflammation and hemorrhage.

REFERENCES:

1. Clinical Classification of Pulmonary Hypertension. 1998 World Symposium on Primary Pulmonary Hypertension.
2. Cardiac Radiology: The Requisites. Miller S. Mosby 1998. pp 23-25.
3. Reading the Chest Radiograph: A Physiologic Approach. Milne E., Pistolesi M. Mosby 1993. pp164-167.
4. Gosselin M, Rubin G. Altered intravascular contrast material flow dynamics: Clues for refining thoracic CT diagnosis. Pictorial Essay AJR 1997;169:1597-1603.
5. High-Resolution CT of the Lung. 3rd edition. Webb R, Muller N, Naidich D. Lippincott, Williams & Wilkins, 2001.
6. Diagnosis of Diseases of the Chest. 4th edition. Fraser, Muller, Colman, Pare. Chapter 50: Pulmonary Hypertension. W.B. Saunders Company: pp 1879-1945.
7. Resten A., Maitre S., Humbert M., et al. Pulmonary Arterial Hypertension: Thin Section CT Predictors of Epoprostenol Therapy Failure. Radiology 2002;222:782-788.
8. Aquino S, Gamsu G, Fahy J, et al. Chronic pulmonary disorders in sickle cell disease: findings at thin-section CT. Radiology 1994;193:807-811.

Notes

Thursday

March 6, 2003

General Session

Thursday

7:00 - 8:00 am Continental Breakfast Americana Foyer

8:00 - 11:00 am Guest Hospitality Suite Moon Room

Thoracic Infection

Moderator: Robert Tarver, MD

Americana 3

7:50 - 8:10 Pulmonary Tuberculosis
Steven Primack, MD

8:10 - 8:30 Non-tuberculous Mycobacterial Infection
David Schwartz, MD

8:30 - 8:50 HIV: Primary and Secondary Lung Infection
Linda Haramati, MD

8:50 - 9:10 Viral Infection on HRCT
Tomas Franquet, MD

9:10 - 9:30 Imaging of Coccidiomycosis
William Berger, MD

9:30 - 9:50 Session Discussion

9:50 - 10:10 am Coffee Break Americana Foyer

The Airway

Moderator: Georgeann McGuinness, MD

Americana 3

10:10 - 10:30 Tracheobronchial Malignancy
Jo-Anne Shepard, MD

10:30 - 10:50 Inflammatory Disease of the Central Airways
Arfa Khan, MD

11:10 - 11:30 Virtual Bronchoscopy
R.C. Gilkeson, Jr., MD

11:30 - 11:50 Session Discussion

11:50 - 12:15 Scientific Presentation and Case of the Day Awards

12:15 pm Meeting Adjourns

Pulmonary Tuberculosis

Steven L. Primack, M.D.

Although there had been an increase in the incidence of tuberculosis (Tb) in the late 1980's, the incidence of tuberculosis has continued to decrease. In the United States, there were 53 cases per 100,000 in 1953. This incidence is now 6 per 100,000 in the year 2000. However, the most recent data from the World Health Organization found that the incidence of tuberculosis in Southeast Asia was 237 per 100,000 in 1995 and the incidence in Sub-Saharan Africa was 191 per 100,000. Risk factors for tuberculosis include lower socio-economic group, prisoners, nursing home residents, immigrants and refugees, health care workers, immunosuppressed patients, alcoholics and diabetics.

Tuberculosis is initially acquired by inhalation of contaminated droplets, which are then ingested by macrophages when in the alveolus. Either a granuloma is formed or extensive tissue necrosis occurs with spread through lymphatics leading to primary tuberculosis. Postprimary tuberculosis occurs at a one percent rate per year in immunocompetent individuals but in a significantly higher rate in immunocompromised patients. The risk of development of active Tb include the contagiousness of the primarily infected individual, adequacy of antimicrobial defense of the exposed individual, the amount of contact and the environment where the contact occurred. Post primary Tb can occur either by reactivation of an endogenous focus of infection acquired early in life or, less commonly, exogenous reinfection. There tends to be an upper lung zone predilection probably related to higher oxygen tension and impaired lymphatic drainage.

The clinical signs and symptoms of tuberculosis are somewhat nonspecific. Systemic symptoms include low grade fever, anorexia, fatigue, weight loss and night sweats. Pulmonary symptoms include cough, which is usually productive as well as hemoptysis on occasion. Severe shortness of breath is somewhat atypical. Patients are asymptomatic in approximately 5%. However, up to 60% of children are asymptomatic at the time of diagnosis. In the elderly, the diagnosis is frequently delayed.

The radiologic manifestations of pulmonary Tb are dependent on host factors including prior exposure, age and immune status. Patients with tuberculosis are typically classified as either having primary or postprimary disease. However, from a clinical standpoint, the important distinction is between active and inactive Tb.

When approached with a patient with possible tuberculosis, classification is based on clinical, bacteriologic and radiographic evaluation. Individuals are typically classified as having no disease, clinically active disease or are clinically inactive. A normal chest radiograph has a high negative predictive value but does have approximately a one percent false negative rate.

Findings indicative of inactive disease on the chest radiograph include the Ghon focus, which is a calcified parenchymal granuloma and the Ranke complex, which is the Ghon focus with associated calcified lymph nodes. Findings sugges-

tive of active disease include consolidation, poorly defined nodules, cavitation and enlarged lymph nodes. When interpreting chest radiographs for possible tuberculosis, it is essential to evaluate with prior radiographs available, particularly older chest radiographs. Prior radiographs other than the most recent should be used since changes can occur slowly. If there is extensive lung disease that is unchanged, the phrase "radiographically stable" is more appropriate than "inactive". If there is indeterminate disease activity, it is appropriate to dictate that it is indeterminate but one should attempt to favor either active or inactive disease. The radiograph is a data point in the evaluation of a patient with suspected tuberculosis.

The radiographic findings of primary Tb include lymphadenopathy, which is present in 95% of pediatric cases. CT scan often demonstrates rim enhancing necrotic lymph nodes. Consolidation is the most common parenchymal finding and is often multifocal with no zonal predominance. Nodules and masses often are also identified. Pleural effusion is present in 5 - 30% of cases, however, this is less common in pediatric patients.

The radiographic findings of postprimary Tb often demonstrate heterogeneous opacities with linear, nodular and consolidative opacities present. Consolidation is the most common radiographic manifestation occurring in 50 - 70% of patients. Cavitation is identified in 20 - 45% of patients. Cavities can have either thin or thick nodular walls and have air fluid levels in up to 20% of cases. Endobronchial spread is often present and is characterized by poorly defined 5 - 10mm nodules in an airway distribution. Well defined nodules or masses with or without satellite nodules can be identified as well. Postprimary Tb has a characteristic radiographic distribution predominantly involving the apical or posterior segments of the upper lobes and the superior segments of the lower lobe. Other segments are often involved but generally occur in association with the characteristic sites. Multiple segments are involved in 70 - 90% of patients. Complications of pulmonary Tb include pneumothorax, bronchiectasis, residual cavities, aspergilloma and broncholithiasis.

Another pattern of tuberculosis is miliary disease, which is more common in immunocompromised patients. This indicates the presence of hematogenous dissemination and is apparent radiographically by the presence of innumerable 1 - 3mm non-calcified nodules throughout both lungs. There is a mild basilar predominance. Interlobular septal thickening is often present which is better identified on CT scanning.

CT scanning can be useful in the evaluation of Tb, particularly for identification of bronchogenic spread with identification of centrilobular nodules ("tree-in-bud"). Satellite nodules associated with masses or nodules are also better identified on CT. Cavitation is also better evaluated. Although CT scanning is helpful to distinguish between active and inactive Tb, it may not be definitive. Consolidation, centrilobular nodules, cavitation suggest active disease.

Non-Tuberculous Mycobacterial Infection

David Schwartz, M.D.

Objective:

The attendee will understand the categorization of the various non-tuberculous mycobacteria, and their relationship to human infection, particularly involving the lungs.

Nomenclature:

The term “Non-tuberculous mycobacteria” (NTMB) is commonly used when referring to this group of organisms, frequently associated with opportunistic infection in man. “MOTT” (Mycobacteria other than tuberculosis) has also been used to describe this group, but neither of these terms is completely accurate, as *M. leprae* is not generally included in this category.

Two of the common mycobacteria, *M.tuberculosis* and *M.leprae* are obligate parasites. All of the others live free in the environment. Therefore, these two may be the “Atypical mycobacteria”, so that terminology is somewhat arbitrary. Perhaps “Environmental Mycobacteria” is the most precise way to refer to these organisms. They are found in water, soil, and milk, as well as fish, birds, and other animals. This is probably the most useful distinction, as these are not usually transmissible by contact with patients. The public health implications are completely different than when dealing with tuberculosis.

Classification:

The common categorization of these environmental mycobacteria is the Runyon methodology, based on culture growth rates and the presence or absence of yellow or orange pigment:

Runyon Group I - Photochromogenic slow growers. These cultures require 2-6 weeks before growth is visible. They develop yellow pigment when exposed to light, but not in the dark.

M. kansasii – Usually associated with pulmonary disease in humans – more common in the Midwest. Occasional disseminated disease.

M. marinum – Causes skin infections – “Swimming pool granuloma” – “Fish tubercle bacillus”.

M. simiae – Rare cause of pulmonary disease.

Runyon Group II – Scotochromogenic slow growers. Pigment is produced in light and in the dark.

M. scrofulaceum – Associated with cervical adenitis, particularly in children. Pulmonary infection in the presence of underlying disease (e.g. emphysema or silicosis).

M. gordonae – Saprophyte found in tap water. Rare pulmonary pathogen.

M. szulgai – Rare pulmonary pathogen.

Runyon Group III – Non-photochromogenic slow growers. Non-pigmented. Very slow growing.

M. avium-intracellulare – *M avium* complex (MAC) - responsible for pulmonary disease, especially in immunocompromised individuals.

M. xenopi – Associated with pulmonary infections.

M. malmoense - Associated with pulmonary infections.

M. terrea – Rare pathogen.

M. ulcerans - Causes Buruli ulcer, the third most common mycobacterial infection in immunocompetent humans (after tuberculosis and leprosy). Infection occurs in skin lesions exposed to stagnant water in low-lying marshes (Uganda, West Africa, Australia). Skin nodules form, followed by ulceration of skin, soft tissues, and bone. Scarring with contractures and severe disabilities occurs.

Runyon Group IV – Rapid growers – These cultures show visible growth in 2-7 days. They may be pigmented or non-pigmented.

M. fortuitum complex (*M. fortuitum*, *M. peregrinum*, *M. abscessus*, *M. chelonae*) - Cause of abscesses, especially at injection sites or surgical wounds. Associated with indwelling catheters, breast implants, or other surgical devices. In one study of 115 hemodialysis centers, water contamination with mycobacteria, mostly *M. fortuitum* complex, was seen in 83%. Pulmonary disease may occur, often related to achalasia and repeated aspiration.

Diagnosis of Pulmonary Infection with Environmental Mycobacteria:

Due to the fact that these mycobacteria are widely present in the environment, the existence of these organisms in the respiratory tract is common. This makes the differentiation of infection from colonization very difficult. The current standards, published by the American Thoracic Society in 1997, state that clinical, radiographic, and bacteriologic criteria must all be satisfied. They refer to three groups of patients:

I. Local immune suppression – HIV Seronegative - Alcoholism, bronchiectasis, cyanotic heart disease, cystic fibrosis, prior mycobacterial disease, pulmonary fibrosis, smoking/COPD, or no risk factors.

II. General severe immune suppression – HIV Seronegative - Leukemia, Lymphoma, organ transplantation, other immunosuppressive therapy.

III. HIV Seropositive with CD4 count <200

1. **Clinical criteria:**
 - a. Compatible signs/symptoms (cough, fatigue, fever, dyspnea, weight loss, hemoptysis)
AND
 - b. Reasonable exclusion of other disease (TB, histoplasmosis, cancer) to explain the clinical presentation
2. **Radiographic criteria:**
 - a. Infiltrates with or without nodules (≥ 2 mo or progressive)
 - b. Cavitation
 - c. Nodules alone (multiple)
 - d. HRCT - Multiple small nodules
 - e. HRCT - Multifocal bronchiectasis with or without small nodules
3. **Bacteriologic criteria:**
 - a. At least three sputum/bronchial wash samples within 1 year
 - Three positive cultures with negative AFB smears
OR
 - Two positive cultures and one positive AFB smear
OR
 - b. Single bronchial wash and inability to obtain sputum samples
 - Positive culture with 2+, 3+, or 4+ growth
(In group II or III patients, includes 1+ or greater growth)
(In group III patients, excludes *M. avium* complex)
OR
 - Positive culture with 2+, 3+, or 4+ smear
OR
 - c. Tissue biopsy
 - Any growth from bronchopulmonary tissue
 - Granuloma and/or AFB on lung biopsy with one or more positive cultures from sputum/bronchial wash
 - Any growth from usually sterile extrapulmonary site

Radiographic Appearance of Pulmonary NTMB Infection:

There are a number of patterns of lung disease described with NTMB infection. The appearance is not specific to the organism, with MAC and *M. kansasii* being the most common pathogens.

1. HIV-negative males, usually in the 60's or 70's may show a pattern of infection similar to that seen in post-primary tuberculosis. Most of these patients have underlying pulmonary disease, and fit in Group I, with alcoholism, bronchiectasis, smoking history, etc. Younger patients with cystic fibrosis may also fit into this category.

There is fibronodular disease, usually involving the apical and posterior segments of the upper lobes. Cavitation frequent-

ly occurs, often with apical pleural thickening. Progression is slow, but there may be volume loss of the affected segments, with hilar retraction and tracheal deviation. Bronchiectasis occurs in the most severely affected portions, but lymphadenopathy and pleural effusion are uncommon.

Endobronchial spread occurs, with the development of scattered nodular densities, 5-15 mm in diameter. On HRCT, these have a centrilobular distribution.

2. HIV-negative females, also in the 60's and 70's, with no predisposing conditions. Cough is common, but constitutional symptoms (fever, weight loss, fatigue) are not. These patients have scattered reticular and nodular densities, typically with associated bronchiectasis. The lingula and right middle lobe are the most commonly affected areas ("Middle Lobe Syndrome").

3. Asymptomatic patients with solitary or multiple pulmonary nodules. Histologically, these are granulomas, indicating infection, not just colonization. Occasionally, surrounding fibrosis or smaller satellite nodules may be present.

4. Patients with achalasia may develop infection with organisms of the *M. fortuitum* complex. The radiographic pattern is that of patchy homogeneous airspace opacities, often bilateral. The appearance suggests aspiration pneumonia. Chronic lung abscesses may develop in a small number of these patients.

5. Immunocompromised patients (AIDS, transplant recipients, leukemia, lymphoma) in Groups II and III, may develop disseminated NTMB infection. 20-30% of AIDS patients develop clinical NTMB infection during their lifetime, and 50% of AIDS patients have MAC infection detected at autopsy. Prophylactic treatment is now recommended for those AIDS patients with CD4 count below 50.

Symptoms are usually non-specific, and the clinical picture is frequently confused by the presence of other pulmonary pathogens.

The lungs may appear clear in the presence of mediastinal and/or hilar lymphadenopathy. Central necrosis of the lymph nodes is not as frequent as in tuberculosis. Airspace opacities may be present, and, less commonly, nodules, cavities, or interstitial infiltrates.

ADDITIONAL READING:

1. Patz EF, Swensen SJ, Erasmus J. Pulmonary Manifestations of Nontuberculous Mycobacterium. *The Radiologic Clinics of North America* 1995;33:719-729
2. Supplement: American Thoracic Society Diagnosis and Treatment of Disease Caused by Nontuberculous Mycobacteria. *Amer J Resp & Crit Care Med* 1997;156:S1-S25
3. Washington L, Miller WT. Mycobacterial Infection in Immunocompromised Patients. *J Thor Imag* 1998;13:271-281
4. Fraser RS, Muller NL, Colman N, Pare PD, eds. *Mycobacteria (Nontuberculous mycobacteria)*. In: *Diagnosis of Diseases of the Chest*. 4th ed. Philadelphia: WB Saunders; 1999. p. 849-861.

HIV-infection: Primary and Secondary Lung Infection

Linda B. Haramati, M.D.

Objectives:

1. To describe and give examples of the various lung infections to which HIV-infected patients are predisposed.
2. To describe the changes in distribution of infection with the waning immunity (as reflected by CD4) that is a usual feature of untreated HIV-infection.
3. To describe changes in lung disease related to partial immune restoration by treatment with highly active anti-retroviral therapy (HAART).

Needs and Attributes:

This lecture is designed for radiologists who interpret chest radiographs and CT scans. All such radiologists should be familiar with the classic and recent finding of HIV-related pulmonary infections.

The recognition of HIV-infection in the early 1980's was prompted by the description of Kaposi sarcoma in several gay men, and then by recognition of *Pneumocystis carinii* pneumonia (PCP) in patients who did not fit previous categories of immune compromise. Since that time, HIV-infection has reached epidemic proportions throughout the world and became a scourge in the United States. Unlike other forms of immune compromise such as organ transplantation and congenital immune deficiencies that are confined to a small population, HIV infection is widespread. Infection is the most common complication of HIV-infection and the lung is the most frequently involved organ. This brief talk will give an overview of the wide variety of infections that occur in HIV-infected patients, how the patients' immune status reflects the type of infections that they acquire, how HAART with partial immune restoration has decreased the prevalence of severe immunocompromise and how it has changed the course of several diseases.

Although PCP is the pulmonary infection thought to be associated with AIDS, even early in the AIDS epidemic, bacterial pneumonia was recognized to occur more frequently. Infection with pneumococcal pneumonia, haemophilus and other usual species is most common. AIDS patients with bacterial pneumonia are more frequently bacteremic than their immune-competent counterparts. Although the incidence of bacterial pneumonia increases as the patients CD4 decreases, two or more episodes of bacterial pneumonia in a single year are AIDS-defining at any CD4 count. The chest radiographic and CT findings of bacterial pneumonia in HIV-infected patients are similar to that of the general population, although some authors describe more frequent multi-lobar involvement and pleural effusion. As a patient's immunity wanes, various unusual bacterial infections including zoonoses are seen in HIV-infected individuals.

PCP is a taxonomic misfit that has bounced from the protozoal to the fungal category-not fully belonging to either. Previously, PCP was a common presenting infection leading to the diagnosis of AIDS. However, this presentation is currently uncommon, except in patients who have reduced access to healthcare. PCP generally occurs in patients with CD4 counts <200/mm³. HAART has made that level of immune compromise unusual. Prophylactic therapy for PCP is standard for

those with CD4 <200/mm³. When the CD4 increased due to therapy with HAART, the prophylaxis can be stopped. The classic radiographic finding in PCP is bilateral perihilar granular or reticular opacities with ground glass opacities on CT. The course may be complicated by cystic changes leading to pneumothorax. Upper lobe predominance and focal disease are more frequently noted in the current era. CT is especially useful in diagnosing focal, mild PCP in the setting of an equivocal or normal radiograph and a high clinical suspicion.

Tuberculosis is more common in HIV-infected patients at any level of immune status. In early HIV-infection when the patients CD4 count is over 200/mm³, tuberculosis is clinically and radiographically similar to the immunocompetent population with reactivation tuberculosis. As the CD4 count declines, tuberculosis tends to occur more randomly in any lobe of the lung, cavitation becomes unusual and lymphadenopathy is frequently a prominent feature. On contrast-enhanced CT the lymphadenopathy can be low attenuation with peripheral enhancement. Disseminated (miliary) disease occurs most frequently in the severely immunocompromised. After anti-tuberculous antibiotic therapy was described in the 1940s and 1950s a paradoxical response was noted in some patients. In those patients, there was worsening of symptoms including fever and worsening of the chest radiographic findings after initiation of anti-tuberculous therapy. This paradoxical response has been recently described to occur with increased prevalence in HIV-infected patients with tuberculosis who are started on HAART. These patients have worsening of their symptoms and radiographic findings. Usually they undergo an extensive work-up to investigate their worsening condition-with the work-up revealing only tuberculosis. This is thought to be due to an exuberant immune response to the tuberculous infection—with the exuberance attributed to the partial immune restoration by HAART. The treatment of paradoxical response is continuation of therapy with anti-tuberculous antibiotics and HAART. If symptoms are severe, steroids may alleviate them.

Mycobacterium avium complex (MAC) infection has caused significant disease in late stage AIDS. MAC usually occurs as a disseminated infection in those with CD4 counts <50/mm³. In this population, MAC can be detected in the blood and bone marrow and causes fever, anemia and wasting. Involvement of the lung is less frequent although the lung is thought to be the portal of entry for the organism. Chest radiographic findings of pulmonary MAC include lymphadenopathy-which is the most frequent finding. Lung parenchymal nodules with or without cavitation can also be seen. In patients who have diagnosed or undiagnosed disseminated MAC and begin therapy with HAART, a lymphadenitis associated with inflammation in a variety of organs including the lung may occur. As the viral load declines and CD4 climbs, chest radiographs and CTs show worsening lymphadenopathy and infiltrates or nodules, which may be cavitory. Other mycobacterial infections also occur with increased frequency in HIV-infected patients. Their clinical presentation and radiographic findings overlap with tuberculosis and MAC.

AIDS patients are also at an increased risk of developing both endemic and opportunistic fungal infections with the manifestations dependant on the patient's immune status. In the New York City area we see reactivation of the endemic fungus histoplasmosis, usually in the disseminated form, in severely immunocompromised patients who have emigrated from endemic areas. The most common chest radiographic and CT findings are innumerable small nodules-usually slightly larger than military nodules-with or without associated lymphadenopathy. The most common opportunistic fungal infection in AIDS patients is cryptococcus. Cryptococcal meningitis is seen more commonly than cryptococcal pulmonary disease, but the lung is the second most frequently involved organ. It can be involved in isolation, or as a manifestation of disseminated disease. The chest radiographic and CT findings of cryptococcal pulmonary disease in AIDS are varied. Diffuse small nodules can be seen-similar to histoplasmosis. However, single or multiple larger nodules or masses with or without cavitation, pleural effusions and lymphadenopathy are all manifestations of cryptococcus in AIDS. Clinical and radiographic findings in AIDS patients with cryptococcal infection also can worsen on HAART. Thus cryptococcus falls within the spectrum of diseases of immune restoration or reconstitution.

Sarcoidosis, which is of unknown etiology has also been observed to develop or worsen on HAART and is one of the thoracic manifestations of immune reconstitution syndrome.

Aspergillus infection, which occurs with some frequency in solid organ and bone marrow transplant patients can occur in late stage AIDS, but is seen infrequently. Host defense against aspergillosis is neutrophil and macrophage activity rather than cellular immunity, while diminution of cellular immunity is the hallmark of HIV-infection. Therefore, additional factors come into play when AIDS patient develop aspergillosis. They may be treated with medication that suppresses bone marrow, or be at an extreme end stage of their disease with diminished neutrophil function. Although aspergillus is a ubiquitous organism-present in the soil- it is reported that marijuana often contains a large amount of aspergillus. Smoking marijuana in a weakened state of immunity can lead to inhalation of a large bolus of aspergillus organisms and consequent infection. When AIDS patients develop aspergillosis, the most common form is semi-invasive disease. Other forms include invasive and bronchial aspergillosis. The chest radiographic and CT manifestation of aspergillosis include ill-defined nodules or infiltrates, thick-walled cavities with dependant soft tissue masses and bronchial abnormalities. Hemoptysis is a dreaded consequence.

Viral infections are often difficult to document in HIV-infection, as in other clinical settings. In the lung, the most commonly documented viral infection is with cytomegalovirus (CMV). These patients are usually severely immunocompromised with CD4 <100 and often have other manifestations of CMV infection including retinitis, esophagitis or enteritis. The chest radiographic findings are usually quite subtle-demonstrating "increased markings". Occasionally areas of confluence or cavitation are noted. On CT, reticular opacities, peribronchial thickening, bronchiectasis and small nodules may be noted.

The last category of infection that I would like to touch upon is the oncogenic viruses. Although a number of neoplasms are associated with HIV-infection, those that were described earliest and are most strongly associated with HIV have been shown to be related to co-infection with other viruses. It is now unequivocally demonstrated the infection with Human herpes virus 8

(HHV-8) is necessary for development of Kaposi sarcoma-including the AIDS-associated, classical (Mediterranean) and endemic (African) forms. HHV-8 infection is also associated with body-cavity lymphoma and Castelman's disease. Kaposi sarcoma is sexually transmitted. In the United States it is seen most frequently in the gay male population, but in Africa, the gender distribution is more even. Kaposi sarcoma is usually manifest as cutaneous disease. Visceral involvement is present in more severely immunocompromised AIDS patients. Pulmonary disease is rare without cutaneous or oropharyngeal disease. Chest radiographic and CT features of pulmonary Kaposi sarcoma include peribronchial thickening, ill-defined nodules with a peribronchovascular distribution and later-thickened interlobular septae, conglomerate masses, pleural effusion and lymphadenopathy.

AIDS-related lymphoma has been demonstrated to often-but not always-be related to Epstein-Barr Virus (EBV) infection with the viral genome identified in many tumors. Pulmonary disease may be a component of systemic lymphoma-although primary pulmonary lymphoma is also reported in AIDS patients. The chest radiographic and CT findings include lung nodules and masses, pleural masses and effusions. In systemic lymphoma, lymphadenopathy is often present on CT, but extra nodal (pulmonary and pleural) disease is usually the dominant finding.

Women with AIDS have long been described to have an increased risk of cervical dysplasia and carcinoma. Gay men with AIDS have an increased risk of anal carcinoma. In both cases it is due to co-infection with the oncogenic strains of Human papillomavirus (HPV). Metastatic disease to the chest from these primary tumors occasionally presents a diagnostic dilemma.

In conclusion, the decline in cellular immunity caused by infection with HIV predisposes HIV-infected patients to a wide variety of pulmonary infections. The types and manifestations of disease vary with the patients' immune status. Highly active retroviral therapy (HAART) causes dramatic improvement in the patients' immune status associated with a rising CD4, declining viral load and a decreased incidence of opportunistic infections. It has also brought to our attention a change in the clinical and radiographic manifestation of certain diseases encompassed in the "immune reconstitution syndrome".

REFERENCE LIST:

1. Afessa B, Green B. Bacterial pneumonia in hospitalized patients with HIV infection: the Pulmonary Complications, ICU Support, and Prognostic Factors of Hospitalized Patients with HIV (PIP) Study. *Chest* 2000;117:1017-1022
2. Boisselle PM, Crans CA, Jr., Kaplan MA. The changing face of *Pneumocystis carinii* pneumonia in AIDS patients. *AJR Am J Roentgenol* 1999;172:1301-1309
3. Fishman JE, Saraf-Lavi E, Narita M, Hollender ES, Ramsinghani R, Ashkin D. Pulmonary tuberculosis in AIDS patients: transient chest radiographic worsening after initiation of antiretroviral therapy. *AJR Am J Roentgenol* 2000;174:43-49
4. Haramati LB, Lee G, Singh A, Molina PL, White CS. Newly diagnosed pulmonary sarcoidosis in HIV-infected patients. *Radiology* 2001;218:242-246
5. Lanzafame M, Trevenzoli M, Carretta G, Lazzarini L, Vento S, Concia E. Mediastinal lymphadenitis due to cryptococcal infection in HIV-positive patients on highly active antiretroviral therapy. *Chest* 1999;116:848-849

6. Mylonakis E, Barlam TF, Flanigan T, Rich JD. Pulmonary aspergillosis and invasive disease in AIDS: review of 342 cases. *Chest* 1998;114:251-262
7. Nalaboff KM, Rozenshtein A, Kaplan MH. Imaging of *Mycobacterium avium-intracellulare* infection in AIDS patients on highly active antiretroviral therapy: reversal syndrome. *AJR Am J Roentgenol* 2000;175:387-390
8. Ognibene FP, Steis RG, Macher AM, et al. Kaposi's sarcoma causing pulmonary infiltrates and respiratory failure in the acquired immunodeficiency syndrome. *Ann Intern Med* 1985;102:471-475
9. Shah RM, Kaji AV, Ostrum BJ, Friedman AC. Interpretation of chest radiographs in AIDS patients: usefulness of CD4 lymphocyte counts. *Radiographics* 1997;17:47-58
10. Shelburne SA, III, Hamill RJ, Rodriguez-Barradas MC, et al. Immune reconstitution inflammatory syndrome: emergence of a unique syndrome during highly active antiretroviral therapy. *Medicine (Baltimore)* 2002;81:213-227

Viral Infection on HRCT

Tomás Franquet, M.D.

Chest Imaging Section, Department of Diagnostic Radiology,
Hospital de Sant Pau, Universitat Autònoma de Barcelona, Barcelona, Spain

Course Objectives

1. To summarize the high-resolution CT findings of some of the most common viral infectious processes seen in both the immunocompetent and the immunocompromised patient.
2. To understand the spectrum of radiological manifestations according to different immune status of the hosts

Introduction

Respiratory viral infections are the most common illnesses afflicting humans. In the United States more than 500 million acute respiratory illnesses are estimated to occur yearly. In healthy persons, respiratory viral infections associated with acute morbidity but low mortality. However, persons with underlying illness or immunosuppression exhibit increased mortality.

Diagnosis of respiratory viral infections relies on tissue culture techniques, special stains and serologic tests. Numerous viruses, including influenza virus, measles virus, Hantavirus, herpesviruses, varicella-zoster virus, cytomegalovirus, papilloma virus, and Epstein-Barr virus, can cause lower respiratory tract infection in adults.

The radiologic manifestations of pulmonary viral infections are protean and include nodular opacities, tree-in-bud appearance, ground-glass opacities, air-space consolidation, bronchial wall thickening, and small pleural effusions. The differential diagnosis is based on the clinical history and the pattern and distribution of findings on high resolution CT

High-resolution CT can be helpful in the detection, differential diagnosis, and management of immunocompromised patients with pulmonary complications. Although accurate clinical information is essential to narrow the differential diagnosis, it is often still impossible to determine the cause of parenchymal abnormalities in this group of patients. Combination of pattern recognition with knowledge of the clinical setting is the best approach to pulmonary infectious processes. A specific pattern of involvement can help suggest a likely diagnosis in many instances.

The aim of this lecture is illustrate the radiographic and high-resolution CT findings of pulmonary viral infections in the normal and the immunocompromised host.

Viral Infections in the Non-Immunocompromised Patient

Epstein-Barr virus

Pulmonary involvement associated with Epstein-Barr virus infection is a rare but potential complication of infectious mononucleosis. Pathologically, mononuclear inflammatory cells predominately in the interstitium along bronchovascular bundles, interlobular septa, and alveolar septa. The most common CT abnormalities consist of interstitial infiltrates and subsegmental areas of consolidation.

Respiratory Syncytial virus

The most common pneumonia in children under three years of age is caused by respiratory syncytial virus (RSV).

Radiographic diagnosis is suggested by the presence of air trapping and patchy bilateral consolidation.

Tracheobronchial Papillomatosis

Squamous papillomatosis of the respiratory tract is an uncommon abnormality caused by human papillomavirus. It usually affects the larynx of children 18 months to 3 years of age. Bronchopulmonary disease may develop subsequently, typically 10 years or more later.

CT may demonstrate small nodules projecting into the lumen of the airway. Involvement of distal airways and parenchyma can result in multiple, sharply circumscribed nodules that may also cavitate. Fluid levels sometimes can be identified.

Long-standing tracheobronchial papillomatosis may be complicated by the development of squamous cell carcinoma.

Hantaviruses

Hantaviruses are lipid-enveloped RNA viruses. In the early 1990s, the Sin Nombre virus was identified as the agent responsible for a frequently more fulminant and clinically severe disease with prominent pulmonary involvement—the hantavirus pulmonary syndrome. This syndrome characteristically presents as noncardiogenic pulmonary edema.

Radiographically, Hantavirus pulmonary syndrome manifests as interstitial edema with or without rapid progression to air-space disease.

Viral Infections in Immunocompromised Patients

Influenza virus

Influenza virus is a common cause of lower respiratory tract infection in adults and children. It can occur in pandemics, epidemics, or sporadically. Pneumonia is uncommon and usually caused by type A organisms. The risk of developing pneumonia is increased in the elderly and in patients with underlying heart disease, chronic bronchitis, and cystic fibrosis. There have been isolated reports of influenza pneumonia in immunocompromised patients. In the immunocompromised patients, the predominant high resolution CT findings consist of ground glass opacities, centrilobular nodules and branching linear opacities (tree-in-bud pattern).

Cytomegalovirus

Cytomegalovirus (CMV) pneumonia is a common life-threatening complication seen in immunocompromised patients. It occurs most commonly following bone marrow and solid organ transplantation and in patients with the acquired immune deficiency syndrome (AIDS). The HRCT manifestations are variable and may consist of a reticular or reticulonodular pattern, ground glass opacities, airspace consolidation, nodular opacities or a combination of these patterns. There is no radiographic finding characteristic enough to allow differentiation of CMV pneumonia from other infections. Pathologic findings of CMV pneumonia include areas of acute interstitial pneumonia or diffuse alveolar damage, and focal inflammatory or hem-

orrhagic lesions. In patients with CMV pneumonia and poorly defined nodules or nodules with an associated “halo” of ground glass attenuation, histologic correlation showed the nodular opacities to represent focal areas of inflammation or hemorrhage.

Herpes simplex virus type 1

Herpes simplex virus type 1 pneumonia is an unusual infection that typically affects immunocompromised patients. It is also common in patients with severe burns. The CT findings include multiple nodular opacities, patchy segmental or subsegmental consolidation, and ground-glass attenuation.

Pathologically, the nodular lesions contain central necrosis as the virus spreads peripherally from the hematogenously seeded foci.

Varicella-zoster virus

In adults, disseminated varicella-zoster infection tends to cause significant complications such as varicella-zoster virus pneumonia. The characteristic radiographic pattern consists of multiple 5- to 10-mm nodular opacities. Progression to extensive air-space consolidation can occur rapidly. The histologic findings parallel the clinical severity. Histologically, lesions vary from tiny microscopic foci of parenchymal necrosis and inflammation to large zones of necrosis and findings suggestive of diffuse alveolar damage.

Measles virus infection

Although measles pneumonia is rare among adults, immunocompromised patients who have lymphoreticular malignancy or congenital immunodeficiency may die as a result of measles pneumonia.

Histologically, measles virus pneumonia is characterized by multinucleated giant cells containing up to 50 nuclei in the alveolar spaces and within bronchiolar epithelium. CT findings include ground-glass attenuation, air-space consolidation, and small centrilobular nodules

Adenovirus infection

Adenovirus is a common cause of bronchiolitis and atypical pneumonia in children and young adults, and may cause a fulminant pneumonia in immunocompromised patients. Pathologically, the lungs are large and heavy and show patchy areas of hemorrhagic consolidation. Nuclear inclusion bodies, most prominent in alveolar lining cells but also found in the airway epithelium, may be identified in infected cells. The bronchiolitis may be necrotizing and results in a necrotizing bronchopneumonia similar to that seen in severe herpes simplex infection. The most frequent radiographic findings of adenovirus pneumonia are unilateral or bilateral bronchopneumonia.

REFERENCES:

1. Kim EA, Lee KS, Primack SL et al. Viral pneumonias in adults: radiologic and pathologic findings. *RadioGraphics* 2002;22:S137-S149
2. Kang EY, Patz Jr EF, Müller NL. Cytomegalovirus pneumonia in transplant patients: CT findings. *J Comput Assist Tomogr* 1996; 20:295-299
3. Franquet T, Lee KS, Müller NL. Cytomegalovirus pneumonia: thin-section CT findings in 32 immunocompromised non-AIDS patients. (submitted)
4. Worthy SA, Flint JD, Müller NL. Pulmonary complications after bone marrow transplantation: high-resolution CT and pathologic findings. *RadioGraphics* 1997;17:1359-1371

Imaging of Coccidioidomycosis

William Berger, M.D.

Objective: To illustrate the various imaging findings related to thoracic *Coccidioides immitis* infection.

Coccidioidomycosis is an infection caused by *Coccidioides immitis*, a dimorphic soil-inhabiting fungus. The disease occurs in endemic areas, essentially confined to the Western Hemisphere, particularly the southwestern United States. Approximately 100,000 new cases of coccidioidomycosis occur in endemic regions each year. Knowledge of the various imaging findings related to coccidioidomycosis is important for radiologists outside of endemic regions as the southwestern United States is a popular tourism destination, and consequently patients with coccidioidomycosis may seek medical attention in nonendemic regions.

Pulmonary manifestations are particularly common, as 99% of coccidioidomycosis infections are acquired by inhalation of arthrospores contained in dust. Approximately 30-40% of patients will develop symptoms following a 1-3 week incubation period, usually mild respiratory illness characterized by pleuritic chest pain and dry cough. Systemic manifestations may occur and include fever, night sweats, and myalgia. "Valley" or "Desert" fever usually implies primary disease combined with characteristic skin lesions such as erythema nodosum. Resolution of the infection usually occurs over 2-6 weeks, after which immunocompetent patients develop immunity. About three quarters of patients with primary coccidioidal pneumonia will go on to complete recovery. Persistent primary or chronic pulmonary Coccidioidomycosis occurs in about 5% of patients. Approximately 0.5% of white and 10-15% of African American and Filipino patients develop disseminated disease.

A diagnosis of Coccidioidomycosis in endemic areas may be established if typical clinical or radiographic findings are present. In nonendemic areas, a travel history is of great importance as the diagnosis may be delayed without knowledge of previous travel to an endemic region. Serologic tests for *C. immitis* are of benefit in establishing the diagnosis of acute or primary coccidioidomycosis, as they are accurate, and generally considered to be the most reliable among currently available serologic markers for mycoses. Occasionally, bronchoscopy, or biopsy of a lymph node, skin lesion, or pulmonary nodule is needed to establish the diagnosis.

Treatment with antifungal medication is usually not necessary, but is often indicated for immunocompromised patients and in those with severe primary or disseminated coccidioidomycosis. Antifungal medication is usually not required for treatment of a nodule or cavity, or following resection of a lung lesion. Symptomatic patients with cavities may be treated with oral azole therapy. Further, cavities that are large, persist, or are subpleural (predisposing to rupture into the pleural space) are usually treated operatively. Chronic coccidioidal fibrocavitary disease is usually treated with azole antifungal therapy.

Primary Coccidioidomycosis occurs after inhalation of the arthrospores, which induce an exudative reaction, producing a typical bronchopneumonia, which eventually is accompanied by a granulomatous reaction. The pneumonia usually remains relatively localized, and frequently completely resolves.

Radiographic findings in primary coccidioidomycosis vary from no abnormalities to areas of air space consolidation, which are

usually unilateral (80%) and often confined to the parahilar and basal regions. Consolidation is the most common radiographic abnormality and may be dense or hazy and ill defined.

Occasionally, areas of consolidation may resolve in one area and develop in another, producing so-called "phantom infiltrates". Mediastinal (5%) and hilar (15%) adenopathy may occur, and small effusions (typically ipsilateral to consolidations) occur in about 10%. Large effusions are rare. Less commonly, a cavity or one or more nodules may be present during the primary phase of the disease.

Chronic Coccidioidomycosis is typically defined when clinical and radiographic manifestations last for longer than 6 weeks. Most commonly, a single nodule develops, frequently in the same area as a pre-existing consolidation, a finding that is particularly suggestive of Coccidioidomycosis. The nodules are usually less than 4 cm, frequently occur in mid to apical portions of the lung (including the anterior segments of the upper lobes in contrast to tuberculosis), and almost never calcify. These nodules may spontaneously cavitate and resolve, remain stable, or enlarge slowly. Less frequently multiple nodules may develop. Multiple nodules are almost always randomly distributed, small, and occasionally show microcavitation. Marked contrast enhancement of Coccidioidal nodules has been reported. Most patients with nodules are asymptomatic and frequently serum coccidioidal antibodies are negative.

Occasionally biopsy of a nodule may be necessary to exclude a malignant etiology if a previous pneumonia in the same location can not be documented. Cavities are usually the result of cavitation of a nodule or excavation of a pneumonia. The cavities are also usually less than 4 cm and frequently have thin-walled "grape skin" morphology, though thick or irregular cavity wall morphology may also be observed. They are well circumscribed and rarely contain air-fluid levels. They also have a propensity for the upper lungs and frequently resolve spontaneously. About half of patients with cavities are asymptomatic, 25% have hemoptysis or respiratory complaints. Subpleural cavities may rupture into the pleural space producing pneumothorax and associated empyema. The most serious form of chronic Coccidioidomycosis is progressive and persistent pneumonia, which may ultimately prove fatal, especially in immunocompromised patients. Chronic progressive coccidioidal pneumonia occurs in less than 1% of patients, and may simulate chronic pulmonary tuberculosis or histoplasmosis due to presence of apical fibronodular changes, cavities, and volume loss.

Disseminated Coccidioidomycosis usually occurs early in the course of the disease, but may develop from chronic progressive pneumonia or extrathoracic coccidioidomycosis. Disseminated disease, is more common in African American and Filipino patients, as well as the immunocompromised. Disseminated coccidioidomycosis has been documented in immunocompetent patients, though is more commonly fatal in immunocompromised patients. Disseminated thoracic coccidioidomycosis usually produces a miliary pattern. Associated mediastinal or hilar adenopathy is common. Extrathoracic disease is also frequently present, usually related to basal meningitis, meningoencephalitis, or vertebral osteomyelitis.

Tracheobronchial Tumors

Jo-Anne O. Shepard, M.D.

Director, Thoracic Radiology
Massachusetts General Hospital

BENIGN TUMORS AND CYSTS

Benign tumors of the trachea are very rare and account for 10% of tracheal tumors. Ninety percent of benign lesions are encountered in the pediatric age group. Benign tumors represent a large group of diverse lesions that manifest as sharply defined masses with no invasive characteristics. They are usually homogeneous, and the majority of lesions have no characteristic features to differentiate them by radiologic means.

Papillomas

Papillomatosis is the result of a multicentric viral infection with the human papilloma virus. Papillomas occur either singly or as multiple, irregular tumor excrescences that generally arise from the true vocal cords. Papillomas most often involve the superior surfaces or free margins of the vocal cords and less commonly occur in the supraglottis and subglottis. Papillomas are divided into juvenile and adult groups. Papillomas of the juvenile group often manifest as multiple lesions most commonly found in the larynx. The papillomas may recur or may spread diffusely through the trachea, bronchi and lungs following excision. In the lungs, sheets of squamous cells proliferate within alveoli forming nodules that characteristically cavitate. The adult type of lesion often presents as a solitary mass with a lesser propensity to recur after removal. Transformation of the lesions into invasive squamous cell carcinoma is well known.

Radiographically, the tracheal walls may appear thickened and nodular in appearance, either in a focal or diffuse fashion, sometimes visible on chest radiographs, but best demonstrated on CT. Multiple pulmonary nodules with and without cavitation can be identified on chest radiographs and CT.

Chondromas

Chondromas of the larynx are uncommon lesions that occur most frequently in middle age men. The tumor is smooth, submucosal, and firm in consistency. On the radiographic and CT examination the tumor presents as a sharply defined mass and frequently contains mottled calcifications. Radiologically, a chondroma cannot be distinguished from a chondrosarcoma; this distinction also may be difficult on histopathologic examination. The most common location is the inner surface of the cricoid lamina (70%). Less often, chondromas arise from the thyroid, arytenoid, or epiglottic cartilages. On rare occasions, chondromas may be situated on the upper surfaces, free margins, or undersurfaces of the vocal cords. Chondromas may occur in the trachea but occur less commonly than laryngeal chondroma.

Hemangiomas

Hemangiomas are uncommon lesions in the larynx and even less commonly in the trachea. The pediatric type of hemangioma usually manifests by 6 months of age, is subglottic in location, and causes signs of airway obstruction. Typically, these children exhibit hoarseness, stridor, and dysphagia with poor feeding. In the anteroposterior radiographic film there is subglottic often asymmetrical narrowing and evidence of a distinctive homogeneous, sharply defined soft tissue mass. In adults, laryngeal

hemangiomas usually arise in the supraglottic larynx as a sharply defined, homogeneous mass that may contain phleboliths. Most of the reported cases are of the cavernous variety, as opposed to capillary hemangiomas, which are seen in infancy.

Other benign tumors

Miscellaneous benign tumors are encountered in the larynx and trachea. These include neurogenic tumors, pleomorphic adenoma, oncocytic tumor, granular cell tumor, paraganglioma, lipoma, fibrous histiocytoma and rhabdomyoma and hamartomas. Conventional radiographs do not usually reveal any characteristic features that allow a specific histopathologic diagnosis. CT can identify fatty attenuation within hamartomas and lipomas and increased contrast enhancement within paragangliomas. A chondroid matrix can be identified within chondromas and chondrosarcomas.

Laryngoceles

Various cystic lesions are encountered in the larynx which are either retention cysts or laryngoceles. Laryngoceles are air- or fluid-filled outpouchings of the mucosa of the laryngeal ventricles. They extend from the ventricle into the adjacent aryepiglottic fold and are then referred to as internal laryngoceles. They may, however, herniate through the thyrohyoid membrane and result in external laryngoceles. They are characterized by an air-filled structure that is usually well defined. Intralaryngeal expansion leads to a variable degree of airway obstruction, depending on the size of the lesion. If these laryngoceles are filled with fluid, they manifest as homogeneous, dense masses and cannot be differentiated from a benign tumor.

Tracheal cyst or tracheocele

A tracheal cyst is a thin walled air containing paratracheal cavity that is visible on chest radiographs and chest CT examinations. The tracheal cyst is a circumscribed saccular tracheal outpouching of the posterior wall of the trachea. The cyst may rarely contain an air-fluid level. Dynamic bulging can be observed during a Valsalva maneuver at fluoroscopy or on CT. This condition occurs through a localized weakness of the membranous part of the tracheal and is theorized to be associated with obstructive lung disease.

MALIGNANT LESIONS

Epithelial tumors

Larynx

The majority of laryngeal malignancies (90%) represent epithelial neoplasms. Among these, about 50 to 70% of laryngeal cancers are glottic in nature, about 30 to 35% represent supraglottic carcinomas, and 4 to 6% represent subglottic carcinomas. Tumor size, location, and histologic grading are important parameters that determine the occurrence of lymph node metastases. Metastatic lymph nodes are more common when the primary tumor in the supraglottic larynx is greater than 2.0 cm in diameter and is poorly differentiated. Supraglottic carcinomas arise

from the laryngeal surface and rim of the epiglottis, aryepiglottic folds, arytenoids, false cords, and laryngeal ventricles. They commonly extend across the midline, invade the extralaryngeal structures by direct extension to the pyriform sinuses, postcricoid region and potentially extend to the cervical esophagus, valleculae, and base of tongue. Vocal cord cancers arise commonly from the anterior two-thirds of the vocal cords and may spread via the anterior commissure to the subglottic space (20%) and infrequently into the cervical trachea. Deep penetration of the cord by tumor into the vocalis muscle causes fixation of the cord.

Carcinomas arising in the cervical trachea may involve by superior extension the subglottic larynx. In larger carcinomas it is often difficult to determine whether the origin is from the cervical esophagus, the cervical trachea or an extension of a subglottic carcinoma into the upper trachea. Stomal recurrence post-laryngectomy is encountered in 5 to 15% of cases. The tumor manifests as single or multiple nodules at or near the stomal margin involving the skin or tracheal mucosa. Deep invasion is commonly present associated with ulceration at the skin margin.

CT evaluation provides valuable information concerning extension of malignant tumor to the following areas: 1) the anterior commissure; 2) the paracordal and para-arytenoidal areas; 3) the preepiglottic and subglottic spaces; 4) cartilage invasion; 5) extralaryngeal extension of an endolaryngeal tumor and 6) extension of pyriform sinus carcinomas through the cricothyroid space to involve the postcricoid region and cervical esophagus. Contrast CT or MRI is utilized to evaluate the tracheal extension and tumor invasion of the upper mediastinum prior to surgery and/or radiation therapy.

Trachea

Although very rare, primary malignancies of the trachea are much more common than benign tumors. Squamous cell carcinoma is the most common tracheal malignancy (50%), followed by adenoid cystic carcinoma (30%), and adenocarcinoma (10%). Other less frequently encountered malignancies include mucoepidermoid carcinoma, undifferentiated carcinoma, small cell carcinoma, and carcinosarcoma.

Squamous cell carcinoma

Squamous cell carcinoma may present as a focal mass with a tendency for exophytic growth and a propensity to invade the mediastinum. Synchronous and metachronous squamous cell carcinomas of the larynx, lungs and esophagus are found in many patients. CT is useful in demonstrating the primary tumor and its extent in the trachea and adjacent mediastinum as well as associated adenopathy within the mediastinum and hilum.

Adenoid cystic carcinoma

Adenoidcystic carcinoma tends to grow with endophytic spread in the submucosal plane of the trachea and bronchi. On radiographs, CT and MRI scans the trachea appears thickened with a smooth nodular appearance, associated with luminal narrowing. The tumor may extend into the adjacent soft tissues of the neck and mediastinum, depicted on CT or MRI as extension into the adjacent mediastinal fat. Regional lymph nodes in the neck and mediastinum are the first to be involved by metastases. Hematogenous metastases to lung, bones and liver do occur later in the disease progression.

Mucoepidermoid tumors

Mucoepidermoid tumors are very uncommon tumors of the trachea, central bronchi and rarely of the lung. They may be of either high or low-grade malignancy. The radiographic findings are of a focal endoluminal soft tissue mass within a large central airway, without characteristic features to distinguish the mass from other tumors.

Carcinoid tumors

Carcinoid tumors are neuroendocrine tumors derived from the Kulchitski cell. Typical carcinoid tumor represents the lowest grade subtype of a spectrum of tumors that includes the more aggressive atypical carcinoid tumor and the highly malignant small cell carcinoma. *Typical carcinoids* present in the fifth and sixth decades and tend to arise in the central bronchi, peripheral lung (10%) and rarely in the trachea. They tend to be smooth, well-defined round masses that present as a nodular filling defect and may be associated with atelectasis, distal pneumonia, and/or bronchiectasis if they cause bronchial obstruction. *Atypical carcinoid tumors* tend to present in the sixth and seventh decades of life, may be either central or peripheral in the lung and have a tendency to metastasize to regional hilar and mediastinal lymph nodes. *Small cell carcinomas* are extremely malignant tumors that present in the seventh and eighth decades. They usually are associated with large bulky central hilar and mediastinal lymphadenopathy and distant metastases at the time of diagnosis. CT scans often reveal a small peripheral primary tumor within the lung, generally not visible on routine chest radiographs.

Carcinoid tumors have several distinguishing features on imaging studies. Typical carcinoid tumors generally exhibit slow growth and may contain calcifications. Carcinoid tumors are highly vascular and will demonstrate a high degree of contrast enhancement with iodinated contrast on CT scans. Because somatostatin receptors are found in carcinoid tumors, radionuclide-coupled somatostatin analogues such as ¹²³I-Tyr3-octreotide and ¹¹¹In-octreotide can be used to identify carcinoid tumors. This diagnostic approach is helpful in identifying occult carcinoid tumors in those patients who present with clinical symptoms referable to serotonin, ACTH or bradykinin production.

Mesenchymal tumors

Mesenchymal tumors are rarely reported to occur in the trachea, and tend to occur in young adults. Fibrosarcoma, leiomyosarcoma, chondrosarcoma, hemangioendotheliosarcoma, and lymphomas have been reported. Except for calcifications in the chondrosarcomas, there are no specific characteristics with which to differentiate mesenchymal tumors from other malignancies.

Secondary malignant tumors

Carcinomas especially papillary and follicular types arising from the thyroid gland may invade the larynx and cervical trachea in up to 5% of cases. The trachea may also be invaded by tumors of the esophagus and lung. The delineation of the extent of these tumors is best accomplished with CT and MRI.

REFERENCES:

- Becker M, Moulin G, Kurt AM, Dulgerov P, Vukanovic S, Zbaren P, Marchal F, Rufenacht DA, Terrier F. Non-squamous cell neoplasms of the larynx: radiologic-pathologic correlation. *Radiographics*. 18(5):1189-209, 1998.
- Kushner DC, Harris GBC: Obstructing lesions of the larynx and trachea in infants and children. *Radiol Clin North Am* 16:181, 1978.
- Grillo HC. Tracheal tumors. In: Choi NC, Grillo HC, eds. *Thoracic Oncology*. New York: Raven Press, 1983.
- Hadu SI, Huvos AG, Goodner JT et al. Carcinoma of the trachea: Clinicopathologic study of 41 cases. *Cancer* 25:1448-1456, 1970.
- Heitmiller RF, Mathisen DJ, Ferry JA, Mark EJ, Grillo HC: Mucoepidermoid lung tumors, *Ann Thorac Surg* 47:3394-399, 1989.
- Mathisen DJ. Tracheal tumors. *Chest Surg Clin N Am* 6(4):853-864, 1996.
- Mathisen DJ. Primary tracheal tumor management. *Surg Oncologic Clin N Am* 8(2):307, 1999.
- Meyers BF, Mathisen DJ. Management of Tracheal Neoplasms. *Oncologist*. 2(4):245-253, 1997.
- McCarthy MJ, Roasado-de-Christenson ML. Tumors of the trachea. *J Thorac Imaging* 10(3): 180-198, 1995.
- Weber AL, Grillo HC: Tracheal tumors: A radiological, clinical, and pathological evaluation of 84 cases. *Radiol Clin North Am* 16: 227, 1978.
- Weber AL, Shortsleeve M, Goodman M et al: Cartilaginous tumors of the larynx and trachea. *Radiol Clin North Am* 16: 261, 1978.
- Zwiebel BR, Austin JH, Grimes MM: Bronchial carcinoid tumors: Assessment with CT of location and intratumoral calcification in 31 patients, *Radiology* 179:48333-486, 1991.

Inflammatory Diseases of Central Airways

Arfa Khan, M.D.

COURSE OBJECTIVES

1. Become familiar with the rare inflammatory diseases of central airways.
2. Describe the radiographic findings and differential diagnosis of the inflammatory disease of central airways.

INTRODUCTION

1. Inflammatory diseases of the central airway are uncommon. The following list contains the most common etiologies of the inflammatory diseases of central airways.
 - Granulomatous Tracheobronchitis
 - Infection - Scleroma, Fungal and T.B.
 - Granulomatous - Wegener's and Sarcoid
2. Tracheopathia osteochondoplastica
3. Relapsing Polychondritis
4. Amyloidosis
5. Ulcerative Colitis

SCLEROMA

Scleroma or rhinoscleroma is a chronic progressive granulomatous infection that affects the respiratory tract from the nose to bronchi. The etiologic agent is a gram-negative diplobacillus, *Klebsiella rhinoscleromatis*. The disease primarily affects the nose, sinuses and pharynx. From 2 to 9 % of patients develop tracheal disease that most commonly affects the proximal trachea; however, it may involve the entire trachea and main bronchi. Scleroma is uncommon in the West, occurring mainly in the underdeveloped countries with low socioeconomic status. The disease manifests in four overlapping stages: the catarrhal stage, characterized by prolonged purulent rhinorrhea, the atrophic stage, with mucosal changes and crust formation; the granulomatous stage, characterized by granulomatous nodule in the nose with or without involvement of other respiratory tract and the sclerotic stage, with dense cicatricial fibrosis of involved tissues.

The radiographic findings include thickening of tracheal wall, nodular deformity of the tracheal mucosa, subglottic stricture and concentric narrowing of the trachea and central bronchi.

The disease can be arrested especially in the granulomatous pre fibrotic stage by appropriate antibiotics. Balloon dilation or mechanical dilation can sometimes be used to treat significant fibrotic stenosis of trachea and bronchus with the rigid bronchoscope. A tracheostomy is occasionally required for severe involvement of larynx or subglottic space.

TUBERCULOSIS

Although common in past, tracheobronchial tuberculosis is now rare. The reported incidence of bronchial tuberculous stenosis in patients with tuberculosis ranges from 40% in the preantibiotic era to 10% in more recent years. It is usually associated with cavitary lung disease and grossly infected sputum. There are three histopathological stages of tracheobronchial tuberculosis, which may exist alone or coexist. In the hyperplastic stage, there is formation of tubercles in the submucosal layer. Ulceration and necrosis of the bronchial wall is followed

by a fibrostenotic stage, in which a residual stenosis is formed. Tracheobronchial stenosis can develop acutely at the time of the pulmonary tuberculosis or can become manifest as many as 30 years later. However, active parenchymal tuberculosis is not a prerequisite to the development of tracheobronchial stenosis.

The radiographic findings of central airway tuberculosis differ according to the stage of the disease. Central airways narrowing are seen in both active and fibrotic stages. However, in patients with active disease, CT shows irregular and thick walled airways, a pattern that usually reverses after appropriate antitubercular therapy, whereas patients with fibrotic disease generally have smooth narrowing of the airways and minimal wall thickening, a pattern that is irreversible.

WEGENER'S GRANULOMATOSIS

Wegener's granulomatosis is a granulomatous vasculitis of the upper and lower respiratory tract that is usually accompanied by renal and other organ involvement. It is a disease of unknown pathogenesis and is more prevalent in men and typically affects middle-aged persons. The classic manifestations include glomerulonephritis in addition to systemic vasculitis. Laryngeal and endobronchial involvement is rare and usually seen late in the disease process. The radiographic features of airway involvement may be focal or diffuse. The diseased portions of trachea typically have circumferential mucosal thickening; irregularity, and ulceration that are best shown with CT. Involvement of the cartilaginous rings is less common but may result in deformity and narrowing of the trachea. Bronchial wall involvement may lead to airway obstruction and atelectasis. Other radiographic findings include parenchymal nodular opacities, which may cavitate; ill-defined areas of increased opacity; and pleural effusions.

SARCOIDOSIS

Sarcoidosis typically affects the hilar and mediastinal nodes and the lung parenchyma. However, 1-3% of patients will have tracheal involvement, primarily in the upper part of trachea. The distal parts of the trachea and primary bronchi are affected infrequently. Narrowing of the airway may be secondary to extrinsic compression from enlarged lymph nodes or may be the result of granuloma formation within the airway mucosa and submucosa.

The radiographic appearance is similar to that of other stenosis. Bronchial wall thickening reflects the presence of granuloma in the bronchial mucosa. Other findings, such as lymph node enlargement, may also be present.

TRACHEOPATHIA OSTEOCHONDROPLASTICA

Tracheopathia osteochondroplastica (TO) is a rare, benign disorder involving the trachea and main bronchi characterized by multiple submucosal osteocartilagenous nodules. TO was originally described by Wilks in 1857. The etiology is not known, although different theories like congenital, familial, chronic infectious-inflammatory, degenerative, metabolic etc have been postulated. The nodules classically affect the lower two-thirds of the trachea and proximal portions of the primary

bronchi. The nodules may be either focal or diffuse, characteristically, these nodules spare the membranous posterior wall of the trachea. There is a 3:1 male predilection and the disease typically manifests between fifth and sixth decades. The disease usually remains asymptomatic and may be detected on bronchoscopy performed for another reason. The prevalence of TO found during routine bronchoscopy for unrelated complaints ranges from 0.02% to 0.7%. When symptomatic, TO has been reported to cause recurrent infection, cough, stridor and hemoptysis. The evolution of the disease is usually slow and prognosis depends on the extent of the disease.

The characteristic CT appearance consists of calcified nodules measuring between 3 and 8mm in diameter resulting in irregular narrowing of the lower trachea and main stem bronchi with sparing of the posterior tracheal wall.

At bronchoscopy, these nodules are typically hard and difficult to biopsy. The diagnosis is made from the visual appearance alone. There is currently no specific treatment to remove the abnormal tissue growth or to prevent the development of new nodules.

RELAPSING POLYCHONDRITIS

Relapsing polychondritis is a rare inflammatory disease of unknown cause involving the cartilage of nose, ears, upper respiratory tract, and the joints. It is thought to be related to abnormal acid mucopolysaccharide metabolism, an association has also been noted in approximately 25% of cases with autoimmune vasculitis.

Histologically, there is evidence of chondritis with perichondral inflammation, loss of basophilic staining of cartilage matrix and fibrous replacement of damaged cartilage. Clinically auricular chondritis is seen in 88% of patients. Nasal chondritis is less frequent. Polyarthrititis occurs in 76% of the patients. The respiratory tract is affected in 56-70% of cases and carries a poor prognosis, accounting for 50% of deaths.

Characterized by episodic inflammation, relapsing polychondritis results in diffuse tracheal and bronchial narrowing secondary to a combination of edema, granulation tissue, cartilage destruction and ultimately fibrosis of the tracheal wall. When severe, this disease may result in airway obstruction and recurrent episodes of atelectasis and pneumonia.

At radiography, diffuse or localized airway involvement may be seen. The larynx and upper trachea are affected most frequently, but disease may involve airways to the subsegmental level.

Trachea narrowing resulting from thickening of the anterior and lateral walls with sparing of the posterior tracheal wall is characteristic. Dynamic imaging during expiration may demonstrate airway collapse.

AMYLIODOSIS

Amyloidosis is characterized by the deposition of abnormal proteinaceous material (amyloid) in extra cellular tissue that characteristically stains with Congo red. Amyloid infiltration of the airways and lung may occur as an isolated phenomenon or as part of diffuse systemic disease. Three patterns of respiratory involvement have been described; (a) tracheobronchial, (b) nodular parenchymal disease, (c) diffuse parenchymal disease. The tracheobronchial pattern is the most common pattern of respiratory amyloidosis. Tracheobronchial amyloidosis is rare and is generally confined to the trachea without evidence of concurrent parenchymal disease. Deposits may be either solitary or multiple, with or without calcifications, and if sufficiently large, they can lead to hemoptysis or airway obstruction with resultant atelectasis or recurrent pulmonary infection.

The classic radiographic appearance of tracheobronchial amyloidosis is nodular and irregular narrowing of the tracheal lumen. Lobar or segmental collapse may be seen with endobronchial obstruction due to amyloid deposition. In certain cases of diffuse involvement, there is significant component of calcification and ossification of the lesions. Unlike tracheopathia osteochondroplastica, in which nodules spare the membranous portion of trachea, amyloidosis involves the entire circumference of the trachea.

ULCERATIVE COLITIS

Rare involvement of both large and small airways has been reported to occur in patients with ulcerative colitis. Findings of submucosal fibrosis and airway narrowing have been described, including the trachea, often in association with bronchiectasis. To date no apparent relationship has been established between disease activity within the colon and airway abnormalities.

On CT, the tracheobronchial walls appear thickened, resulting in an irregular narrowing.

REFERENCES:

- Prince JS, Duhamel DR, Levin DI, Harrell JH, Friedman PJ: Nonneoplastic Lesions of the Tracheobronchial Wall: Radiographic Findings With Bronchoscopic Correlation. *RadioGraphics* 2002; 215-230.
- Shepard JO: The Bronchi: An Imaging Perspective. *Journal of Thoracic Imaging* 1995, Vol. 10, No. 4, 230-255.
- Daun TE, Specks U, Colby TV, Edell ES et al: Tracheobronchial Involvement in Wegener's granulomatosis. *Am J Respiratory Care* 1995 151: 522-6.
- Port JL, Khan A, Barbu RR: Computed Tomography of Relapsing Polychondritis. *J Compt Rad.* 1993, 17(2): 119-23.
- Pickfor HA, Swensen SJ, Utz JP: Thoracic Cross-Sectional Imaging of Amyloidosis. *AJR* 1997, 168(2): 351-5.
- Moon WK, Im JG, Yeon KM, Han MC: Tuberculosis of the Central Airways. *AJR* 1997, 169 (3): 649-53.

Virtual Endoscopy in the Thorax: Present and Future Applications

R.C. Gilkeson, M.D.

University Hospitals of Cleveland
CWRU Medical School

Learning Objectives:

1. To understand the imaging appearances of large and small airway disease
2. To gain a basic understanding of virtual bronchoscopy and its clinical utility.
3. To understand the virtual bronchoscopic appearance of a variety of airway diseases.

In the clinical evaluation of pulmonary disease, fiberoptic bronchoscopy is a crucial tool in the diagnosis of a variety of chest diseases. Though often instrumental in the diagnosis of a variety of neoplastic, inflammatory and infectious diseases, fiberoptic bronchoscopy (FOB) has important limitations: It is invasive, time consuming, and requires sedation. It is often not well tolerated in the young, the critically ill, or in patients with coagulopathies. In patients with significant airway disease/stenoses, the bronchoscopic evaluation of the airway distal to areas of stenoses/narrowing is technically difficult and can often significantly compromise patient oxygenation. Equally important, the evaluation of extraluminal pathology is significantly limited in fiberoptic bronchoscopy. Moreover, the diagnostic capabilities of FOB in the evaluation of extraluminal pathology is limited. The last decade has seen incredible advances in thoracic imaging. The advent of spiral CT, and the acquisition of volumetric data sets, has allowed anatomic depiction of axially acquired data. MPR, MIP, and volume rendering techniques are now standard in chest imaging. With increasingly sophisticated software, axial images can be reconfigured to display this data from an endoscopic perspective. This has clearly been important in the evaluation of bowel pathology, and virtual colonoscopy offers promising results in the non-invasive screening evaluation of colon cancer. Similar advances have been made in other gastrointestinal organs, the paranasal sinuses and vascular structures. Virtual bronchoscopy has similarly become an important tool in the evaluation of chest diseases. While original virtual bronchoscopy programs were often time consuming and impractical to the practicing radiologist, increasingly sophisticated post processing techniques have improved the speed and accessibility of the user interface, enabling rapid virtual endoscopic depiction of the airways. This presentation will outline these advances, and present the use of virtual bronchoscopy in the evaluation of a variety of neoplastic and non neoplastic processes. Other endoscopic applications in the thorax will be presented, along with a discussion of their possible future in chest imaging.

Several principles in image acquisition are crucial in the successful performance of virtual bronchoscopy. A number of studies have demonstrated the importance of narrow collimation and reconstruction overlap of at least 50% to optimize any type of three dimensional imaging; and these parameters are similarly important to virtual bronchoscopic evaluation. For single slice CT scanners a slice thickness of 3-5mm is preferred. While pitch values up to 2 are usually acceptable for the volumetric depiction of pathology, most published protocols prefer a pitch of 1 for virtual bronchoscopic rendering using a single slice scanner. With the advent of the dual slice CT scanner, slice collimation of 2.5mm

with 1mm slice reconstruction has been published. With the advent of multislice scanning slice acquisitions of 4-32 slices and gantry rotation times of 500msec, virtual bronchoscopic imaging can now be routinely performed with 1mm slice collimation. While there is not a significant amount of data on the role of multislice CT in virtual bronchoscopy, examination of these improved imaging parameters would strongly suggest their superiority in VB imaging. While the use of IV contrast is not necessary in most virtual bronchoscopy, it is often used for the depiction of extraluminal pathology. To optimize contrast opacification of extraluminal vascular structures, 100-140cc of IV contrast is used at injection rates that range from 2-5cc/sec. As will be discussed later, accurate integration of extraluminal pathology with the virtual bronchoscopic data helps optimize virtual bronchoscopy diagnostic capabilities. Accurate segmentation of extraluminal structures is optimized with IV contrast, and is therefore important to advanced VB protocols. At our institution, cases in which virtual bronchoscopy is considered is now performed entirely on our multislice scanners. Decisions on 1 or 2.5mm scanning is depends on the clinical question and anatomic coverage required. The speed of the multislice scanner allows dynamic inspiratory/expiratory endoscopic imaging, which has proven important to our referring pulmonologists in the evaluation of tracheomalacia and suspected upper airway collapse. Future research in image optimization in VB includes the role of cardiac gating in the accurate depiction of airway stenoses, and will be presented here.

Following the acquisition of the spiral CT data, transfer of the DICOM data to advanced imaging workstations can be performed. There are a variety of advanced imaging products capable of virtual endoscopic imaging. These products include General Electric Navigator (General Electric Medical Systems, Milwaukee, Wis), Vital Images Voxel View (Vital Images, Fairfield Connecticut), Iris Explorer (Silicon Graphics, Mountain View, USA). A number of advanced, hybrid imaging techniques have been developed at individual institutions to further optimize the VB data. At our institution we have used Voyager Software (Phillips Medical Systems) for virtual bronchoscopy. The recent transition to a Windows NT workstation has significantly improved the speed for image reconstruction of this data and made virtual bronchoscopic imaging increasingly accessible to the less experienced operator. The effective use of virtual bronchoscopy necessitates an understanding of the anatomy seen during fiberoptic bronchoscopy. In particular, the perspective of the bronchoscopist, with the bronchoscope displaying the anatomy in a cranial-caudad direction with the patient in a supine position, needs to be easily understood by the thoracic radiologist. For those radiologists involved with virtual bronchoscopy, a solid understanding of the anatomy seen at fiberoptic bronchoscopy is important, and participating/correlation with fiberoptic bronchoscopy is important in understanding the capabilities and limitations of virtual bronchoscopy. In most virtual bronchoscopy software packages, both surface and volume rendering can be performed. Surface rendering is most often used because with traditional software, reconstruction times for virtual bronchoscopy is faster than volume rendering. Standard

threshold values for surface rendering techniques have been described by Summers as ~ 500 . While these thresholds are effective in the main and lobar bronchi, artifacts can occur in the smaller airways, and may also result in an overestimation of stenoses. Faster reconstruction times have made volume rendered techniques more accessible and are used increasingly at our institution.

As we have seen with more recent literature in virtual colonoscopy, an original fascination with the technology has given way to a more realistic assessment of VBs particular capabilities and weaknesses. One of the greatest strengths of virtual bronchoscopy is the added benefits inherent in CT imaging. Unlike fiberoptic bronchoscopy, the data used in the generation of the virtual bronchoscope is not limited to the lumen: CT bronchoscopy has the ability to accurately depict extraluminal anatomy not available to the bronchoscopist. Integration of this intraluminal and extraluminal data will be discussed later. Many of the imaging limitations of virtual bronchoscopy have been well defined by Summers, but often describe the markedly limited ability of the virtual bronchoscope to depict mucosal abnormalities. The unavoidable integration of cardiac and respiratory motion into the virtual bronchoscope introduces subtle error into the depiction of VB data and therefore limits the ability to evaluate the mucosal and submucosal pathology.

A number of papers have been written comparing the diagnostic value of virtual bronchoscopy with standard CT images as well as fiberoptic bronchoscopy. One of the values of virtual endoscopy in the airways is the evaluation of the upper airways. In a paper by Burke, Vinings and others using FreeFlight software, evaluation of airway obstruction was evaluated using virtual bronchoscopy. This study included 30 patients with upper airway disease ranging from airway stenosis, laryngotracheomalacia, tumors and webs. There was excellent agreement between VB and FOB in the evaluation of airway stenoses. The differences in ratios of stenoses/lumen was within 10% for VB vs upper airway endoscopy. The evaluation of dynamic airway collapse was much less reliable with virtual endoscopy, but there was clearly established a role for virtual endoscopy in airway stenoses.

Several papers have been written defining the role of virtual bronchoscopy in patients with airway stenoses secondary to bronchogenic carcinoma. In the paper by Liewald et al, 30 patients with bronchogenic carcinoma were studied. While central lesions were well identified by virtual bronchoscopy, stenosis secondary to smaller lobar lesions were not accurately identified. In a paper by Rapp Bernhardt, a number of visualization techniques were compared, including axial, MPR, MinIP and virtual bronchoscopy. Virtual bronchoscopy evaluation of stenoses showed the lowest interobserver variability. There was no significant difference between virtual and fiberoptic bronchoscopy in the estimation of stenoses, though there tended to be some overestimation of stenoses, felt to be due to thresholding limitations of stenoses in virtual bronchoscopy. Mucosal abnormalities were not well evaluated with virtual bronchoscopy. Other work has looked

at the success of bronchial stenoses in a lung transplant population. In this paper, stenoses at the anastomosis was evaluated by axial and virtual bronchoscopy. Stenoses at the anastomotic sites were better visualized by virtual bronchoscopy than axial CT, though this was not statistically significant. Surface irregularities due to infection were equally visualized with virtual and fiberoptic bronchoscopy.

There is an increasing literature on the use of virtual bronchoscopy in improving the diagnostic accuracy of fiberoptic bronchoscopy. In a paper by McAdams, the virtual bronchoscopy was reviewed by the pulmonologist for evaluation of lymph node biopsy, and was preferred to the axial CT slices. There was a slight improvement in diagnostic yield compared to standard axial images when VB images were reviewed. In a paper by Hopper, a technique of lymph node highlight was described. Mediastinal lymph nodes were manually segmented and highlighted and integrated into the surface rendered virtual bronchoscopy. By the use of varying the transparency of the bronchial wall, the involved lymph node could be chosen before the procedure. While there was no significant difference in the diagnostic sampling of subcarinal lymph nodes, these techniques improved diagnostic yield significantly for hilar and pretracheal lymph nodes.

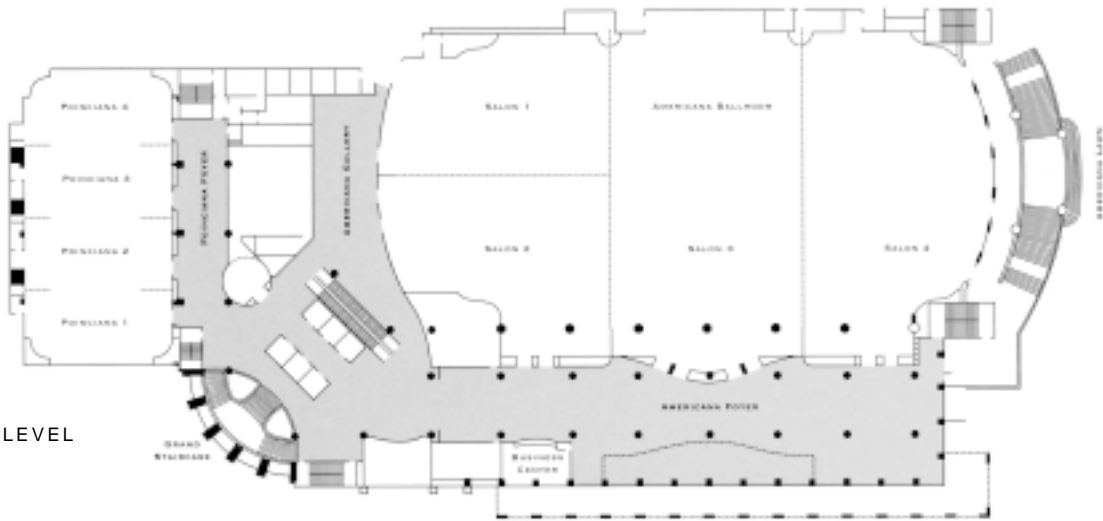
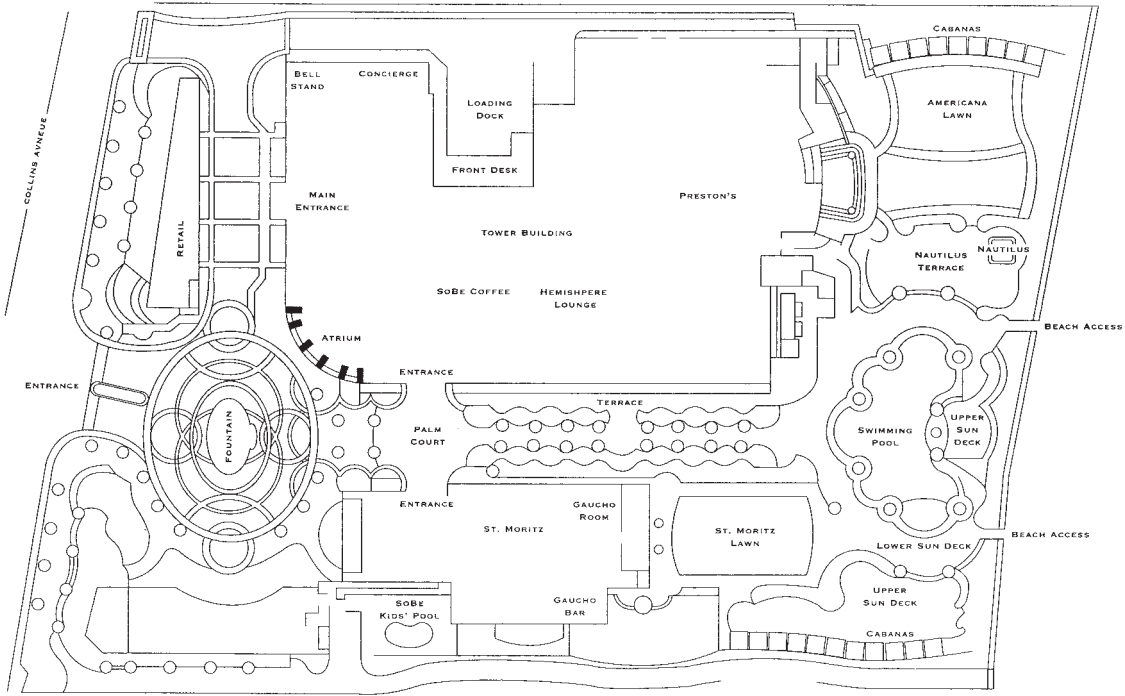
We have used virtual endoscopy in the chest to also evaluate the esophagus and aorta. Virtual endoscopy has been used extensively by our thoracic surgeons to preoperatively assess the aorta. Evaluation of atherosclerotic disease, endoscopic evaluation of dissections, aneurysms and stenoses have helped the presurgical planning of pulmonary thromboendarterectomy. It has been used in the coronary arteries, and pulmonary arteries for evaluation of stenoses and embolic disease. As our techniques improve, virtual endoscopic techniques will only improve, as will their clinical applications.

REFERENCES:

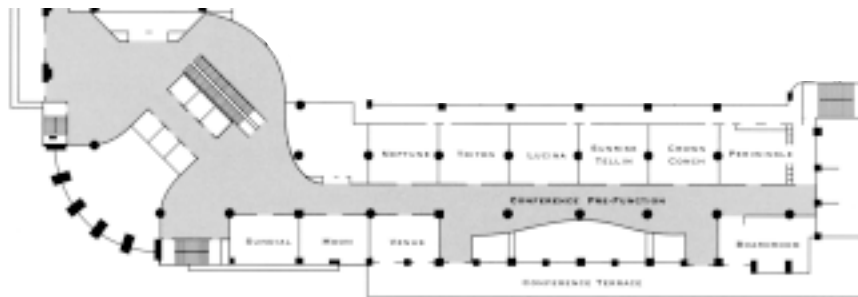
- Haponik E, Aquino S, Vining D, Virtual Bronchoscopy Clinics in Chest Medicine 20;201-217 1999
- Burke A, Vining DJ, McGuirt W, et al Evaluation of airway Obstruction Using Virtual Bronchoscopy. Laryngoscope;110 23-29 2000
- McAdams N, Palmer S, Erasmus JJ et al. Bronchial Anastomotic Complications in Lung Transplant Recipients:Virtual Bronchoscopy for Noninvasive Assessment Radiology 1998;209:689-695
- Hopper K, Lucas TAS, Gleeson K, et al. Transbronchial Biopsy with Virtual CT Bronchoscopy and Nodal Highlighting. Radiology 2001;221:531-536.
- Seeman M, Claussen C, Hybrid 3D Visualization of the chest and virtual endoscopy of the tracheobronchial system:possibilities and limitations of clinical application. Lung Cancer 32 (2001)237-246
- Rapp-Bernhardt U, Welte T, Doerhing W, et al Diagnostic potential of virtual bronchoscopy:advantages in comparison with axial CT slices, MPR and mIP. Eur. Radiol.10,981-988 (2000).

A large L-shaped black line forming a frame for notes, consisting of a vertical line on the right and a horizontal line at the bottom, meeting at a rounded corner.

Notes



SECOND LEVEL



THIRD LEVEL